

The Efficiency of Plastic Skylight Panels as Smoke Vents in the Event of Fire

A thesis submitted in partial fulfilment
of the requirements for the Degree
of Master of Engineering in Fire Engineering
in the University of Canterbury
By J. M. Gaskin

University of Canterbury
Christchurch, New Zealand

2010

Abstract

Concerns have been raised over the use of plastic skylights as smoke vents in large single story buildings. The plastic skylights provide natural light to the building. There has been an assumption that these plastic panels will melt and provide smoke and heat venting during a fire.

The plastics commonly used in New Zealand, polyvinyl chloride (PVC), polycarbonate, acrylic and glass fibre-reinforced polyester (GRP) have been tested in small scale experiments to further the understanding of the behaviour of the materials at elevated temperatures. The behaviour of particular interest is the effectiveness of the skylight as a vent for hot buoyant gases.

Small scale experiments have been conducted to find the mass flow rate of an unobstructed vent. Experiments have then been carried out on samples of the four skylight materials for a range of exposure temperatures and times. The mass flow has been measured for the deformed sample and compared to the unobstructed flow.

The results of the small scale experiments have been analysed and an empirical relationship has been developed for the PVC and polycarbonate material. The acrylic behaviour does not provide enough data to include it in the empirical relationship. The GRP failed to melt and was therefore also excluded from the empirical relationship.

A model has been developed to demonstrate the use of the empirical relationship. The model compares four cases, the vents always open, the vents always closed, the vents opening at a single value and the area when calculated using the empirical relationship.

Acknowledgements

I wish to acknowledge the following people for their support and help.

My supervisor, Mike Spearpoint for guiding me through this long process.

Bob Wilsea-Smith, for turning my thoughts into reality and making the experiments possible.

Mum and Dad for their help and encouragement.

Isabelle for being a good friend.

The parishioners of Upper Riccarton-Yaldhurst, for their friendship and support, especially Craig, Nicola and Olivia for sharing their home.

The New Zealand Fire Service Commission for their support of the Fire Engineering programme at the University of Canterbury.

Table of Contents

Abstract	ii
Acknowledgements	iii
Table of Contents	iv
List of Figures	vii
List of Tables	ix
Chapter 1 Introduction	1
1.1 Problem Background.....	1
1.2 Scope and objectives.....	2
1.3 Road Map	3
Chapter 2 Literature Review	5
2.1 Codes and Standards	5
2.1.1 New Zealand.....	5
2.1.2 Australia	8
2.1.3 United Kingdom	8
2.2 Construction Practice	9
2.3 Materials.....	10
2.3.1 Polycarbonate	12
2.3.2 Polyvinyl Chloride	13
2.3.3 Acrylic.....	13
2.3.4 GRP.....	14
2.3.5 Material Selection.....	15
2.4 Single Story Building Fires	15
2.5 Research	16
Chapter 3 Methodology.....	18
3.1 Experimental Apparatus.....	20
3.1.1 Oven.....	20

3.1.2	Reference Frame.....	20
3.1.3	Windtunnel.....	21
3.1.4	Universal Data Logger.....	24
3.2	Preliminary Experiments.....	25
3.2.1	Method.....	26
3.3	Wind-tunnel Characterisation.....	27
3.3.1	Baseline.....	28
3.4	Main Series.....	28
3.4.1	Experimental Procedure.....	29
3.4.2	Data Analysis.....	31
Chapter 4	Experimental Results.....	36
4.1	Preliminary Results.....	36
4.1.1	Polyvinyl Chloride.....	36
4.1.2	Polycarbonate.....	39
4.1.3	Acrylic.....	41
4.1.4	Glass-fibre reinforced polyester (GRP).....	42
4.1.5	Alternative Sealing.....	44
4.2	Characterisation Results.....	45
4.2.1	Wind Tunnel Profiles.....	45
4.2.2	Fan Settings.....	46
4.2.3	Baseline Measurements.....	48
4.3	Glass-fibre Reinforced Polyester.....	52
4.4	Polycarbonate.....	54
4.5	Polyvinyl Chloride.....	57
4.6	Acrylic.....	63
4.7	Angled Plate.....	66
4.7.1	Experimental Results.....	74

4.8	Empirical Relationship.....	75
Chapter 5	Modelling.....	81
5.1	Building Geometry.....	81
5.2	Calculation Procedure.....	83
5.3	Limitations.....	91
5.4	Results.....	92
Chapter 6	Discussion.....	96
6.1	Research Limitations.....	96
6.2	Angled Plate.....	97
6.3	Polycarbonate.....	98
6.4	Polyvinyl Chloride.....	99
6.5	Acrylic.....	99
6.6	GRP.....	100
6.7	Prediction of Vent efficiency.....	100
6.8	Modelling.....	101
Chapter 7	Conclusion.....	102
7.1	Further Research.....	102
Chapter 8	References.....	104
Appendix A	Baseline Results.....	106
Appendix B	Polycarbonate Experiments Results.....	113
Appendix C	Polyvinyl Chloride Experiment Results.....	167
Appendix D	Acrylic Experiment Results.....	215
Appendix E	Glass-Fibre Reinforced Polyester Results.....	227
Appendix F	Calculation of Biot number.....	231
Appendix G	Model Results.....	235

List of Figures

Figure 1: Connection detail	10
Figure 2: Chemical structure of polycarbonate	12
Figure 3: Chemical structure of PVC.....	13
Figure 4: Chemical structure of PMMA	14
Figure 5: Ceiling jet and wind tunnel flow comparison.....	19
Figure 6: Oven used to deform the plastic	20
Figure 7: Wind tunnel schematic	22
Figure 8: Cross-section of the wind tunnel and measuring duct	22
Figure 9: Hatch to admit inlet air.....	23
Figure 10: Pressure transducer.....	24
Figure 11: Diagram showing the measuring points, dimensions in mm.....	31
Figure 12: Plan view of measuring points defining the coordinate system.....	33
Figure 13: Graphical representation of the integration	35
Figure 14: Small hole found after 120 minutes at 100°C.....	36
Figure 15: PVC after 50 minutes exposure at 150°C.....	37
Figure 16: The PVC shrinking from the first side after 10 minutes exposure to 200°C.....	38
Figure 17: PVC, two sides shrinking after 30 minutes exposure at 200°C.....	38
Figure 18: PVC at the end of the 250°C experiment	39
Figure 19: The polycarbonate after 10 minutes exposure to 200°C.	40
Figure 20: The slumped polycarbonate after 15 minutes exposure at 250°C	40
Figure 21: The polycarbonate after being exposed to 300°C	41
Figure 22: The large bubbles formed during the acrylic test at 200°C	42
Figure 23: Deterioration of the acrylic at 250°C	42
Figure 24: GRP, bubbles formed during the test at 250°C.....	43
Figure 25: GRP, dark brown colour at the end of the 300°C test.....	43
Figure 26: Building showing direction of primary connection	45
Figure 27: Centre-line velocity profile at 100°C	46
Figure 28: Average velocities at different fan settings	47
Figure 29: Velocity at different fan settings and temperature at 100°C	48
Figure 30: Raw data output from the pressure transducer for the 150°C baseline.....	49
Figure 31: Raw thermocouple readings for the 150°C baseline.....	49
Figure 32: Density time series	50

Figure 33: Velocity time series.....	51
Figure 34: Time series of mass flow per unit area.....	51
Figure 35: Velocity record, GRP, 120 minutes exposure to 300°C.....	53
Figure 36: Temperature record, GRP, 120 minutes exposure to 300°C	54
Figure 37: Summary of Polycarbonate results	57
Figure 38: Temperature record, PVC, test 1, 5 minutes exposure to 200°C	58
Figure 39: Velocity record, PVC, test 1, 5 minutes exposure to 200°C	59
Figure 40: Image of deformed sample, test 1, and note flow is from bottom to top	59
Figure 41: Temperature record, PVC, test 3, 5 minutes exposure to 200°C	60
Figure 42: Velocity record, PVC, test 3, 5 minutes exposure to 200°C	60
Figure 43: Image of deformed sample, test 3, hole inside the circle	61
Figure 44: Summary of polyvinyl chloride results	63
Figure 45: Velocity record, acrylic, 20 minutes exposure at 250°C.....	65
Figure 46: Temperature record, acrylic, 20 minutes exposure at 250°C	65
Figure 47 Physical deflection of air flow by the plastic sample.....	66
Figure 48: Cross-section defining the angle of the plastic plate.....	67
Figure 49: Angled plate reversed.....	68
Figure 50: Graphical representation of theoretical model.....	69
Figure 51: Comparison of theoretical and experimental efficiency.....	75
Figure 52: E vs. $\tau T_e/T_m$	78
Figure 53: E vs. $\tau T_e/T_m$ with modified acrylic melting temperature	80
Figure 54: Model building dimensions with skylight location.....	82
Figure 55: Elevation of model building showing important physical dimensions	82
Figure 56: Flow diagram of the model calculations	84
Figure 57: Comparison between the step-wise temperature and unrounded temperature	90
Figure 58: Layer heights for PVC skylights with a fast fire growth rate	93
Figure 59: Layer heights for polycarbonate skylights with a fast fire growth rate.....	94
Figure 60: Layer heights for acrylic skylights with a fast fire growth rate.....	95

List of Tables

Table 1: Summary of plastic melting temperatures (°C)	12
Table 2: Experimental matrix for preliminary experiments	25
Table 3: Target pressure transducer readings	28
Table 4: Experimental matrix for polycarbonate	29
Table 5: Experimental matrix for PVC	29
Table 6: Experimental matrix for acrylic	29
Table 7: Wind tunnel settings and velocity	46
Table 8: Summary of the mass flows for the baseline experiments	52
Table 9: GRP Results	52
Table 10: Polycarbonate Results.....	56
Table 11: Polyvinyl Chloride Results	62
Table 12: Acrylic Results	64
Table 13: Depth of angled plate.....	70
Table 14: Theoretical mass flow through vent for an angled plate	73
Table 15: Experimental mass flows for an angled plate	74
Table 16: Characteristic material values	77

Chapter 1 Introduction

This thesis examines the behaviour of plastic skylights at elevated temperatures. The behaviour of interest is the efficiency of the skylights for use as a smoke vent during a fire. Concerns have been raised in New Zealand about the performance of plastic skylights used as smoke vents particularly those made of glass-fibre reinforced polyesters (Edwards et al. 2007; Department of Building and Housing 2008a).

The efficiency of the skylights as smoke vents has been determined with small scale tests using the wind tunnel developed at the University of Canterbury. The wind tunnel was designed for testing and characterising sprinklers (Chin 2002; Tsui 2004; Yu 2007). The wind tunnel was modified to incorporate a horizontal vent and allow the measuring of buoyant gases flowing through the vent.

There are many questions surrounding the use of plastic skylights. The questions include but may not be limited to the following:

- The effectiveness of plastic skylights in becoming vents during a fire.
- The definition of effective venting.
- When the effective venting needs to occur.
- The appropriateness of a specified venting area.
- The benefits of venting.

This thesis is concerned with the behaviour of the plastic skylight material at elevated temperatures. When the material melts and what proportion of the area is available as a smoke vent.

1.1 Problem Background

Industrial and large commercial buildings are often undivided due to reasons of practicality. Dividing the building into smaller spaces require doors and walls. The presence of these doors and walls can reduce the efficiency of the building operations. The Compliance Document to the New Zealand Building Code limits the fuel load of buildings by limiting the size of fire cells.

Under the Compliance Document solution there are three options for extending the size of fire cells in single story buildings. The first option is the provision of a sprinkler system. The

second option is to provide smoke ventilation. The smoke ventilation system can be provided in a passive manner such as drop out panels, louvre vent or ridge vents. These vents operate as natural vents but have no active initiator such as a fusible link but instead are always open or rely on plastic panels melting. The final option is to build in a location such that the building does not require a structural fire resistance rating.

Plastic roof panels which are installed to meet the requirements for natural lighting (NZ Metal Roofing Manufactures Inc. 2003) have been used by fire engineers to provide a low cost method of providing large areas of venting. There is cost saving using this method of venting for the fire engineer as the plastic roof panels are already provided. Extra fire protection equipment, such as dedicated smoke vents or a sprinkler system, are therefore not required.

In the New Zealand environment plastic roofing has historically been used to provide a level of smoke venting from buildings which exceed firecell size limits and present a fire spread exposure risk to neighbouring properties. Glass fibre-reinforced polyester roofing has been used due to the strength and durability of the material however the New Zealand Fire Service have raised concerns based upon anecdotal evidence that this material does not perform well as a vent during a fire. No verification of the effectiveness of the venting capability has been established for this or any plastic roofing.

1.2 Scope and objectives

This work focuses on the materials and their performance under elevated temperatures. The main body of this report is concerned with the results of small scale experiments. The simulations at the end of this work are an attempt to put the experimental results in context of a large undivided single storey building. The simulation is designed to show the difference between the current knowledge and the new knowledge generated from this work.

The following are commented upon but are outside the scope of this project:

- The specific area requirement for passive venting.
- The use of passive smoke vents.
- What constitutes effective venting.
- The codes and standards.

The above items are mentioned as background and no conclusions should be drawn on the aforementioned items from this report.

Therefore the objectives of this thesis are:

- To further the fire engineering communities understanding of the plastic materials used for skylights at elevated temperatures.
- To provide experimental data on the idealised behaviour of plastic skylights at elevated temperature to assist fire engineers and approval authorities to determine if a design meets the requirements of the Compliance Document.

1.3 Road Map

The thesis attempts to answer the question of how effective the plastic skylight are as smoke vents during fire through the following process.

The thesis first examines the previous knowledge of passive ventilation. The literature review looks at the codes and standards and their development in the New Zealand context. The literature review also briefly covers the regulations in other countries such as Australia and the United Kingdom. The literature review then examines the construction methods in New Zealand and the plastics used for skylights. The literature review finally covers the previous research in this area of fire protection.

Chapter 3 then covers the methodology. This section covers the experiments in three sections. The first section covered is the preliminary experiments that were conducted to gather data about the behaviour of the materials when exposed to elevated temperatures and allow the development of parameters for the main series of experiments. The second section covers the characterisation tests conducted to determine the performance of the wind tunnel itself. The chapter finally covers the experimental procedure for the main series of experiments on the skylight plastic. The methodology then covers how the data was analysed to come up with a percentage flow through the vent. The methodology section also describes the experimental apparatus used to conduct the experiments and the modifications of the wind tunnel.

Chapter 4 outlines the results of the preliminary experiments and the main series results. Further experiments that looked at the effect of the plastic physically deflecting the flow of hot gases are described and the results analysed. The results section also presents an

empirical relationship developed relating the exposure temperature, exposure time and the efficiency.

Chapter 5 presents an exemplar building used to simulate the smoke layer. The section contains the development of the model, the equations used and the results of the simulations. The model shows the difference between the current knowledge and the new knowledge developed by this work.

Chapter 6 contains the discussion. The discussion covers each of the plastics and tries to explain and understand the behaviour seen during the experiments. The discussion also covers the possible implications of this work. The modelling is also discussed in this section. Finally the limitations of this work are discussed.

Chapter 7 contains the conclusion of the work and recommendations are also made as to further work.

Chapter 2 **Literature Review**

The first step in conducting a thesis is to determine what is already known. The literature review covers material that may be outside the scope of the inquiry to give context to the issue.

The literature review covers the following areas:

- Codes and Standards covering smoke venting and roof construction in New Zealand and overseas.
- The materials used as plastic skylights.
- Past research into the use of plastic skylights as smoke vents.

2.1 Codes and Standards

This section of the literature review covers codes and standards from New Zealand, Australia, and the United Kingdom. The author recognizes that other codes and standards do exist; however the research has come about through concerns raised in New Zealand. The Australian codes and standards have been considered due to the proximity to New Zealand and the close functioning of each country for example joint Standards. The United Kingdom has been considered due the influence of British Codes and Standards on the development of New Zealand documents (Edwards et al. 2007).

2.1.1 New Zealand

The governing piece of legislation in New Zealand is the Building Act 2004. The Building Act allows the issuing of the Building Code. The New Zealand building code is a performance code. That is it specifies what the performance of the building should be but not how to obtain it. There are currently two ways to meet the Building Code an engineering based solution or by following Acceptable Solution. In the case of a fire design the relevant document is Compliance Document for New Zealand Building Code Clauses C1, C2, C3, C4 Fire Safety (C\AS1) (Department of Building and Housing 2008b).

As stated previously the genesis of this problem is the design of large undivided single story buildings using the Acceptable Solution. Clause 4.2.4 reproduced below allows the use of passive fire venting.

4.2.4 In an unsprinklered single floor building where the building elements supporting the roof are not fire rated, the firecell floor area may be unlimited provided that no less than 15% of the roof area (distributed evenly throughout the firecell) is designed for effective fire venting (Department of Building and Housing 2008b).

The following are defined by C/AS1 (Department of Building and Housing 2008b) as

Building has the meaning ascribed to it by sections 8 and 9 of the Building Act 2004.

Building element Any structural and non-structural component or assembly incorporated into or associated with a *building*. Included are *fixtures*, services, *drains*, permanent mechanical installations for access, glazing, partitions, ceilings and temporary supports.

Fire The state of combustion during which flammable materials burn producing heat, toxic gases, or smoker flame or any combination of these.

Firecell Any space including a group of contiguous spaces on the same or different levels within a *building*, which is enclosed by any combination of *fire separations*, *external walls*, roofs, and floors.

However, there is no definition of effective fire venting. As no criterion exists to determine what effective venting is, it is difficult to assess if any of the plastic skylight materials available are appropriate.

Read in the context of Clause 4.2.3 the purpose of the fire venting is to prevent fire spread to neighbouring properties.

The required S-rating is determined from Table 5.1 of C/AS1 (Department of Building and Housing 2008b). The ratio of the area of roof openings to floor area assists in determining the

fire resistance time required, the higher the ratio the lower the rating required. The notes to the table state:

4. Effective openings

...

c) only roof venting which is specifically designed to open or melt rapidly in the event of fire shall be included in the area A_h

In November 2008 the following comment was added to C\AS1 after clause 4.2.4

COMMENT:

Roof venting systems such as drop-out panels, louvre vents or ridge venting shall be designed and proven for the purpose of facilitating fire fighting operations. The Australasian Fire and Emergency Services Authorities Council's Fire Brigade Intervention Model (www.afac.com.au/awsv2/learning/fbim.htm) provides guidance on performance criteria for firefighters. Less than 15% roof area for venting may be acceptable if total system performance can be demonstrated (Department of Building and Housing 2008b).

The comment indicates that the roof venting is for the purposes of assisting Fire Service operations. The performance criteria for fire fighters in the FBIM are:

As part of the performance criteria for firefighters the following tenability criteria are given for Fire Brigade personnel in full turnout gear:

- Routine – 25 minutes exposed to 100°C lower layer temperature of 1kW/m².
- Hazardous – 10 minutes exposed to 120°C lower layer temperature or 3kW/m².
- Extreme – 1 minute exposed to 160°C lower layer temperature of 4.5kW/m².
- Critical - <1 minute exposed to >235°C lower layer temperature or 10kW/m².

The above criteria of the FBIM indicate that the measure of fire fighter tenability is in terms of exposure to radiant heat or convective heat assessed through the lower layer temperature. Criteria are not strictly given for the structural performance of building elements.

The New Zealand Fire Service (NZFS) are required by the Fire Service Act 1975 to protect life and property. This contrasts with the requirements of the New Zealand Building Act for life safety and protection of other property. As a consequence the New Zealand Fire Service has a bias towards property protection.

2.1.2 Australia

The Building Code of Australia (BCA) (Australian Building Codes Board 2009) discusses roof lights in Clause C3.2 of Specification C1.1 discusses the use of skylights in terms of their combustibility and ability to prevent fire spread by their location. As the buildings of interest in this report are single storey buildings this clause has no relevance to the discussion.

Smoke and heat vents are one of the permitted methods for increasing the area of unsprinklered fire cells in Table C2.2 of the BCA. The increase in size is only applicable for Class 7 and 8 buildings which generally comprise of warehouses and industrial buildings. The heat and smoke vents are required to comply with AS 2665 (Standards Association of Australia 2001). Alternatively permanently open natural vents can be used.

The Australian standard covering heat and smoke venting is AS 2665: Smoke/heat venting systems: design, installation and commissioning. The standard requires that the vents be activated at a temperature of 68°C or 5°C above the activation temperature of any sprinkler system installed. The activation of the vents may also be achieved through smoke alarms. The vents are also required to be manually overridden. The failure position of all vents is required to be open (Edwards et al. 2007).

The requirements of AS 2665 and of natural ventilation openings to be permanently open prevent the use of melting skylights under the Deemed to Satisfy Provisions of the BCA.

2.1.3 United Kingdom

Between 1985 and 2000 the United Kingdom Approved Documents contained a similar provision for the use of passive skylights. The requirement was for 10% of the floor area (Edwards et al. 2007). The design of portal frames is now required to be carried out using the method set out by Newman (Newman 1990). The structural benefit that may be provided by passive roof venting is no longer required when using the design method.

The 1985 version of United Kingdom document was an important source when the New Zealand Acceptable Solution was first written circa 1990 (Edwards et al. 2007).

2.2 Construction Practice

The particular design of a building is dependent on the environment in which it is built both physically and legislatively. The issues that prompted this research have been created in the New Zealand context and as such the building practices examined are those in New Zealand. The basis for the construction practice has been the New Zealand Metal Roof Manufacturers Code of Practice (NZ Metal Roofing Manufacturers Inc. 2003).

The plastic sheets are fastened to the building structure using screws or nails. The holes for the fastener are required to be over sized to allow for thermal movement load spreading washers should also be used. It is important that the fasteners are installed correctly as over tightening can cause distortion to the plastic. The recommended spacing for the fasteners is every second corrugation for corrugated profile. For trapezoidal profiles the fasteners shall be placed every rib.

The support for the roof is provided by purlins. For purlin spacing of greater than 1200 mm a span breaker is required in the centre of the span. All plastic roof light sheets shall be laid on top of the metal sheeting at both edges.

A detailed connection is shown below in Figure 1. The connection shows the plastic over the metal. Figure 1 is an adaption from the NZ metal Roof Manufacturers Association Code of Practice (NZ Metal Roofing Manufacturers Inc. 2003).

There exists an option for using two sheets of the material to provide increased insulation to the building.

To meet health and safety provisions for working at a height a wire mesh is required. The mesh is installed over the top of the purlins. The roof sheeting is then installed on top of the wire mesh. The wire mesh fulfils a secondary purpose of providing support for insulation or an underlay.

The safety mesh is required to meet the requirements of AS/NZS 4389:1996 (Standards Association of Australia. & Standards New Zealand. 1996a). The standard requires that the safety mesh be made from galvanised welded steel wire with a minimum diameter of 2 mm and a tensile strength of 450 MPa.

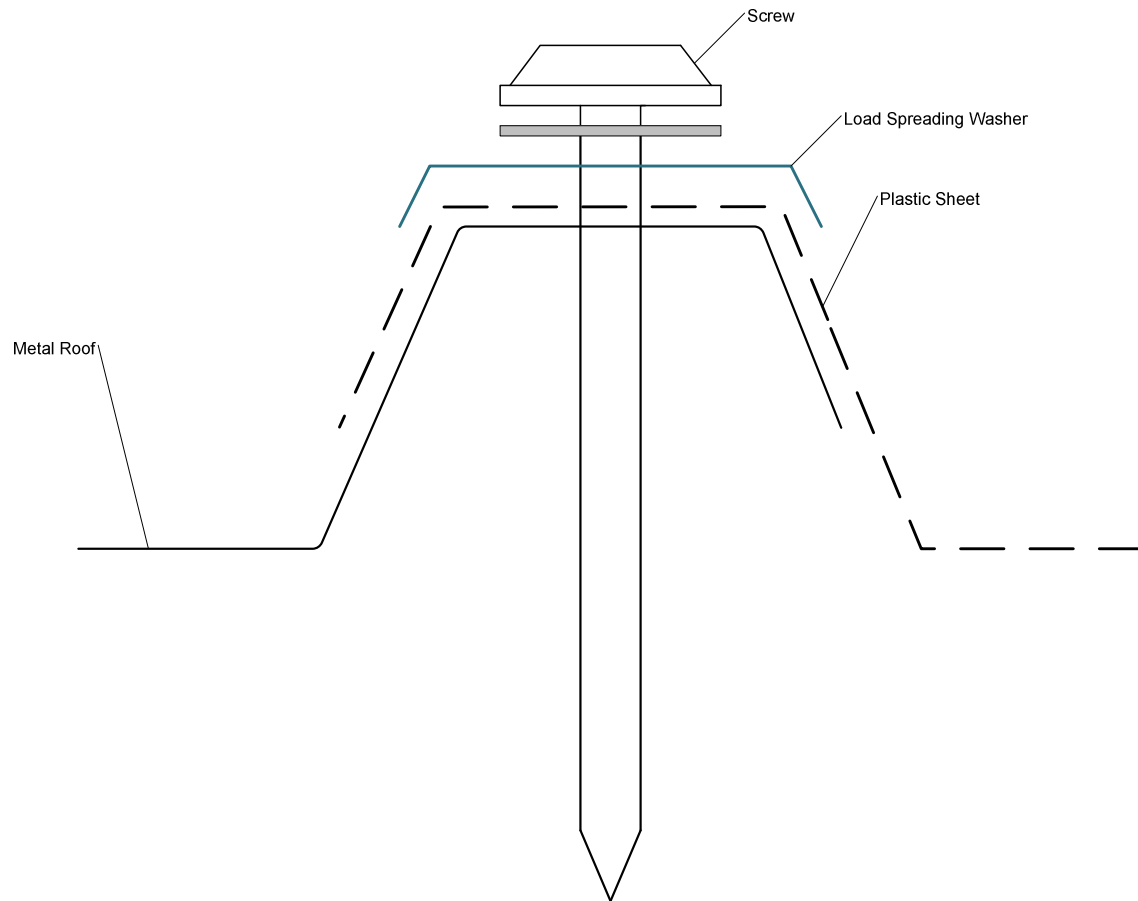


Figure 1: Connection detail

2.3 Materials

The thesis focuses on four plastic materials commonly used in New Zealand for skylights. The materials are:

- Polycarbonate
- Polyvinyl Chloride (PVC)
- Acrylic
- Glass Fibre Reinforced Polyester (GRP)

There are other plastics that can be used for skylight such as the proprietary product Texlon®. This report has not considered these as they are not readily available in New Zealand. It is possible that some of these materials may be appropriate for smoke venting.

The following discussion is based on material from Erhard (Erhard 2006).

When discussing polymers an important distinction needs to be made between thermoplastics and thermosetting plastics. Thermoplastics are polymeric materials made up of linear or branched macromolecules. Thermoplastics contain both crystalline and amorphous structures. The molecules are attached by physical binding forces such as Van der Waals forces and hydrogen bonding which can be overcome by thermal energy. The properties of the materials can be altered by fillers, stabilizer, flame retardants, pigments and other additives to the plastic.

The thermosetting materials are close-meshed cross-linked polymeric chains. The thermosetting material does not soften and melt but chars.

A method of determining a melting point for thermoplastics is the glass transition temperature when the crystalline structures become amorphous and the material loses strength. The glass transition temperature is approximately the Vicat softening temperature. This is the temperature at which a 1 mm² needle penetrates the plastic 1 mm under a 50 N load.

Of the four materials examined by this thesis three are thermoplastics (Polyvinyl Chloride, Polycarbonate and Acrylic). The fourth material, GRP comprises both a resin of polyester and glass fibres. The polyester is a thermosetting resin and as such chars. The glass fibres are made of glass pulled from a furnace at approximately 1300°C at a rate of 3000 to 4000 m/min.

Table 1 summarises the melting temperatures found in the literature. The temperatures are for generic plastics. The melting temperature can be altered by the addition of additives such as those that reduce ultra-violet light and are contained in skylights.

Table 1: Summary of plastic melting temperatures (°C)

	BRANZ (SR165) (Edwards et al. 2007)	NZ Metal Roofing Code of Practice (NZ Metal Roofing Manufactures Inc. 2003)	Design Data for Plastics Engineers (Rao & O'Brien 1998)	Modern Plastics Handbook (Harper 2000)
Polyvinyl Chloride	80	86	80	75-105
Polycarbonate	135-200	133	150	149-250
Acrylic (PMMA)	50-140		105	90-165
GRP	180-200	245		220-260

2.3.1 Polycarbonate

Polycarbonate is a thermoplastic. The chemical structure is shown below in Figure 2. The melting temperature of the polycarbonate was found to range from 135°C (Edwards et al. 2007) to 250°C (Harper 2000). The most common temperature from Harper was 150°C.

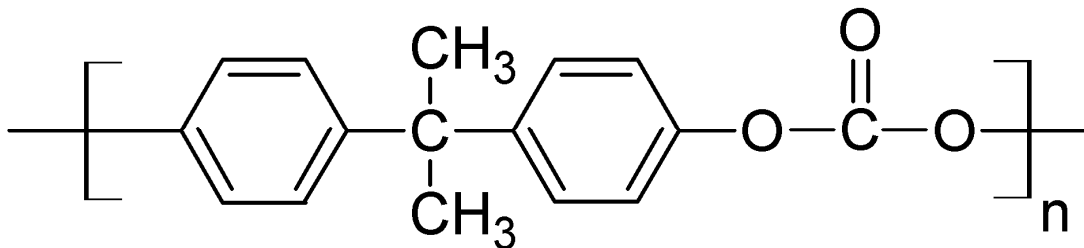


Figure 2: Chemical structure of polycarbonate

The material must conform with AS/NZS 4256 (Standards Association of Australia. & Standards New Zealand. 1995). The polycarbonate blocks ultra violet light up to 99.9% whereas glass only provides 95% blocking. The polycarbonate light transmission is between 89% and 92% (Pringle 1998) for clear profiles. For twined wall setups and a clear sheet the light transmission reduces to 82% (Pringle 1998).

2.3.2 Polyvinyl Chloride

Polyvinyl chloride is a thermoplastic made up of repeating chains containing a chlorine atom as shown below in Figure 3. The melting temperatures were lower than the polycarbonate melting temperatures ranging from 75°C to 105°C (Harper 2000).

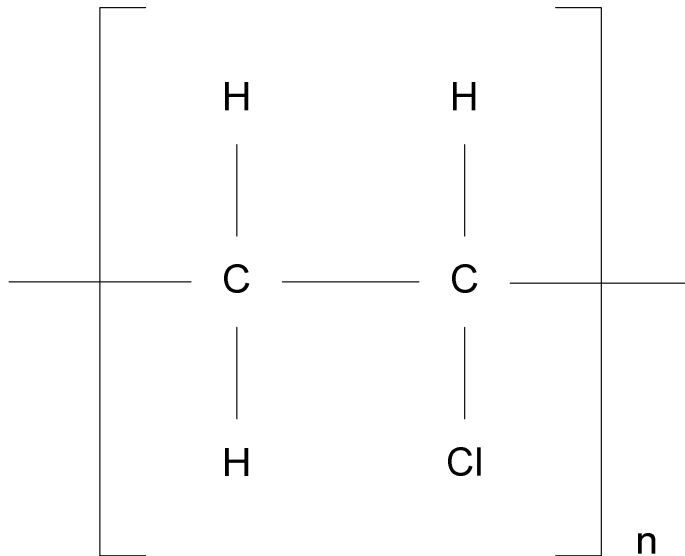


Figure 3: Chemical structure of PVC

The standard governing the PVC material is AS/NZS 4256.2 (Standards Association of Australia. & Standards New Zealand. 1994a).

PVC can block up to 99.9% of ultra violet light. The light transmission value for clear PVC is 78% (Pringle 1998).

2.3.3 Acrylic

Acrylic is a plastic. The acrylic is very clear and strong. The acrylic is also known as polymethylmethacrylate (PMMA) (Edwards et al. 2007). The chemical structure is given below in Figure 4. The melting temperature of the PMMA ranges between 50°C (Edwards et al. 2007) and 165°C (Harper 2000).

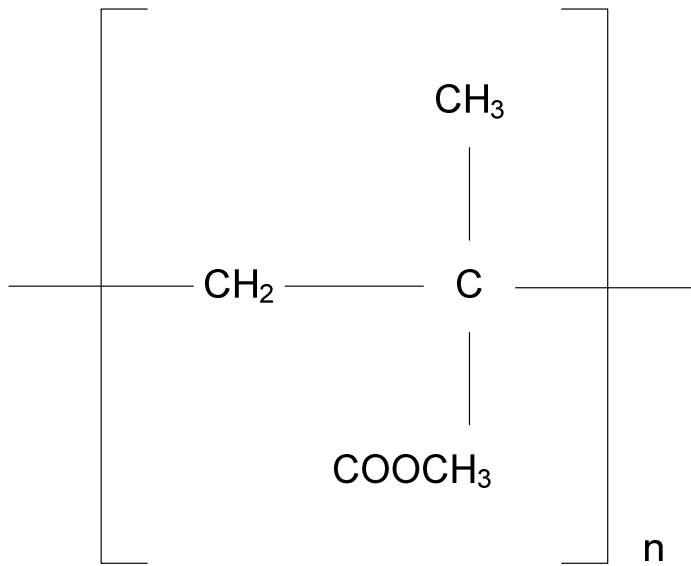


Figure 4: Chemical structure of PMMA

The acrylic achieves a transmission factor of 92% and has superior optical clarity. The material will melt and burn vigorously rather than just breaking (Pringle 1998).

Part 6 of AS/NZS 4256 (Standards Association of Australia. & Standards New Zealand. 1996b) covers acrylic sheets.

2.3.4 GRP

The resin used in the manufacture of GRP is polyester. The melting temperature of the polyester ranges from 180°C (Edwards et al. 2007) to 260°C (Harper 2000). The melting point of the glass fibres used is dependent on formula but is in the range of 700 to 840°C. The melting temperatures are those found in post flash over compartments (Karlsson & Quintiere 2000). The GRP can protect up to 99.9% of UV light.

The GRP light transmission is dependent on the grade, the higher the grade, the higher the glass content and the lower the light transmission. For 1200 grade the transmission is 84-85%. For 1800 grade the transmission is 74-76% (Pringle 1998).

The GRP is covered by part 3 of AS/NZS 4256 (Standards Association of Australia. & Standards New Zealand. 1994b).

2.3.5 Material Selection

In determining the plastic material to be used in the construction of the building the performance as a smoke vent is rarely considered. The major factors affecting the selection of the material are:

- Appearance.
- Cost.
- Wind loading and snow loading.
- Durability.
- Maintenance requirement.
- Fire, acoustic and insulation properties.

The fire properties considered are the combustibility of the product.

2.4 Single Story Building Fires

Clause 4.2.4 relates to the design of single story industrial buildings. According to Cosgrove (Cosgrove 1996) the development of a fire in an industrial building with only a passive venting system would typically develop in the following way

- ~ 1 minutes: initial fire growth
- ~ 3 minutes: developing fire
- ~ 10 minutes: racks fully involved in fire, rack to rack fire spread by radiation
- ~ 20 minutes: flashover and full compartment involvement
- ~ 30 minutes: Structural failure and open air fire

The plastic translucent roof panels are thought to melt and start to provide ventilation around 10 to 20 minutes after the start of the fire.

As discussed in Section 2.1.1, prior to the November 2008 amendments the only comment on the performance of horizontal vents was in relation to the determination of the S-rating required. For a horizontal vent to be included in the ratio A_h/A_f (Area of horizontal vents/Floor Area):

Only roof venting which is specifically designed to open or melt rapidly in the event of fire shall be included in the area A_h .

From the above the time period of interest is the first half hour of the fire. After this time it can be expected that the roof structure has begun to collapse and the fire is beginning to transition from a compartment fire to an open air fire.

The development of the fire in the compartment is in general the following. The fire ignites and as the fire grows the air is heated. As the temperature of the air increases above ambient the air rises due to buoyancy. When the hot air reaches the ceiling the hot air is forced outwards horizontally as a momentum driven circular jet.

Typical ceiling jet velocities in the early stages of a fire are between 1 m/s and 4 m/s (Cox 1977). The velocity of the ceiling jet is dependent on the heat output of the fire, the height of the ceiling and the distance of the ceiling jet from the fire source. As the distance from the centre of the fire increases, the temperature and velocity of the ceiling jet decrease. In a large structure such as an industrial building the variances in temperature and velocity can be expected to be considerable over the length of the building. Near the fire a hot and fast moving ceiling jet is expected while further afield the ceiling jet could be expected to be slow moving and near ambient.

2.5 Research

The research into the use of plastic roof panels melting to provide smoke vents dates back to work done in the 1960's. The research came about from a collaborative research program conducted by Colt Ventilation and Heating Limited and the Fire Offices' Committee Joint Fire Research Organization. The research was undertaken due to a number of fires in large undivided single story buildings (Thomas et al. 1963). The research was reported in three technical papers. The first technical paper was entitled Investigations into the flow of hot gases in roof venting (Thomas et al. 1963). The research found that small levels of venting assisted in maintaining a layer cool layer near the floor of the building. The clear layer assists firefighters in reaching the fire and extinguishing it.

The second paper is entitled Design of Roof Venting Systems for Single Story Buildings (Thomas & Hinkley 1964).

The initial research suggested that to prevent the spread of fire the area of roof venting would need to be much greater than that to provide a clear layer. The area suggested was up to 20% of the floor area.

To provide an economical method for achieving the large area of venting it was proposed that thermoplastic roof panels with a low melting point could be used. This led to the third paper entitled PVC Rooflights for venting fire in Single Story Buildings (Hinkley & Theobald 1966).

The research consisted of full scale experiments on a building with an asbestos cement roof. The PVC panels were installed to the British Standard. The fire used to conduct the test was from wood cribs. The temperature was measured for all experiments. The heat flux was measured for some experiments.

The PVC behaved in the following way. The material softened leading to the collapse of the corrugations. The material then tore in one or two places leaving a clear hole through which the hot gases and flames could be vented.

The conclusion was that the PVC would melt when the hot gas layer below the plastic was 300°C.

More recent research has been conducted by BRANZ Ltd. This work has included a Literature Review (Edwards et al. 2007) and medium scale tests and modelling (Robbins & Wade 2008a, b, c).

The work of most interest to this report is that of the medium scale testing where test methods and criteria such as AS 2428.3 (2004) and BS 7346 Part 1 (1990) undertaken on skylight vents. The report recommends that these current methods are not appropriate for the plastic panels due to the nature of their opening behaviour. The tests are designed for the use in dedicated fire vents which have a binary state of either open or closed. The plastic panels however, open over a period of time and do not necessarily reach a fully open state.

It is noted in the conclusion that the intention was not to test the material or system but to evaluate potential test methods.

The report into the modelling concludes that FDS can model the passive venting. The plastic vent was modelled as a small cell each with a heat detector. When the heat detector activated the plastic vent became a hole.

Chapter 3 Methodology

Small scale experiments were carried out to determine the efficiency of the vent. The efficiency is to be determined by taking the percentage of the mass flow rate of an obstructed vent and dividing by the mass flow rate of the unobstructed vent. This is defined mathematically in Equation 1.

$$Efficiency = \frac{Obstructed\ mass\ flow}{unobstructed\ mass\ flow} \times 100 \quad \text{Equation 1}$$

Each material was tested at a range of temperatures and times. To determine the parameters used for these tests a series of preliminary tests were carried out. The preliminary tests consisted of observing a plastic sample at a single temperature over a period of time. The results from these tests provided information on when and how the different plastics melt. The knowledge was then used to determine times and temperatures for the main series of tests using the wind-tunnel.

The experiments attempted to replicate the conditions found within the building during a fire. The vents in the roof are exposed to the ceiling jet. The ceiling jet replicated using the wind tunnel at the University of Canterbury that was constructed to conduct sprinkler plunge test. Though attempting to mimic the reality some compromises have had to be made. The plastic samples are kept horizontal in contrast to the sloped roofs used in many buildings. The results are therefore only valid for a flat roof condition.

The efficiency is determined using mass flows. The design of smoke control systems are often based on mass or volume flows.

The mass flow is measured by proxy through the temperature and velocity. The flows through the vent are expected to be non uniform and therefore a number of measurements are taken to determine the total mass flow through the vent. A five by five measurement grid would result in 25 points. If the time taken to measure each point is 30 seconds then the total measurement time would be 12 minutes and 30 seconds. To get a reliable measurement it would be necessary for the vent to remain stable during the measurement of the temperature and the velocity.

In an attempt to keep the sample static during the experiment the plastic was deformed in an oven at a set temperature for a set time and then cooled before being exposed to the wind tunnel.

Figure 5 shows the idealised real world condition on the top and the experimental condition underneath. The top section is for a fire occurring under a flat ceiling. The area inside the box is that which the wind tunnel is intended to replicate.

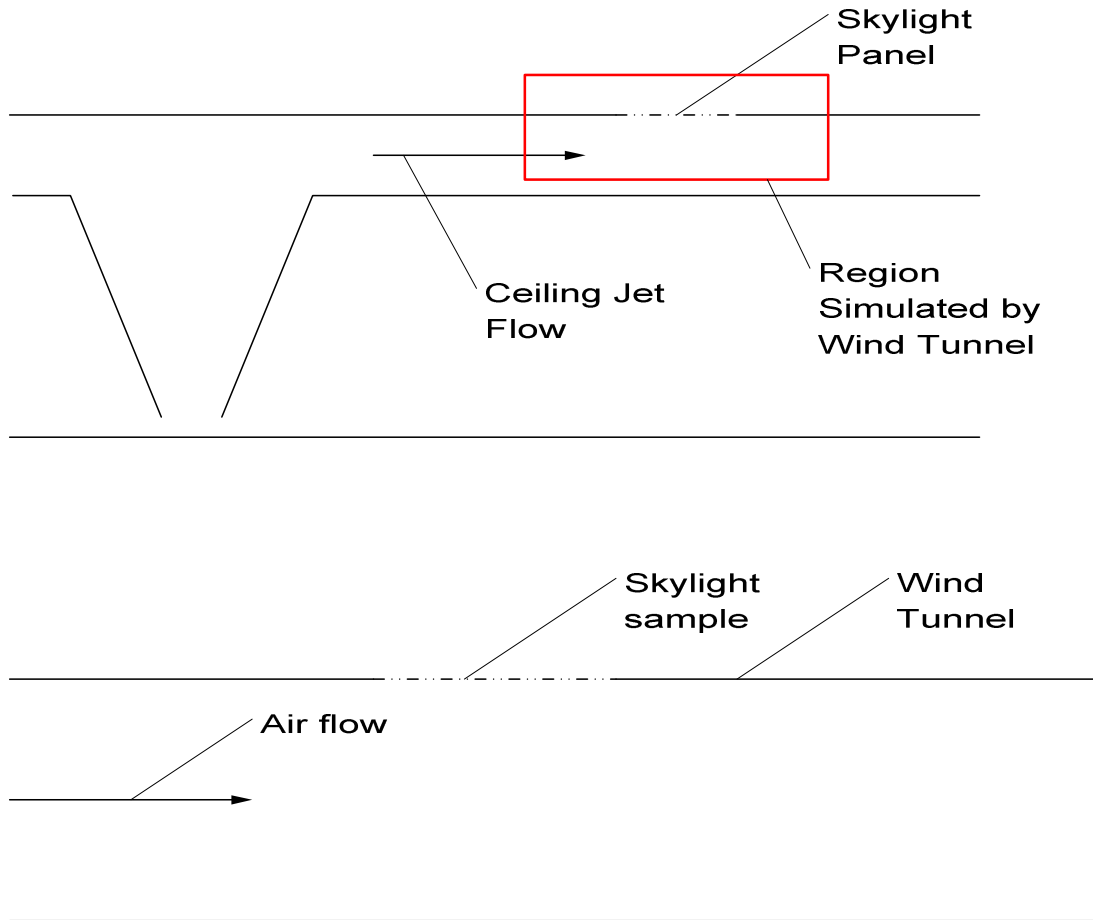


Figure 5: Ceiling jet and wind tunnel flow comparison

3.1 Experimental Apparatus

Two main pieces of apparatus were used in the experiments an oven to heat and deform the samples and a wind tunnel to replicate the ceiling jet and conduct mass flow measurements.

3.1.1 Oven

The oven is a Contherm Digital series oven as seen in Figure 6. The oven contains four racks upon which the samples could be placed. The temperature is set using a digital control on the front of the panel.

The oven is a self contained piece of equipment. The only additional apparatus required for use is the reference frame.



Figure 6: Oven used to deform the plastic

3.1.2 Reference Frame

The samples were tested in a frame that provided a reference area to allow comparison. The frame was made of stainless steel with dimensions of 330 mm by 275 mm. The frame was 50 mm high. Three frames were constructed. Plastic roof sheeting from which the samples were cut had dimensions of between 760 mm wide and 840 mm wide. The lengths of sheeting available are from 1.8 m to 7.2 m long. The behaviour of full scale sheets is not to be addressed by this thesis and there is scope for further research to determine the validity of the small scale results.

3.1.3 Windtunnel

The wind tunnel is more complex in the composition and operation than the oven. The wind-tunnel consists of a number of major parts, the ducting, heating element, fan, and measuring equipment. Figure 7 shows a schematic of the wind-tunnel used for the experiments.

The ducting is made of steel. The cross-section of the wind tunnel is 300 mm by 300 mm. The duct is insulated using a glass wool fibre blanket.

The testing section of the wind tunnel, where the measuring occurs, consists of three sections. Each section contains a side window and an opening on the top side that can be removed. The openings are covered with wooden covers insulated on the underside.

To obtain the required measurements and observations for the experiments a number of modifications were needed.

The first modification was to the testing section. It was desired to be able to film the tests to obtain a visual record of the deformed sample. Thus a window was inserted on the underside of the centre of the testing section. This allowed the camera to film the sample from below. To assist the filming an oven light was installed in the tunnel to add extra light to the underside of the plastic.

The modification required for measurement involved the construction of a stainless steel duct. This duct was located on the top of the wind-tunnel. Five bars were placed along the top of this duct, parallel to the flow. A thermocouple was located on each bar hanging approximately 50 mm below the bar. A cross-section of the measuring duct and the wind-tunnel is shown in Figure 8.

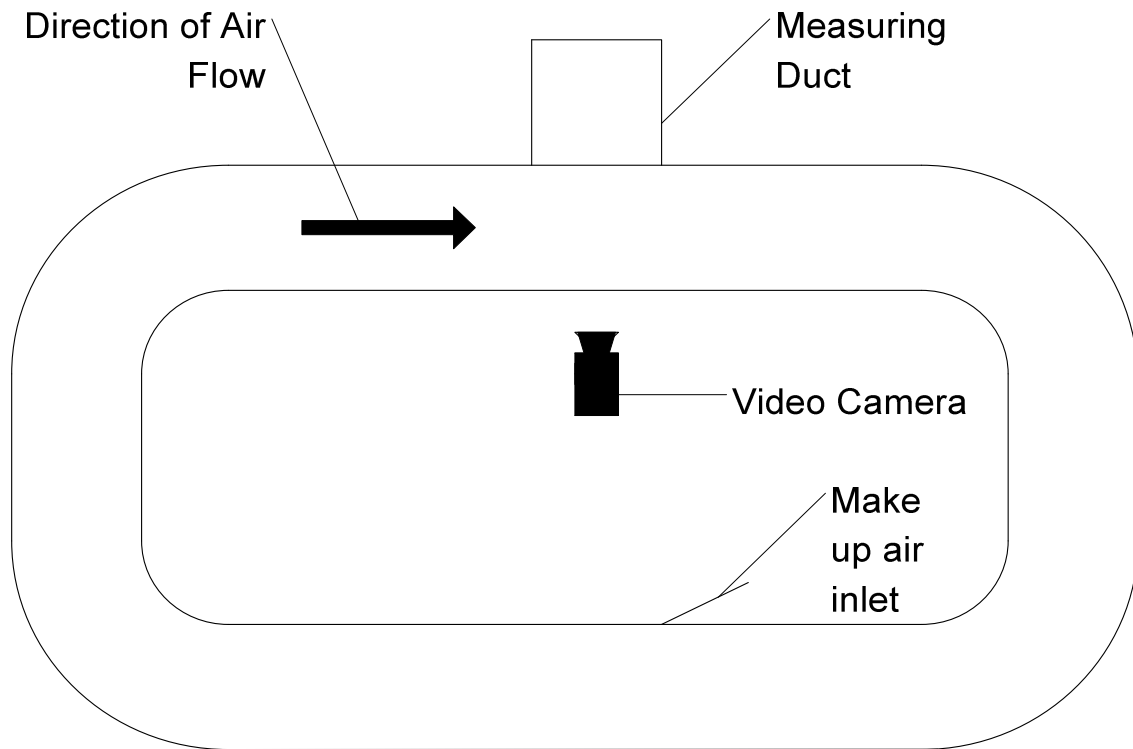


Figure 7: Wind tunnel schematic

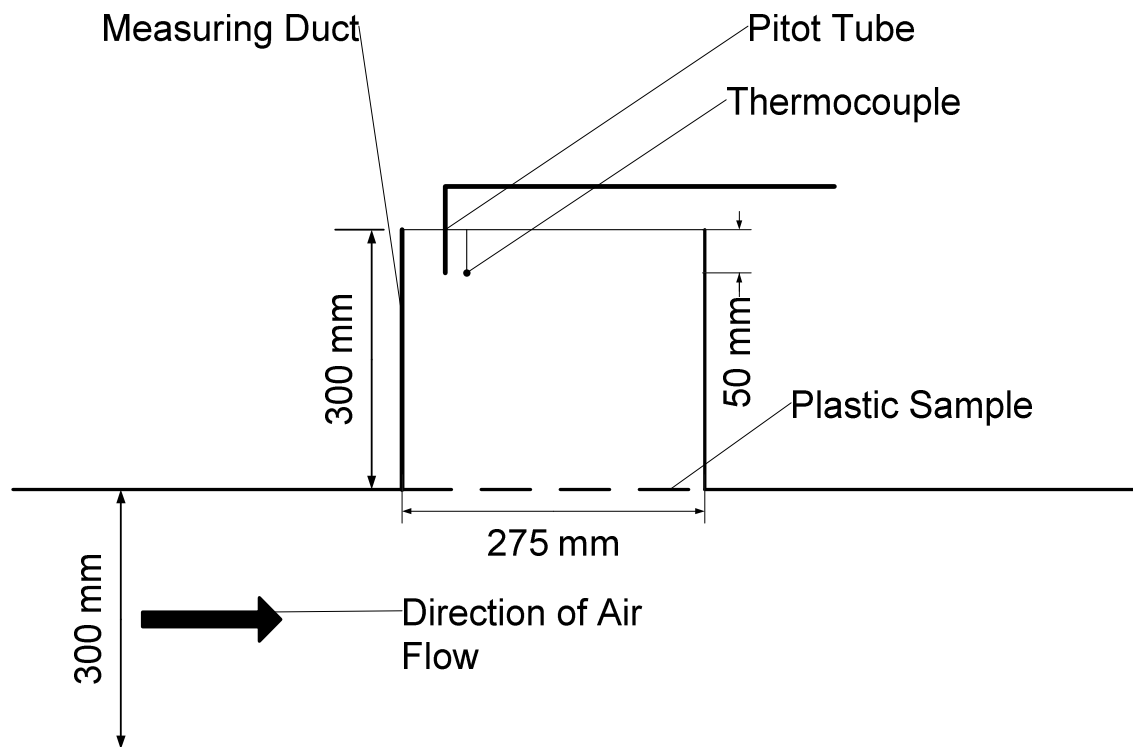


Figure 8: Cross-section of the wind tunnel and measuring duct

The locating of a vent on the top of a wind tunnel results in air leaving the system. Therefore it was necessary to make a provision for make-up air. This was accomplished by including a vent opening on the lower section of the wind-tunnel as pictured in Figure 9. This vent consists of an opening with dimensions of 250 mm long by 100 mm wide.



Figure 9: Hatch to admit inlet air

The heating of the air is accomplished through the use of a 9 kW heating element. The wind tunnel is capable of heating the air to 300°C. The fan is capable of providing an air velocity of up to 2.94 m/s.

Three different measurements were taken during the experiments, pressure difference, temperature and visual observations. The pressure difference was measured using a pitot tube. The pitot tube consists of two tubes. One tube is directed into the flow and one which is parallel to the flow. The tube directed into the flow measures the dynamic pressure and the tube parallel measures the static pressure. The pressure transducer (MKS INSTRUMENTS Inc. MODEL NUMBER2233BD-000.2AAB), Figure 10, measured the difference between the two tubes. The output is measured in volts. The maximum pressure difference is 0.2 Torr and the maximum voltage output is 1 volt. This leads to the following relationship in Equation 2. This pressure difference can then be easily converted into SI units using Equation 3 based on the conversion factors from the SFPE handbook (SFPE 2008).

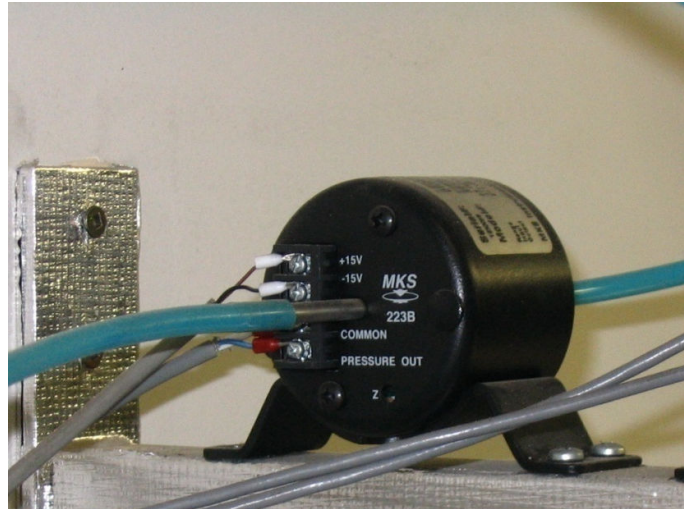


Figure 10: Pressure transducer

$$\Delta P_{Torr} = 0.2V \quad \text{Equation 2}$$

Where

ΔP_{Torr} The pressure difference (Torr)

V The output in volts

$$\Delta P = 133.3\Delta P_{Torr} \quad \text{Equation 3}$$

Where

ΔP_{Torr} The Pressure difference (Torr)

ΔP The Pressure difference in Pa

The measurement of temperature was accomplished by using five k-type thermocouples. The thermocouple measurements are simpler as the output is recorded directly as degrees Celsius ($^{\circ}\text{C}$).

The visual observations were taken with a Canonxm2 digital video camera. The video was recorded onto DVD. Still images were then obtained from the DVD.

3.1.4 Universal Data Logger

The data output was recorded using the Universal Data Logger software. The software stores the data as a comma separated value file. The software allows the user to input a description of the test which is displayed in the file.

The data recorded is dependent on the instruments attached. Each instrument output is assigned a Channel. The experiments created 7 Channels of output. The first Channel recorded the pressure transducer output in volts. Channels 3 to 7 recorded the thermocouple data.

The software records the time at which each measurement is recorded.

The universal data logger allows the user to determine the sampling rate. The sampling rate used for the experiments was 1 sample every second.

3.2 Preliminary Experiments

The preliminary experiments were carried out using the Contherm digital oven located in the Transportation Laboratory at the University of Canterbury. The temperature of the oven was set by a digital control. The oven is able to reach a maximum temperature of 300 °C. This coincides with the maximum temperature performance of the wind-tunnel (Yu 2007). The plastics were tested at 50°C intervals. The size of the interval is due to the range of literature temperatures from 80 to 260°C and the limitations of time and cost. Table 2 below shows the temperatures at which material was tested. Two additional tests were carried out using the PVC at 150°C to investigate the effect of alternates to fully sealing the sample. One sample was sealed along the long edge and one along the short edge. The experiments were conducted to determine the effect of the connection on the behaviour of the melting plastic. As mentioned in section 2.2 the connections consist of screws in rows along the short edge of the plastic sheet. The partial sealing along the short edge replicates the real world connection the best, where screws are used along the short axis of the sheet.

Table 2: Experimental matrix for preliminary experiments

Temperature (°C)	PVC	Polycarbonate	Acrylic	GRP
50	✓			
100	✓		✓	
150	✓	✓	✓	✓
200	✓	✓	✓	✓
250	✓	✓	✓	✓
300		✓		✓

3.2.1 Method

The following describes the procedure used to conduct the preliminary experiments.

The first step involved cutting the material to the dimensions 275 mm by 328 mm. The plastic sample was then placed into the frame and sealed along all edges using ADOS Gasket 260 sealant. The sealant was then left overnight to cure.

The next day the oven temperature was set to the required temperature. The oven was left for 10 minutes after the required temperature was reached to allow the temperature to stabilise. The oven was then opened and the frame containing the sample placed inside the oven.

The sample was observed at intervals. The observation was taken by opening the oven door, looking and photographing the sample. This had to be done rather quickly as opening the door decreased the temperature.

The desired time intervals for the observations were every five minutes for the first half hour, every 10 minutes for the second half hour and every 15 minutes for the last hour. For the samples that started to deform the observation interval reverted to five minutes. This was not always the case as these preliminary tests were something of trial and error and the testing procedure evolved over time.

The length of the experiments differed. The time of most interest was the first half an hour. Prior to Amendment 7 to C/AS1 the only comment on the performance of roof venting came from note 4c to Table 5.1 stating that:

Only roof venting which is specifically designed to open or melt rapidly in the event of fire shall be included in the area A_h .

Cosgrove (1996) indicates that roof collapse is expected to occur after about 20 minutes. Once the roof begins to collapse or has large deflections the behaviour of the plastic skylights is of less consequence as large openings in the roof will vent smoke and heat from the building.

The majority of the experiments were run for one and an half hours. The exception was when the material had become fully disconnected from the frame or when significant deformation had occurred and the plastic was producing noticeable quantities of smoke. A number of the GRP samples were run for two hours in an attempt to deform the sample.

At the end of the experiment the samples were removed from the oven and photographed.

3.3 Wind-tunnel Characterisation

The first experiments carried out using the wind tunnel were a series of experiments designed to characterise the temperature and velocity profiles in the wind-tunnel and the measuring duct. The characterisation tests were carried out in two phases before the main series and after the main series of experiments.

The characterisation tests were conducted to determine the behaviour inside the wind tunnel.

The first test was to create a velocity profile vertically along the duct to determine the most appropriate position in which to conduct further measurements. This was achieved by taking measurements starting 50 mm from the bottom of the duct and then at 25 mm intervals.

The second characterisation tests involved determining the fan settings that should be used to run the main series of tests at to achieve the desired velocity.

This was accomplished by setting the wind tunnel to the required temperature. The fan settings were then varied and the temperature and pressure difference recorded. The fan settings consisted of an arbitrary scale. The fan setting was increased by intervals of 1 or 0.5. Before the experiment was run the predicted voltage output of the pressure transducer was calculated using Equation 5 to get the required pressure difference and then converting this value into a voltage. The interval of the fan speed was reduced when this reading was neared on the computer screen. Unfortunately this method did not work exceedingly well because of the rate at which the individual readings changed. The predicted values were calculated by rearranging Equation 2, Equation 3, Equation 5.

$$\Delta P_{Pa} = \frac{\rho u^2}{2}$$

$$\Delta P_{Torr} = \frac{\Delta P_{Pa}}{1333}$$

$$V = \frac{\Delta P_{Torr}}{0.2}$$

For example for a target velocity of 2.5 m/s at a temperature of 100°C the voltage would be

$$\Delta P_{Pa} = \frac{0.95(2.5)^2}{2}$$

$$\Delta P_{Torr} = \frac{2.97}{133.3}$$

$$V = \frac{0.02}{0.2}$$

$$V = 0.1110 V$$

The targeted pressure transducer reading for each temperature is given in Table 3.

Table 3: Target pressure transducer readings

Temperature (°C)	Velocity (m/s)	Volts (V)
100	2.5	0.1110
150	2.5	0.0978
200	2.5	0.0875
250	2.5	0.0791

3.3.1 Baseline

The efficiency as defined by Equation 1 requires a measurement of the unobstructed flow. The unobstructed flow is a baseline to which the experimental flows are compared. The unobstructed baseline flows were found experimentally by measuring the temperature and pressure difference with a frame without a sample in it. The baseline flow is defined as 100% efficient.

3.4 Main Series

The main series of experiments are the experiments used to determine the efficiency of the vent. A total of 62 experiments were conducted. The experiments conducted are shown below in Table 4, Table 5 and Table 6. In addition two experiments were conducted on the GRP at an exposure temperature of 300°C for an exposure time of 120 minutes.

The lowest exposure temperature for each material was chosen as it was believed that there would be no melting and the vent would be completely blocked. From Equation 1 this would result in an efficiency of 0%. The maximum temperature for the materials that melted was 250°C as this was the highest temperature that the wind tunnel could sustain with the vent open. The GRP could be tested at 300°C as there was no deformation and hence the plastic sealed the vent and prevented the air flowing out.

The times for the PVC, polycarbonate and the acrylic were chosen to be 5, 10 and 20 minutes. This gives a range of times showing the fast effect and the longer term effect.

Table 4: Experimental matrix for polycarbonate

Temperature Time	150	200	250
5 minutes	3	3	3
10 minutes	3	3	3
20 minutes	3	3	3

Table 5: Experimental matrix for PVC

Temperature Time	100	150	200	250
5 minutes	-	3	3	3
10 minutes	-	3	3	-
20 minutes	3	3	3	-

- Not tested

Table 6: Experimental matrix for acrylic

Temperature Time	250
10 minutes	3
20 minutes	3

3.4.1 Experimental Procedure

The first step in the experimental procedure was the preparation of the plastic sample. The sample was cut to dimensions of 328 mm x 275 mm.

GRP: The GRP was cut to the required dimensions. The preparation was simple as the plastic was flat and did not have any directional difference.

Acrylic: The acrylic was cut to the required dimensions by using a band saw. The acrylic was also isotropic.

PVC: The PVC was cut using shears. The sample was cut so that the long edge was perpendicular to the troughs.

Polycarbonate: The polycarbonate was cut using shears. The sample was cut so that the long edge was perpendicular to the troughs.

Both the PVC and the polycarbonate were stiffer parallel to the corrugations than perpendicular.

Different profiles are available, from flat sheets to corrugated and trapezoidal profiles. A profile with troughs slightly increases the surface area available for heat transfer. In small scale experiments the difference is not expected to impact the results.

The next step in the preparation is to seal the sample into the reference frame. This was done by using the same gasket sealant used in the preliminary experiments. The sealant was used along the short edges of the frame only. The results from the preliminary experiments showed that there was different melting behaviour between the partially sealed samples and the fully sealed samples.

The samples and frames are then left overnight so that the sealant strengthened.

The next day the samples were placed on the wind-tunnel and filmed to provide a before reference image.

The samples are then taken to the oven to be exposed to the elevated temperature. The oven is set to the required temperature. When the required temperature is met the oven is left for approximately 10 minutes to stabilise. The samples are then placed in the oven and left for the exposure time, 5, 10 or 20 minutes. At the end of this time the samples are removed from the oven. The samples were removed by taking the tray upon which the frame was sitting from the oven and letting the plastic cool. This was done to reduce the risk of damage to the plastic samples.

The samples were cooled until they could be safely moved to the wind-tunnel. The samples were then videoed for an image of the deformed sample. After the images were gathered the samples were left to cool for a further hour to ensure that the plastic was at ambient.

The wind-tunnel was then set to the required temperature and wind velocity. When the wind-tunnel had reached a constant temperature the sample was placed on the wind tunnel. The data recorder was started.

The data was recorded for 30 seconds before the measurements began. This pause was to allow time for the measuring equipment to settle.

Each of the 25 points was then measured as shown in Figure 11. The measurement started in the downstream corner furthest from the wall. The measurements proceeded upstream along the first bar. The Pitot tube and thermocouple were moved every 30 seconds. In the data analysis only the last 10 seconds of data was used, as the first 10 to 15 seconds were disrupted by moving the measuring apparatus. After the first bar had been completed the Pitot tube was moved to the second bar and the process continued.

Once the sample had been measured the next sample was placed on the wind tunnel and was measured.

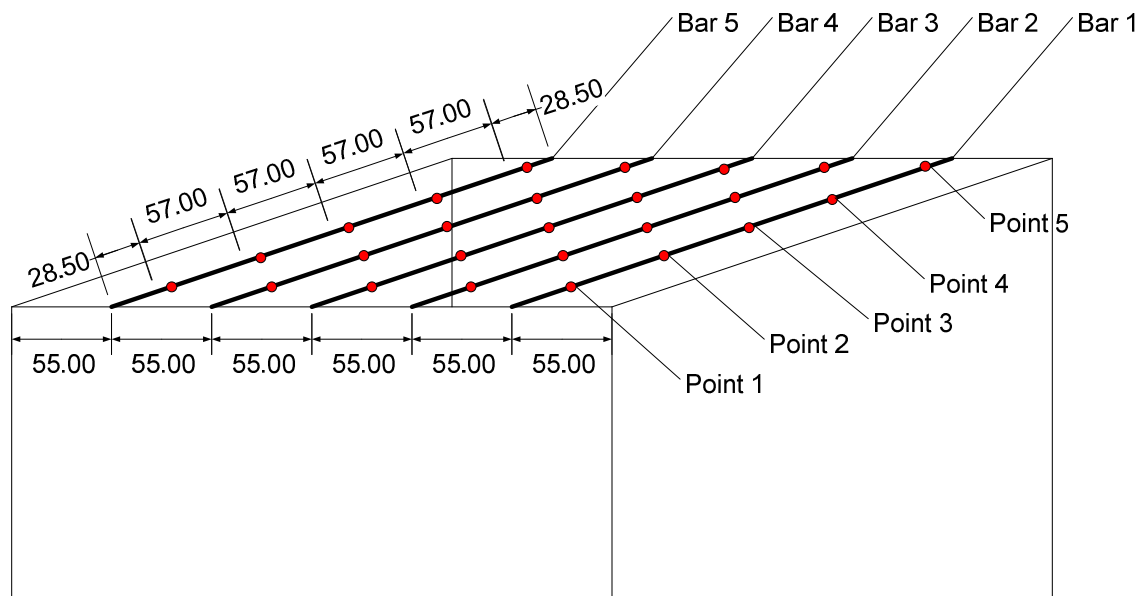


Figure 11: Diagram showing the measuring points, dimensions in mm

3.4.2 Data Analysis

To gain any meaningful results the data need to be processed. This was done using a Microsoft Excel Spreadsheet. The first stage involved copying the data from the comma separated value file (.csv) produced by the Universal Data Logger program. The five bars on which the thermocouples were hung were numbered 1 through 5 in the order that they were

used for example the first bar was number 1 and the second bar number 2 and so forth. This was done to allow the spreadsheet to choose the correct temperature Channel when calculating the density. The mass flow per unit area was calculated using the average density and velocity values.

The first step in the calculation is to find the density of the air using Equation 4 (Emmons & Tanaka 2008).

$$\rho = \frac{352.8}{T} \quad \text{Equation 4}$$

Where

ρ	Density $\left(\frac{kg}{m^3}\right)$
T	Temperature (K)

The density is an important parameter as it is used in the calculation of the velocity and mass flow per unit area. The velocity can be calculated using Equation 5 (Emmons & Tanaka 2008).

$$u = \sqrt{\frac{2\Delta P}{\rho}} \quad \text{Equation 5}$$

Where

u	velocity $\left(\frac{m}{s}\right)$
ΔP	pressure difference (Pa)
ρ	density $\left(\frac{kg}{m^3}\right)$

The mass flow per unit area, Equation 6, can be found by multiplying the density from Equation 4 and the velocity from Equation 5.

$$\dot{m}'' = u\rho \quad \text{Equation 6}$$

Where

\dot{m}''	mass flow per unit area $\left(\frac{kg}{sm^2}\right)$
u	Air Velocity $\left(\frac{m}{s}\right)$
ρ	Air density $\left(\frac{kg}{m^3}\right)$

With the mass flow per unit area known at each point, the overall mass flow is found by integrating in both directions, parallel and perpendicular to the flow. The points have been numbered in the form of (i, j) where i is the bar number and j is the point on the bar. The points are numbered sequentially from downstream to upstream. Figure 12 shows the layout of the measurement points. The dimensions are in units of meters. The flow direction is from the bottom of the page to the top.

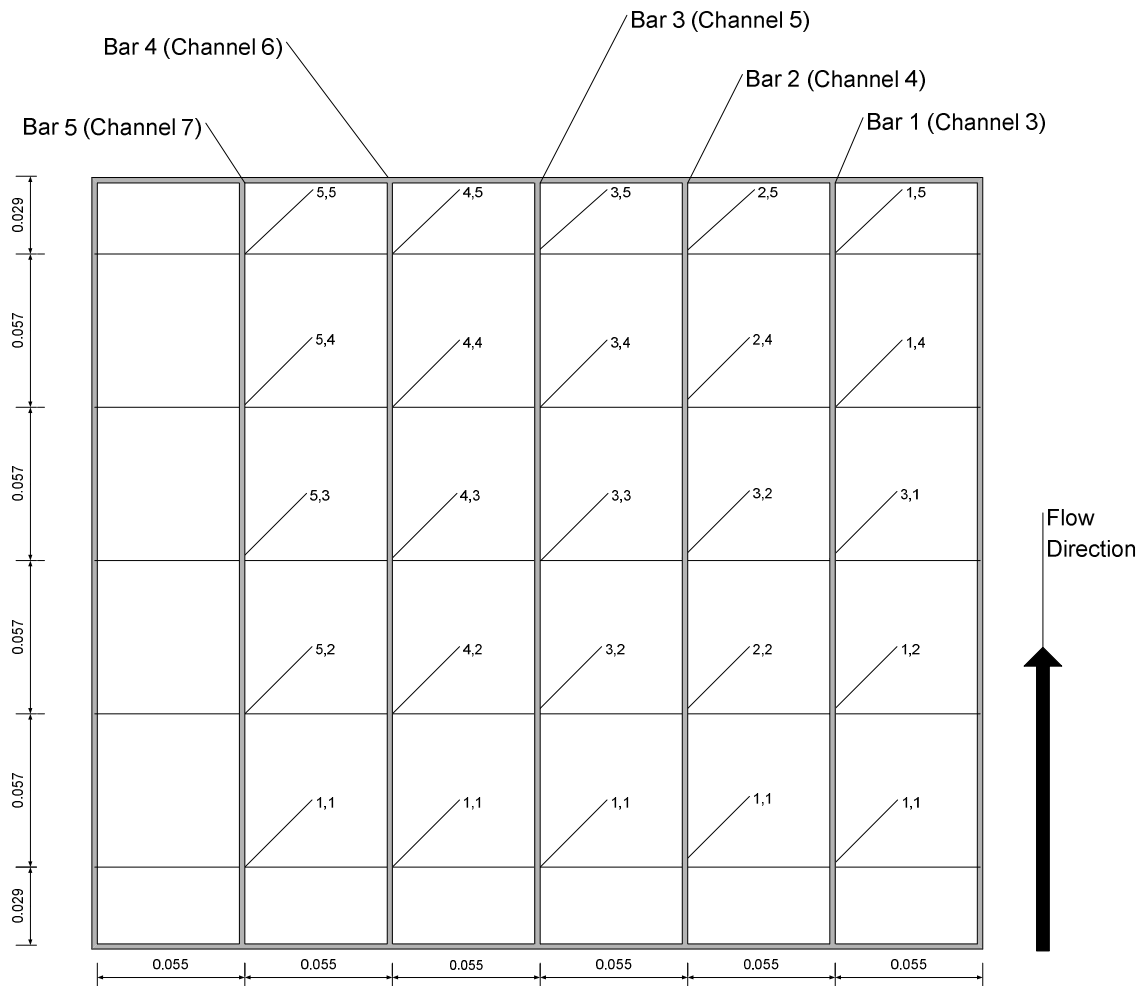


Figure 12: Plan view of measuring points defining the coordinate system

The integration is accomplished using a trapezoidal rule with the end panels being rectangles. This is accomplished in two steps the first step is to integrate in the x direction. This is accomplished using Equation 7. The second step is to integrate the result of Equation 7 along the y direction using Equation 8. The calculation and equations were developed from Excel for Scientists and Engineers (Billo 2007).

$$a_j = \frac{x}{2} z_{1,1} + \sum_{i=2}^5 x \left(\frac{z_{i-1,1} + z_{i,1}}{2} \right) + \frac{x}{2} z_{5,1} \quad \text{Equation 7}$$

$$\dot{m} = ya_1 + ya_5 + \sum_{j=2}^5 y \frac{(a_{j-1} + a_j)}{2} \quad \text{Equation 8}$$

where

\dot{m}	mass flow $\left(\frac{kg}{s}\right)$
y	distance between bars (m)
x	distance between points (m)
a_j	mass flow per unit length along bar j $\left(\frac{kg}{ms}\right)$
$z_{i,j}$	mass flow per unit area at point i, j $\left(\frac{kg}{m^2s}\right)$

Equation 8 is shown graphically for the data in the 200°C baseline. The first integration is already complete. The equation calculates and sums the six areas shown in Figure 13.

With the mass flows known for the baseline cases and the tested samples the percentage of the flow can be calculated by Equation 9.

$$\% = \frac{\dot{m}_{sample}}{\dot{m}_{baseline}} \times \frac{100}{1} \quad \text{Equation 9}$$

The three results are then averaged as shown by Equation 10 (Johnson & Miller 2005).

$$\bar{m} = \sum_{i=1}^n \frac{\dot{m}_i}{n} \quad \text{Equation 10}$$

The standard deviation is calculated using Equation 11 (Johnson & Miller 2005).

$$\sigma = \sqrt{\frac{\sum_{i=1}^n (\dot{m}_i - \bar{m})^2}{n - 1}} \quad \text{Equation 11}$$

The results are then plotted in the form of a histogram. The bars show the average percent of the baseline flow through the vent. The standard deviation is shown as error bars.

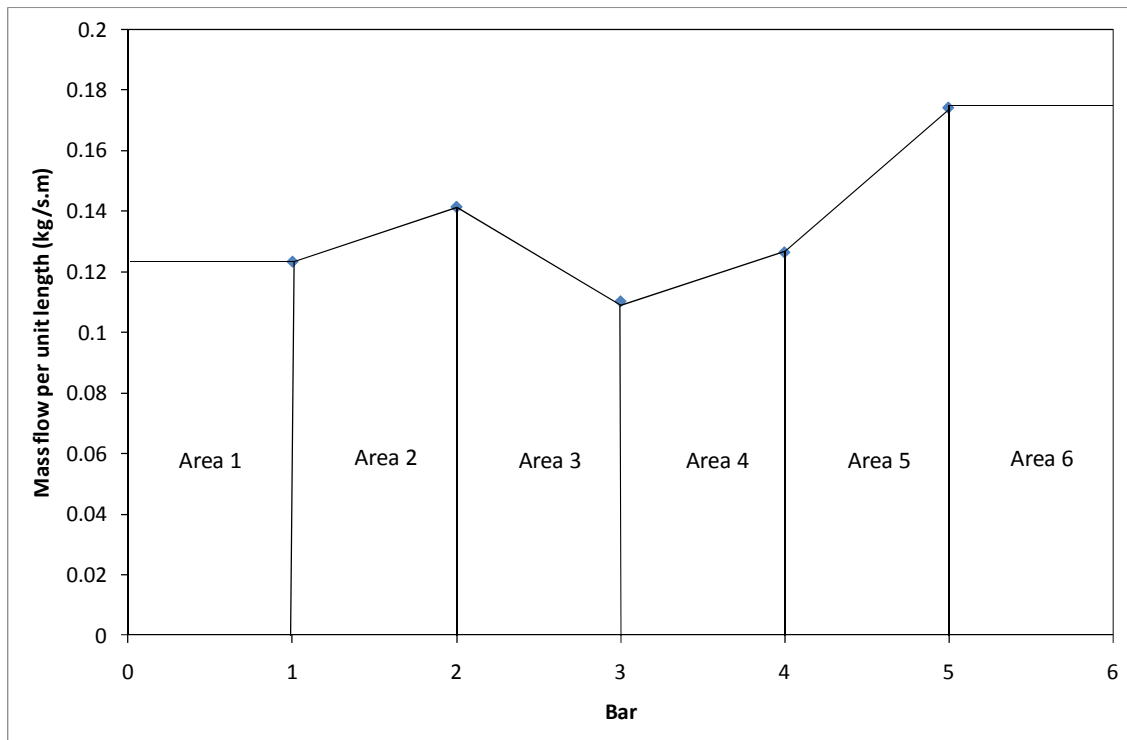


Figure 13: Graphical representation of the integration

The area shown in Figure 13 is the result of Equation 7 and represents the mass flow per unit length between the bars. Area 1 is the mass flow per unit length between the edge and bar 1.

Chapter 4 **Experimental Results**

This chapter presents the results of the experiments. Example results are given to demonstrate the analysis and explain the results. The results for the polycarbonate experiments are given in Appendix B, the results for the PVC experiments in Appendix C, the acrylic experiments in Appendix D and the GRP experiments in Appendix E. The first results presented are the qualitative results for the preliminary test. The next results are the results of the characterisation of the wind-tunnel. The final results are those for the efficiency of the plastic skylights.

4.1 Preliminary Results

The results for the preliminary tests are observations taken during the experiment. The results were based on visual observations taken at the time and reviewing the photographs taken during the experiments.

4.1.1 Polyvinyl Chloride

The PVC was exposed to the following temperatures 50°C, 100°C, 150°C, 200°C, 250°C. The results varied from no visible change at 50°C to major and rapid changes at 250°C.

The test at 50°C was run for 130 minutes and as mentioned above there was no visible change to the plastic itself or the geometry of the sample.

The test at 100°C lasted for 120 minutes. After five minutes exposure the plastic was noted as being soft but there was no change to the geometry. After 60 minutes exposure the plastic appeared to have a bluer colour and possible a cloudy appearance. When the sample was removed after 120 minutes a small hole was seen on one side. The hole was about 6 mm wide. Figure 14 shows a view looking down on the hole.

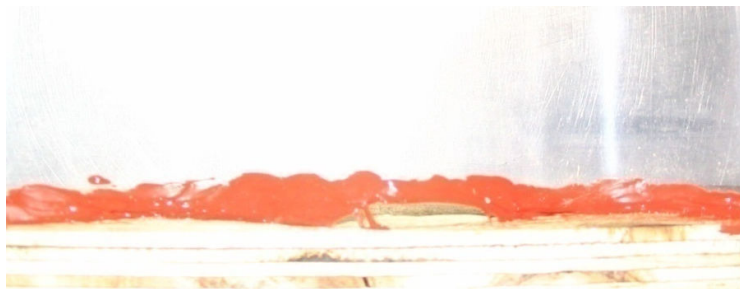


Figure 14: Small hole found after 120 minutes at 100°C

The test at 150°C was run for 60 minutes. The sample again was noted as being soft after five minutes. After 45 minutes the plastic had lost its rigidity and had slumped on to the oven rack. After 50 minutes the plastic had pulled away from one corner as seen in Figure 15. The loss of shape is also visible by the smooth plastic.



Figure 15: PVC after 50 minutes exposure at 150°C

The test at 200°C lasted 45 minutes. As expected the change proceeded faster than the previous tests. After five minutes the plastic had collapsed towards the oven rack. After 10 minutes it was noted that the plastic was pulling away from one side of the frame as shown by Figure 16. After a further five minutes the whole edge had become detached. The opposite edge began to pull away from the frame after 25 minutes. The plastic continued to shrink along the opposite sides as can be seen in Figure 17.



Figure 16: The PVC shrinking from the first side after 10 minutes exposure to 200°C

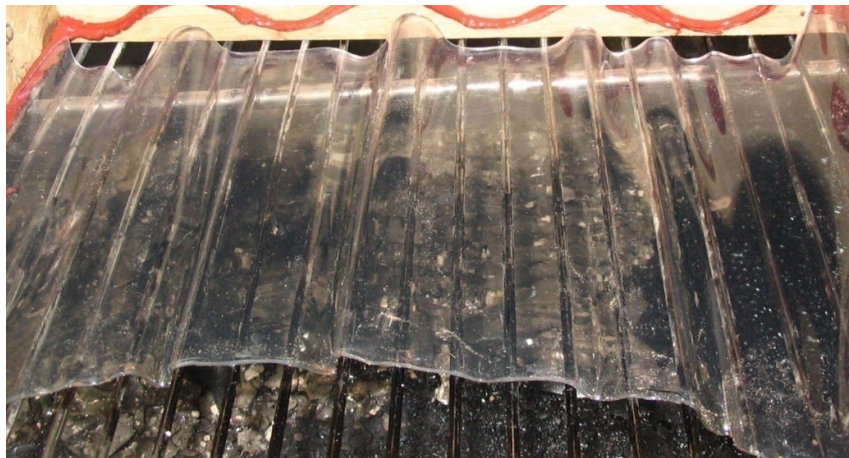


Figure 17: PVC, two sides shrinking after 30 minutes exposure at 200°C

The test at 250°C lasted for 15 minutes. The plastic collapsed onto the oven rack after 5 minutes. After 10 minutes it was noticed that the plastic was going yellow in colour. The test was stopped after 15 minutes due to the plastic starting to smoke. The plastic had deteriorated, with a black brown residue left as shown in Figure 18.



Figure 18: PVC at the end of the 250°C experiment

4.1.2 Polycarbonate

The first polycarbonate experiment was conducted at a temperature of 150°C. The test was run for a total of 120 minutes. During that time no change to the plastic sample was observed. Some damage occurred to the sample when it was being removed from the oven.

The experiment at 200°C was run for 65 minutes. After five minutes the plastic appeared cloudy and to have softened. The plastic started deforming after 10 minutes exposure as seen in Figure 19. This was observed for a further 10 minutes after which no further deformation was seen.

The 250°C experiment lasted 25 minutes. At the five minute observation mark the polycarbonate was slumped down and touching the oven rack. After 10 minutes exposure the sample was cloudy. Small bubbles began to form after 15 minutes as displayed in Figure 20. After 20 minutes some holes were observed in the plastic.

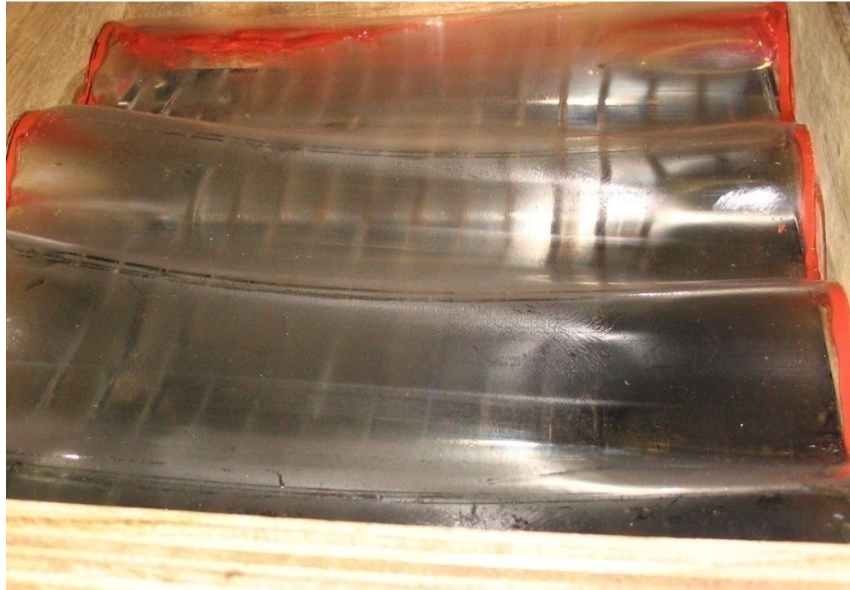


Figure 19: The polycarbonate after 10 minutes exposure to 200°C.



Figure 20: The slumped polycarbonate after 15 minutes exposure at 250°C

A test was conducted at 300°C this test lasted 25 minutes. The plastic had slumped and was going cloudy after five minutes. After 10 minutes it was noticed that the plastic was melting from the sides of the frame after 15 minutes the sample was completely detached from the

frame and after 20 minutes beginning to display fluid like behaviour dripping from the rack. The effect can be seen in Figure 21.

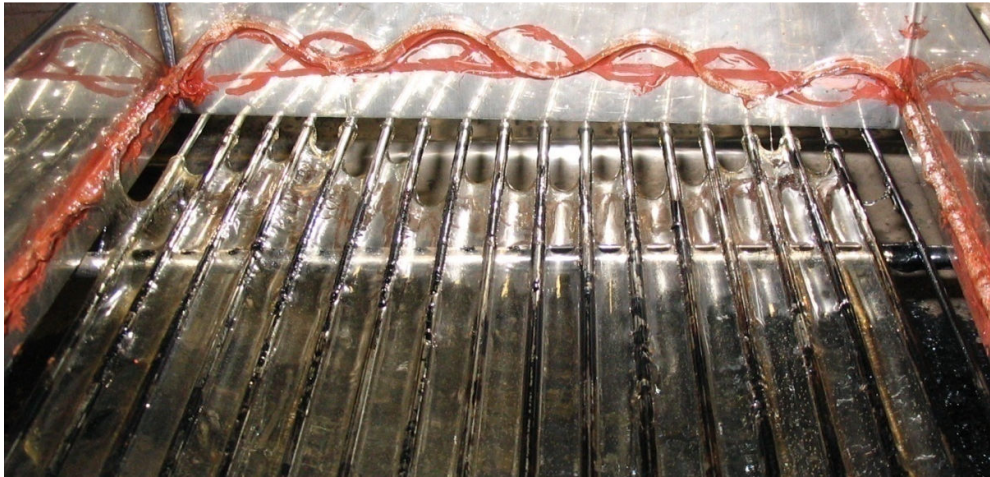


Figure 21: The polycarbonate after being exposed to 300°C

4.1.3 Acrylic

The first experiment on the acrylic material occurred at 100°C and lasted 90 minutes. During the test no changes were noted to the material.

The second test occurred at 150°C and lasted for 90 minutes. There was no visible change to the material however after 25 minutes the material was soft to touch.

The third test at 200°C lasted 80 minutes. The first change was noticed after 10 minutes when the material began to sag in the middle. No further change was noticed until 50 minutes when bubbles were seen on the plastic. Over the next 30 minutes the number of bubbles spread across the surface of the plastic as seen in Figure 22. The material became fully detached from the frame and had dropped out after 80 minutes at which time the test ended.



Figure 22: The large bubbles formed during the acrylic test at 200°C

The final test occurred at 250°C and lasted 25 minutes. The material was soft and slumping after 5 minutes. After 15 minutes the plastic was beginning to deteriorate with small white bubbles as seen in Figure 23 forming in the plastic. After 25 minutes the plastic had dropped out of the frame and the test ended.



Figure 23: Deterioration of the acrylic at 250°C

4.1.4 Glass-fibre reinforced polyester (GRP)

The first GRP test occurred at 150°C and lasted 120 minutes. The first change was noticed at 45 minutes with the plastic starting to appear yellow. No further changes were noted.

The second of the GRP tests occurred at 200°C. The results were similar to those noted at 150°C but with the yellow colouring beginning after 10 minutes of exposure. The sample ended with a deeper yellow colour than the previous sample.

The third test had an exposure temperature of 250°C and lasted for 90 minutes. The sample was yellow after five minutes and there was a plastic smell. After 10 minutes the top surface had bubbles forming. After 50 minutes the plastic was a dark yellow with bubbles covering the top surface as seen in Figure 24. Smaller bubbles appeared to be forming inside the larger bubbles on the top surface.



Figure 24: GRP, bubbles formed during the test at 250°C

The final experiment was conducted at 300°C and lasted for 90 minutes. The material again turned yellow. However there were no large bubbles as seen in the previous experiment. The material turned a dark orange brown colour but remained intact. Figure 25 shows the colour that the GRP has turned and the lack of holes or movement.



Figure 25: GRP, dark brown colour at the end of the 300°C test

The GRP in contrast to the three other plastics did not soften or lose strength throughout the experimental domain.

4.1.5 Alternative Sealing

The previous samples were connected to the frame by sealing around all sides. However it was wished to investigate what would happen if the sealing was conducted only along two opposite edges. Therefore, two further tests were carried out. The tests were conducted at 150°C with the sample material being PVC.

The sample sealed along the straight edge slumped down onto the oven rack after five minutes. The sample lost all its shape becoming nearly flat. The plastic shrunk parallel to the sealed edges.

The sample sealed along the oscillating edges did not slump onto the oven rack. The sample did shrink though this time perpendicular to the sealed edge and thus in the same direction as before.

The connection therefore makes a difference in the behaviour of the material. The case where the plastic was sealed around the entire perimeter took 50 minutes for the sample to pull away from the side. In the two sealed side experiments both showed signs of shrinking after five minutes.

The decision then on how to connect the samples to the frame is important. The connections in practice involve screws or nails being inserted along the short axis of the sheet. This connection method would correspond to the oscillating edge being connected to the frame. The long axis is laid over the metal roofing but not directly connected.

To mimic the real construction of the skylights the samples were only to be sealed along the oscillating edge for the PVC and polycarbonate; this corresponds to the short edge. The GRP and the acrylic will be similarly sealed along the short edge.

The sealed edge is parallel to the flow in the wind tunnel. The flow of hot gases in a ceiling jet along a flat roof is radial and the connection could be at any angle. Buildings are mostly rectangular as shown in Figure 26. The solid lines show the location of the screw or nail connections on the plastic panels. The general direction of the hot gases in such a building would be parallel to the connection.

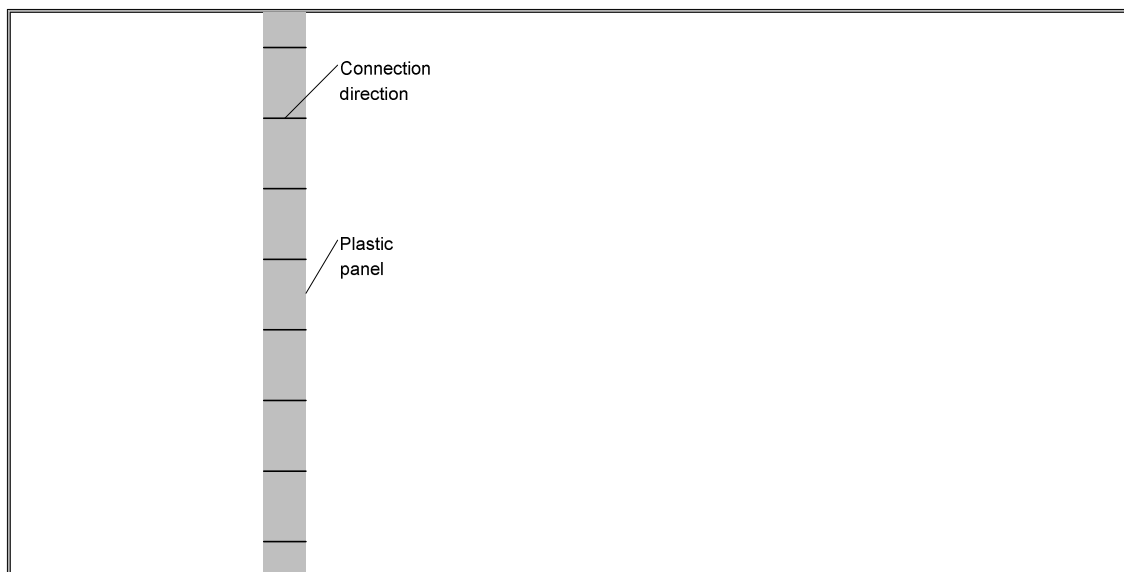


Figure 26: Building showing direction of primary connection

4.2 Characterisation Results

The results of the characterisation test are displayed in three parts; wind-tunnel profile, baseline measurements; angled obstruction.

The wind-tunnel profile results describe the velocity and temperature inside the closed wind-tunnel. The purpose of these tests was to determine the fan settings required to produce the desired velocity.

The baseline measurements were conducted to provide a mass flow through the open vent. The baseline was considered the 100% case.

4.2.1 Wind Tunnel Profiles

The intention was to test the samples at a wind velocity of 2.5 m/s. The value of 2.5 m/s falls within the range of ceiling jet velocities in the early stage of a fire as discussed in section 2.4. The fan setting is an arbitrary scale and has no units. Thus it was not possible to set the velocity with the same simplicity as setting the temperature. A number of experiments were conducted to determine the wind velocity at each temperature. The wind tunnel performance was measured for each temperature. The velocity was recorded. The first part was taking a velocity profile across the depth of the wind tunnel in the centre of the flow.

The velocity profile at 100°C and a fan speed setting of 20 is shown below as Figure 27. The profile shows that the velocity varies by approximately 0.4 m/s from 0.9 m/s to 1.3 m/s. The velocity for determining the settings was recorded 100 mm from the top of the tunnel.

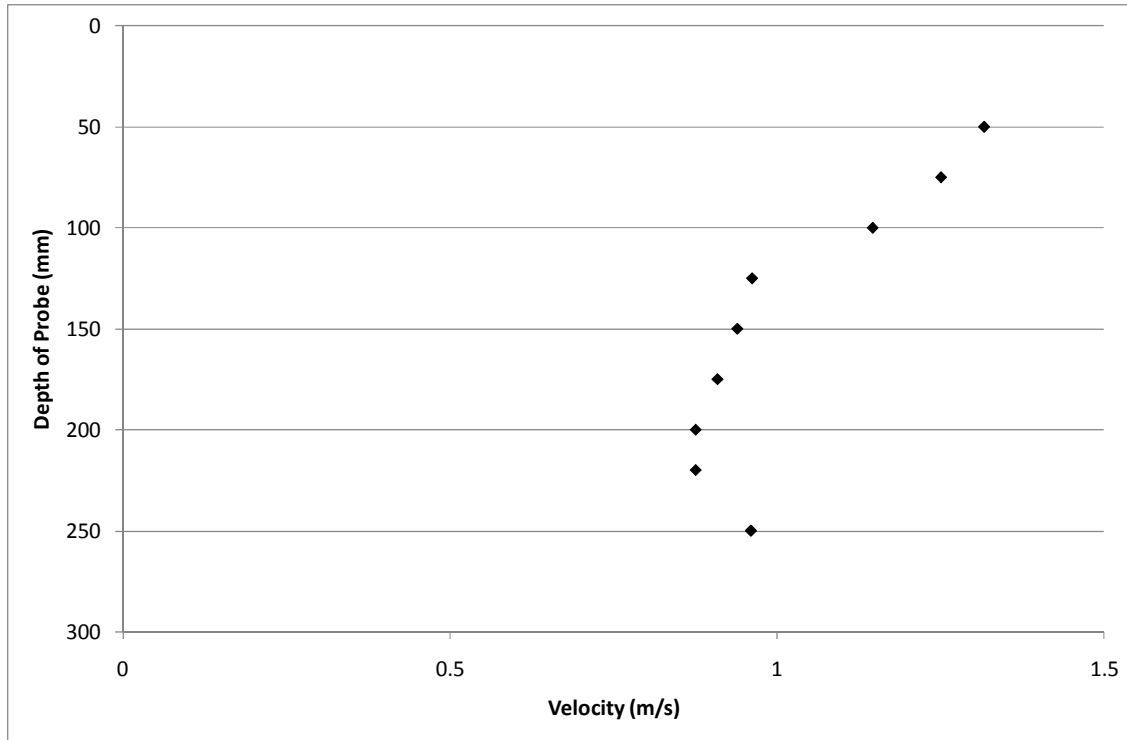


Figure 27: Centre-line velocity profile at 100°C

4.2.2 Fan Settings

The velocities measured in the wind tunnel were less than the planned velocity of 2.5 m/s. Table 7 details the velocity and fan setting used at each temperature. There is a general trend of the velocity decreasing with an increasing temperature as would be expected.

Table 7: Wind tunnel settings and velocity

Temperature (°C)	Fan setting	Velocity (m/s)	Standard deviation
50	37	2.013	0.135
100	39	2.170	0.156
150	37	1.888	0.170
200	39	1.792	0.164
250	37	1.454	0.378

The velocity values are somewhat more variable than would have been desired. The difficulty in selecting an appropriate fan setting is highlighted by the 250°C case where the average velocity increases and then decreases with an increase in the fan setting. This is shown in Figure 28. By adding error bars showing the standard deviation it becomes clear that there is

little causal relationship between the fan setting and velocity at this temperature and in this range of settings.

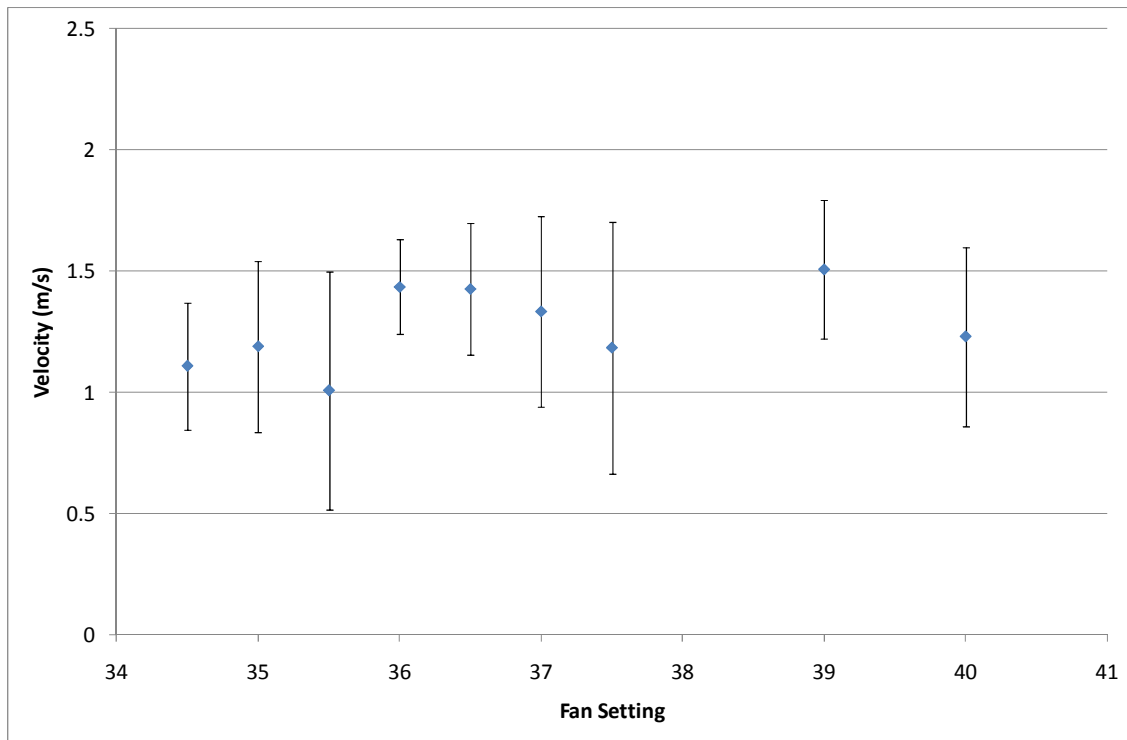


Figure 28: Average velocities at different fan settings

Figure 29 shows the average velocity at the different fan settings but when the fan is run at a temperature of 100°C. There is an increase in the average velocity with the increase in the fan setting. The error bars showing the standard deviation are smaller indicating that the data is more closely grouped. The error bars also overlap less.

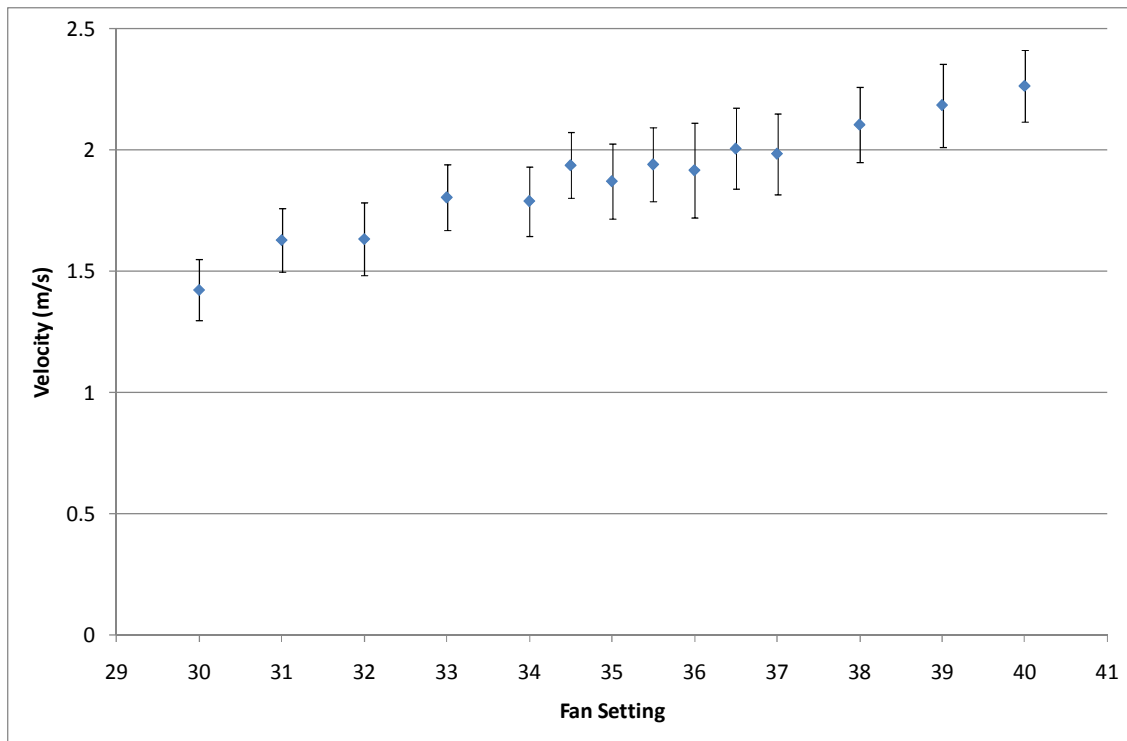


Figure 29: Velocity at different fan settings and temperature at 100°C

4.2.3 Baseline Measurements

The baseline is the basis for determining the efficiency of the subsequent vents. The baseline was measured as by using the empty frame. This baseline is defined as 100% efficient. The full results are shown in Appendix A. The results for the 150°C baseline are shown. The raw results are in volts and degrees celsius and are given in Figure 30 and Figure 31 respectively.

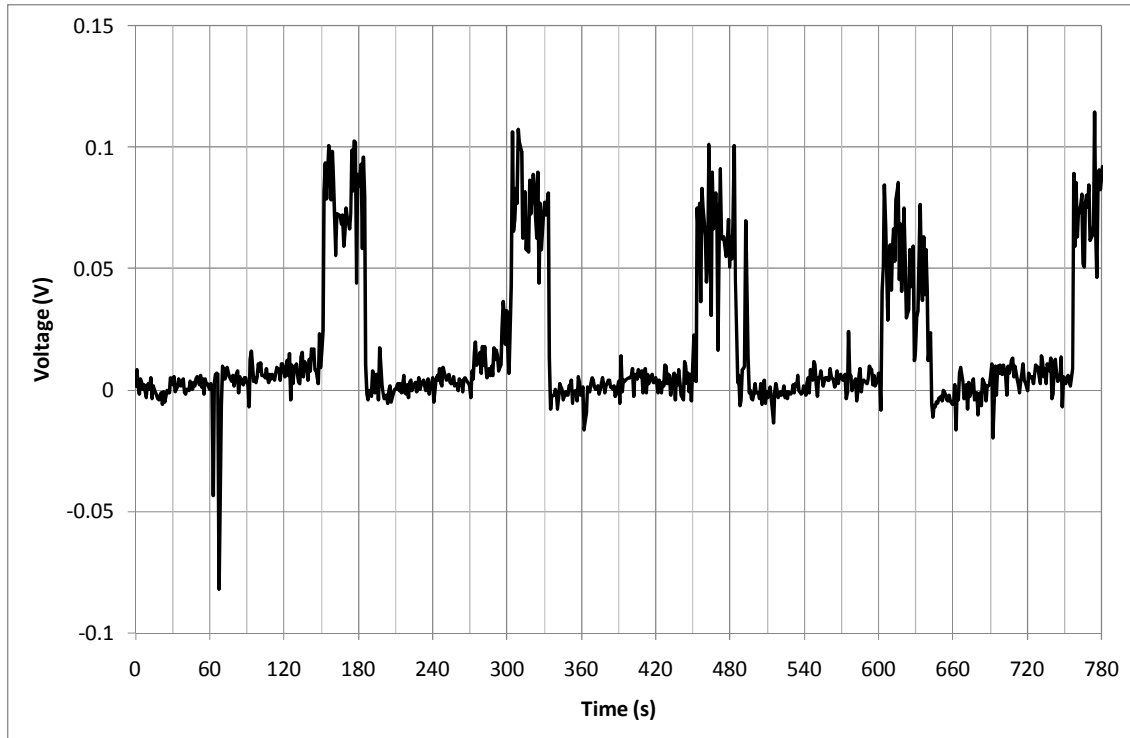


Figure 30: Raw data output from the pressure transducer for the 150°C baseline

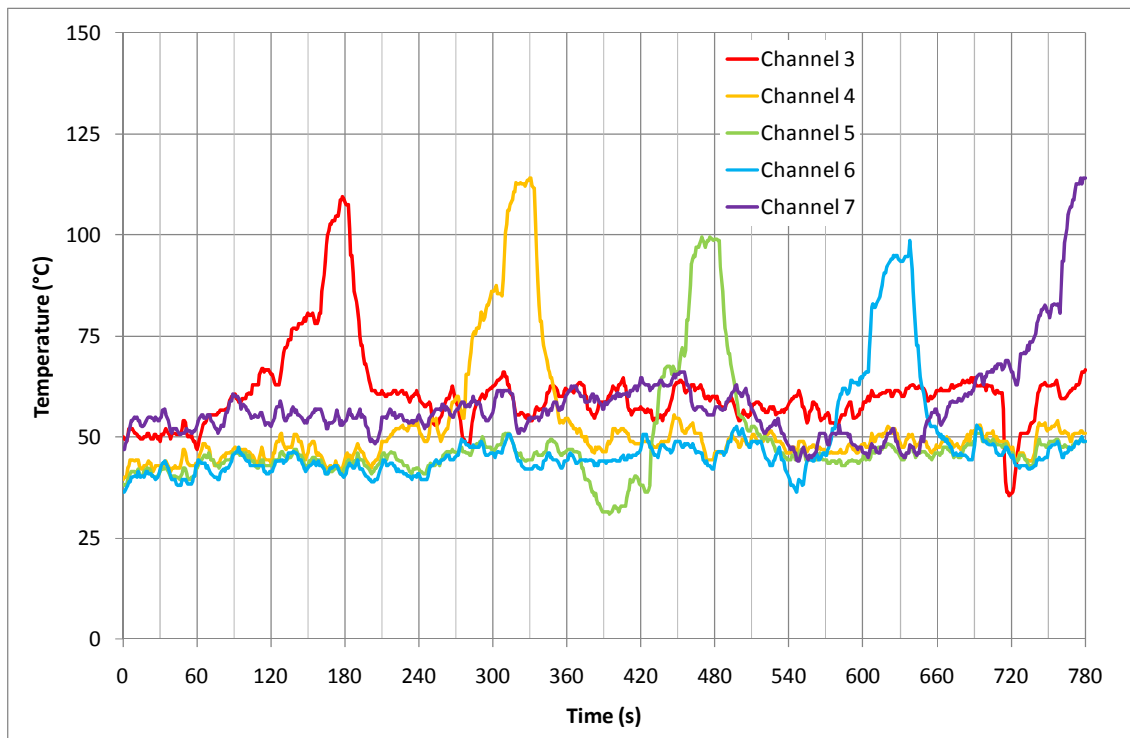


Figure 31: Raw thermocouple readings for the 150°C baseline

The required quantities are density and velocity. The thermocouple data can be used to calculate the density using Equation 4. By selecting the relevant temperature Channel the density as a time series can be shown as Figure 32. The point data shows the density based upon a 10 point average of the temperature.

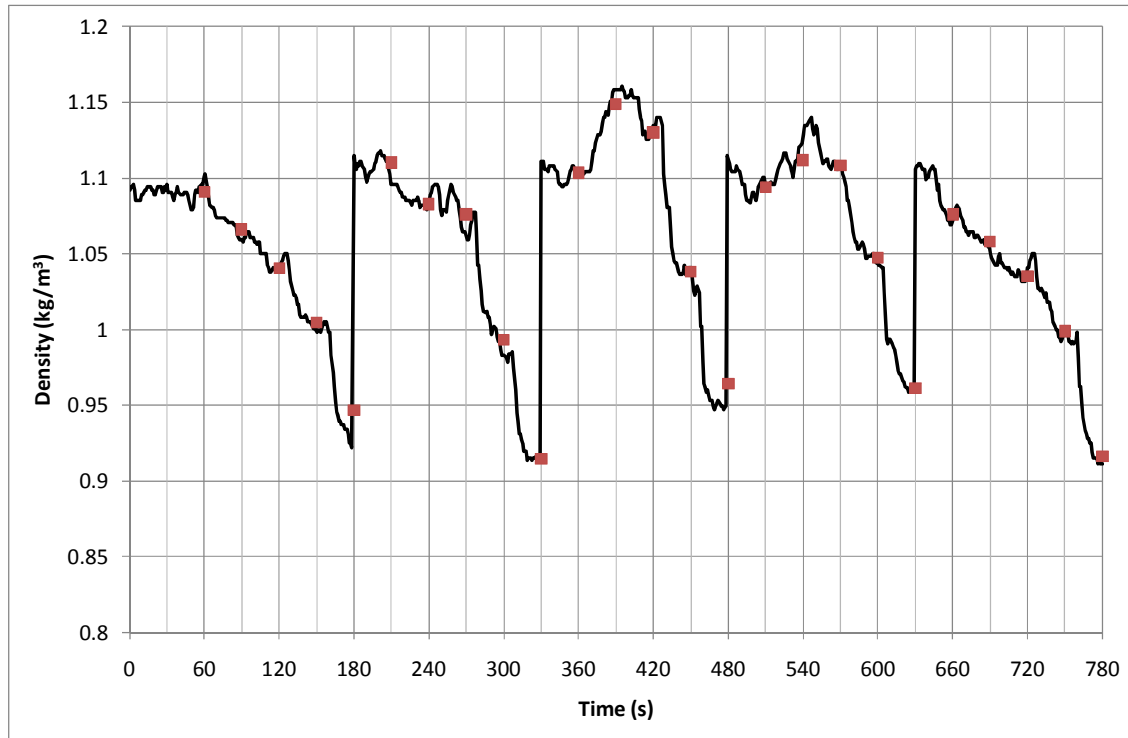


Figure 32: Density time series

Similarly Figure 33 shows the calculated velocity as a time series and an averaged velocity as point data. The average velocity was calculated using the average density, the points shown in Figure 32 and a 10 point average of the pressure transducer output. The need to use average values is best seen by looking at the velocity. The potential error would be great if a single point was used as the data is noisy.

The next step in the analysis is the calculation of the mass flow per unit area. This is accomplished by multiplying the velocity and the density. Figure 34 again shows the time series data and the average data.

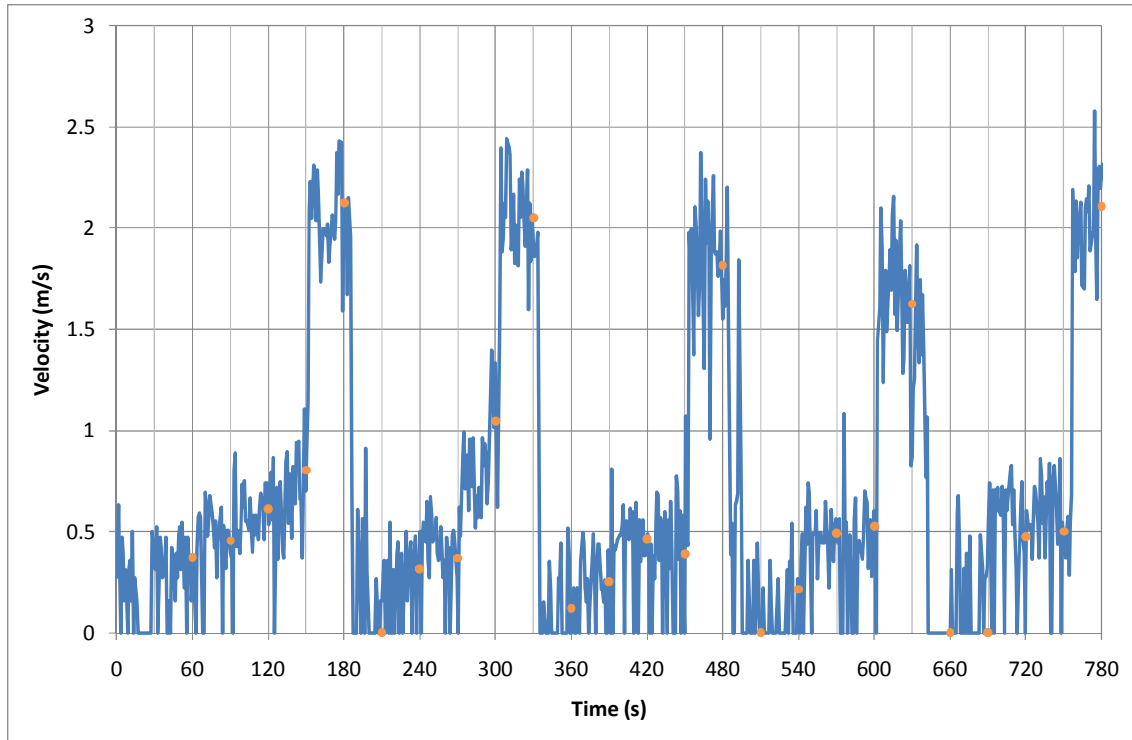


Figure 33: Velocity time series

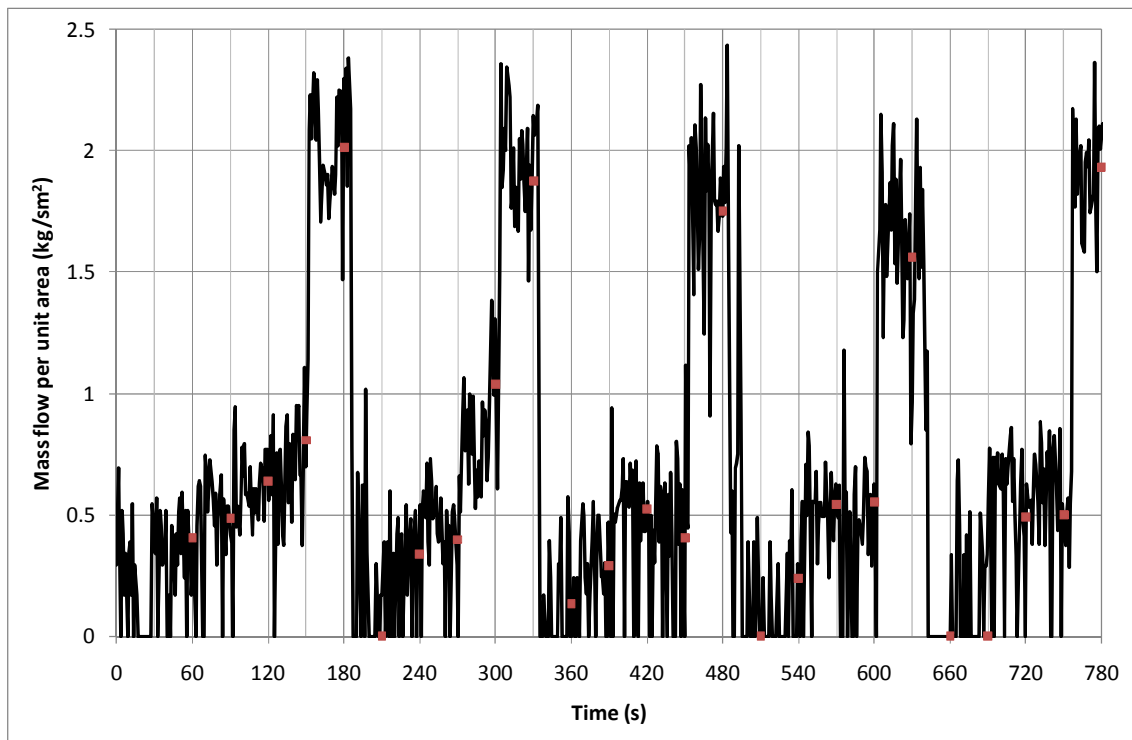


Figure 34: Time series of mass flow per unit area

The final set in the process is to integrate the data across the area. Table 8 gives a summary of the mass flows for the baseline experiments. There is a trend of decreasing mass flow with increasing temperature. The increasing temperature increases the buoyancy and would be expected to give an increase in the mass flow; however the increased temperature reduces the density of the air. Therefore less mass is travelling past the vent.

Table 8: Summary of the mass flows for the baseline experiments

Temperature (°C)	Mass flow (kg/s)
100	0.073
150	0.064
200	0.045
250	0.038

4.3 Glass-fibre Reinforced Polyester

The behaviour of the GRP was as expected from the initial oven tests. Due to the resistance to deformation under heat the material was exposed to a temperature of 300°C for 120 minutes (two hours). During this time the material developed a deep brown colour but retained the initial shape.

Two samples were then tested in the wind tunnel. Small flows were measured though these could not have been through the sample. Due to the high temperature it was not possible to create a baseline flow as the heating element could not maintain a temperature of 300°C with the vent open. As such the mass flows can only be presented as an absolute number.

Table 9: GRP Results

Temperature (°C)	Time (minutes)	Test	Mass Flow (kg/s)	Average (kg/s)	Standard Deviation
300	120	Test 1	0.001	0.001	0.000
		Test 2	0.001		

The velocity record for test 2 is shown below. The velocity reading is often 0 m/s though there are areas of higher flow such as the first 60 seconds of the record due to the movement of the probe between measurement points.

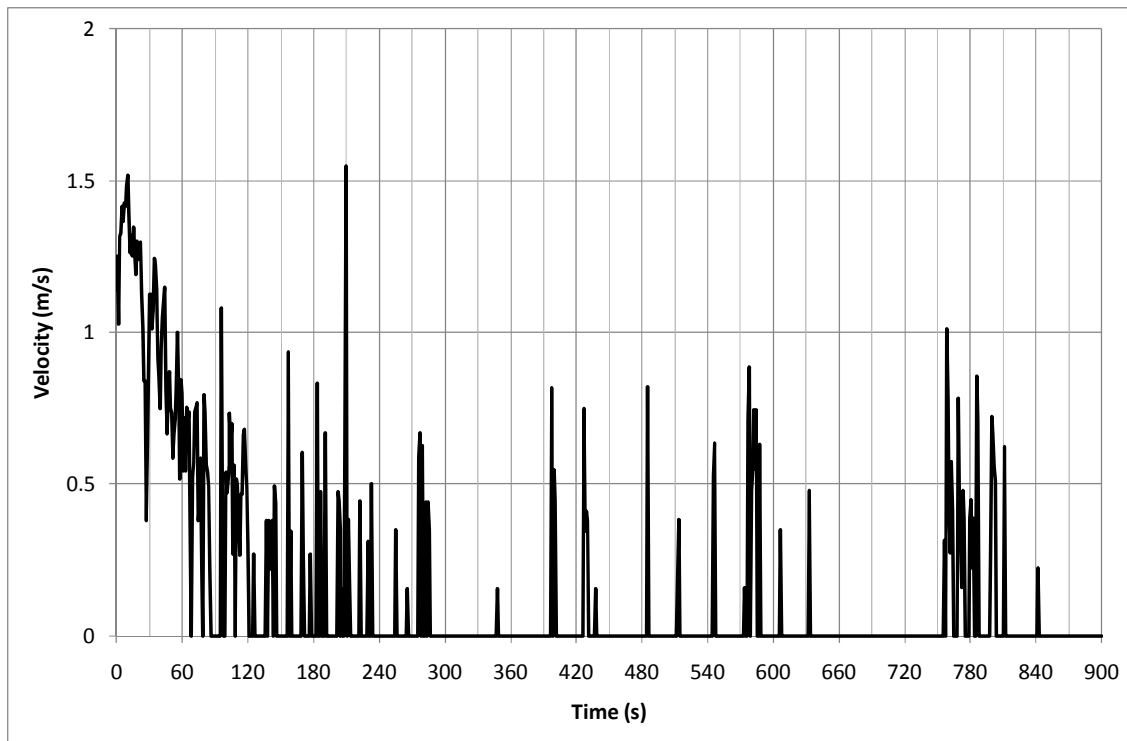


Figure 35: Velocity record, GRP, 120 minutes exposure to 300°C

The temperature record, Figure 36 is as expected for tests where little or no flow is recorded. The temperature sits around 50°C. Channel 4 and Channel 5 show a definite decrease in temperature as the thermocouple moves away from the side of the measuring duct and increase again as the thermocouple passes the half way point. The temperature of Channel 1 also shows some of this decreasing behaviour.

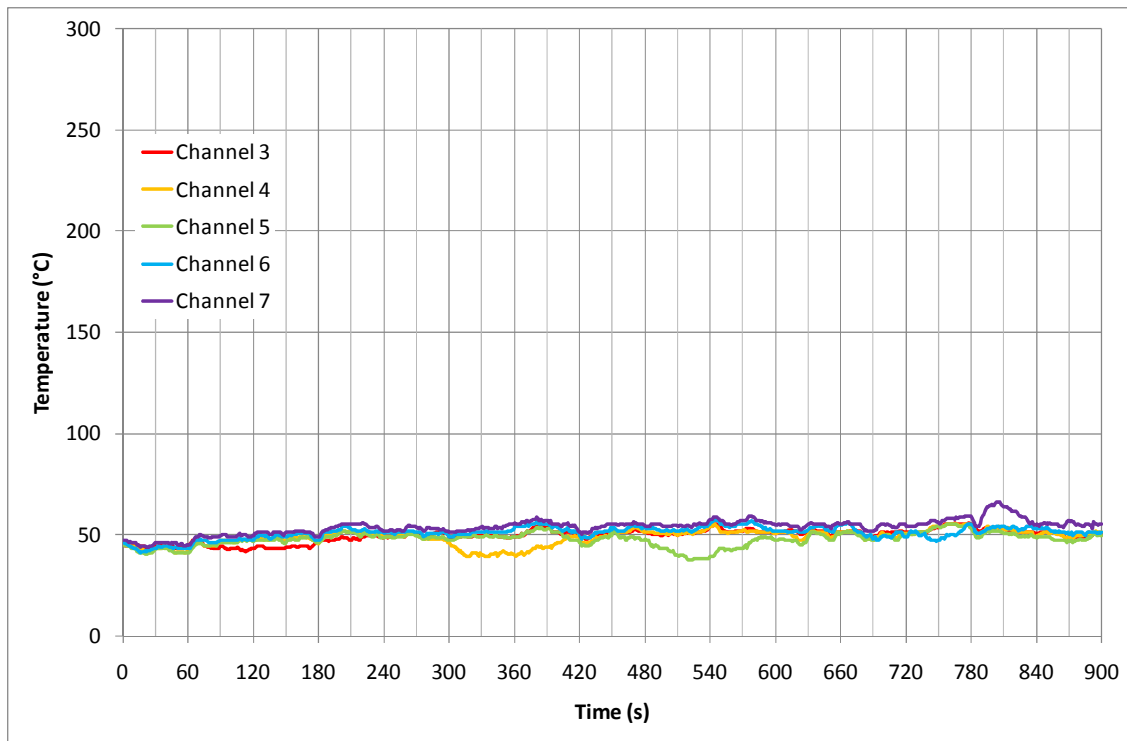


Figure 36: Temperature record, GRP, 120 minutes exposure to 300°C

4.4 Polycarbonate

A total of 27 experiments were carried out on the polycarbonate. The experiments consisted of three exposure temperatures, 150°C, 200°C and 250°C. For each exposure temperature three exposure times of 5 minutes, 10 minutes and 20 minutes were used. For every time and temperature combination three repeats were conducted.

The exposure to the 150°C temperature did not produce large deformations in the plastic. The samples after five minutes exposure did not appear damaged at all, while small amounts of shrinking perpendicular to the long axis were seen. Similarly after 20 minutes exposure small amounts of shrinking were seen and discolouration of the plastic but not changes in the shape.

The plastic exposed to 200°C experienced shrinking and loss of shape.

The plastic experienced large deformation at an exposure temperature of 250°C. After five minutes exposure the plastic had dropped down and was resting upon the oven rack with some of the long edges shrinking parallel to the flow short axis. The contact between the oven rack and the plastic is not of great concern. As discussed in section 2.2 the construction of the roof includes installing a safety mesh. The oven rack and the mesh will both limit the vertical displacement of the plastic. The measurement time for these samples was reduced to

20 seconds per point due to the difficulties encountered earlier after the 20 minute exposure. After 10 minutes exposure the samples were also showing signs of deformation and some signs of liquid melting. Some tendrils were hanging from the long edges indicating dripping behaviour. The first two experiments were completed but with some minor movement of the plastic sample during the measurement and the plastic sample collapsing within a minute of the measuring finishing. The third test was conducted unsuccessfully with collapse of the plastic and the temperature of the wind tunnel being significantly reduced after three minutes of measurement. As a complete set of data was not obtained for this sample the result has been excluded from the analysis.

Similar behaviour was seen during the test after 20 minutes exposure but with greater deformation to begin with. The first and third tests were completed successfully. The second test showed large deformation and though the measuring could continue a significant decrease in the wind tunnel temperature was noted. The temperature after 8 minutes was only 220°C instead of the 250°C before the partial collapse. On analysis of the results it was decided that the second experiment would be excluded as the test had become dynamic during the measuring process in contrast to the other samples.

The collapse of the above samples is believed to have been caused by the heating of the plastic by the wind tunnel and a subsequent loss of strength.

The mass flows and percentages are shown in Table 10. The table also shows the percentage of the unimpeded flow and the average percentage.

The results are shown in graphical form in Figure 37. The error bars show ± 1 standard deviation.

Table 10: Polycarbonate Results

Temperature (°C)	Time (Minutes)	Experiment	Mass Flow (kg/s)	Efficiency (%)	Average Efficiency	Standard deviation
150	5	1	0.022	34.3	15.3	16.5
		2	0.005	7.1		
		3	0.003	4.3		
	10	1	0.0067	10.4	9.3	8.7
		2	0.0111	17.4		
		3	0.000	0.0		
	20	1	0.021	32.6	19.9	14.3
		2	0.015	22.6		
		3	0.003	4.4		
200	5	1	0.010	21.5	25.2	3.6
		2	0.013	28.8		
		3	0.012	25.3		
	10	1	0.032	70.5	38.2	35.6
		2	0.020	44.0		
		3	0.000	0.0		
	20	1	0.029	64.3	56.7	7.2
		2	0.025	55.8		
		3	0.023	50.0		
250	5	1	0.010	27.5	38.6	14.6
		2	0.013	33.2		
		3	0.021	35.2		
	10	1	0.026	69.7	55.4	20.2
		2	-	-		
		3	0.015	41.0		
	20	1	0.030	79.6	69.8	14.0
		2	0.023	59.9		
		3	-	-		

- Data excluded due to failure during measurement

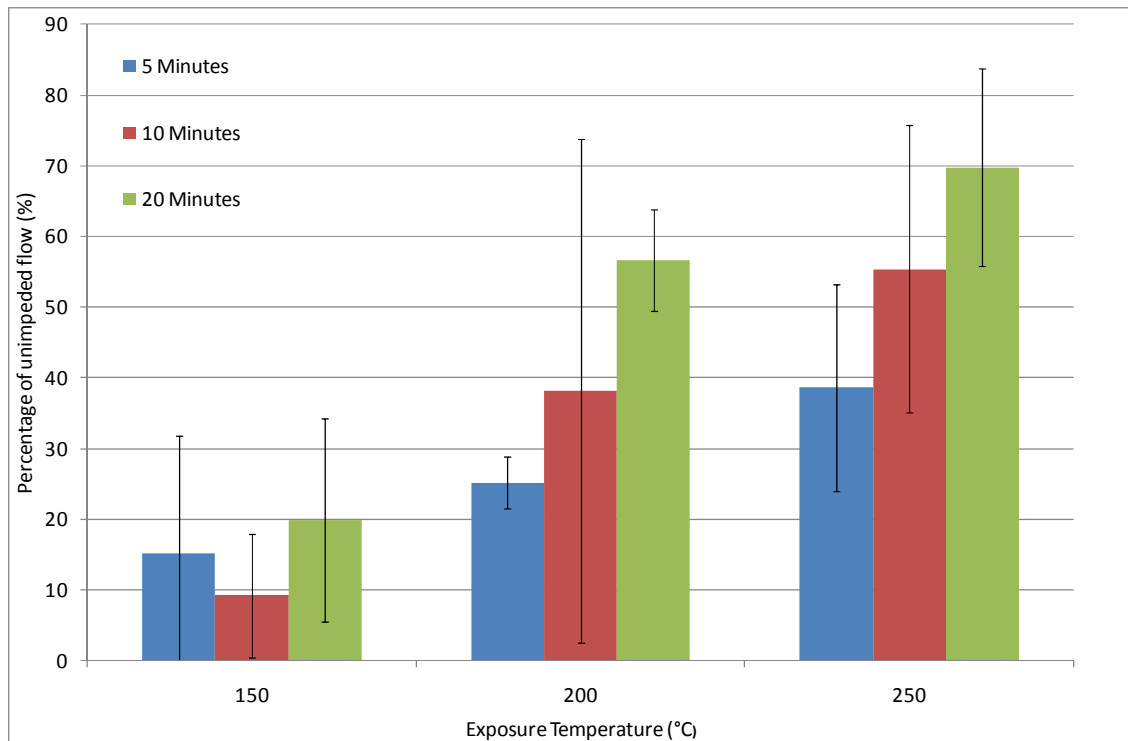


Figure 37: Summary of Polycarbonate results

4.5 Polyvinyl Chloride

The range of temperature tested ranged from 100°C to 250°C. The initial range of 150°C to 250°C was extended to include one set of tests at 100°C as the initial results of the tests conducted at 150°C indicated that a significant flow was still being measured despite there being very little visible evidence.

The material was therefore exposed to 100°C for 20 minutes. The velocity and temperature results monitored during the experiments did not indicate any flow and the preliminary results gave a result of 0 kg/s. Fuller examinations of the results found that the average flow of the three experiments was 0.001 kg/s. The mass flow corresponds to an efficiency of 2%.

The number of experiments at 250°C was limited. The first three experiments found that the PVC had become detached from the frame. Thus, the result was the same as the baseline and no further experiments were conducted at this temperature.

The results at 200°C showed a large amount of variation from 0.007 kg/s to 0.070 kg/s. The variance in the results can be seen from the following figures. The first three figures show the temperature (Figure 38), the velocity (Figure 39) and an image of the deformed sample in the wind tunnel (Figure 40). The flow for test 1 was measured at 0.068 kg/s. This results in an

efficiency of 148%. What Figure 40 does not show clearly is the vertical displacement of the plastic into the wind tunnel duct.

The next set of figures is for test three. This test had a measured flow of 0.007 kg/s. This flow corresponds to an efficiency of 15.8%. The temperature profile, Figure 41, shows only minor increases in temperature of approximately 30°C whereas in test one the temperature increases were in the order of 50°C.

Figure 42 shows the velocity record. There is one large peak of around 1.5 m/s between 300 to 360 seconds and a smaller peak of 0.5 m/s between 450 and 480 second. This compares to Figure 39 where a large portion of the time the measured velocity is greater than 0.5 m/s.

Figure 43 shows an image of the test 3 sample. The hole is located inside the circle. This compares to Figure 40 where there are large openings on both sides. The cause of the difference is not obvious. Possible causes are variation in the strength of the connection or variation in the plastic.

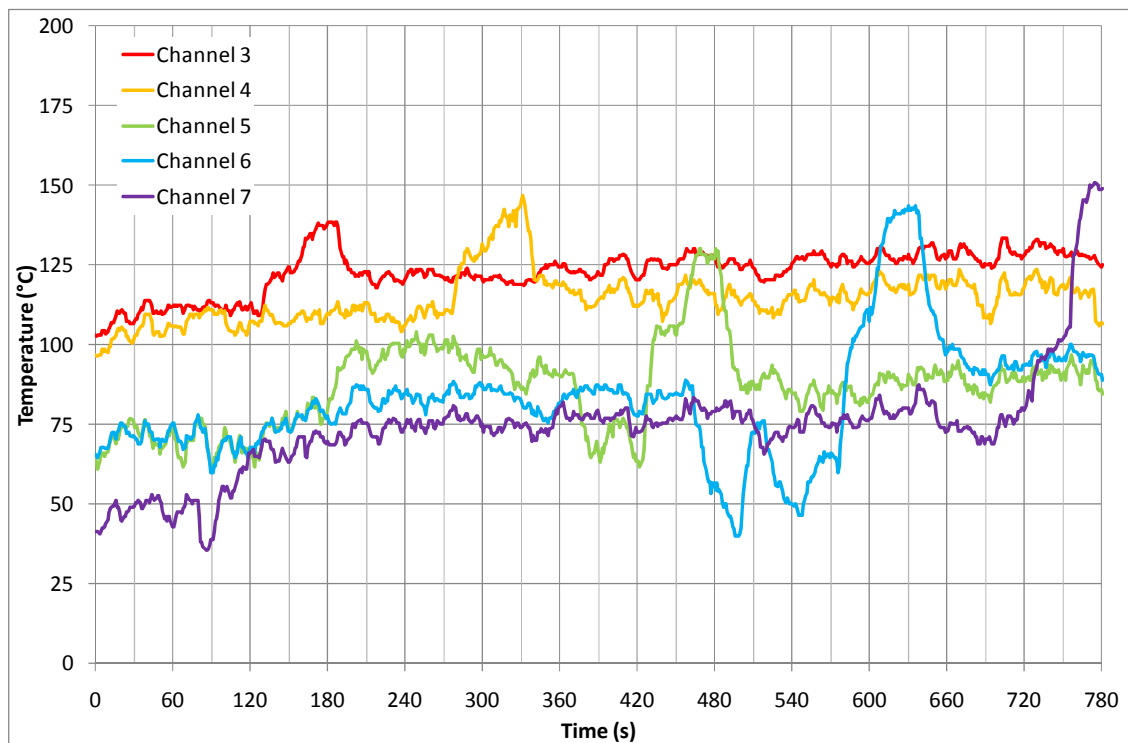


Figure 38: Temperature record, PVC, test 1, 5 minutes exposure to 200°C

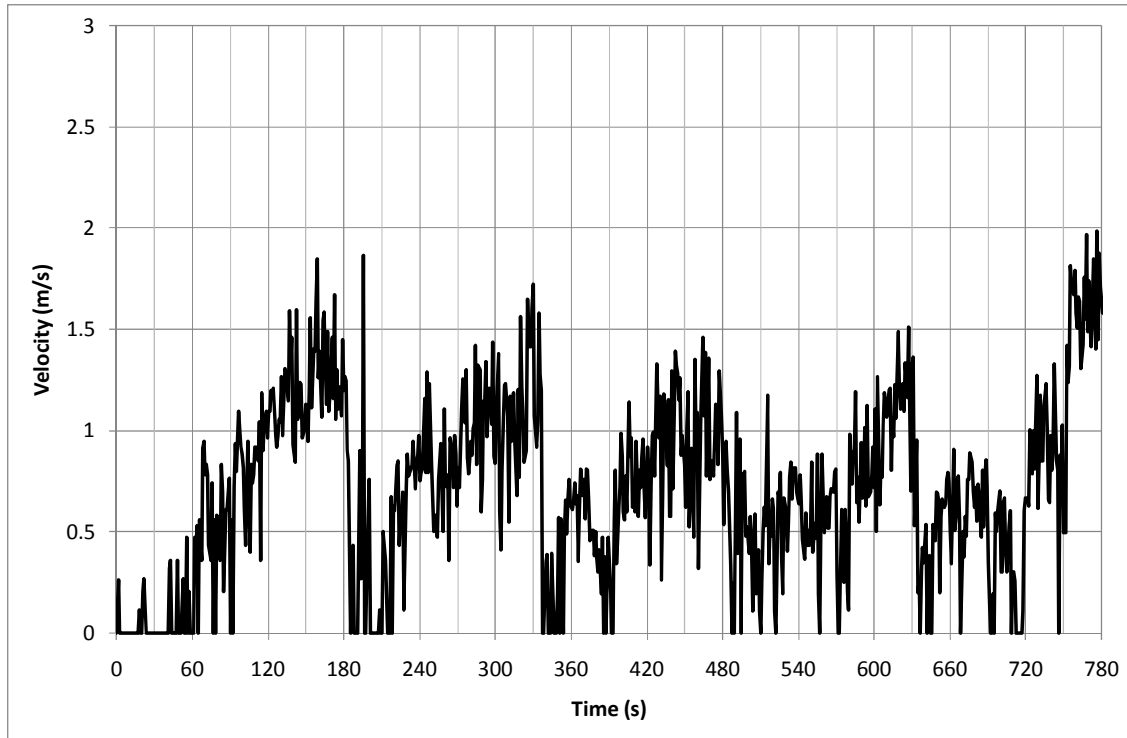


Figure 39: Velocity record, PVC, test 1, 5 minutes exposure to 200°C



Figure 40: Image of deformed sample, test 1, and note flow is from bottom to top

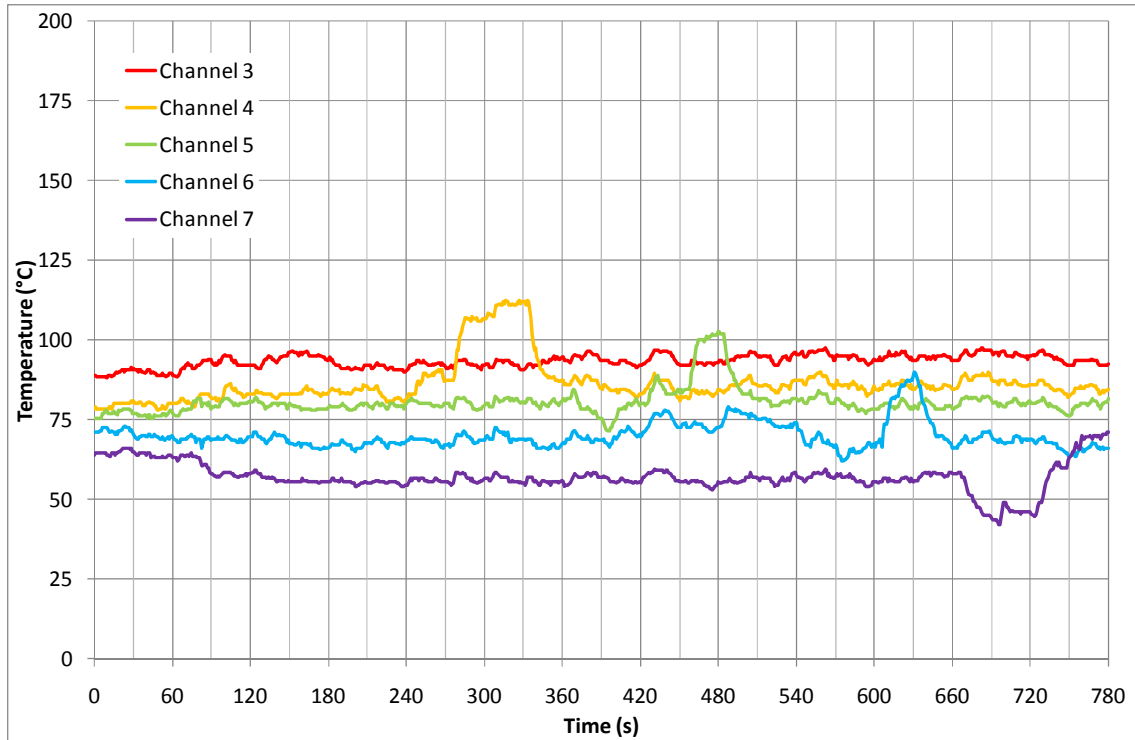


Figure 41: Temperature record, PVC, test 3, 5 minutes exposure to 200°C

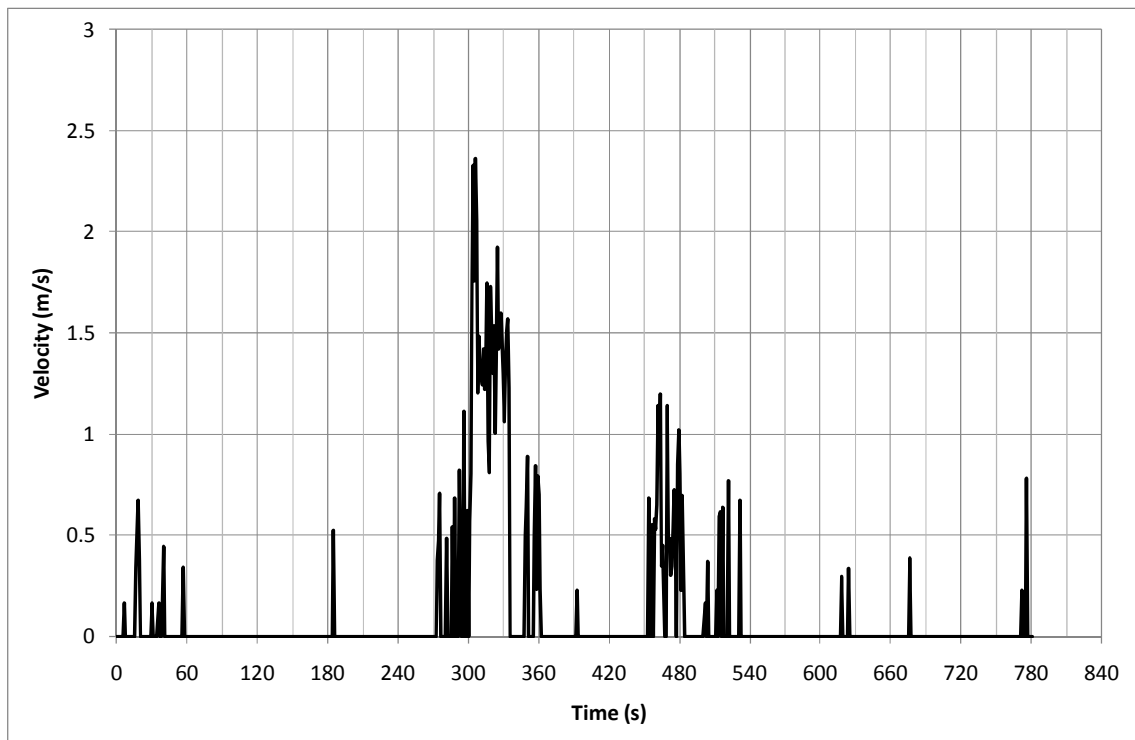


Figure 42: Velocity record, PVC, test 3, 5 minutes exposure to 200°C



Figure 43: Image of deformed sample, test 3, hole inside the circle

The entire data set is given as Table 11.

Table 11: Polyvinyl Chloride Results

Temperature (°C)	Time (min)	Experiment	Mass Flow (kg/s)	Efficiency (%)	Average Efficiency (%)	Standard Deviation (%)
100	20	1	0.005	7.2	4.1	3.7
		2	0.004	5.0		
		3	0.000	0.0		
150	5	1	0.005	8.3	20.7	12.3
		2	0.021	33.0		
		3	0.013	20.9		
	10	1	0.034	52.8	27.7	23.6
		2	0.016	24.2		
		3	0.004	6.0		
	20	1	0.013	20.3	36.4	19.0
		2	0.020	31.5		
		3	0.037	57.4		
200	5	1	0.068	148.9	100.5	148.9
		2	0.063	136.7		
		3	0.007	15.8		
	10	1	0.036	78.9	73.3	56.6
		2	0.017	37.0		
		3	0.053	115.9		
	20	1	0.027	59.1	98.5	45.4
		2	0.067	148.2		
		3	0.040	88.1		
250	5	1	0.029	77.6	103.0	29.0
		2	0.030	96.8		
		3	0.051	134.6		

Figure 44 displays a summary of the results obtained. The solid bars represent the average value. The error bars indicate the range over which results were obtained. The transparent bars are nominal values. The nominal values exist as there were no experiments conducted at those times. The result after 5 minutes exposure to 250°C resulted in the plastic detaching from the frame. This condition has already been defined in section 3.3.1 as 100%. The bars were included in the chart for completeness.

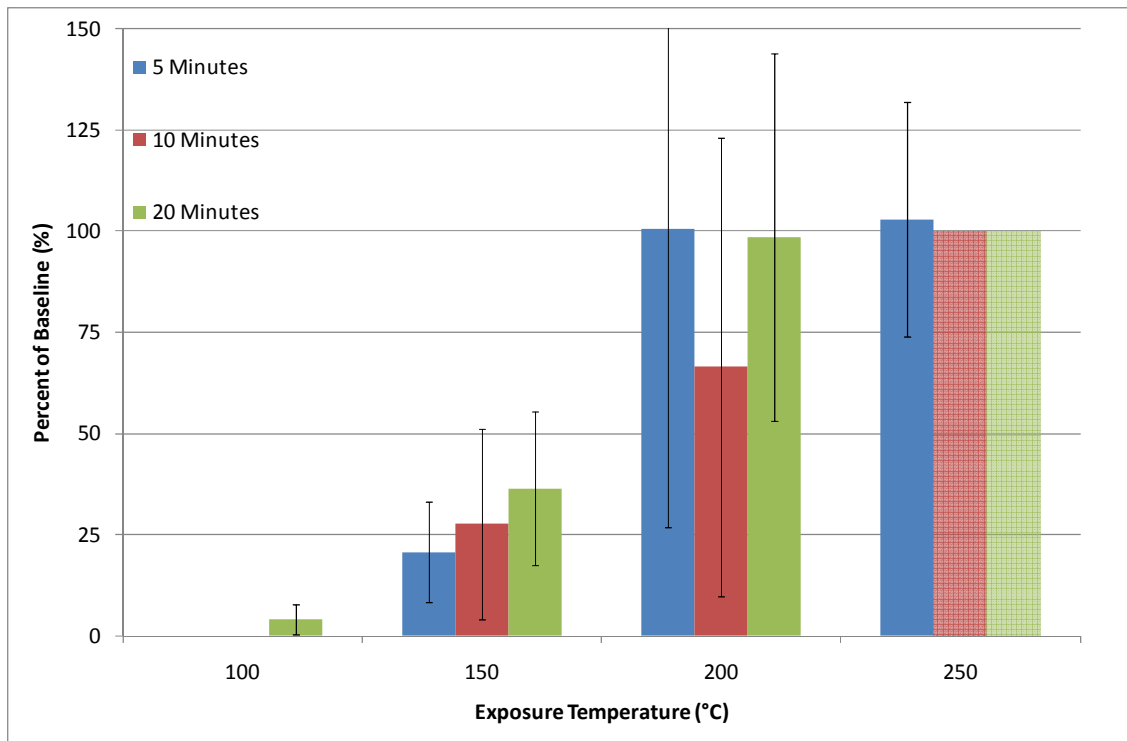


Figure 44: Summary of polyvinyl chloride results

The PVC as with the polycarbonate displays a progressive melting pattern moving from no melting to fully melted. As discussed earlier the experiment at 100°C displays very poor venting behaviour. As the temperature increased the efficiency of the vent increased.

The PVC shrunk along the long axis and thus the connection was important. The biggest effect is noticeable for the tests at 200°C. In these experiments there is a wide range of values. Some of the material had pulled away from one edge and partially dropped into the wind tunnel resulting in a high flow of greater than 100%. When the connection remained intact, preventing the material from pulling away the sample remained horizontal and only small flows were recorded.

4.6 Acrylic

Six experiments were carried out on the acrylic samples. From the preliminary tests it was thought that the only results would occur at the temperature of 250°C. The first three tests were carried out at 20 minutes exposure. The results indicated small flows of air through the vents. Three tests were then carried out for 10 minutes. The samples did not appear to deform and the measurements during the tests did not show any indication of air flow. The subsequent analysis found very small flows. The results are given in Table 12.

As can be seen from the results the flow after 20 minutes exposure at 250°C the average flow was 9.4%. The flow after 10 minutes was 3.0%.

Table 12: Acrylic Results

Temperature (°C)	Time (min)	Experiment	Mass Flow (kg/s)	Efficiency (%)	Efficiency Average (%)	Standard Deviation (%)
250	10	Test 1	0.001	1.6	3.0	1.7
		Test 2	0.002	4.9		
		Test 3	0.001	2.4		
	20	Test 1	-	-	9.4	3.4
		Test 2	0.003	7.0		
		Test 3	0.004	11.8		

The results of Test 1 of 20 minutes exposure to 250°C were ruled out as the sample was damaged being removed from the oven and one end was broken.

Figure 45 shows the velocity record for test 2 for the 20 minute exposure to 250°C. The majority of the velocity readings are single spikes. A number of spikes, such as that about 420 seconds are caused due to the movement of the Pitot tube between measurement points. Figure 46 gives the corresponding temperature record. The temperature is reasonably constant throughout the record. The most interesting Channel is Channel 7 where the temperature increases at the end matching the velocity reading seen at the end of Figure 45.

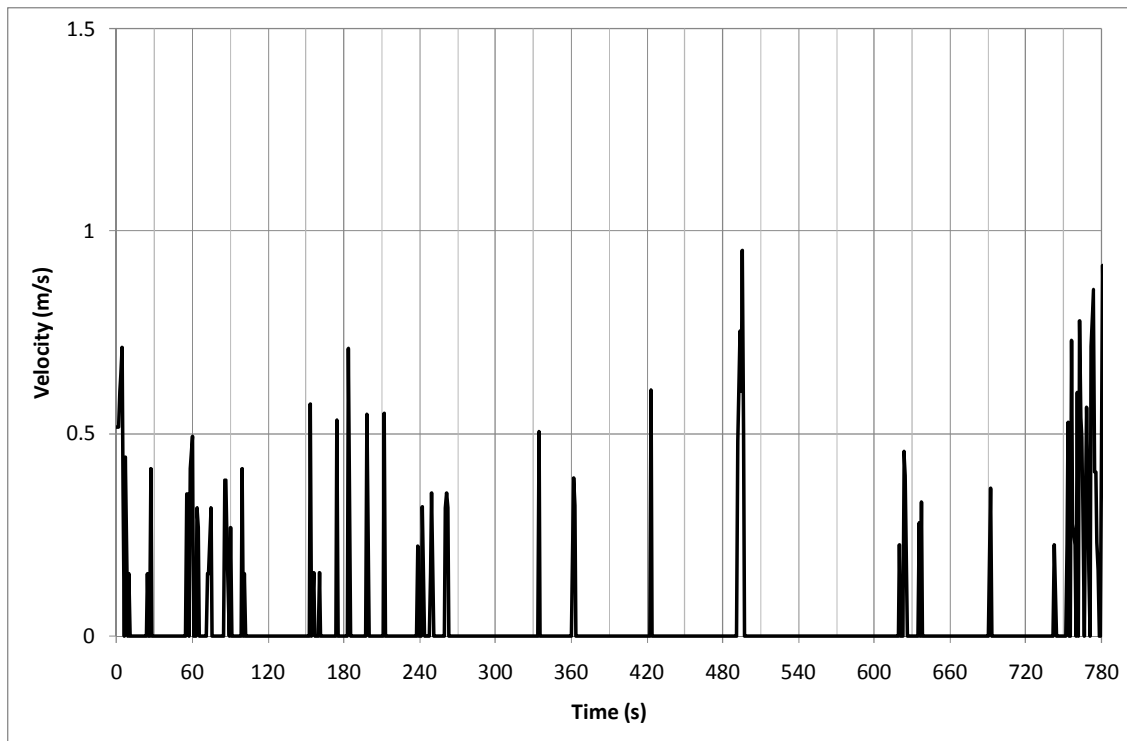


Figure 45: Velocity record, acrylic, 20 minutes exposure at 250°C

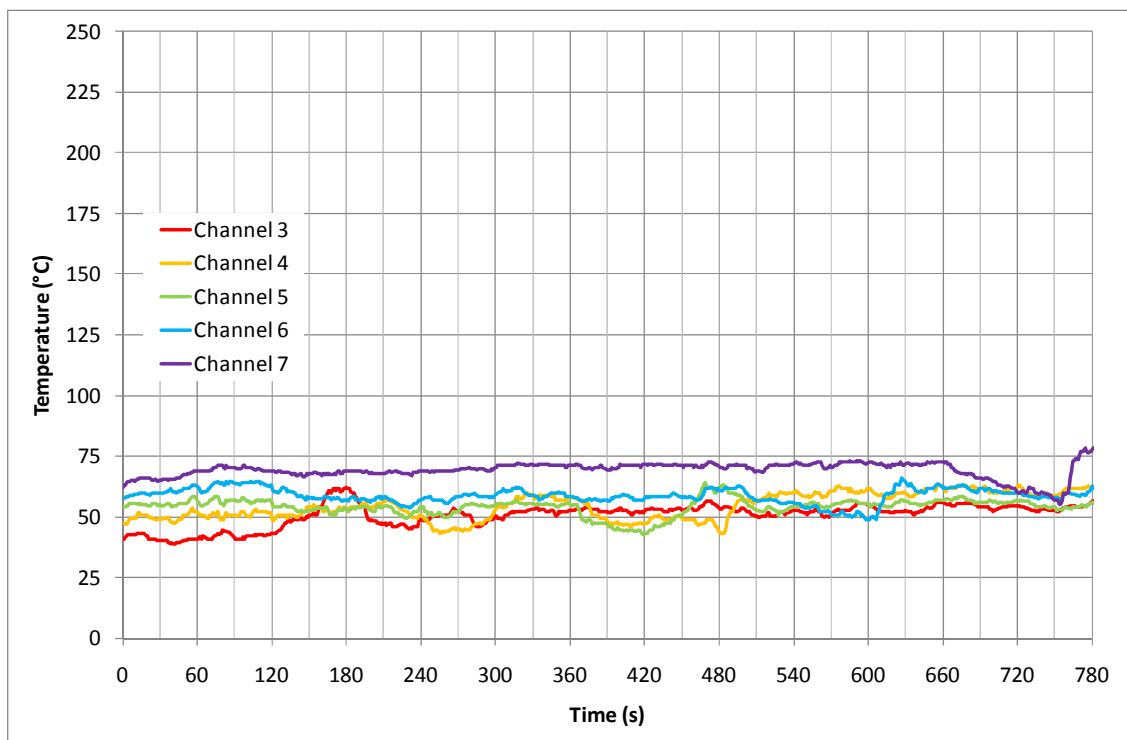


Figure 46: Temperature record, acrylic, 20 minutes exposure at 250°C

4.7 Angled Plate

The above results gave some unexpected efficiency values. The results above 100% did not make sense as the baseline with no plastic obstructing the vent was thought to be the most flow possible. During these experiments with higher than expected results it was noticed that the edges perpendicular to the flow were dipping below the top of the wind tunnel and into the flow of hot air as shown in Figure 47.

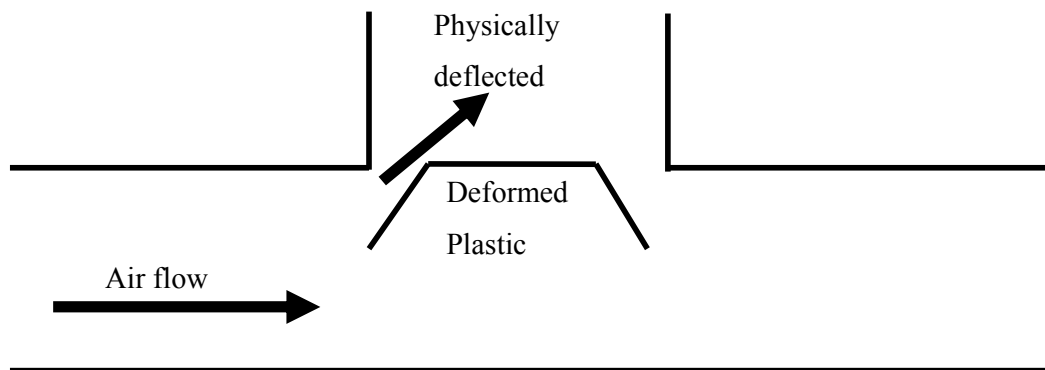


Figure 47 Physical deflection of air flow by the plastic sample

This phenomenon was examined by placing a plate of the GRP into the wind tunnel at varying angles. The mass flow through the vent was then measured. The general setup and definition of the angle is shown in Figure 48 which is a cross-section through the testing section.

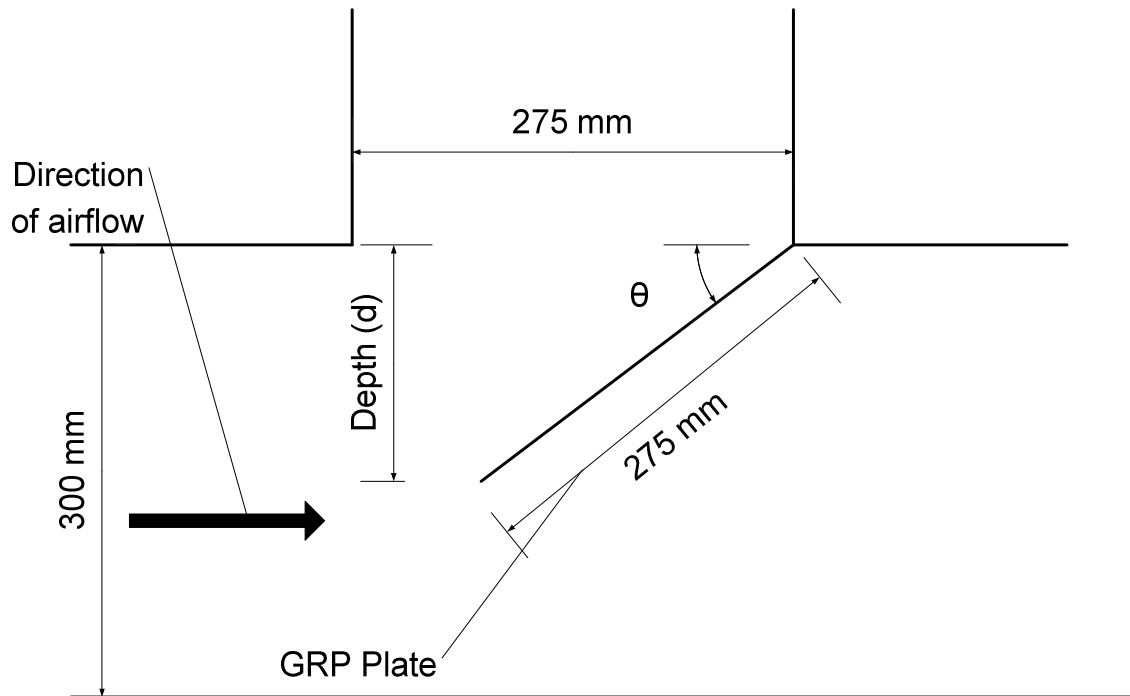


Figure 48: Cross-section defining the angle of the plastic plate

The following angles were tested

- 15°
- 45°
- 60°
- 90°

A further experiment was undertaken where the plate was angled from the downstream edge at 45° as shown in Figure 49.

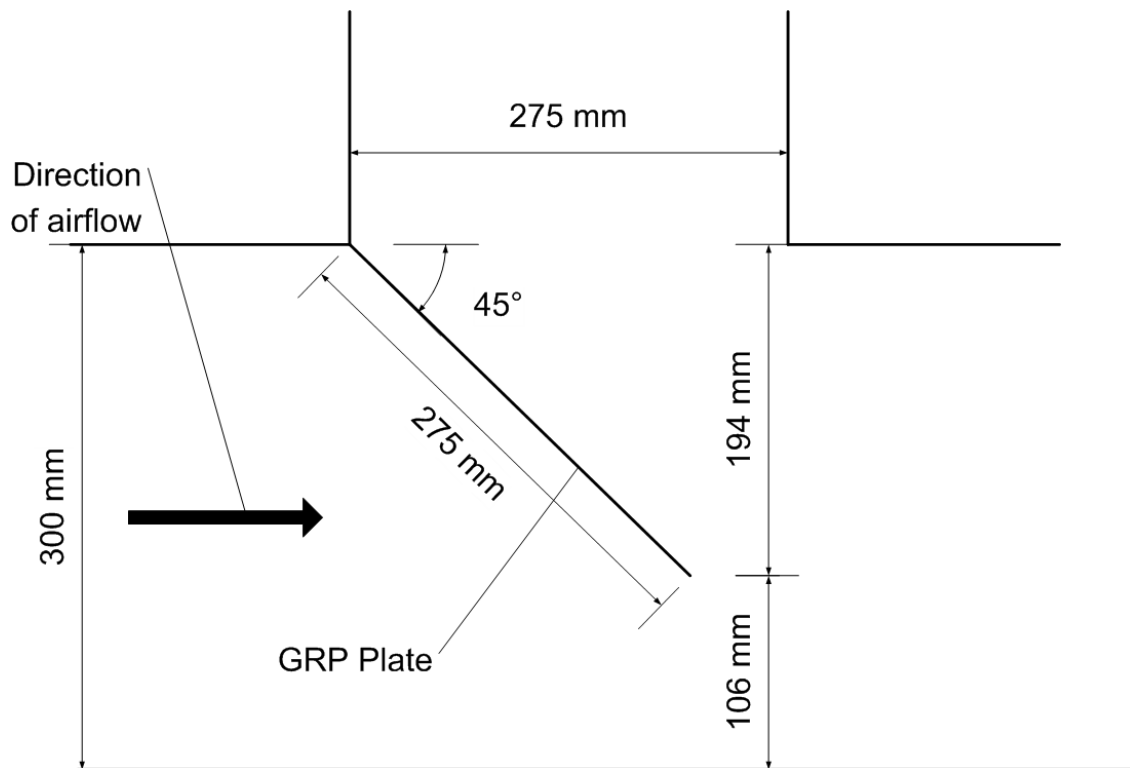


Figure 49: Angled plate reversed

An attempt has been made to theoretically predict the flow from the deflected plate. The premise of this prediction is that all the air above the bottom of the plate is deflected up and through the vent and that all the air below the plate does not move through the vent and recirculates. Because of the limited number of velocity and temperature profiles recorded at the time, the average temperature and velocity have been used as a basis for determining the flow in the duct. The assumption is shown graphically in Figure 50. The air above the dashed line flows up and through the vent and the air below flows past the vent.

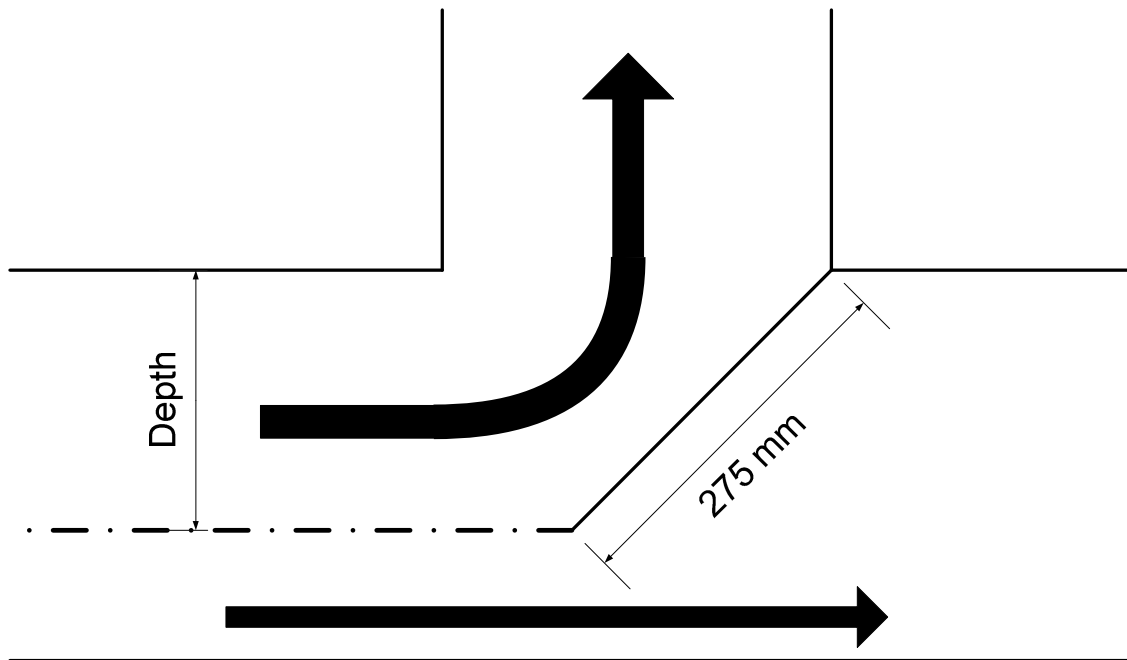


Figure 50: Graphical representation of theoretical model

Two theoretical flow profiles have been used. The first is a plug flow. This assumes that the velocity and temperature are constant throughout the cross-section. This is expected to over predict the flow as it does not take into account the effects of the corners or boundaries of the duct.

The second theoretical model used is the equivalent circular area method (Chartered Institution of Building Services Engineers, 2001; Howell et al. 2005). This approximates the flow area of a square duct to a circular duct.

The depth that the plastic plate extends into the flow can be calculated using the trigonometric relationship shown as Equation 12.

$$O = H \sin \theta \quad \text{Equation 12}$$

The depth of the plate increases as the angle increases, the depths for each angle and the proportion of the wind tunnel section that represents is given below in Table 13. The proportion is calculated using Equation 13, the depth of the plate is divided by the depth of the wind tunnel, 300 mm.

$$P = \frac{\text{depth}}{300} \quad \text{Equation 13}$$

Table 13: Depth of angled plate

Angle (degrees)	Depth (mm)	Proportion of tunnel depth
0	0	0.000
15	71	0.237
45	194	0.648
60	238	0.794
90	275	0.917

As the flow is being distributed pro rata the proportion of the tunnel depth is used to determine the mass flow, for example the flow for a plate at 45° would be 64.8% of the total mass flow.

Two methods were found and used to calculate the equivalent diameter of the duct. The simpler method is displayed as Equation 14 (Howell et al. 2005). The more complex is Equation 15 (Chartered Institution of Building Services Engineers. 2001).

$$d_c = \frac{1.30ab^{0.625}}{a + b^{0.250}} \quad \text{Equation 14}$$

where

d_c	The equivalent diameter
a	A side of the duct (mm)
b	The adjacent side (mm)

$$d_c = \frac{32\lambda_c w^3 h^3}{\pi^2 \lambda_r (w + h)} \quad \text{Equation 15}$$

Where

d_c	The equivalent diameter (mm)
λ_c	Pressure loss coefficient of the circular galvanized duct equivalent
λ_r	The pressure loss coefficient of the rectangular duct
w	The width of the duct (mm)
h	The height of the duct (mm)

The equivalent diameter is calculated by assuming that the friction loss coefficient for the same volume flow is constant and hence λ_r and λ_c are equal and therefore cancel each other out.

The equivalent diameters calculated were 328 mm from Equation 13 and 330 mm Equation 14.

Plug Flow Calculation

The calculation of the theoretical mass flows were calculated at the temperature and velocity used in the experiments. The temperature was 150°C (423 K) and the velocity 1.88 m/s.

$$T = 423 \text{ K}$$

$$\rho = \frac{352.8}{T}$$

$$\rho = \frac{352.8}{423}$$

$$\rho = 0.83 \frac{\text{kg}}{\text{m}^3}$$

$$u = 1.88 \text{ m/s}$$

$$\dot{m}'' = u\rho$$

$$\dot{m}'' = 1.56 \frac{\text{kg}}{\text{s}}$$

$$\dot{m} = \dot{m}''A$$

$$A = 0.09 \text{ m}^2$$

$$\dot{m} = 0.014 \text{ kg/s}$$

The mass flow above is the total mass flow through the wind tunnel section.

Howell Calculation

The equivalent diameter of the duct is found and then the flow is calculated as above for the plug flow.

$$d_c = \frac{1.30ab^{0.625}}{a + b^{0.250}}$$

$$a = 0.3$$

$$b = 0.3$$

$$d_c = 0.328 \text{ m}$$

$$A = \frac{\pi d^2}{4}$$

$$A = 0.084 \text{ m}^2$$

$$\dot{m}'' = 1.56 \frac{\text{kg}}{\text{s}}$$

$$\dot{m} = 0.132 \text{ kg/s}$$

CIBSE Calculation

$$d_c = \frac{32\lambda_c w^3 h^3}{\pi^2 \lambda_r (w + h)}$$

$$w = 0.3$$

$$h = 0.3$$

$$\lambda_r = \lambda_c$$

$$d_c = 0.330 \text{ m}$$

$$A = \frac{\pi d^2}{4}$$

$$A = 0.086 \text{ m}^2$$

$$\dot{m}'' = 1.56 \frac{\text{kg}}{\text{s}}$$

$$\dot{m} = 0.134 \frac{\text{kg}}{\text{s}}$$

Having determined the mass flow through the wind tunnel the next step is calculating the proportion of the flow going through the vent.

$$\dot{m}_{vent} = \dot{m}P$$

For the 45° flow the following calculations are carried out.

Plug Flow

$$\dot{m}_{vent} = 0.14 \times 0.648$$

$$\dot{m}_{vent} = 0.117 \frac{\text{kg}}{\text{s}}$$

Howell

$$\dot{m}_{vent} = 0.132 \times 0.648$$

$$\dot{m}_{vent} = 0.110 \frac{kg}{s}$$

CIBSE

$$\dot{m}_{vent} = 0.134 \times 0.648$$

$$\dot{m}_{vent} = 0.111 \frac{kg}{s}$$

A summary of the theoretical mass flows are given in Table 14.

Table 14: Theoretical mass flow through vent for an angled plate

Angle	Plug Flow (kg/s)	Equivalent diameter (Howell) (kg/s)	Equivalent diameter (CIBSE) (kg/s)
0	0.000	0.000	0.000
15	0.043	0.040	0.041
45	0.117	0.110	0.111
60	0.143	0.134	0.136
90	0.165	0.155	0.157

4.7.1 Experimental Results

As the angle of the plate increases from 0° to 90° the flow through the duct increases from 0 kg/s to 0.142 kg/s respectively. The results have been normalized by the baseline flow at 150°C of 0.064 kg/s. This is the flow where there is no obstruction to the vent. The flow with a plate at 0° is 0% as expected as the plate covers the opening preventing buoyant flow. A further experiment was carried out with the plastic plate angled at 45° down from the downstream edge. As expected this produced a radically different result. The measured flow was 0.006 kg/s or 9%. The 45° case when set up as in Figure 49 had a measured flow of 0.058 kg/s or 131%. This result is not surprising as in the backward case the plate deflects the air down towards the bottom of the wind tunnel but in the normal case the air is deflected upwards towards the vent.

The results for the angled plate experiments are given in Table 15.

Table 15: Experimental mass flows for an angled plate

Angle	Mass flow (kg/s)	Percent
0	0.000	0
15	0.029	45
45	0.084	131
60	0.113	177
90	0.142	195
-45	0.006	8

The comparisons between the theoretical and experimental results are shown in Figure 51.

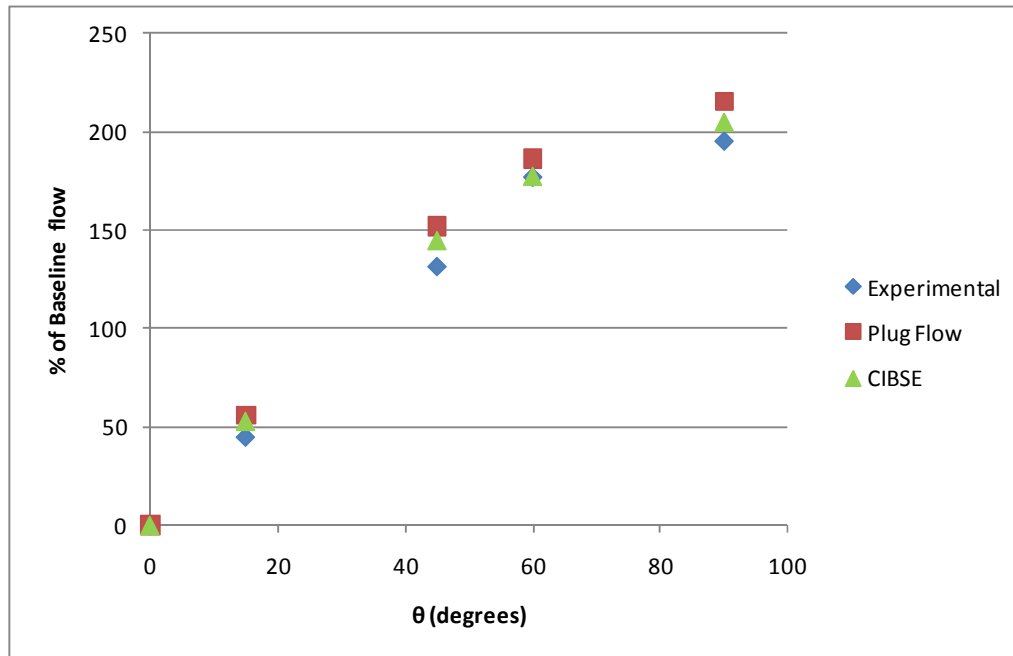


Figure 51: Comparison of theoretical and experimental efficiency

The results using the formula from Howell are not displayed due to the closeness of the CIBSE and Howell results.

The results show that it is possible to boost the buoyancy driven flow by physically deflecting it, therefore the flows greater than 100% in the main tests have an explanation.

There is a strong agreement between the theoretical and experimental flow. This is despite the simple nature of the theoretical relationship. The experimental results are less than those predicted. This result is expected as the effects of the boundary layer would reduce the velocity and the mass flow.

4.8 Empirical Relationship

An objective of this work is to provide designers with experimental data to assist in determining the efficiency of the vent. To aid in achieving that objective an empirical equation was developed from the experimental data.

The equation was developed using the data from the PVC and polycarbonate experiments. The GRP data was not used due to the plastic not deforming to a point that allowed venting. The acrylic data is plotted but due to the limited number of experiments was not used to

develop the equation. The intention is to develop a general relationship that can be used for different types of plastic.

From Figure 37 and Figure 44 it can be seen that as the temperature increases the efficiency increases. It is also evident that the efficiency increases the longer the material is exposed. Therefore the efficiency is a function of the exposure time, exposure temperature and the material.

The heat transfer problem of a lump of material at constant temperature being placed into a thermally different environment might be seen as representing the method of heating used in the experiments, where the plastic at ambient temperature was placed into the hot oven.

The time for the material to reach some temperature T , can be found using the lumped heat capacitance method if the Biot number is less than 0.1 (Incropera et al. 2007). The calculation of the Biot number is given in Appendix F. The calculation required a convective heat transfer coefficient. A range of values for free convection were given as 2 to 25 W/m²K (Incropera et al. 2007). The maximum Biot number for the PVC was 0.078 and for the polycarbonate was 0.054. It is therefore reasonable to use the lumped capacitance method for these materials. The Biot number for the acrylic had a range of 0.018 to 0.225. The lumped heat capacity method may not be applicable to this material. It is assumed that the time taken to reach the melting temperature t_m is given by Equation 16 (Incropera et al. 2007).

$$t_m = -\frac{1}{k} \ln \left(\frac{T_m - T_e}{T_i - T_e} \right) \quad \text{Equation 16}$$

Where

t_m	Time to reach the melting temperature (s)
T_m	melting temperature (°C)
T_e	exposure temperature (°C)
T_i	initial temperature (°C)

The constant k is defined as

$$k = \frac{hA_s}{\rho V c}$$

Where

ρ	density $\left(\frac{kg}{m^3}\right)$
--------	---------------------------------------

V	<i>volume</i> (m^3)
c	<i>specific heat</i> ($\frac{J}{kg}$)
h	<i>convective heat transfer coefficient</i> ($\frac{W}{m^2K}$)
A_s	<i>Surface Area</i> (m^2)

Since the materials were of the same nominal size and thickness and the oven conditions similar for each experiment the surface area volume and convective heat transfer coefficient is constant and arbitrarily set to 1 since the purpose is to determine the proportional relationship.

The melting temperature was taken as an average of the values in Table 1. The density and specific heat values are from Roa and O'Brien (Rao & O'Brien 1998).

Table 16: Characteristic material values

Material	Melting Temperature ($^{\circ}C$)	Density (kg/m^3)	Specific heat (J/kg)
PVC	86	1100	1400
Polycarbonate	133	1170	1200
Acrylic	111	1180	1450

The melting time incorporates the material properties. A non dimensional time is defined as Equation 17.

$$\tau = \frac{t_e}{t_m} \quad \text{Equation 17}$$

Where

t_e	The exposure time (s)
t_m	Melting time (s) from Equation 16

The efficiency is now proportional to the non dimensional time and the exposure temperature. To create a non dimensional temperature the exposure temperature is normalised by the melting temperature. The independent variables are plotted on the x-axis and the dependant variable on the y-axis resulting in Figure 52.

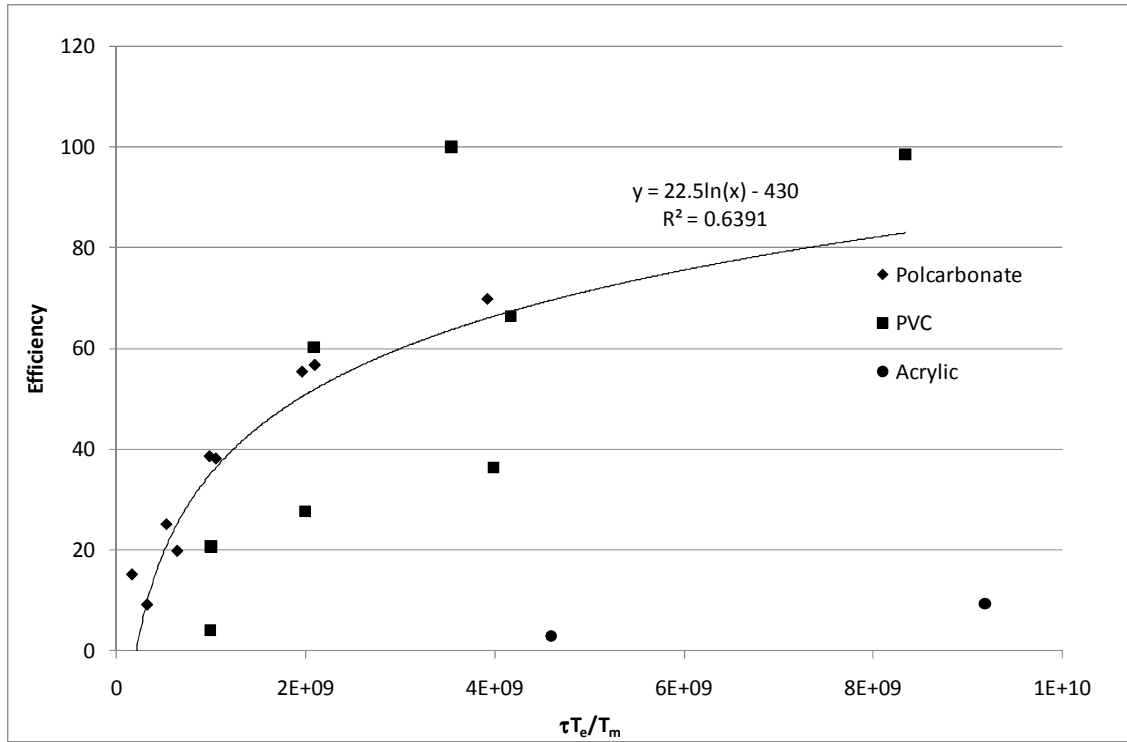


Figure 52: E vs. $\tau T_e / T_m$

A line of best fit has been drawn through the data resulting in the following relationship.

$$y = 22.5 \ln x - 430$$

$$y = E$$

$$x = \tau \frac{T_e}{T_m}$$

Rearranging to make the efficiency the subject results in

$$E = 22.5 \ln \left(\tau \frac{T_e}{T_m} \right) - 430 \quad \text{Equation 18}$$

Inserting Equation 16 and Equation 17 into Equation 18 results in Equation 19

$$E = 22.5 \ln \left(\left(\frac{t}{-\frac{1}{k} \ln \left(\frac{T_m - T_e}{T_i - T_e} \right)} \right) \frac{T_e}{T_m} \right) - 430 \quad \text{Equation 19}$$

The equation has the following limits

$$T_m < T_e \leq 250 \text{ } ^\circ\text{C}$$

$$5 < t < 20 \text{ minutes}$$

$$0 \leq E \leq 100\%$$

The result fit to the polycarbonate results is surprisingly good. The results for the PVC are somewhat disappointing with there being a large amount of scatter. There are PVC data points that lie near the 100% line. The leftmost point was limited in value to 100%. The data point is in fact above 100%. This is caused by the melted plastic physically deflecting the flow as discussed in the previous section it was not possible to determine how much of the flow was caused by deflection and how much through buoyancy. This explains why the data point is so far above the line of best fit.

The results for the acrylic material are disappointing but not surprising. It is possible that due to the higher Biot number the lumped heat capacitance method is not appropriate. It is also noted that for the PVC and the polycarbonate the melting temperature is about 10°C less than the lowest temperature tested, whereas the melting temperature for the acrylic is 139°C less than the temperature at which the material melted. The melting temperatures that were taken from the literature were for generic materials and not those specifically for skylights. It is therefore possible that a higher melting temperature is more appropriate. An increased melting temperature of 240°C was used and the acrylic data was plotted in Figure 53. The temperature of 240°C was used as this is 10°C less than the exposure temperature as was seen with the polycarbonate and the PCV. The data points shift near the line of best fit.

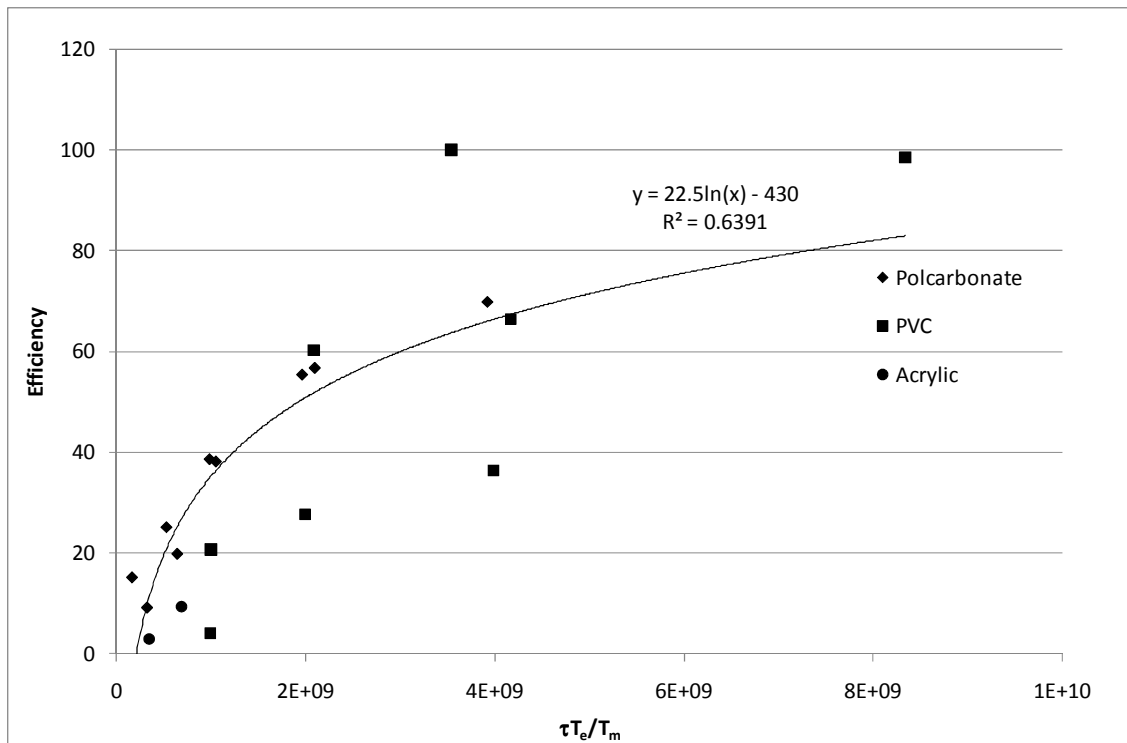


Figure 53: E vs. $\tau T_e / T_m$ with modified acrylic melting temperature

The lumped capacitance method may not account for all of the process going on in the melting of the plastic. The values of specific heat and density are assumed to be constant with temperature and this may not be appropriate especially when there is a phase change from solid to liquid.

The empirical equation should not be used for the acrylic material as there is not enough experimental data to determine if the relationship is appropriate. Users of the equation should be aware of the limitations of the experiments as discussed in Section 6.1 and the limits discussed in this section.

Chapter 5 **Modelling**

An exemplar building has been modelled. The intention of the modelling is to examine the effects of the vent opening behaviour. The model makes a number of assumptions and the absolute numbers should be treated with care.

The following variables have been examined.

The materials:

- Polycarbonate.
- Polyvinyl Chloride.
- Acrylic.

The ventilation condition:

- Ventilation always closed.
- Ventilation always open.
- Opening at the melting temperatures from literature.
- Opening based on the aforementioned results.

The fire growth rate:

- Slow.
- Medium.
- Fast.
- Ultra Fast.

The GRP has not been modelled as the GRP does not melt below 300°C and it is unknown what occurs above this temperature.

5.1 Building Geometry

The building geometry is arbitrary. The building is 80 m by 40 m and 15 m high. The area of the skylight material is based upon the requirements of clause 4.2.4 of C/AS1 (Department of Building and Housing 2008b). The clause requires 15% of the floor area as effective venting. It has for the sake of simplicity been assumed that the skylight material provides effective venting on a 1:1 ratio. The area of the skylight is thus calculated.

$$A_{vent} = A_{floor} \times 15\%$$

$$A_{vent} = (40 \times 80) \times \frac{15}{100}$$

$$A_{vent} = 480 \text{ m}^2$$

To further simplify the problem it has been assumed that the width of the skylights is 1 m. To comply with the requirement of the vents being distributed evenly through the space an odd number of vents were chosen. The length of the vents needed to be less than 40 m, the width of the building. It was found that 15 vents would result in a required length of 32 m and a distance between centre lines of 6.67m. The layout of the skylights is shown in Figure 54 along with the important dimensions.

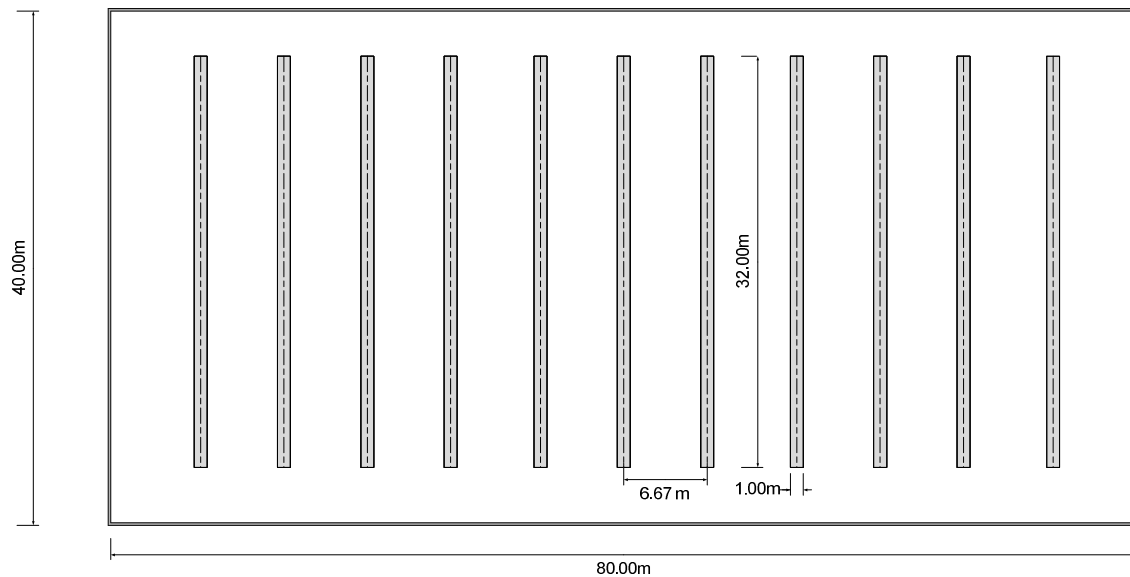


Figure 54: Model building dimensions with skylight location

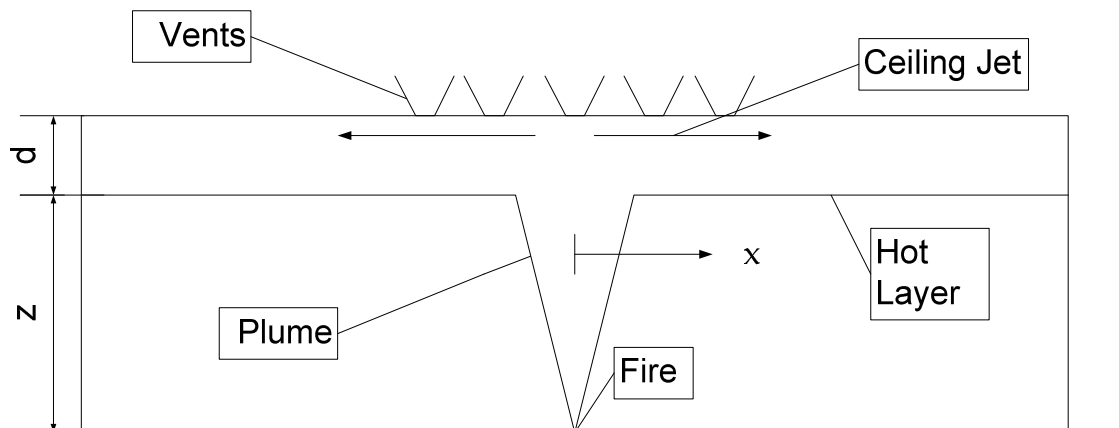


Figure 55: Elevation of model building showing important physical dimensions

The important aspects and physical dimensions are shown in Figure 55. The important parts are:

- The fire size (\dot{Q} in kW).
- The plume (volume flow).
- The layer (depth below ceiling).
- The ceiling jet temperature.
- The vent area.
- The vent flow.

5.2 Calculation Procedure

The model is relatively simple. The relationships between the important parts of the model calculation are shown in Figure 56. The following inputs are required to run the model.

- Fire Growth rate, α in kW/s².
- Distance of the vent centre line from the fire, x in m.
- Area of each vent at distance x , A_v in m².
- Inlet area, A_i in m².
- Area of the building, A in m².
- The height of the building, h in m².

The first calculation required is that of the fire size in kW. This is achieved using Equation 20 (Karlsson & Quintiere 2000).

The next step is the calculation of the plume characteristics. The characteristic of interest was the volume flow rate at the height of the hot layer. This required the calculation of intermediate values of the mass flow rate and temperature. The plume correlation chosen was for a point source axisymmetric plume. There are a number of good reasons for doing this. The first is that the model is an idealised case. The second reason is that the only fire input required is the heat release rate. The mass flow was calculated using Equation 21 (Karlsson & Quintiere 2000) and the rise in temperature calculated using Equation 22 (Karlsson & Quintiere 2000). The local temperature could then be calculated using Equation 23. Equation 4 was then used to calculate the local density. With the mass flow rate and the density known the volumetric flow rate could be calculated using Equation 24.

$$\dot{m}_p = 0.20 \left(\frac{\rho_\infty^2 g}{c_p T_\infty} \right)^{\frac{1}{3}} \dot{Q}^{\frac{1}{3}} z^{\frac{5}{3}}$$

Equation 21*Where*

ρ_∞ ambient density of air $\left(\frac{kg}{s}\right)$

g gravity $\left(\frac{m}{s^2}\right)$

c_p specific heat $\left(\frac{J}{kgK}\right)$

T_∞ ambient temperature (K)

\dot{Q} heat release rate (kW)

z height of rise (m)

$$\Delta T = 5.0 \left(\frac{T_\infty}{g c_p \rho_\infty^2} \right)^{\frac{1}{3}} \dot{Q}^{\frac{2}{3}} z^{-\frac{5}{3}}$$

Equation 22

$$T = T_\infty + \Delta T$$

Equation 23

$$\rho = \frac{352.8}{T}$$

Equation 4*where*

ρ The density (kg/m³)

T The temperature (K)

$$\dot{V} = \frac{\dot{m}}{\rho}$$

Equation 24*where*

\dot{V} The volumetric flow rate m³/s

\dot{m} The mass flow rate (kg/s)

ρ The density (kg/m³)

After calculating the volume of air going into the hot layer the next step is to calculate the volume going out. The model assumes that the only volume exiting the upper layer is that from the horizontal vents in the roof. The model does not consider vertical vents such as doors and windows. The flow through the vertical vent has been calculated from Equation 9 (Klote et al. 2002). This flow is in terms of kg/s again with the volumetric flow rate can be calculates using Equation 24 if the density has been calculated using Equation 4.

$$\dot{m}_v = C_d A_v \rho \frac{\left(2gd(T_s - T_\infty) \left(\frac{T_\infty}{T_s}\right)\right)^{\frac{1}{2}}}{T_s + \left(\frac{A_v}{A_i}\right)^2 T_\infty} \quad \text{Equation 25}$$

Where

\dot{m}_v	The mass flow rate through the vent (
C_d	The discharge coefficient
A_v	The geometric area of the vent (m^2)
ρ	The air density in ($\frac{kg}{m^3}$)
g	The acceleration due to gravity ($\frac{m}{s^2}$)
d	The depth of the smoke layer
T_s	The smoke temperature ($^{\circ}C$)
T_∞	The ambient temperature ($^{\circ}C$)
A_i	The area of the inlet air (m^2)

A number of unknowns still need to be calculated, the area of the vent which will be discussed later and the temperature of the smoke. The temperature used for the determination of the area is that of the ceiling jet. This value will also be used to calculate the local smoke flow. In keeping with the models simplicity and idealisation the ceiling jet temperature has been calculated using Alpert's Correlation rather than some more complex expression for ceiling jet temperatures. Alpert's Correlation for temperature is given below as Equation 26 and Equation 27 (Alpert 2008).

$$T - T_{\infty} = 16.9 \frac{\dot{Q}^{\frac{2}{3}}}{H^{\frac{5}{3}}} \quad \text{for } \frac{r}{H} \leq 0.18 \quad \text{Equation 26}$$

$$T - T_{\infty} = 5.38 \frac{\dot{Q}^{\frac{2}{3}}}{\left(\frac{r}{H}\right)^{\frac{2}{3}}} \quad \text{for } \frac{r}{h} > 0.18 \quad \text{Equation 27}$$

Where

T	<i>Temperature of the ceiling jet (°C)</i>
T_{∞}	<i>Ambient Temperature (°C)</i>
r	<i>The radial distance from the fire (m)</i>
H	<i>The height of the ceiling (m)</i>
\dot{Q}	<i>The heat release rate of the fire (kW)</i>

The calculation of the area is the heart of the model and as such is the most complex. The area of the vent available for venting is what is of real interest. The smoke layer which is being used to compare the outcome is really just a proxy. Five different equations were used to calculate the area of the vent depending on the behaviour being examined. The following lists the conditions that were tested.

- Vents closed throughout the simulation (Always Closed).
- Vents open throughout the simulation (Always Open).
- Vents open at the melting in the literature review (Open (Melting Temperature)).
- Vents open using the results developed in this thesis (Open (Formula)).

The description in brackets corresponds to the legend displayed on the results. The first two simulations were conducted to define the extremes of the model and verify that the other results made sense. The smoke layer for example should not be deeper than the case where the vent is always closed nor should it be higher than when it is always open.

The area for the vent being always closed was defined using Equation 28.

$$A = 0$$

Equation 28*where* A

The Area of the open vent

Similarly the open case was calculated from Equation 29.

$$A = A_v$$

Equation 29*Where* A

The Area of the open vent

 A_v

The area of the plastic skylight

The case of the material opening at the melting temperature was achieved using a simple if statement if the ceiling jet temperature was less than the melting temperature the area was 0. If the ceiling jet temperature was greater than the melting temperature the whole panel was considered melted out and the area was 32m².

Using Equation 18 developed in Section 4.8. The area was calculated as Equation 30.

$$A_{open} = C_e A_{total}$$

Equation 30*Where* A_{open}

The open area available for smoke to vent through

 A_{total}

The total area of the plastic panel

 C_e

The efficiency coefficient

$$C_e = \frac{E}{100}$$

$$E = 22.5 \ln \left(\left(\frac{t}{-\frac{1}{k} \ln \left(\frac{T_m - T_e}{T_i - T_e} \right)} \right) \frac{T_e}{T_m} \right) - 430$$

Equation 18*Where* E

Efficiency (%)

t	<i>Time (s)</i>
T_e	<i>Exposure Temperature (°C)</i>
T_m	<i>Melting Temperature (°C)</i>
k	<i>Constant</i>

$$k = \frac{hA_s}{\rho V c}$$

Where

ρ Material density $\left(\frac{kg}{m^3}\right)$

c Specific heat $\left(\frac{J}{kg}\right)$

$\frac{hA_s}{V}$ 1

The melting temperature to be used above is material specific. The material properties used for the empirical equation are from Table 16 reproduced below. The higher estimated melting temperature has been used for the acrylic.

Table 16: Characteristic material values

Material	Melting Temperature (°C)	Density (kg/m ³)	Specific heat (J/kg)
PVC	90	1100	1400
Polycarbonate	141	1170	1200
Acrylic	240	1180	1450

The temperature curve has been broken into a stepwise function to gain a time in excess of 1 second. The results were calculated using an arbitrary 25°C step using the excel function MROUND. The time was calculated by using a simple VBA script that took the temperature from the previous time step and compared it to the current temperature. If the temperature differed the time was reset to 1 second. If the temperatures were the same it added 1 second to the time of the previous time step. The time was output in terms of minutes as this is the time unit used to determine the performance of the plastic skylights. Figure 57 shows a comparison of the calculated temperature at two locations, radius of 1 m calculated using Equation 26 and a radius of 10 m using Equation 27. The heat release rate is based upon a

fast fire where $\alpha = 0.047 \frac{kw}{s^2}$ (Karlsson & Quintiere 2000). The chart shows the calculated value and the step wise function created by rounding to the nearest multiple of 25 using the MROUND function in Microsoft Office Excel 2007. Over the range of temperatures found in the model this is not significant and the shape of the curve is not largely altered.

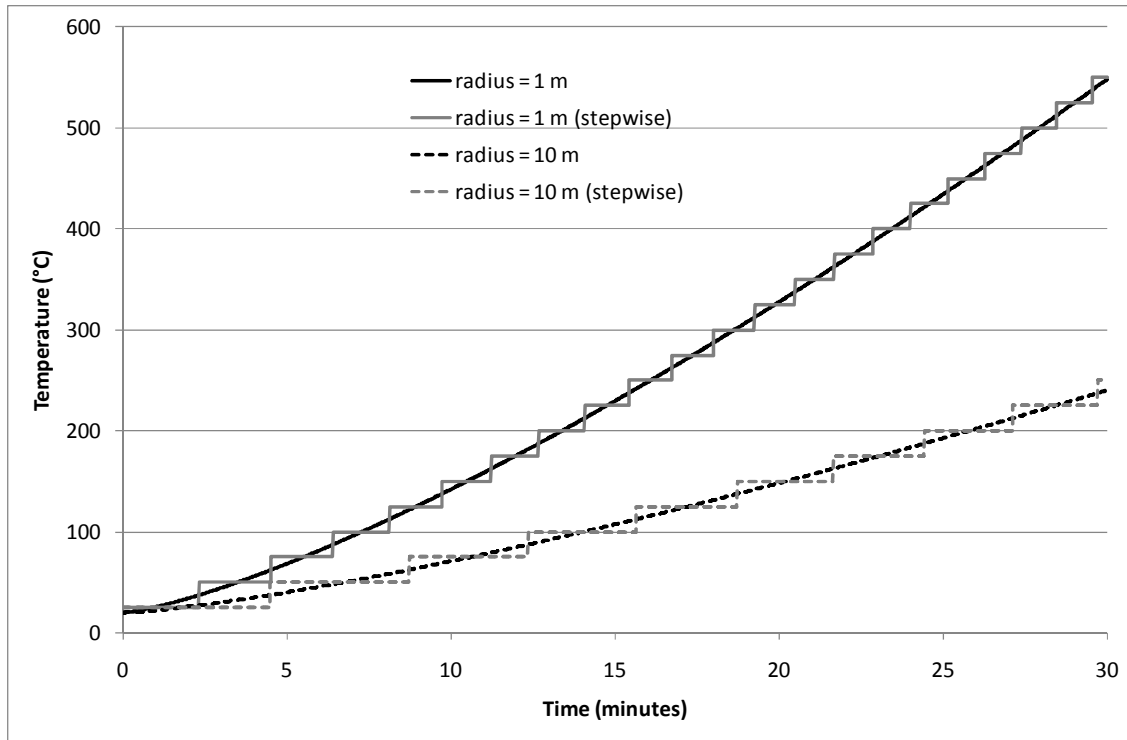


Figure 57: Comparison between the step-wise temperature and unrounded temperature

The change in the volume of the layer is calculated from Equation 31

$$\frac{dV}{dt} = (\dot{V}_{in} - \dot{V}_{out})t$$

Equation 31

Where

$$\frac{dV}{dt}$$

Is the change in volume

$$t$$

Is the time step (s)

$$\dot{V}_{in}$$

The volumetric flow into the layer $\left(\frac{m^3}{s}\right)$

$$\dot{V}_{out}$$

The volumetric flow out of the layer $\left(\frac{m^3}{s}\right)$

The volume of the layer can then be calculated by adding the change in volume to the volume from the previous time step as shown by Equation 32.

$$V = V_{t-1} + \frac{dV}{dt} \quad \text{Equation 32}$$

Where

V_{t-1}	<i>The volume of the hot smokelayer at the previous time step</i>
$\frac{dV}{dt}$	<i>The change in volume from Equation 31</i>

The final step is to calculate the depth of the layer. This is achieved using Equation 33.

$$d = \frac{V}{A} \quad \text{Equation 33}$$

Where

d	<i>Depth of the hot layer (m)</i>
V	<i>Volume of smoke (m³)</i>
A	<i>Area of the building (m²)</i>

5.3 Limitations

The number of assumptions made impress a number of limitations upon the model. The first is in terms of the geometry. The flat roof is not commonly used especially with this design of building and roof system. The flat roof allowed the use of Alpert's Ceiling Jet correlation (Alpert 2008).

The ceiling jet correlation ignores the effect of the vent opening. This may lead to a premature opening of the vent.

The model does not include any venting through vertical openings. The vertical openings in industrial buildings can be significant. However the openings are only relevant if they are open and the smoke layer descends below the top of the opening.

The temperature of the panel is assumed to be constant along the entire length of the panel. The temperature represents the point value at the centre of the panel. Lower temperatures at the end of the panel would produce smaller opening areas and as such a deeper smoke layer.

5.4 Results

The results of the modelling are somewhat predictable, the always open case resulted in a layer height that remained very near the ceiling, while the always closed case resulted in a layer that quickly descended towards the floor. The opening criteria of the melting temperature followed the always closed case until the layer jumped up as the first and then subsequent groups of panels reached the required temperature. The layer height calculated from the empirical relationship resulted in a curve that followed the always closed case and gradually moved from decreasing to increasing smoke layer height.

The modelling displays significant difference in the behaviour of the layer height for different opening mechanisms. The limitations are great and the results give only an indicative and not absolute result. Further work is needed as the current model is very simple and not appropriate for decision making.

Figure 58 show the simulation results for the polycarbonate material with a fast fire growth rate. The always open line remains near the roof level as expected. The always closed line drops down towards the floor again as expected. The behaviour of the opening on reaching the melting temperature produces a sharp point. In this case all the vents open and the smoke layer matches the always open case. Each of the opening vents can be seen the centre vent opens first followed by the seven sets each side.

This contrasts with the smooth gradual result found using the results of the experiments. The beginning of the venting also occurs at a later stage. This is not surprising as the melting temperatures found in the literature values were found to underestimate when holes would be formed.

The figure shows that 15% venting may be over conservative in providing protection. This is an area of potential future research in determining an optimum level of venting. It is noted that the Building Code of Australia (Australian Building Codes Board 2009) requires only 1.5% venting.

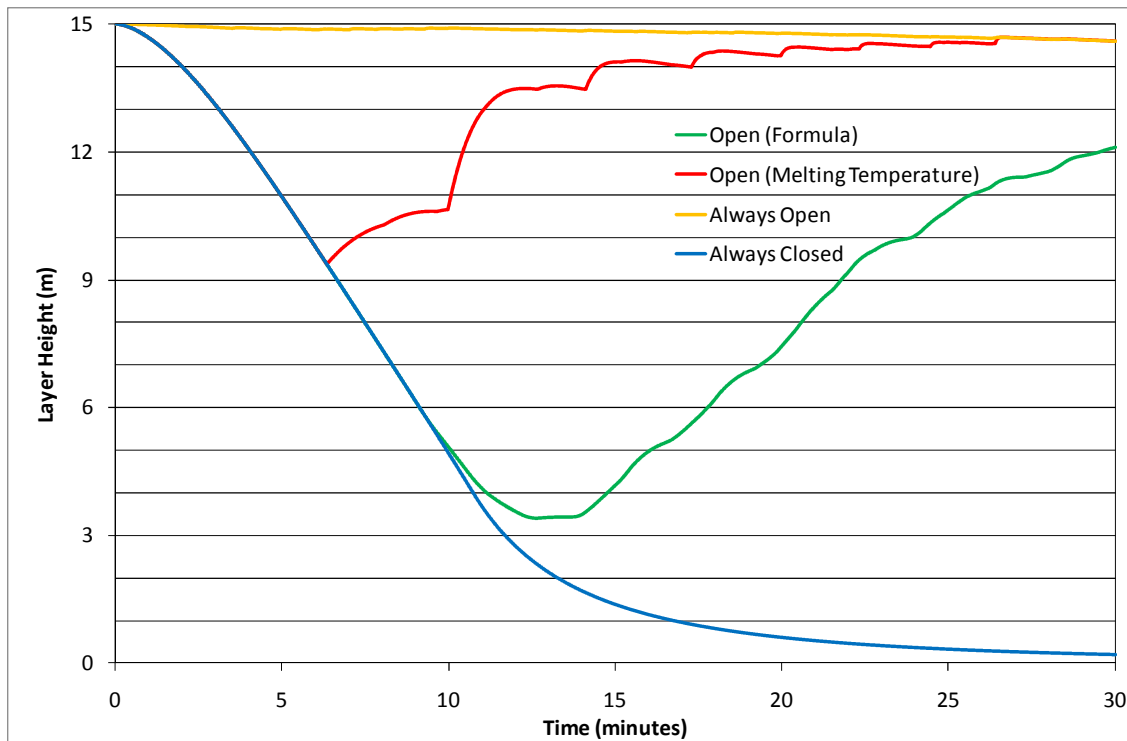


Figure 58: Layer heights for PVC skylights with a fast fire growth rate

The polycarbonate behaved in a similar manner to the PVC but with the two opening behaviours occurring later. The behaviour is as expected, due to the higher temperatures required to create openings in the polycarbonate.

Figure 59 displays this delayed melting behaviour. The step wise nature of the opening at a melting temperature is also more visible in this plot due to the greater jumps in layer height achieved.

The behaviour at the other fire growth rates was similar in a gross sense. The melting occurred earlier with the ultra fast t-squared fire and later with a medium t-squared fire. The simulation provided no melting with the slow growth fire.

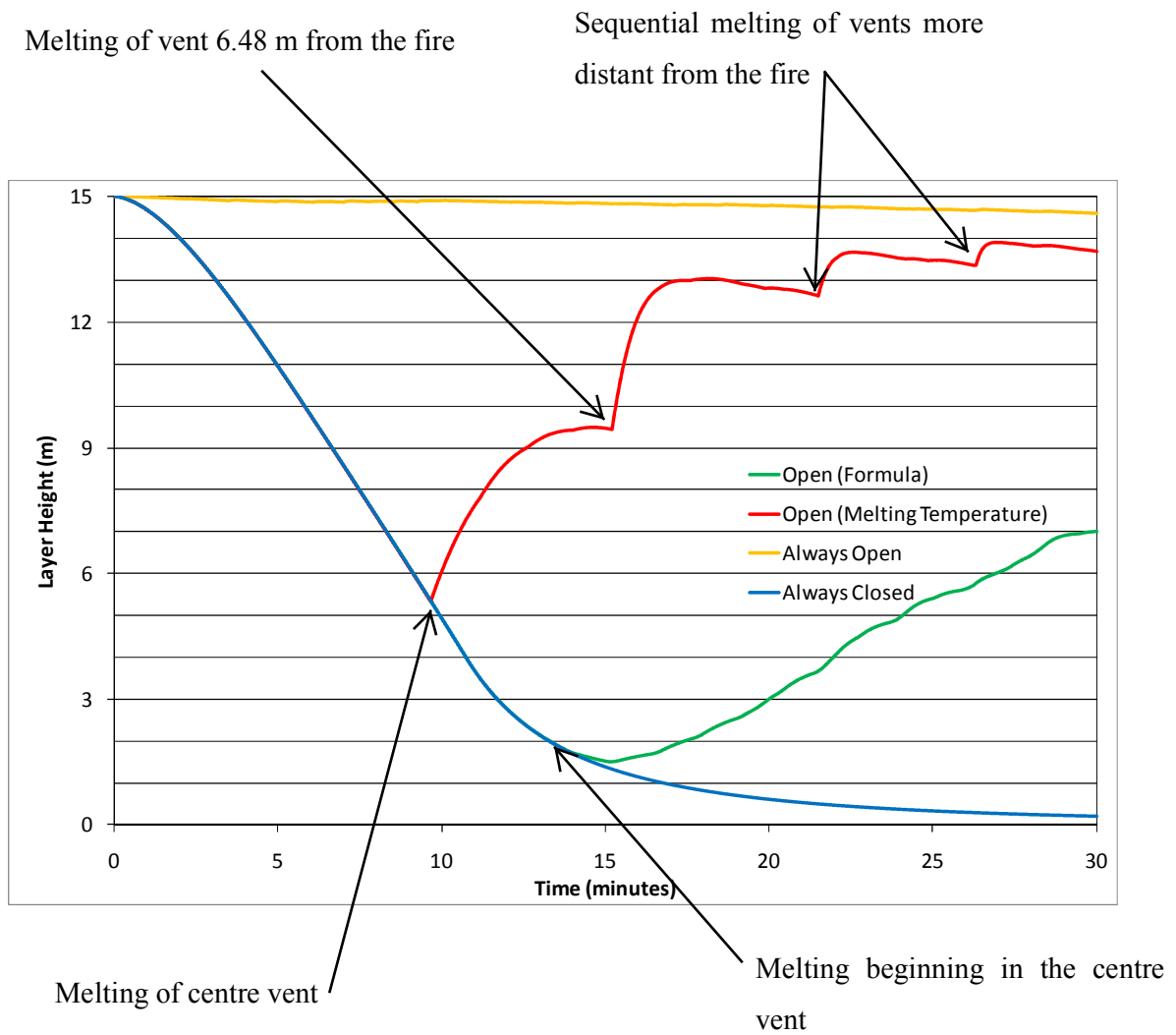


Figure 59: Layer heights for polycarbonate skylights with a fast fire growth rate

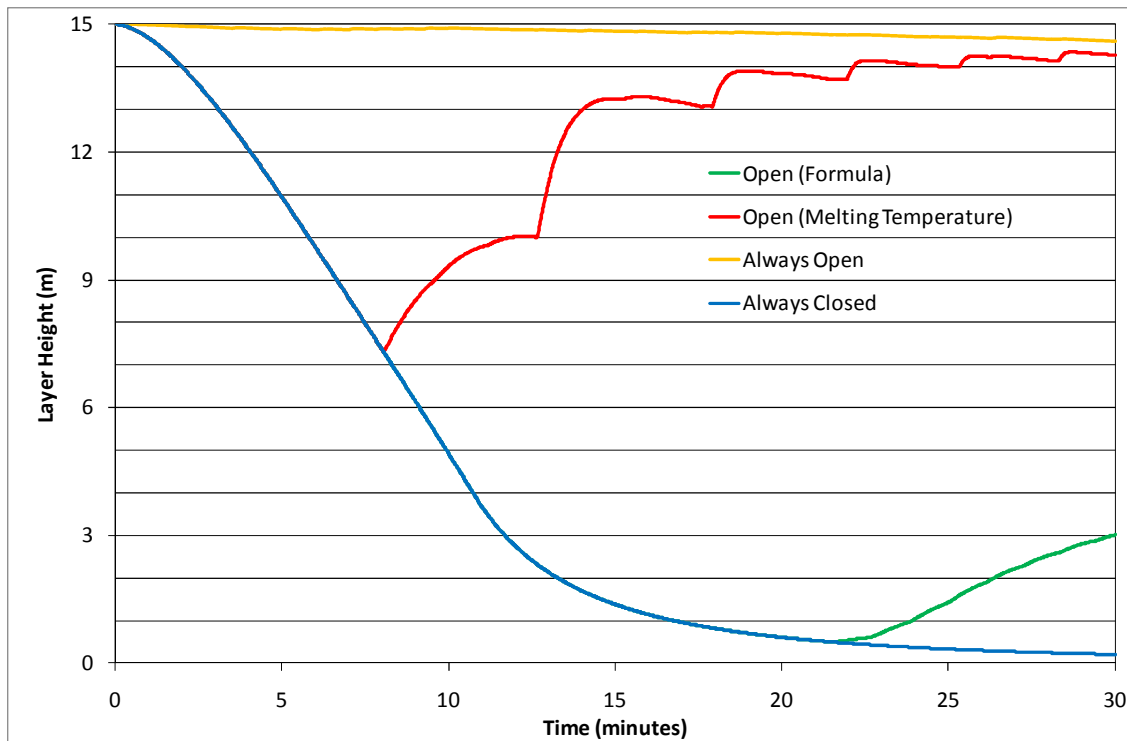


Figure 60: Layer heights for acrylic skylights with a fast fire growth rate

Figure 60 shows that the behaviour of the acrylic is similar to the polycarbonate and PVC. It should be noted that the melting temperature for the formula was 240°C while for the simple melting case it was 111°C. This was done as the intention was to compare the current knowledge with the new knowledge.

As stated in section 4.8 the use of the empirical equation for acrylic cannot be supported with the current experimental data.

Chapter 6 Discussion

6.1 Research Limitations

There are limitations to this research. The experiments were all carried out at small-scale, compromises were made for reasons of practicality, a limited range of temperatures and times were examined, and a limited range of materials.

The small scale tested resulted in a number of compromises. The compromises come in the detail of the connection. The connection was continuous across the short axis of the plastic sheet, whereas, full scale connections are discrete points of restraint across the short axis. The real world conditions would create localised stresses that combined with a softened material could lead to earlier failure.

Due to limitations on cost, time and equipment a limited number of temperature and time combinations could be tested. The oven limited the testing of all the materials to 300°C. The wind-tunnel performance limited the testing of materials that melted and therefore acted as vents to 250°C. As discussed in Section 7.1 there is scope for future research at higher temperatures to provide an increased understanding of the plastic behaviour.

The number of repeats at each temperature was also limited. This presents the issue that the results may be affected by the presence of outliers. This limitation is especially evident for the tests that were undertaken on the PVC at 200°C. The melting direction being away from the connections resulted in some of the samples staying connected and some not. Those that stayed connected resulted in reasonably small flows not much greater than seen at 150°C. The times when the connection failed the plastic occupied a smaller area of the horizontal plane of the vent but at the same time occupied part of the vertical plane. This resulted in cases where part of the wind tunnel was blocked and the flow was deflected out of the vent. This resulted in the flow being greater than 100%. With only three tests it is difficult to gauge the most appropriate flow to use.

Only one brand of each material was tested. Though the results are presented as general results it should be recognised that a complete testing of all materials available was not undertaken. Differences in processing and additive use may result in different behaviour.

The method of heating is something of a limitation on the applicability of this research. The oven heated the sample in a still environment. The heating in real buildings however is from

a ceiling jet which is moving a velocity. The oven heats both sides of the plastic whereas the ceiling jet only heats the underside of the plastic. Heat is then lost from the top of the plastic. The heating does not include the effects of the thermal radiation from the fire and is an area of possible future research.

This report is not intended to characterise the thermal properties of the skylight.

6.2 Angled Plate

The results from the angled plate provide some interesting data. The flows with the angled plate were higher than would be expected from a purely buoyant flow. This is indicated by the values over 100% and the high flow for the 15° angle. The results indicate that the flow is being physically deflected. This behaviour provides an explanation for the greater than 100% flows seen in some of the polyvinyl chloride experiments. It is also possible that the flow for the polycarbonate samples tested at 250°C may have provided a higher reading than those simply from buoyant flow.

The physical deflection of the flow is an issue in predicting the performance in a real building. This report has tried to limit the influence of this through limiting the flow to 100% efficiency when attempting to develop a formula to predict the efficiency.

The result when the plate was put in backwards with the plate connected to the downstream edge of the vent instead of the upstream edge the results were widely different. The backward result gave only 8% efficiency while the normal case gave a value of 131%. This is entirely expected as the normal case forces the air up and through the vent while the backward case forces the air flow down away from the vent. This though provides a problem for the designer depending on which part of the vent melts; either an enhancement or a degradation of efficiency may result.

There was surprisingly good agreement between a theoretical flow through the vent due to the deflection and the experimental results. The theoretical approach was rather crude as it assumed a plug flow, which is a large simplification and simply apportioned the flow pro rata between going through if it was above the bottom of the plate, or not if it was below. The model was improved by using an equivalent diameter formula (Chartered Institution of Building Services Engineers. 2001) to convert the square duct into a circular flow. The resulting equivalent diameter is very similar to that found using a simpler formula in the Howell (Howell et al. 2005).

As can be seen from Figure 51 an increase in the angle θ results in an increase in the percentage of the unimpeded baseline flow. The flow at 0° is 0. This is expected as at this angle the plate covers the entire outlet area. At an angle of 45° the flow is nearly the equivalent of the baseline flow. At 90° the flow is nearly double that of when no plate is present at all.

The results however are only indicative of the behaviour and very simplified. The melting behaviour of the plastic is much more complex. The plastic melts in numerous places and ways and results in changing angles. For example the polycarbonate had edges that melted down into the flow on the downstream and upstream edges. The results indicate that the flow may have been both boosted and restrained.

Due to the complexity of the issue around the boosted flows this thesis will restrict in the analysis and conclusion the flow to 100%.

6.3 Polycarbonate

The literature values for the melting of the polycarbonate ranged from 133°C to 250°C . Two of the sources gave a single value for the melting temperature of 133°C (NZ Metal Roofing Manufactures Inc. 2003) and 150°C (Rao & O'Brien 1998). The BRANZ literature review on the subject gave the melting temperature as a range from $135\text{-}200^\circ\text{C}$ (Edwards et al. 2007). A number of values were given in the Modern Plastic Hand book. These values ranged from 149°C to 250°C ; however the most common value was 150°C (Harper 2000).

The range of temperature indicates the difficulty that an engineer may encounter when designing, especially when dealing with a generic material such as polycarbonate. There is also another layer of complexity added when investigating the melting temperature of plastics as a single value such as that for a simple material. The differing level of additives to improve the plastic properties such as reducing the level of ultra violet light transmission can alter the temperature at which melting occurs.

The testing method and hence the definition of the temperature also impact on the value reported. For example a melting temperature calculated using the Vicat-B (Rao & O'Brien 1998) method defines melting as a point at which the plastic deflects under a load. Thus an engineer using a melting temperature found using this method and expecting the plastic to immediately change from a solid to a liquid, may end up with a design that is inappropriate.

The ideal melting temperature for this application of venting would be one in which the temperature is defined as when the plastic leaves the entire area of the vent clear.

The polycarbonate was tested at 150°C, 200°C and 250°C. At none of these values did the entire plastic sample melt from the frame. The plastic was observed to move from a state of no deformation to one where some minor dripping was seen. The preliminary test at 300°C showed a larger amount of the plastic dripping and had the plastic been left for a long enough time the plastic would likely have completely melted out. The same is true if the temperature was increased, with the time required to reach the fully melted stage decreasing.

The melting behaviour of the polycarbonate is possibly concerning as the dripping hot plastic could possibly result in spot fires or injuries to fire-fighters distant from the main fire.

6.4 Polyvinyl Chloride

The polyvinyl chloride material has long been used for this purpose and the initial testing of this type of system used this type of plastic. The UK report concluded that if the temperature of the ceiling jet was 300°C then the PVC panel would fall out and provide a vent (Hinkley & Theobald 1966). This report found that when exposed to a temperature of 250°C for five minutes the plastic melted from the vent and provided a clear area.

The lower temperature can be explained by a number of factors. The first is that the tests occurred over 40 years apart. During that time there may have been alterations to the additives used.

The second possible reason for the difference in the temperature at which the plastic melted is the way in which the heating of the sample occurred. The heating in the UK test occurred on only the underside of the plastic panel while the samples in this thesis were heated on both sides.

The final difference is that the UK test occurred at full scale while these test occurred at bench-scale.

6.5 Acrylic

The acrylic material behaviour was difficult to fully assess. The temperature at which the material displayed melting behaviour was 250°C. This temperature was also the maximum test temperature available.

The melting at this temperature was found to give an efficiency of 3% after 10 minutes of exposure and 9.4% after 20 minutes exposure. The behaviour at higher temperatures is unknown.

The temperature at which this melting occurred however is much higher than the values given in the BRANZ literature review, 50 – 140°C (Edwards et al. 2007), design data for plastic engineers, 105°C (Rao & O'Brien 1998) or the modern plastic handbook, 90-165°C (Harper 2000). The result was seen in the other products tested but not to the extent seen for the acrylic. This highlights the difficulty of using data for products which are generic. The four resins, polycarbonate, polyvinyl chloride, Acrylic and polyester are used for many applications and not exclusively for plastic roofing.

6.6 GRP

The GRP material is very different from the other three materials. For one the GRP is a composite material consisting of a glass fibre matrix and a plastic resin. The other three materials are pure materials. The second major difference is that the plastic resin is a thermo setting plastic. The thermo setting plastic does not melt as the thermo plastic does but chars.

The differences continued into how the material behaved in the oven. The material unlike the other three plastics did not lose strength and sag nor did it shrink. The GRP turned yellow and then an orange brown. The glass fibre is used to increase the strength of the material. The melting temperature of glass is around 600°C (Buchanan 2001). The plastic is polyester and has a melting temperature of 245°C. However the plastic does not really melt but burn.

The GRP was exposed for two hours at 300°C. The plastic did not deform, melt or ignite. The material did change colour and some smoke was observed and the material did seem thinner than at the start. However, the thickness of the material was not measured before or after the experiments.

The resistance of the GRP to heat resulted in the material being inefficient as a smoke and heat vent when the temperature is at or below 300°C.

6.7 Prediction of Vent efficiency

The empirical equation developed to predict the vent efficiency provides a good match for the polycarbonate data. However, the results for the PVC are disappointing. Some of the data scatter may be due to the extra flow caused by physical deflection of the flow. To get a

reasonable result for the acrylic the melting temperature had to be increased from 111°C to 240°C. This value is arbitrary and is not supported by the literature values in Table 1. There is also insufficient experimental data to determine if the empirical relationship is appropriate for this material.

The empirical relationship is

$$E = 22.5 \ln \left(\left(\frac{t}{-\frac{1}{k} \ln \left(\frac{T_m - T_e}{T_i - T_e} \right)} \right) \frac{T_e}{T_m} \right) - 430$$

With the following limits

$$T_m < T_e \leq 250 \text{ } ^\circ\text{C}$$

$$5 < t < 20 \text{ minutes}$$

$$0 \leq E \leq 100\%$$

The material should be PVC or polycarbonate.

6.8 Modelling

The results of the modelling must be interpreted carefully. The model contains many limitations and simplifications as discussed in Chapter 5. There has been no attempt to match the model to experimental data and the model only reflects an idealised case and not a real world case.

The model does however show greatly varying behaviour. The vent opening at a literature melting temperature value opens first and earlier than a simulation based on the results of the experiments. The earlier provision of area brought about by the literature value temperature resulted in the layer of the hot gases being higher throughout the test period, than the layer height calculated when the vent opened based on the results of the experiments.

The above behaviour is as expected due to the melting during the experiments beginning at or above the values in Table 1.

Chapter 7 **Conclusion**

The thesis increases the knowledge on the behaviour of the skylight plastic used in New Zealand. The melting behaviour is complex and involves changes in the geometry and strength of the material. The material may either become liquid and flow or char.

The thesis has provided experimental data on the efficiency of the plastics. The GRP has no efficiency below 300°C. The acrylic has a small efficiency at 250°C. The polycarbonate and PVC materials were more complex with the efficiency increasing with both increased time and temperature. An empirical relationship has been developed for the PVC and polycarbonate plastics however this is based on small scale experiments in an ideal geometry. The maximum temperature that the PVC, polycarbonate and acrylic were tested to was 250°C. The GRP was tested to 300°C.

7.1 Further Research

This work improves the knowledge on the use of plastic skylights as smoke vents however it does not answer all the questions. The following are recommendations on areas of further research

- Full scale experiments to compare the validity of the small-scale experiments with the full-scale behaviour of the material.
- Further experiments at higher temperatures and more intermediate times, this is especially necessary for the acrylic and GRP material.
- Undertake further tests on material from multiple manufactures and suppliers to obtain a more generic empirical relationship.
- Investigate the heat transfer between the hot gas and the plastic panels.
- Further work on the reliability of the skylights. This should look at the problem in terms of the design and the consequence of that. For example if the average value is used and the true performance of the skylight is less what is the consequence on the performance of the building.

- A cost/benefit study of the skylights when compared to alternate options for example sprinklers, automatically activated natural vents, mechanical ventilation or no ventilation
- More detailed modelling of this type of building investigating the behaviour of the layer height, temperature, gas concentrations and visibility. This should include the effects of the heat being lost through the vent.
- Investigate the appropriateness of the 15% vent area for the various materials.
- Undertake experiments on material from a number of manufactures to quantify the effects of the generic material.

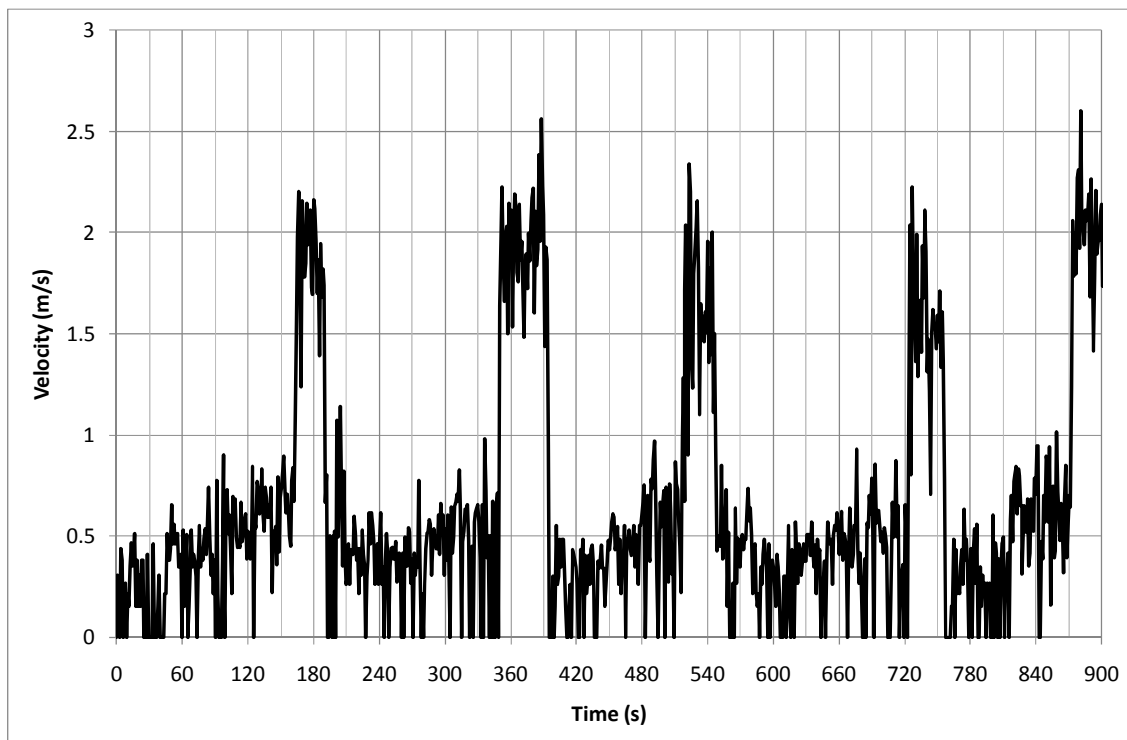
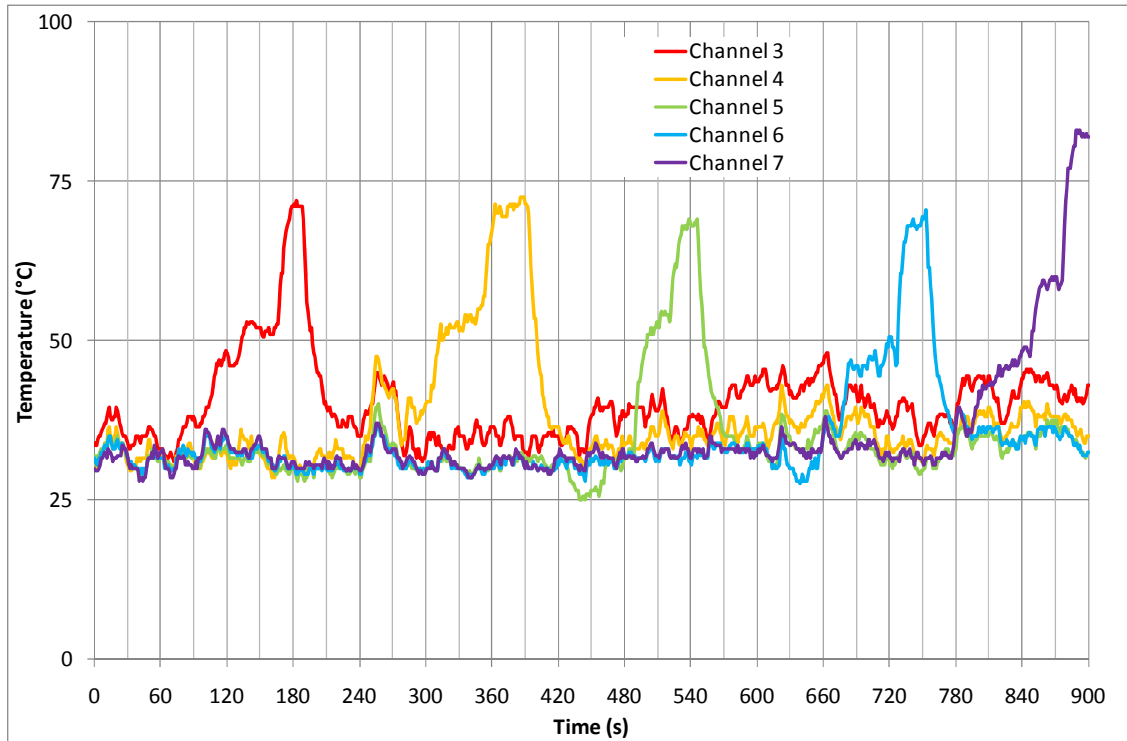
Chapter 8 References

- Alpert RL 2008. Ceiling Jet Flows. In: DiNunno PJ ed. SFPE Handbook of Fire Protection Engineering. 4th Edition ed. Quincy, National Fire Protection Association.
- Australian Building Codes Board 2009. BCA : Building Code of Australia. Canberra, A.C.T., CanPrint Communications on behalf of the ABCB. v p.
- Australian Fire Authorities Council 2004. Fire Brigade Intervention Model. Version 2.2.
- Billo EJ 2007. Excel for scientists and engineers : numerical methods. Hoboken, N.J., Wiley. xix, 454 p.
- Buchanan AH 2001. Structural design for fire safety. Chichester, England ; New York, Wiley. xxii, 421 p.
- Chartered Institution of Building Services Engineers. 2001. Reference data : CIBSE guide C. [New]. ed. Oxford, Butterworth-Heinemann. 1 v. (various pagings) p.
- Chin KS 2002. Development of bench-scale testing of sprinkler and smoke detector activation/response time : this report was presented as a project report as part of the M.E. (Fire) degree at the University of Canterbury. vii, 82 leaves p.
- Cosgrove BW 1996. Fire design of single storey industrial buildings : a report submitted in partial fulfilment of the requirements for the degree of Master of Engineering at the University of Canterbury, Christchurch, New Zealand. xiv, 159 p.
- Cox G 1977. Gas velocity measurement in fire by the cross-corellation of random thermal fluctuations - a comparison with conventional technique. Combustion and Flame.
- Department of Building and Housing 2008a. Effective venting for single storey buildings. Codewords(25).
- Department of Building and Housing 2008b. Compliance Document for New Zealand Building Code Clauses C1, C2, C3, C4 Fire Safety. Wellington, Vic Books.
- Edwards APR, Soja E, Wade CA 2007. Effective Passive Roof Venting in the Event of Fire - Literature Review. BRANZ Study Report SR 165.
- Emmons HW, Tanaka T 2008. Vent Flows. In: DiNunno PJ ed. SFPE Handbook of Fire Protection Engineering. 4th Edition ed. Quincy, National Fire Protection Association.
- Erhard G 2006. Konstruieren mit Kunststoffen
Designing with plastics. Cincinnati, Hanser Gardner Publications. xii, 517 p.
- Harper CA 2000. Modern plastics handbook. New York, McGraw-Hill. 1 v. (various pagings) p.
- Hinkley PL, Theobald CR 1966. PVC Rooflights for Venting Fires in Single-Storey Buildings.
- Howell RH, Sauer HJ, Coad WJ 2005. Principles of heating, ventilating, and air conditioning. Atlanta, Ga., American Society of Heating Refrigerating and Air-Conditioning Engineers. 494 p.
- Incropera FP, DeWitt DP, Bergman TL, Lavine AS 2007. Fundamentals of heat and mass transfer Frank P. Incropera ... [et al.]. 6th / ed. Hoboken, N.J., Wiley. xxv, 997 p.
- Johnson RA, Miller I 2005. Miller and Freund's probability and statistics for engineers. Upper Saddle River, NJ, Pearson Prentice Hall. xi, 642 p.
- Karlsson B, Quintiere JG 2000. Enclosure fire dynamics. Boca Raton, FL, CRC Press. 315 p.
- Klote JH, Milke JA, American Society of Heating Refrigerating and Air-Conditioning Engineers., Society of Fire Protection Engineers. 2002. Principles of smoke management. Atlanta, Ga., American Society of Heating Refrigerating and Air-Conditioning Engineers. x, 377 p.
- Newman GM 1990. Fire and Steel Construction: the Behaviour of Steel Portal Frames in Boundary Conditions. 2nd Edition ed. Berkshire, The Steel Construction Institute.

- NZ Metal Roofing Manufactures Inc. 2003. NZ Metal Roof and Wall Cladding Code of Practice.
- Pringle T 1998. Selecting roof claddings : a guide to choosing roof materials. [Porirua, N.Z.], Branz. 118 p.
- Rao NS, O'Brien KT 1998. Design data for plastics engineers. Munich Cincinnati, Hanser ; Hanser/Gardner Publications. x, 207 p.
- Robbins AP, Wade CA 2008a. Effective Passive Roof Venting in the Event of Fire Part 1: Preliminary Modelling Results. BRANZ Study Report SR 197.
- Robbins AP, Wade CA 2008b. Effective Passive Roof Venting in the Event of Fire Part 2: Preliminary Experimental Results. BRANZ Study Report SR 198.
- Robbins AP, Wade CA 2008c. Effective Passive Roof Venting in the Event of Fire Part 3: Summary. BRANZ Study Report SR 199.
- SFPE 2008. Conversion Factors. In: DiNunno PJ ed. SFPE Handbook of Fire Protection Engineering. 4th Edition ed. Quincy, National Fire Protection Association.
- Standards Association of Australia 2001. AS 2665: Smoke/Heat Venting Systems: design instalation and commissioning. Sydney, Standards Association of Australia.
- Standards Association of Australia., Standards New Zealand. 1994a. AS/NZS 4256.2 Part 2:Unplasticized polyvinyl chloride building sheets. Homebush, N.S.W. Wellington, N.Z., Standards Australia ; Standards New Zealand. 8 p.
- Standards Association of Australia., Standards New Zealand. 1994b. AS/NZS 4256.3 Part 3:Glass fibre reinforced polyester (GRP). Homebush, N.S.W. Wellington, N.Z., Standards Australia ; Standards New Zealand. 12 p.
- Standards Association of Australia., Standards New Zealand. 1995. AS/NZS 4256.5 Part 5: Polycarbonate. Homebush, N.S.W. Wellington, N.Z., Standards Australia ; Standards New Zealand. 12 p.
- Standards Association of Australia., Standards New Zealand. 1996a. AS/NZS 4389 Safety mesh. Homebush, N.S.W. Wellington, N.Z., Standards Australia ; Standards New Zealand. 16 p.
- Standards Association of Australia., Standards New Zealand. 1996b. AS/NZS 4256.6 Part 6: Acrylic. Homebush, N.S.W. Wellington, N.Z., Standards Australia ; Standards New Zealand. 12 p.
- Thomas PH, Hinkley PL 1964. Design of Roof Venting Systems for Single Story Buildings.
- Thomas PH, Hinkley PL, Theobald CR, Simms DL 1963. Investigation into the Flow of Hot Gases in Roof Venting.
- Tsui A 2004. Statistical analysis of sprinkler response time index and conduction factor using the plunge test : a thesis submitted as partial fulfilment of the Masters [i.e. Master] of Fire Engineering at the University of Canterbury. ii, 175 p.
- Yu X 2007. Investigation of recessed and concealed sprinklers activation in wind tunnel plunge test and in BRANZFIRE computer model : a thesis submitted in partial fulfilment of the requirements for the degree of Master of Engineering in Fire Engineering, Department of Civil Engineering, University of Canterbury. 260 p.

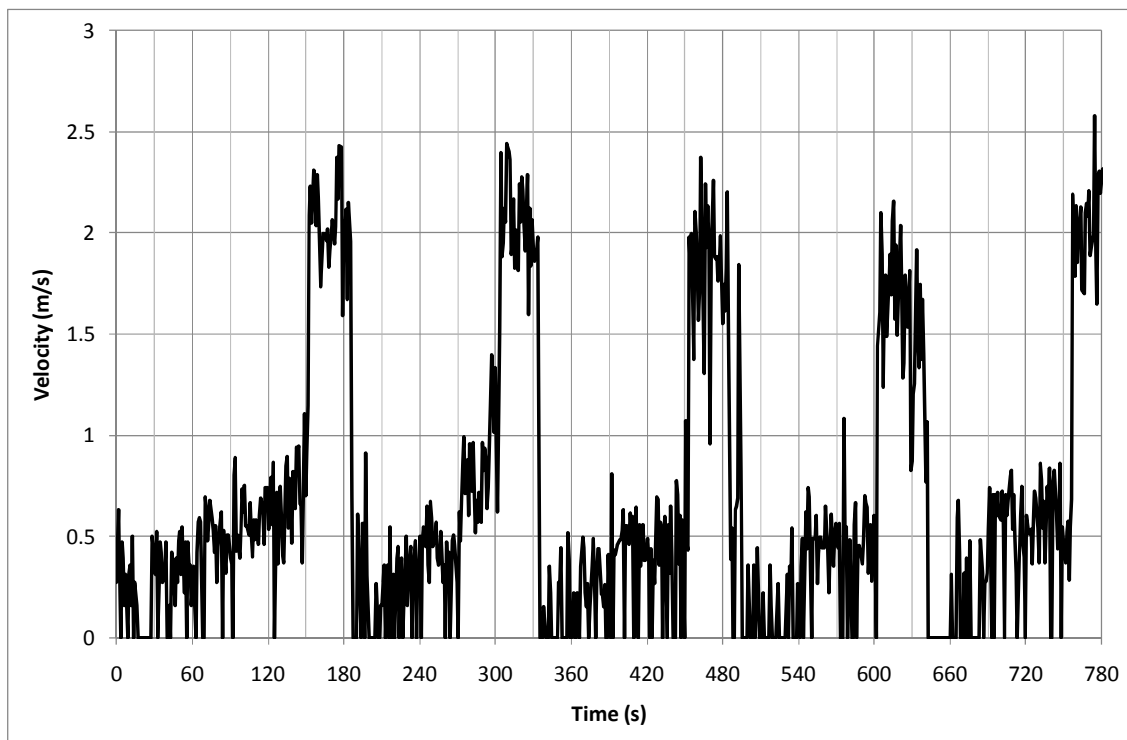
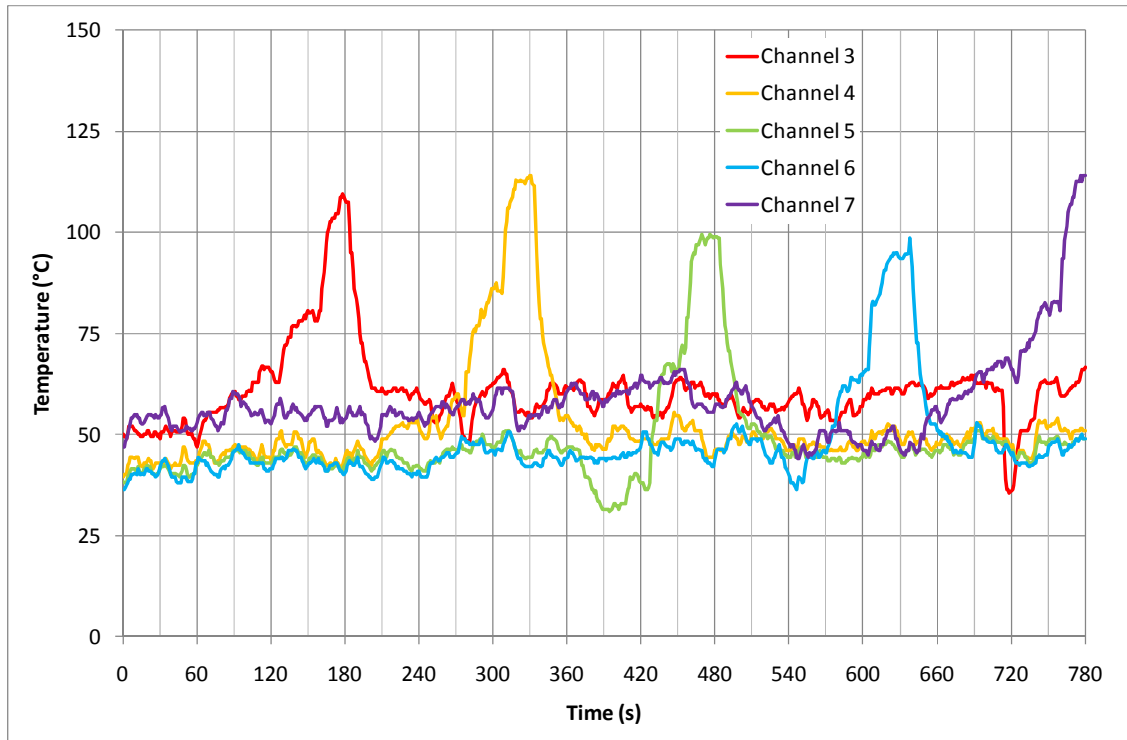
Appendix A Baseline Results

Baseline 100°C



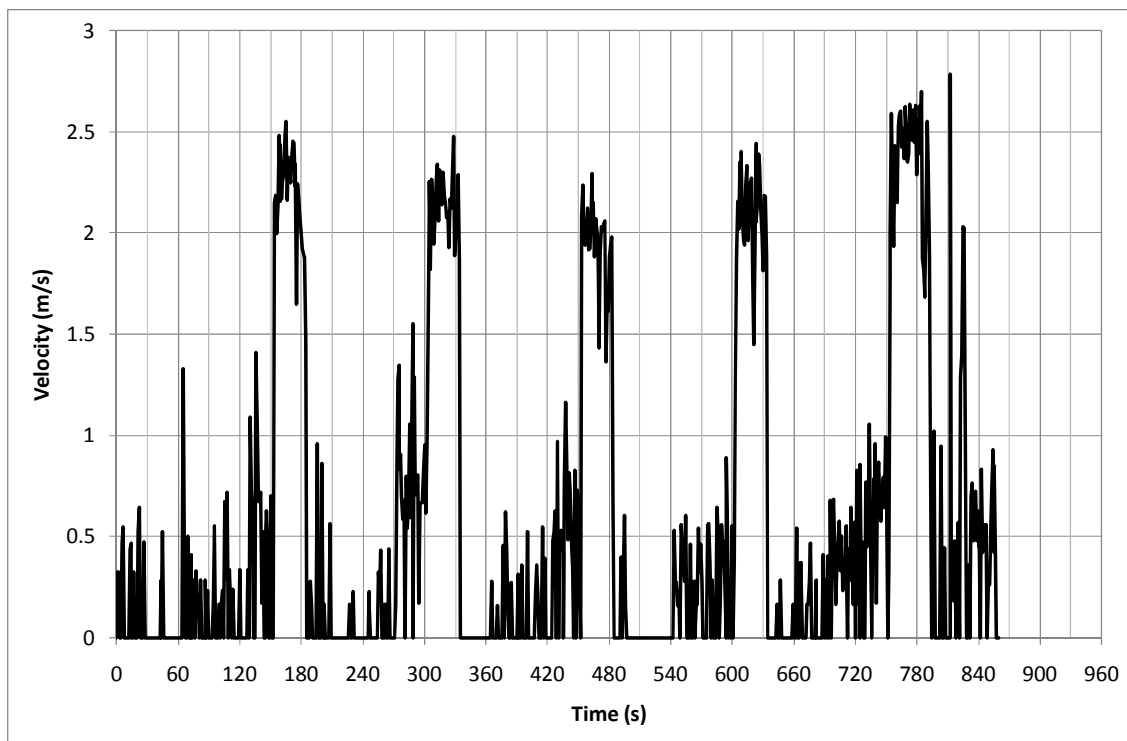
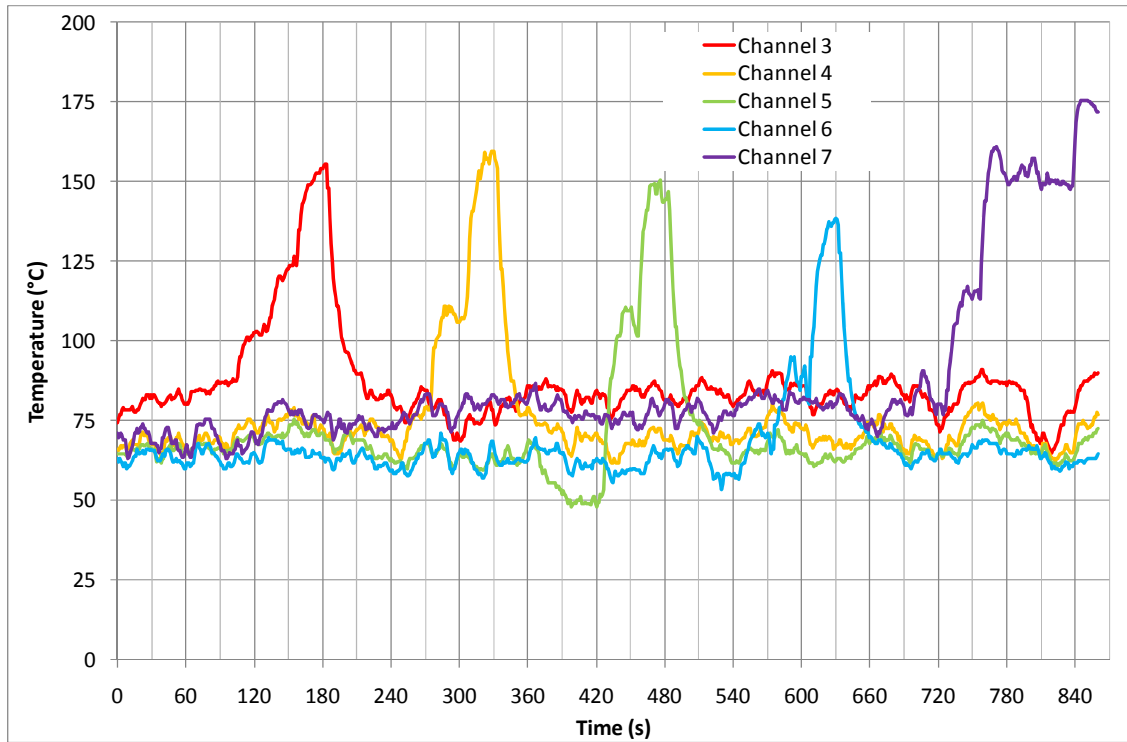
Bar	Point	Time (s)	Temperature (°C)	Velocity (m/s)
1	1	60	34.70	0.44
1	2	90	37.40	0.45
1	3	120	46.75	0.52
1	4	150	52.45	0.56
1	5	180	67.60	1.95
2	1	240	30.95	0.46
2	2	270	42.25	0.37
2	3	300	38.40	0.51
2	4	330	52.20	0.49
2	5	360	61.00	1.91
3	1	420	30.45	0.24
3	2	450	25.60	0.36
3	3	480	30.50	0.47
3	4	510	51.70	0.43
3	5	540	67.75	1.67
4	1	600	33.20	0.34
4	2	630	32.30	0.41
4	3	660	31.40	0.51
4	4	690	45.10	0.45
4	5	750	68.15	1.45
5	1	780	32.55	0.36
5	2	810	42.10	0.33
5	3	840	46.55	0.59
5	4	870	59.20	0.60
5	5	900	82.40	1.97

Baseline 150°C



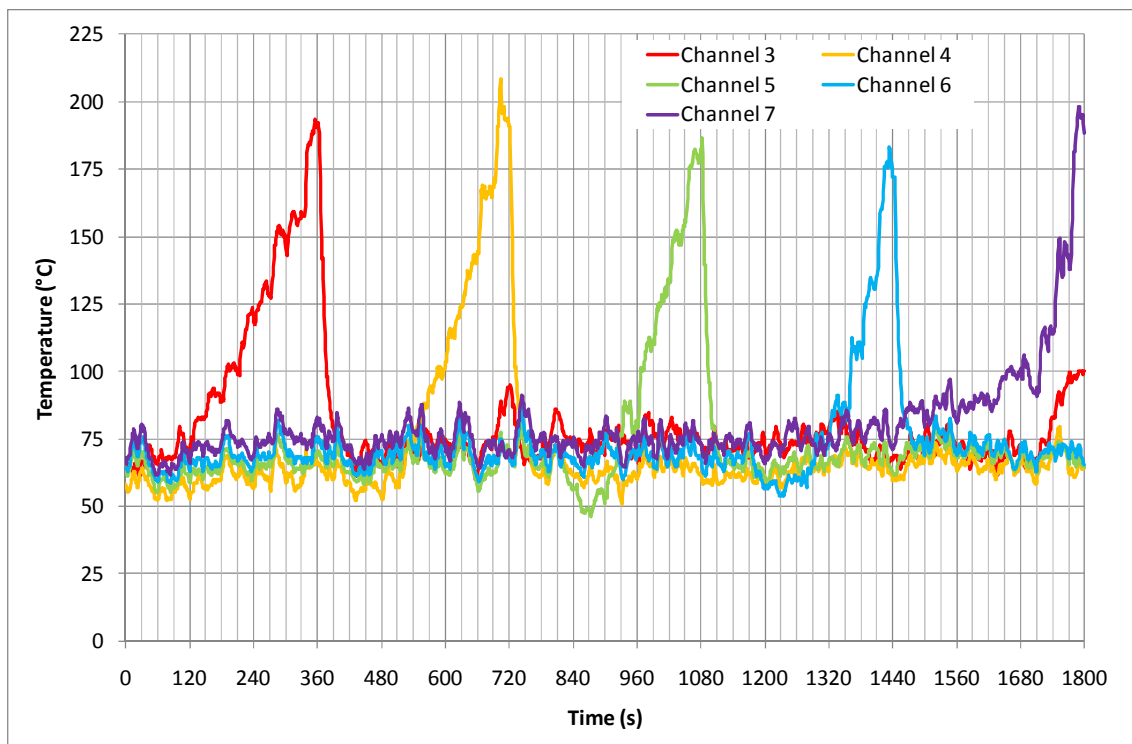
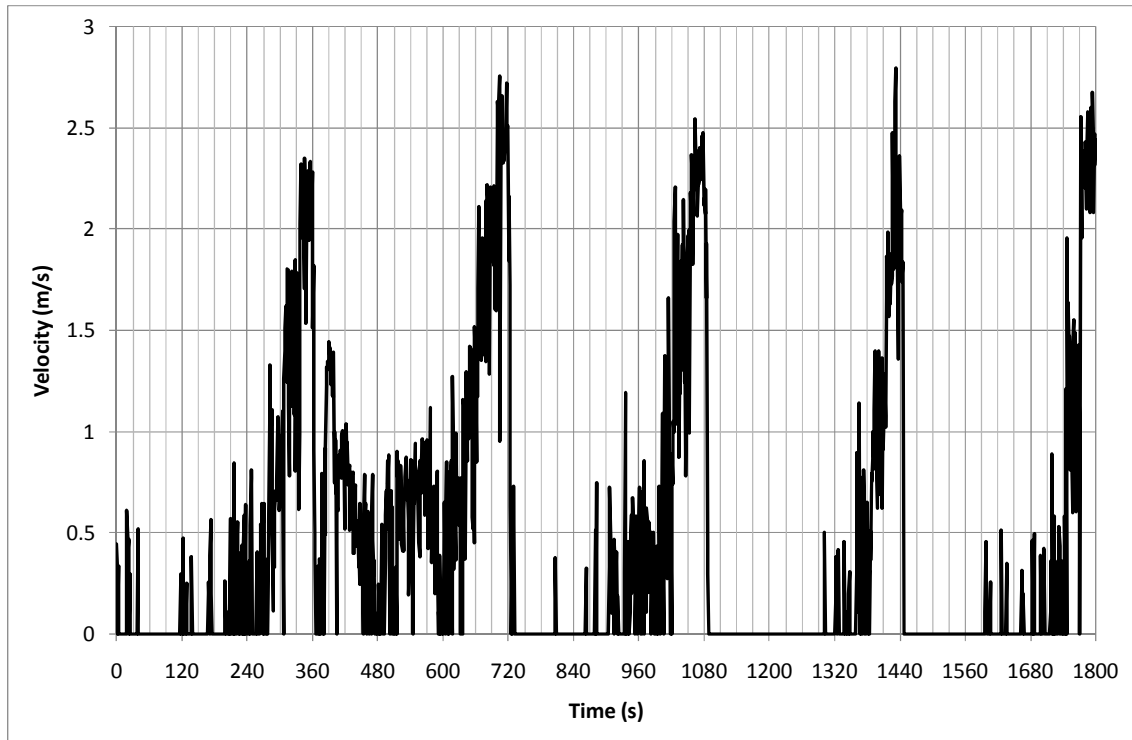
Bar	Point	Time (s)	Temperature (°C)	Velocity (m/s)
1	1	60	50.40	0.37
1	2	90	57.95	0.46
1	3	120	66.00	0.61
1	4	150	78.10	0.80
1	5	180	99.65	2.13
2	1	210	44.75	0.00
2	2	240	52.80	0.31
2	3	270	54.90	0.37
2	4	300	82.25	1.05
2	5	330	112.75	2.05
3	1	360	46.70	0.12
3	2	390	34.10	0.25
3	3	420	39.15	0.46
3	4	450	66.85	0.39
3	5	480	92.90	1.82
4	1	510	49.50	0.00
4	2	540	44.30	0.22
4	3	570	45.25	0.49
4	4	600	63.85	0.53
4	5	630	93.95	1.63
5	1	660	54.85	0.00
5	2	690	60.45	0.00
5	3	720	67.80	0.48
5	4	750	80.10	0.50
5	5	780	112.00	2.11

Baseline 200°C



Bar	Point	Time (s)	Temperature (°C)	Velocity (m/s)
1	1	60	82.35	0.00
1	2	90	85.75	0.00
1	3	120	100.25	0.00
1	4	150	120.25	0.34
1	5	180	143.85	2.21
2	1	210	70.75	0.00
2	2	240	70.15	0.00
2	3	270	76.95	0.00
2	4	300	108.25	0.80
2	5	330	157.45	2.14
3	1	360	63.55	0.00
3	2	390	54.40	0.00
3	3	420	49.50	0.00
3	4	450	107.20	0.45
3	5	480	139.45	1.79
4	1	510	66.60	0.00
4	2	540	57.35	0.00
4	3	570	71.70	0.04
4	4	600	90.30	0.41
4	5	630	135.55	2.08
5	1	660	74.30	0.00
5	2	690	80.70	0.00
5	3	720	81.50	0.35
5	4	750	114.40	0.74
5	5	780	156.55	2.49

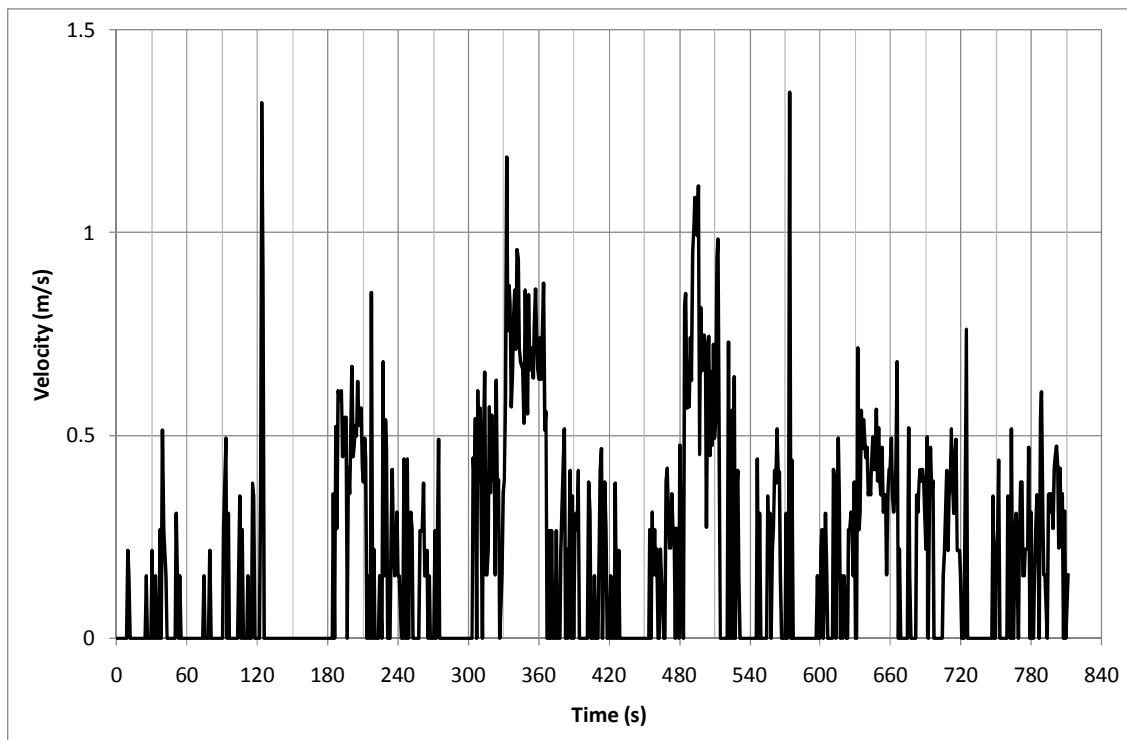
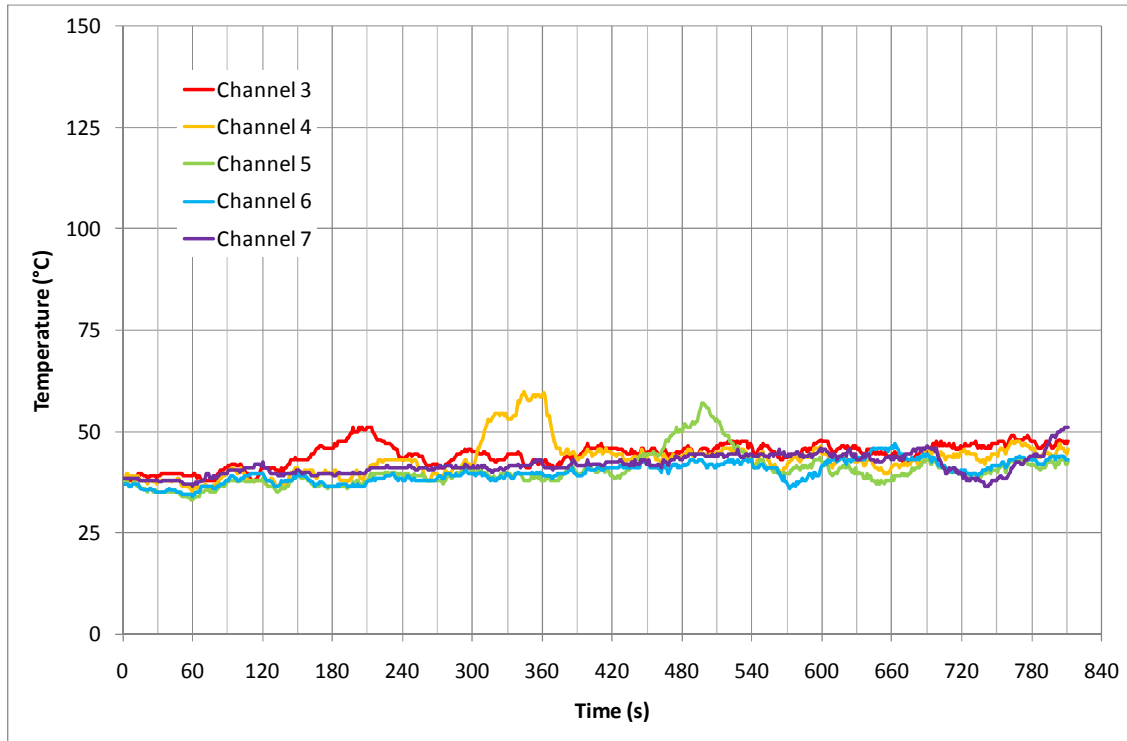
Baseline 250°C



Appendix B Polycarbonate Experiments Results

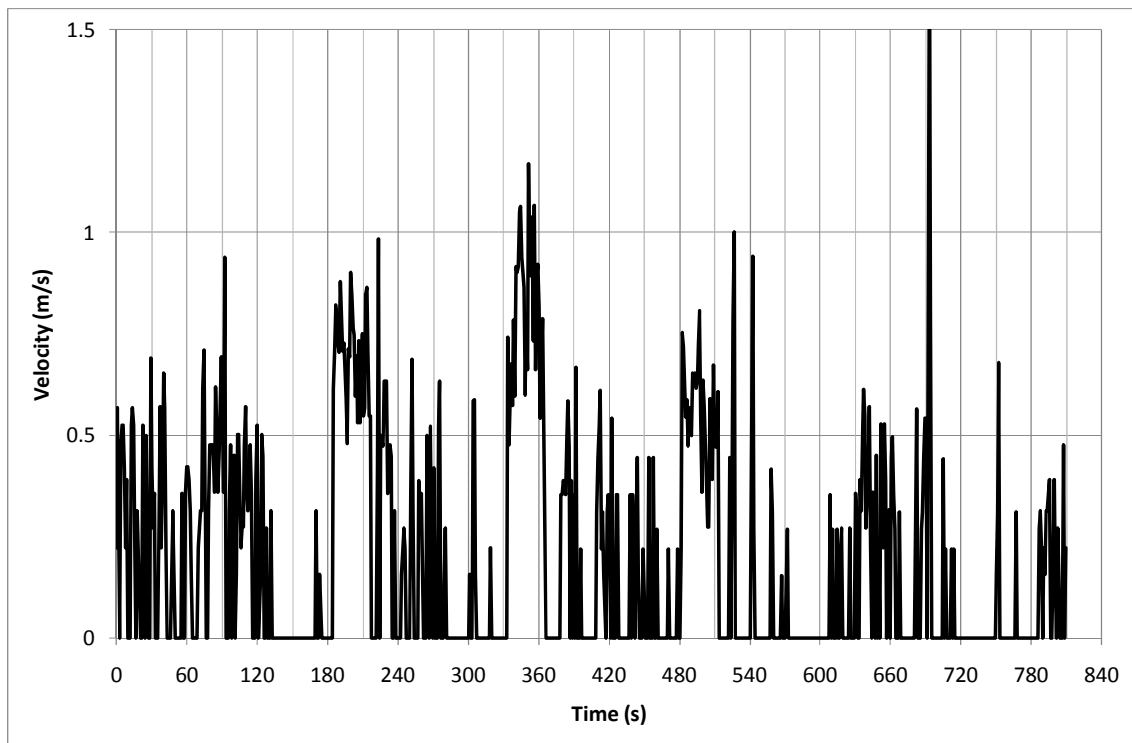
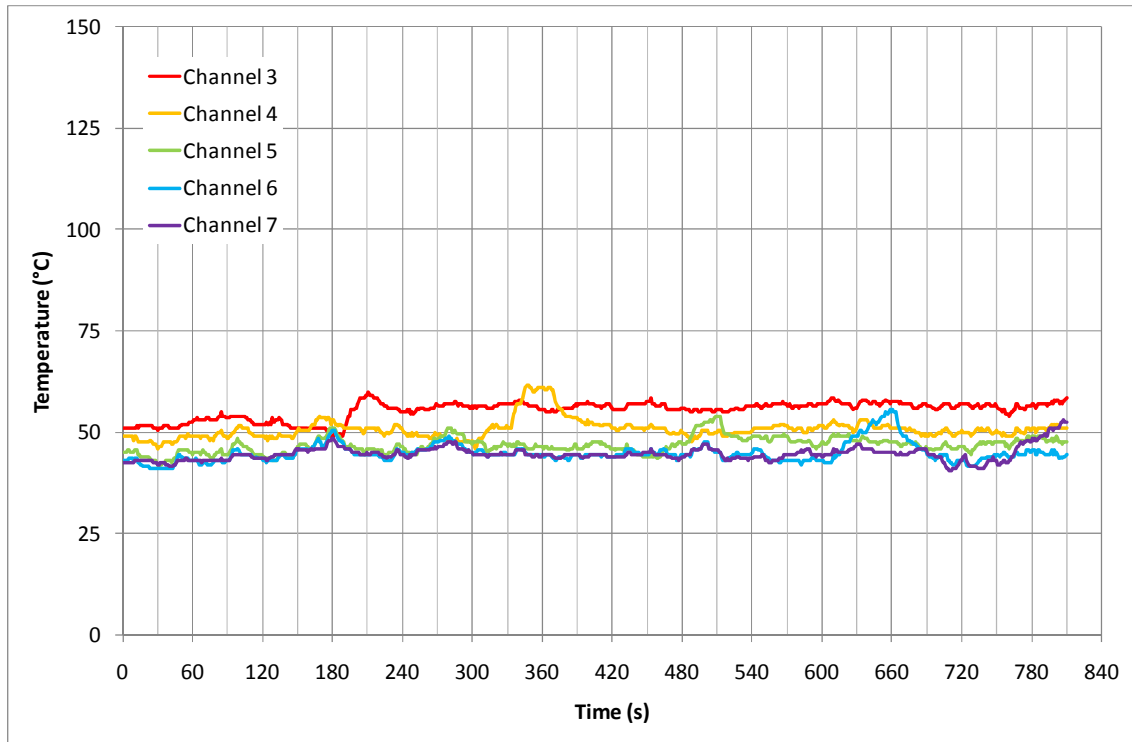
150°C 5 Minutes

Test 1



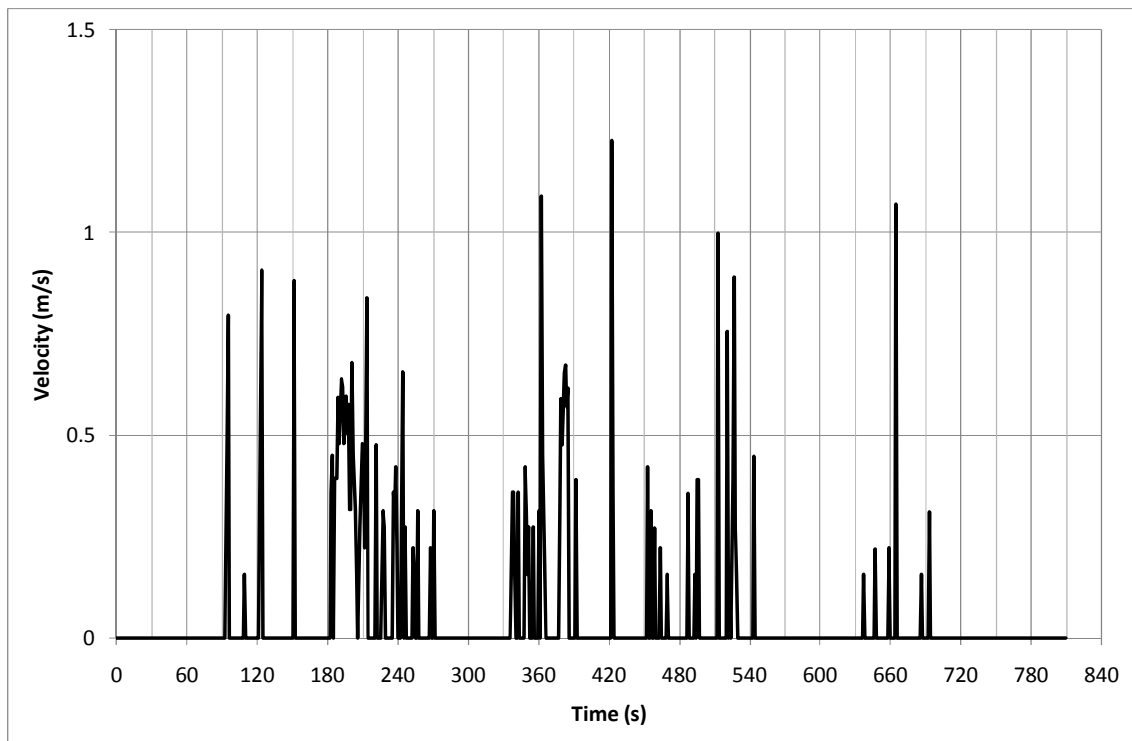
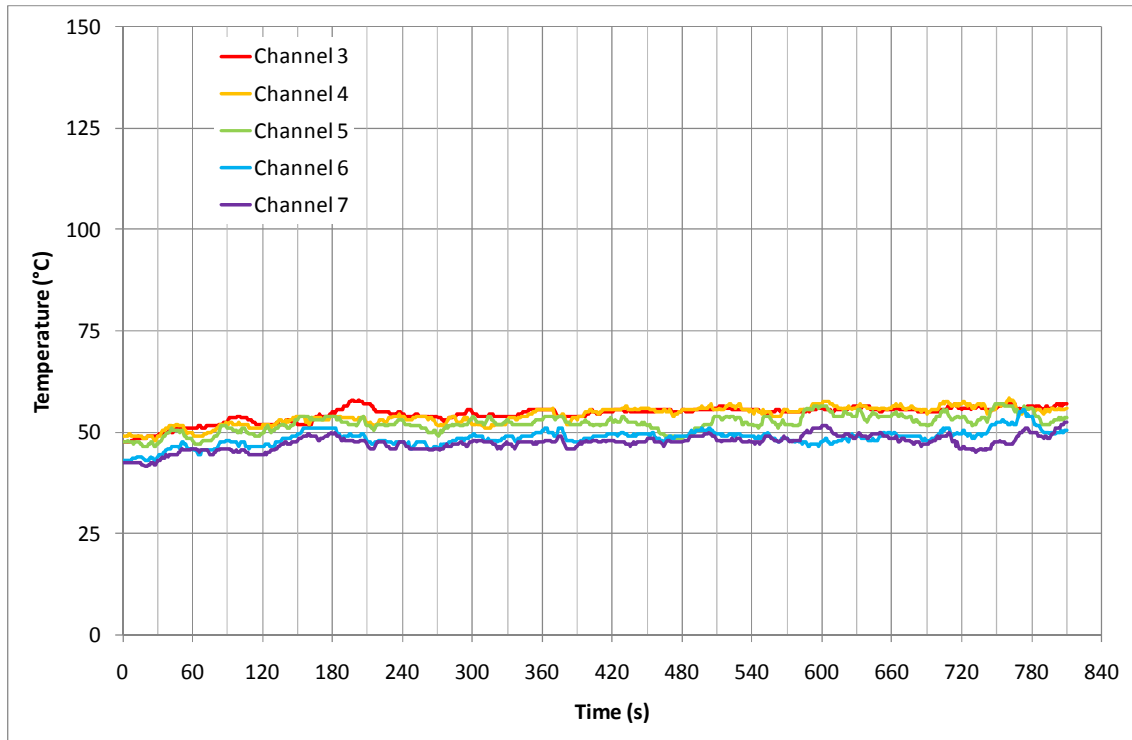
Bar	Point	Time (s)	Temperature (°C)	Velocity (m/s)
1	1	90	40.30	0.00
1	2	120	38.90	0.00
1	3	150	42.50	0.00
1	4	180	46.10	0.00
1	5	210	50.50	0.53
2	1	240	43.00	0.22
2	2	270	38.75	0.13
2	3	300	42.10	0.00
2	4	330	54.35	0.39
2	5	360	58.70	0.72
3	1	390	40.55	0.27
3	2	420	40.30	0.22
3	3	450	43.85	0.00
3	4	480	49.85	0.18
3	5	510	53.05	0.62
4	1	540	42.70	0.00
4	2	570	39.15	0.31
4	3	600	39.75	0.00
4	4	630	42.85	0.20
4	5	660	45.80	0.39
5	1	720	40.40	0.37
5	2	750	37.20	0.00
5	3	780	42.90	0.29
5	4	810	50.15	0.34
5	5	840	50.40	0.31

Test 2



Bar	Point	Time (s)	Temperature (°C)	Velocity (m/s)
1	1	90	53.85	0.00
1	2	120	52.20	0.00
1	3	150	51.30	0.00
1	4	180	50.10	0.00
1	5	210	57.30	0.43
2	1	240	51.20	0.00
2	2	270	49.00	0.00
2	3	300	47.75	0.00
2	4	330	51.25	0.00
2	5	360	60.65	0.74
3	1	390	46.10	0.00
3	2	420	46.65	0.00
3	3	450	44.40	0.00
3	4	480	47.00	0.00
3	5	510	52.15	0.00
4	1	540	44.50	0.00
4	2	570	42.90	0.00
4	3	600	43.25	0.00
4	4	630	48.35	0.00
4	5	660	54.35	0.00
5	1	690	45.90	0.00
5	2	720	41.60	0.00
5	3	750	42.80	0.00
5	4	780	47.55	0.00
5	5	810	51.85	0.00

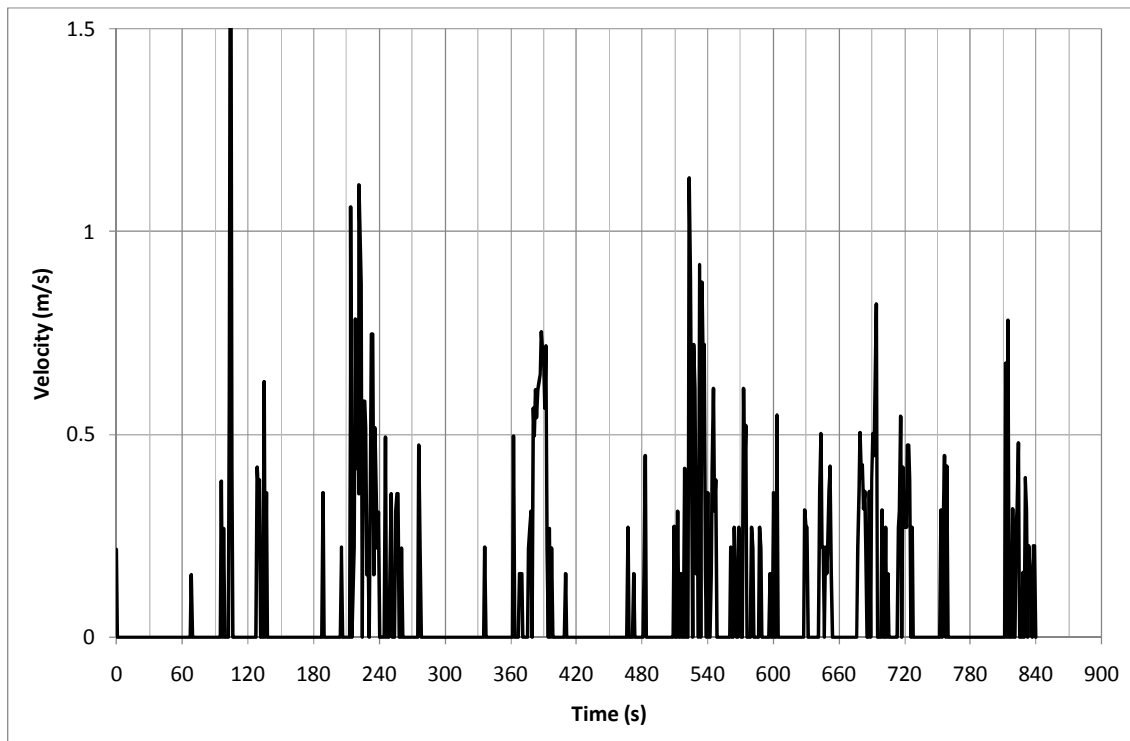
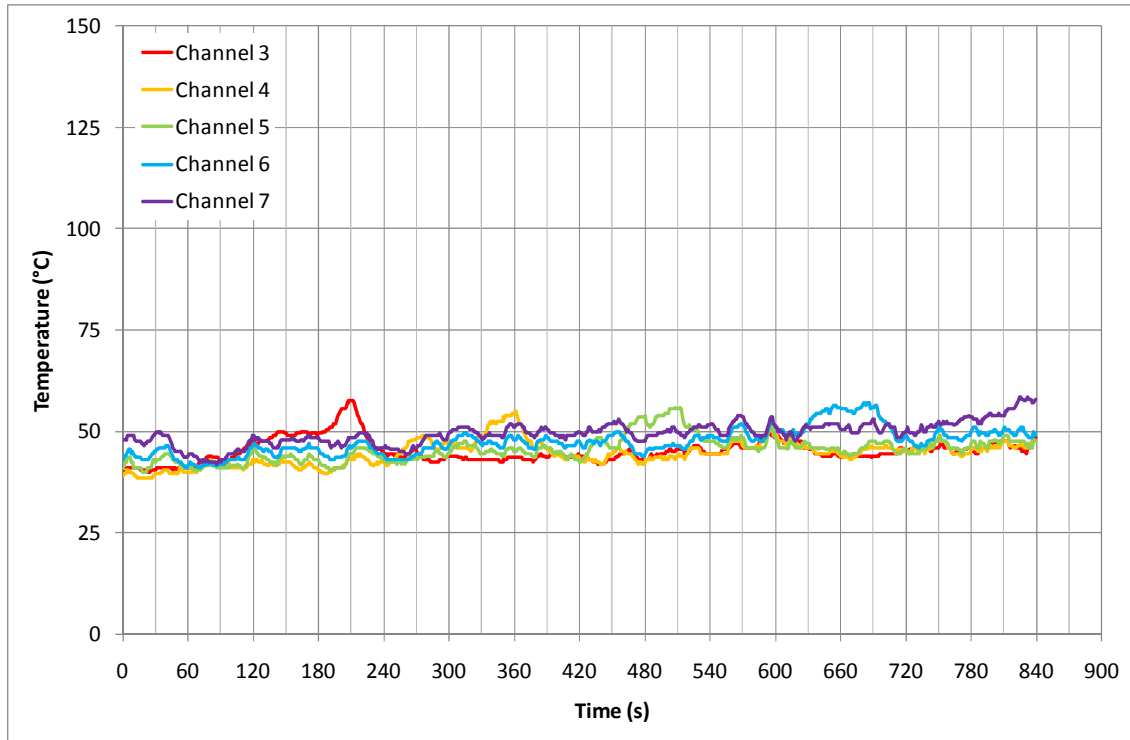
Test 3



Bar	Point	Time (s)	Temperature (°C)	Velocity (m/s)
1	1	90	52.10	0.00
1	2	120	52.35	0.00
1	3	150	52.75	0.00
1	4	180	54.20	0.00
1	5	210	56.90	0.37
2	1	240	53.95	0.00
2	2	270	53.15	0.00
2	3	300	52.85	0.00
2	4	330	52.05	0.00
2	5	360	55.15	0.00
3	1	390	52.20	0.28
3	2	420	52.35	0.00
3	3	450	52.20	0.00
3	4	480	48.70	0.00
3	5	510	52.35	0.00
4	1	540	49.05	0.00
4	2	570	48.15	0.00
4	3	600	47.05	0.00
4	4	630	48.65	0.00
4	5	660	49.65	0.00
5	1	690	47.15	0.00
5	2	720	47.20	0.00
5	3	750	46.45	0.00
5	4	780	50.45	0.00
5	5	810	51.60	0.00

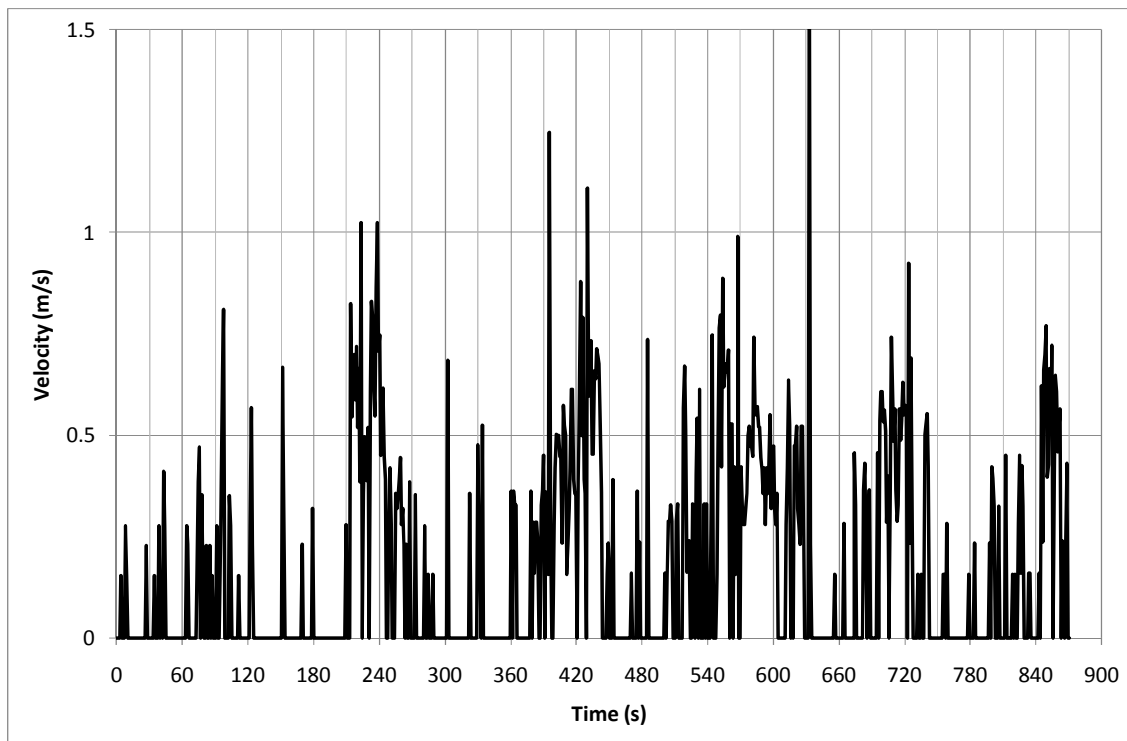
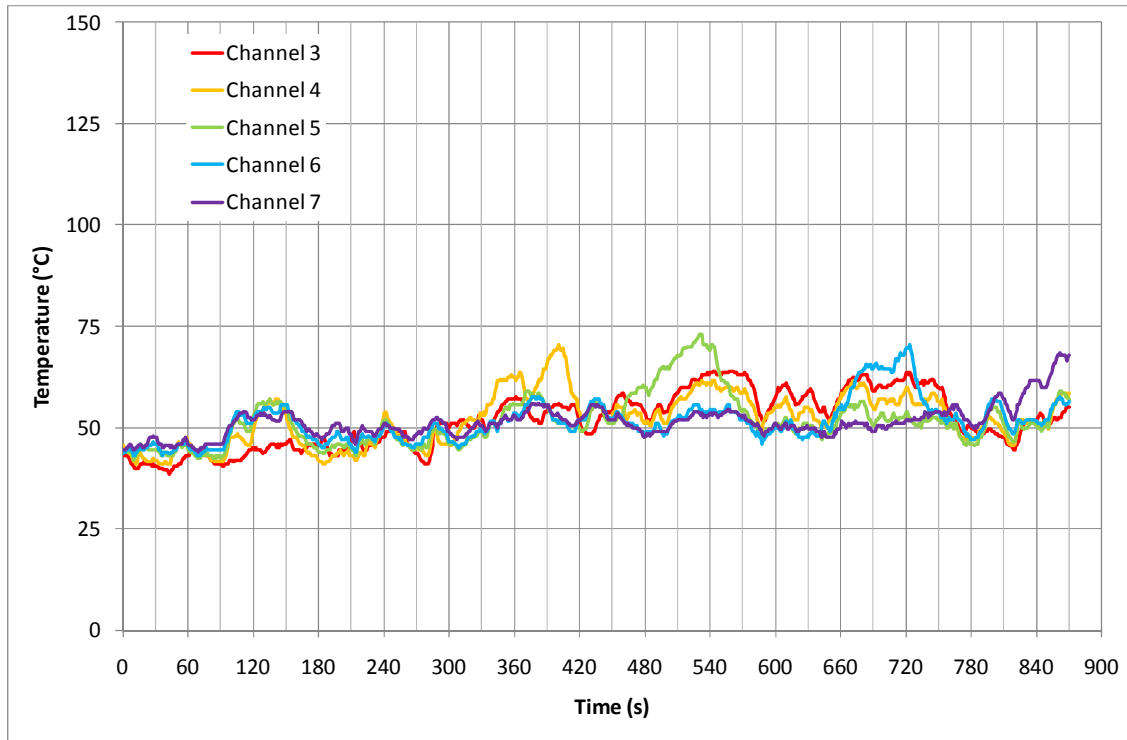
10 Minutes

Test 1



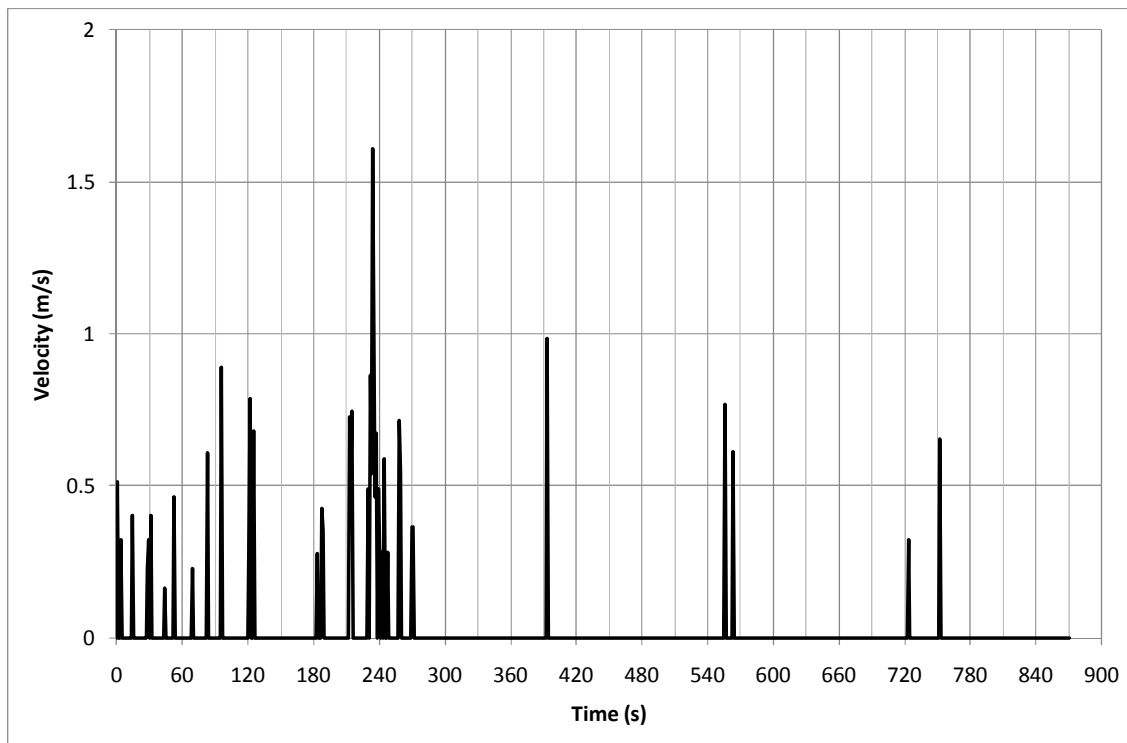
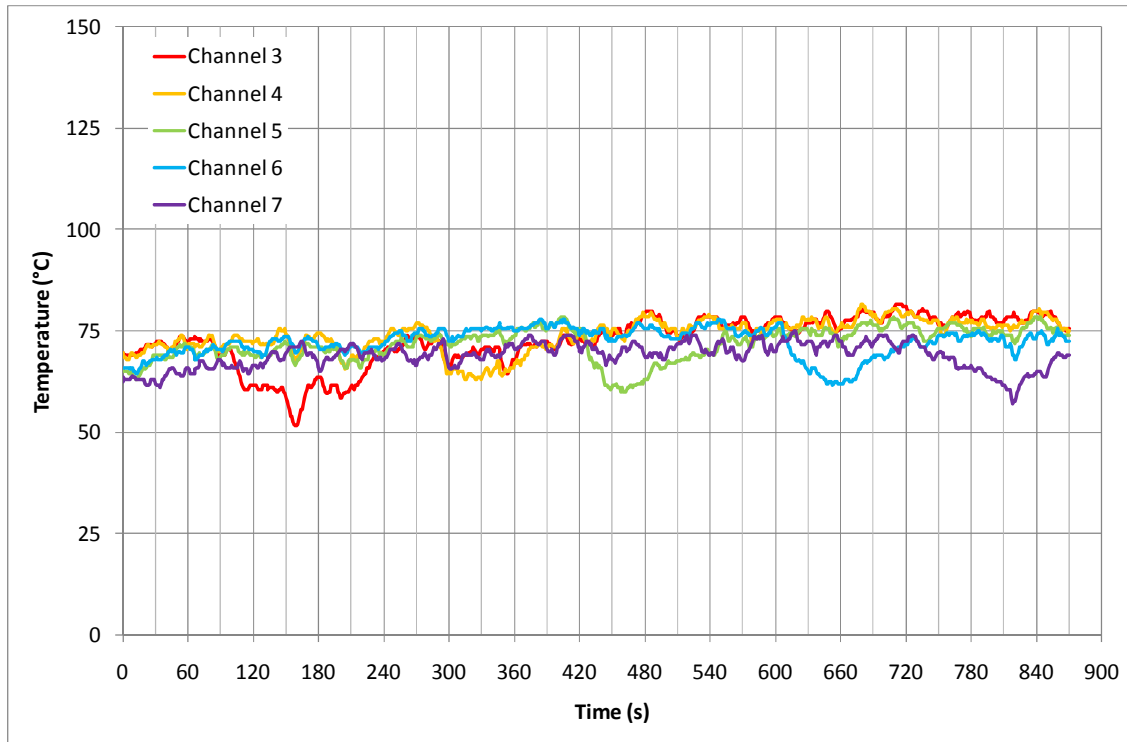
Bar	Point	Time (s)	Temperature (°C)	Velocity (m/s)
1	1	90	43.45	0.00
1	2	120	46.30	0.00
1	3	150	49.80	0.00
1	4	180	49.35	0.00
1	5	210	56.20	0.00
2	1	240	42.15	0.43
2	2	270	47.55	0.00
2	3	300	46.50	0.00
2	4	330	47.35	0.00
2	5	360	53.00	0.00
3	1	390	45.80	0.59
3	2	420	43.50	0.00
3	3	450	46.95	0.00
3	4	480	53.25	0.00
3	5	510	55.25	0.00
4	1	570	51.00	0.00
4	2	600	50.65	0.00
4	3	630	50.10	0.00
4	4	660	55.95	0.00
4	5	690	56.55	0.32
5	1	720	49.25	0.23
5	2	750	51.45	0.00
5	3	780	53.30	0.00
5	4	810	54.05	0.00
5	5	840	57.75	0.19

Test 2



Bar	Point	Time (s)	Temperature (°C)	Velocity (m/s)
1	1	90	41.60	0.00
1	2	120	43.70	0.00
1	3	150	45.65	0.00
1	4	180	45.85	0.00
1	5	210	45.00	0.00
2	1	270	45.20	0.12
2	2	300	46.30	0.00
2	3	330	52.20	0.00
2	4	360	62.20	0.00
2	5	390	62.30	0.15
3	1	420	49.70	0.42
3	2	450	52.35	0.29
3	3	480	59.70	0.00
3	4	510	65.80	0.12
3	5	540	69.50	0.23
4	1	600	48.60	0.40
4	2	630	47.60	0.34
4	3	660	52.55	0.00
4	4	690	64.90	0.00
4	5	720	65.75	0.49
5	1	750	53.55	0.00
5	2	780	52.50	0.00
5	3	810	57.60	0.00
5	4	840	60.90	0.00
5	5	870	65.05	0.53

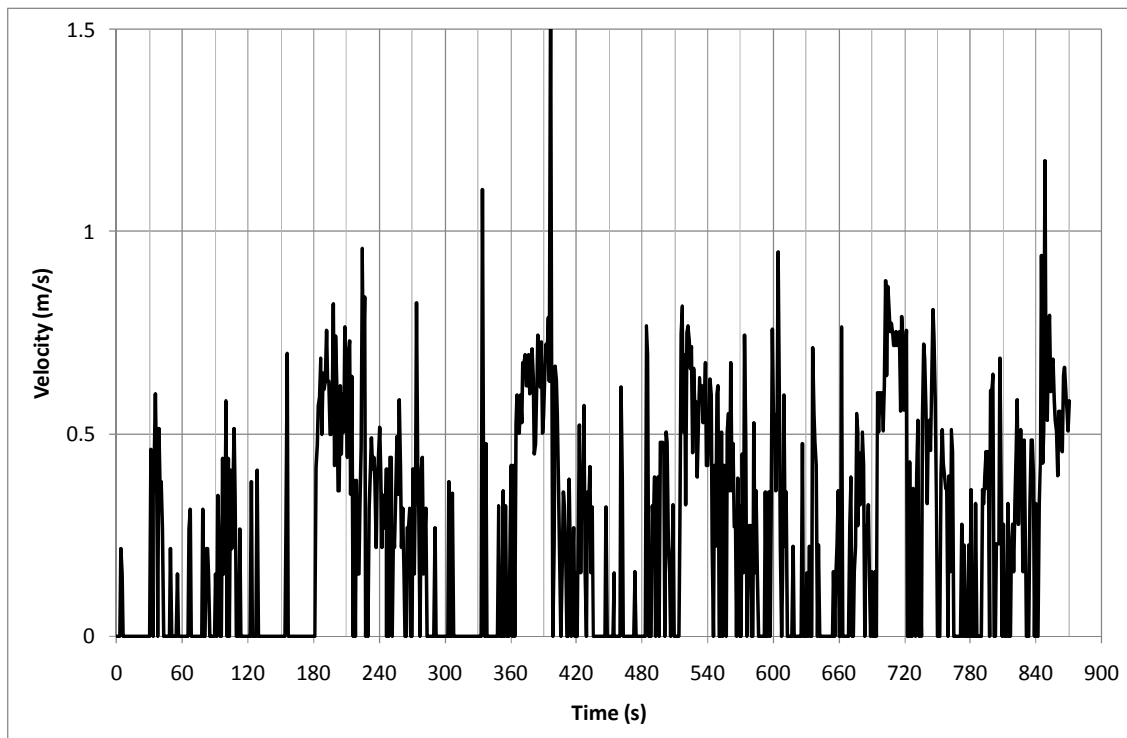
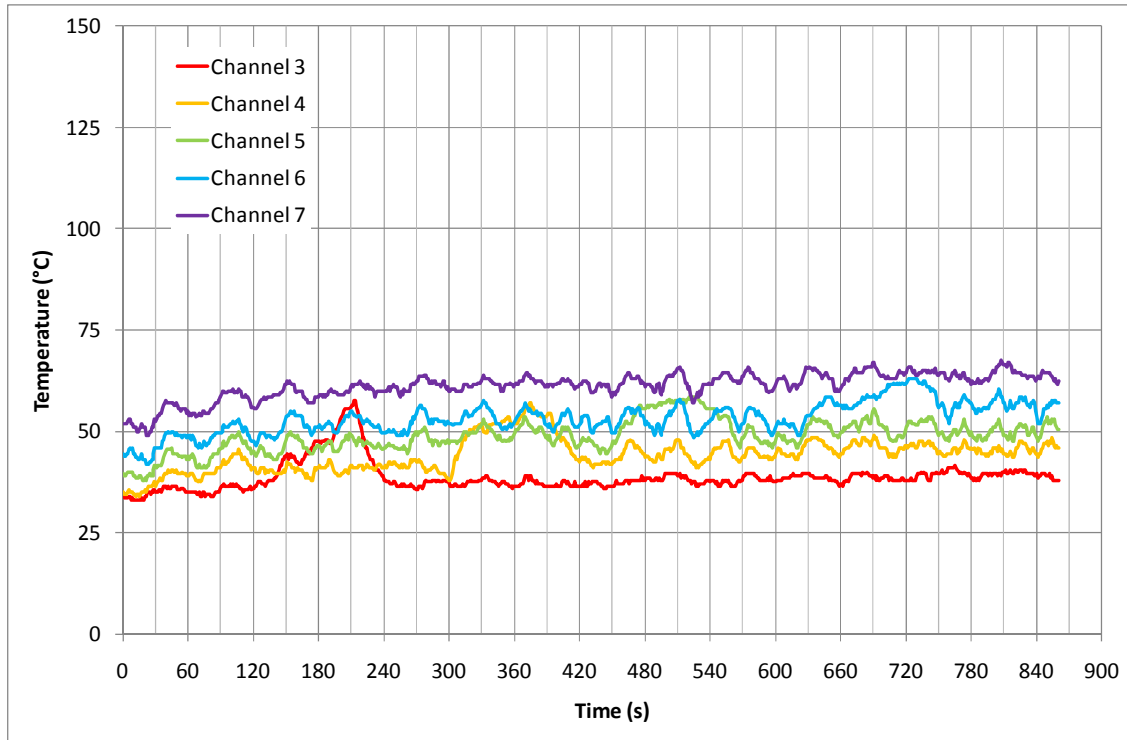
Test 3



Bar	Point	Time (s)	Temperature (°C)	Velocity (m/s)
1	1	90	71.05	0.00
1	2	120	61.00	0.00
1	3	150	60.35	0.00
1	4	180	62.15	0.00
1	5	210	59.50	0.00
2	1	270	75.55	0.00
2	2	300	68.15	0.00
2	3	330	63.55	0.00
2	4	360	65.35	0.00
2	5	390	71.20	0.00
3	1	420	75.15	0.00
3	2	450	62.15	0.00
3	3	480	62.00	0.00
3	4	510	67.05	0.00
3	5	540	70.15	0.00
4	1	600	74.80	0.00
4	2	630	67.05	0.00
4	3	660	62.20	0.00
4	4	690	67.55	0.00
4	5	720	70.95	0.00
5	1	750	68.85	0.00
5	2	780	66.10	0.00
5	3	810	62.45	0.00
5	4	840	64.10	0.00
5	5	870	68.00	0.00

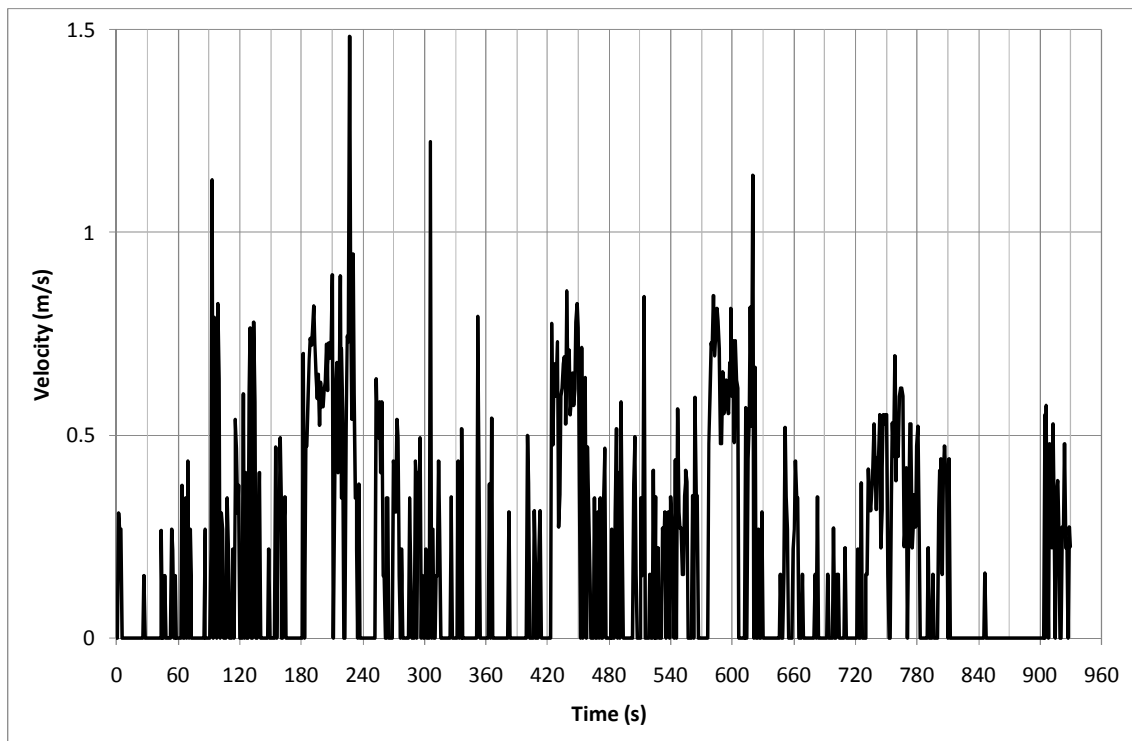
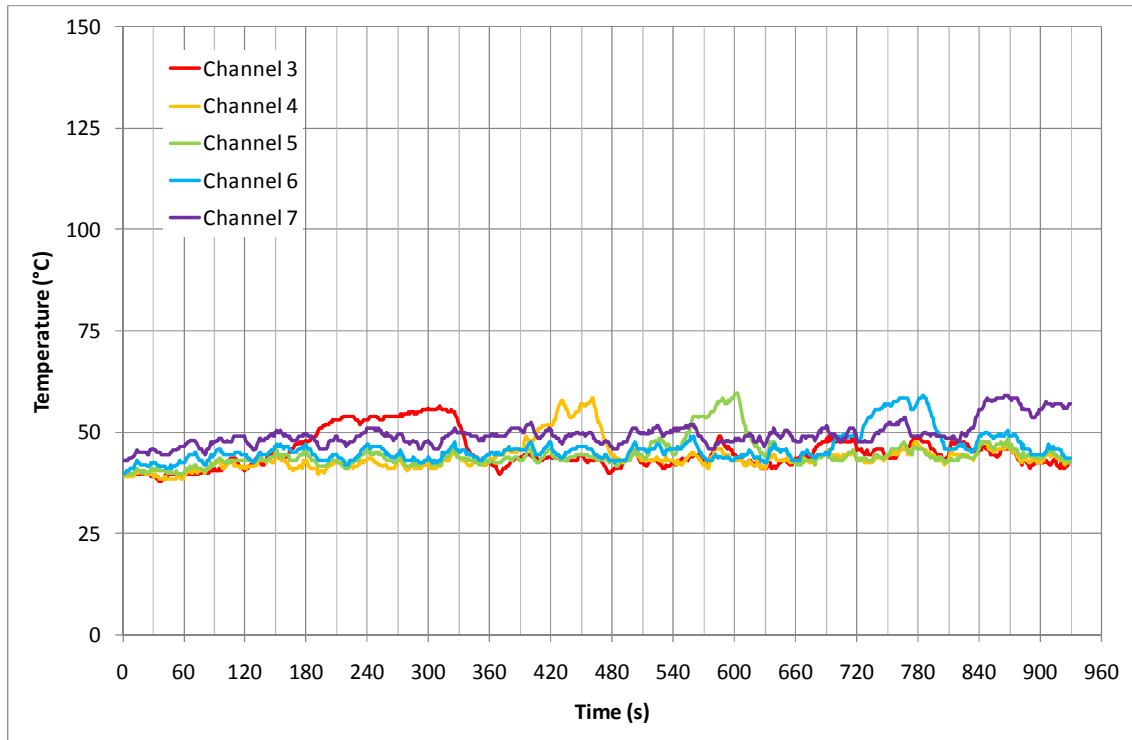
20 Minutes

Test 1



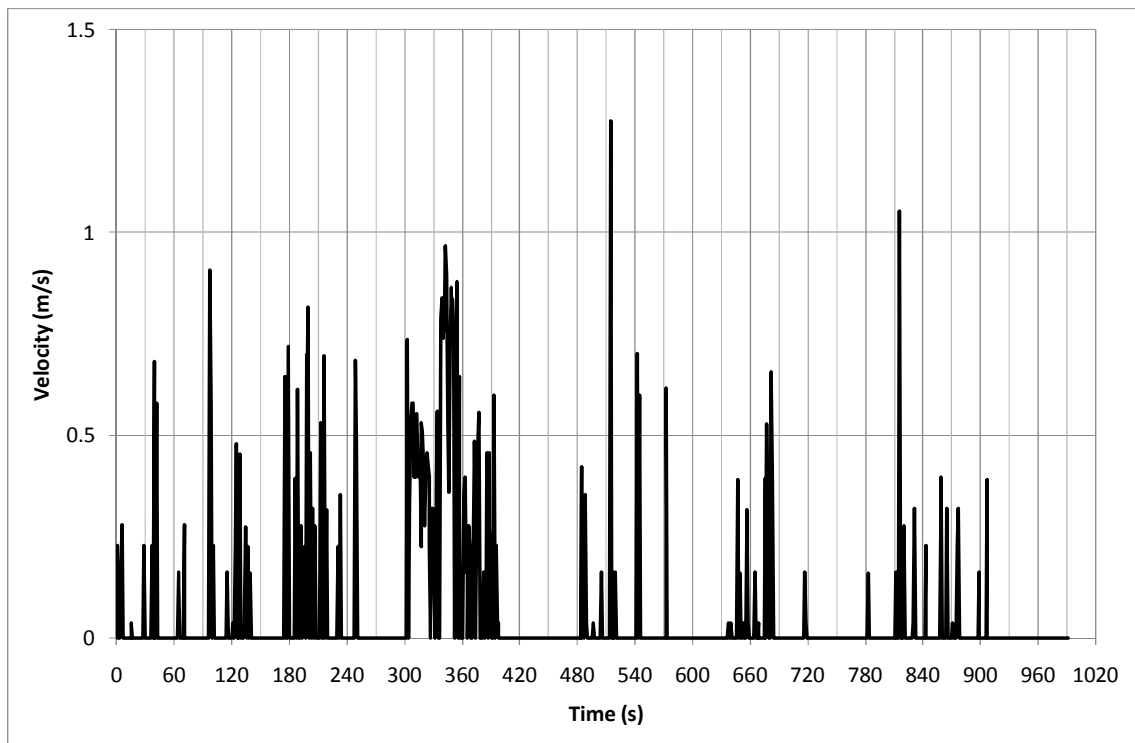
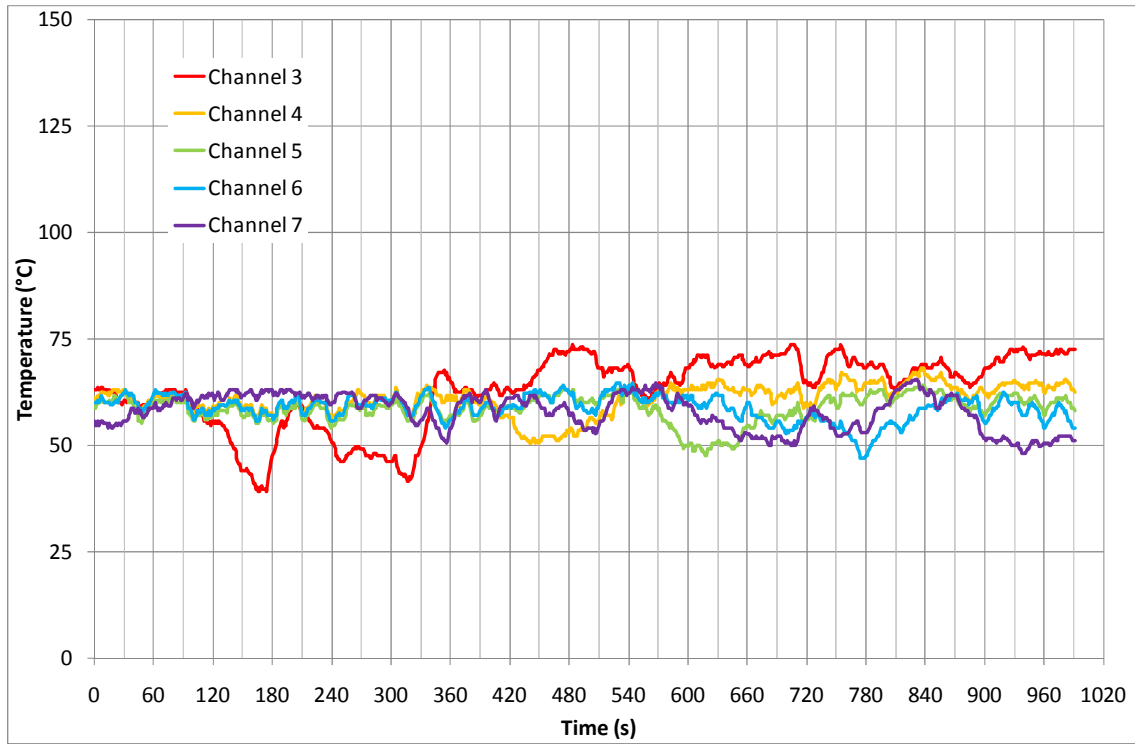
Bar	Point	Time (s)	Temperature (°C)	Velocity (m/s)
1	1	90	34.70	0.00
1	2	120	35.65	0.00
1	3	150	41.45	0.00
1	4	180	46.05	0.00
1	5	210	54.90	0.58
2	1	270	42.05	0.19
2	2	300	39.30	0.00
2	3	330	50.95	0.00
2	4	360	52.55	0.00
2	5	390	53.85	0.62
3	1	420	47.65	0.17
3	2	450	45.45	0.00
3	3	480	55.40	0.00
3	4	510	57.35	0.26
3	5	540	56.00	0.54
4	1	600	50.65	0.11
4	2	630	51.40	0.00
4	3	660	57.15	0.00
4	4	690	58.45	0.30
4	5	720	62.00	0.70
5	1	750	64.65	0.52
5	2	780	63.30	0.00
5	3	810	66.00	0.37
5	4	840	63.30	0.28
5	5	870	61.70	0.55

Test 2



Bar	Point	Time (s)	Temperature (°C)	Velocity (m/s)
1	1	90	40.45	0.00
1	2	120	41.95	0.22
1	3	150	44.25	0.00
1	4	180	47.35	0.00
1	5	210	52.55	0.65
2	1	330	44.55	0.00
2	2	360	42.35	0.00
2	3	390	45.15	0.00
2	4	420	51.40	0.00
2	5	450	54.95	0.67
3	1	480	43.05	0.00
3	2	510	44.80	0.00
3	3	540	46.45	0.10
3	4	570	53.95	0.00
3	5	600	57.85	0.62
4	1	660	44.10	0.00
4	2	690	44.55	0.00
4	3	720	49.10	0.00
4	4	750	56.20	0.45
4	5	780	55.50	0.37
5	1	810	48.85	0.34
5	2	840	52.35	0.00
5	3	870	58.75	0.00
5	4	900	54.20	0.00
5	5	930	56.45	0.19

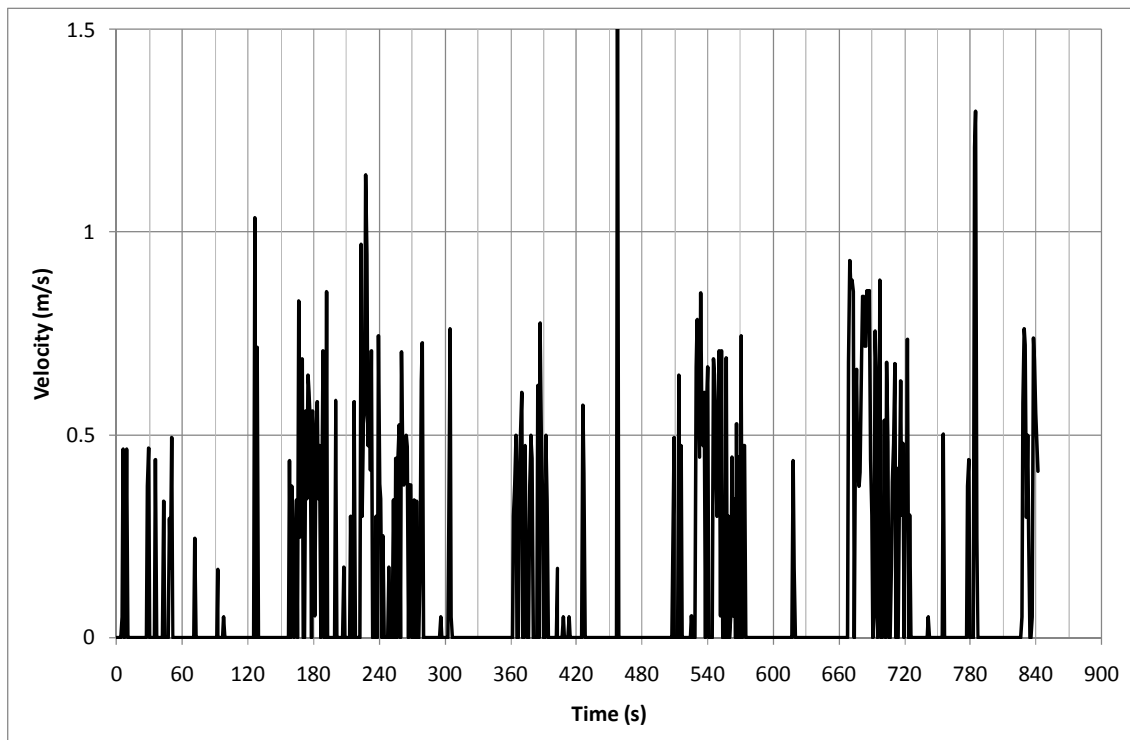
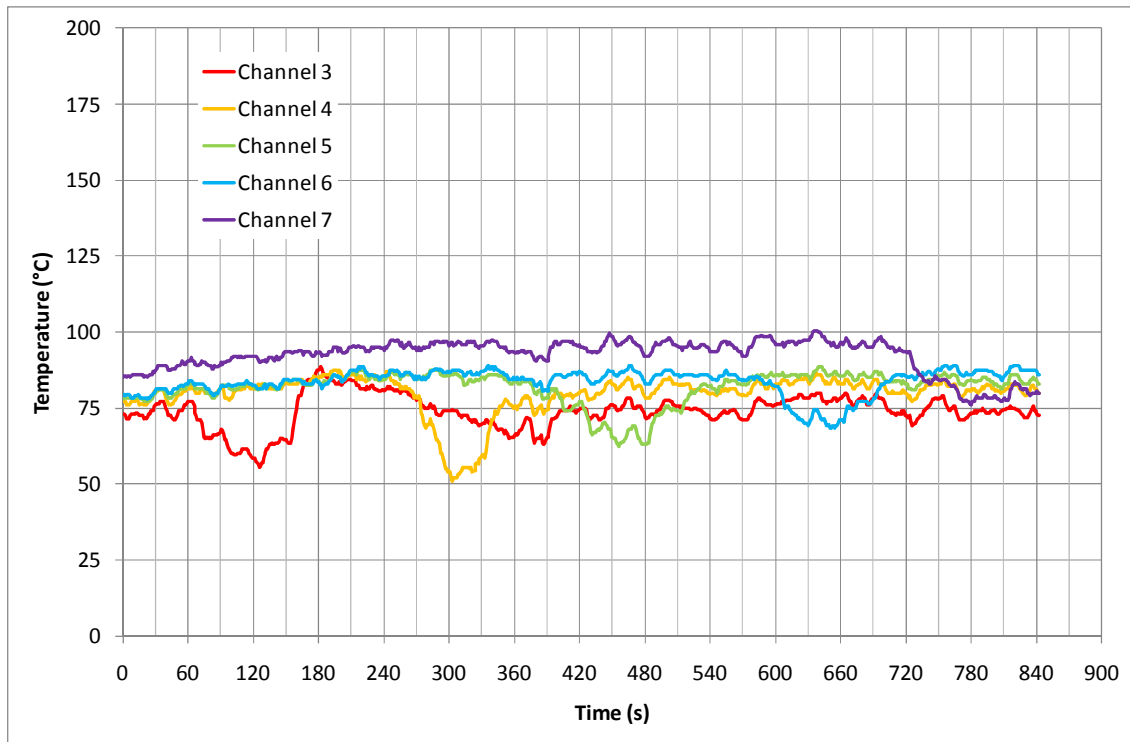
Test 3



Bar	Point	Time (s)	Temperature (°C)	Velocity (m/s)
1	1	90	62.40	0.00
1	2	120	55.40	0.00
1	3	150	46.80	0.00
1	4	180	41.90	0.00
1	5	210	59.50	0.00
2	1	270	49.10	0.00
2	2	300	48.05	0.00
2	3	330	59.70	0.34
2	4	360	60.70	0.49
2	5	390	60.40	0.03
3	1	420	56.75	0.00
3	2	450	50.90	0.00
3	3	480	52.35	0.00
3	4	510	55.85	0.00
3	5	540	61.65	0.00
4	1	600	50.40	0.00
4	2	630	49.90	0.00
4	3	660	53.20	0.00
4	4	690	54.35	0.00
4	5	720	55.20	0.00
5	1	750	54.95	0.00
5	2	780	47.75	0.00
5	3	810	55.05	0.00
5	4	840	58.15	0.00
5	5	870	61.50	0.00

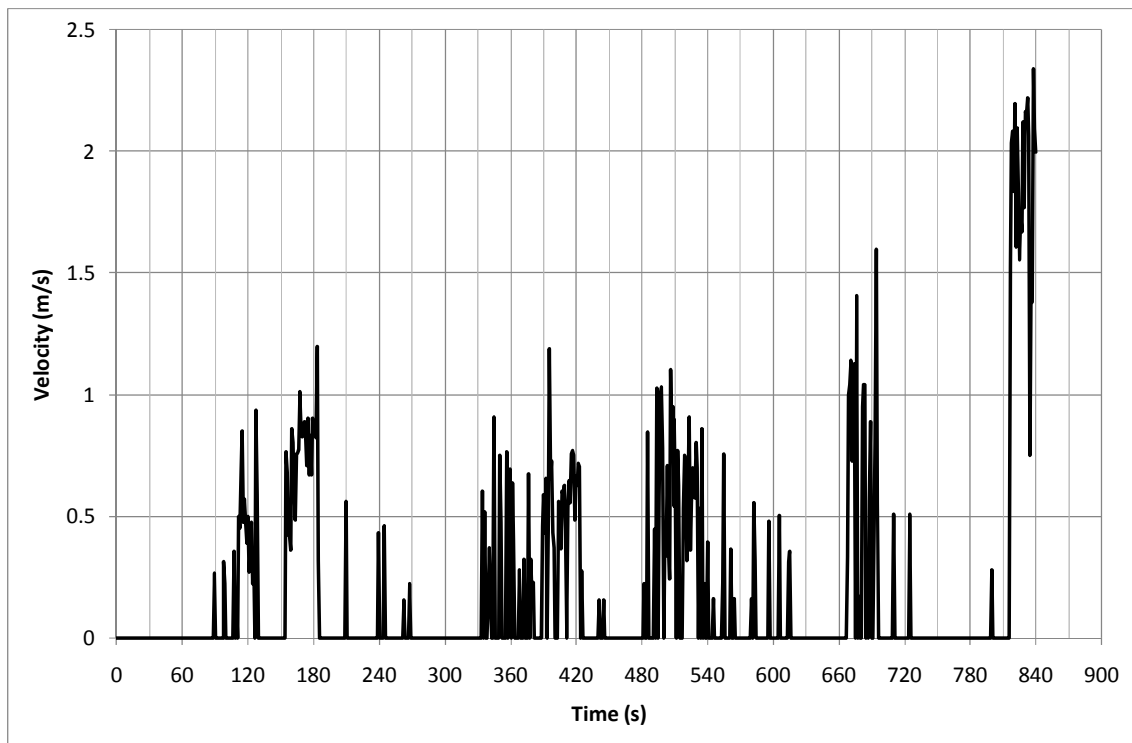
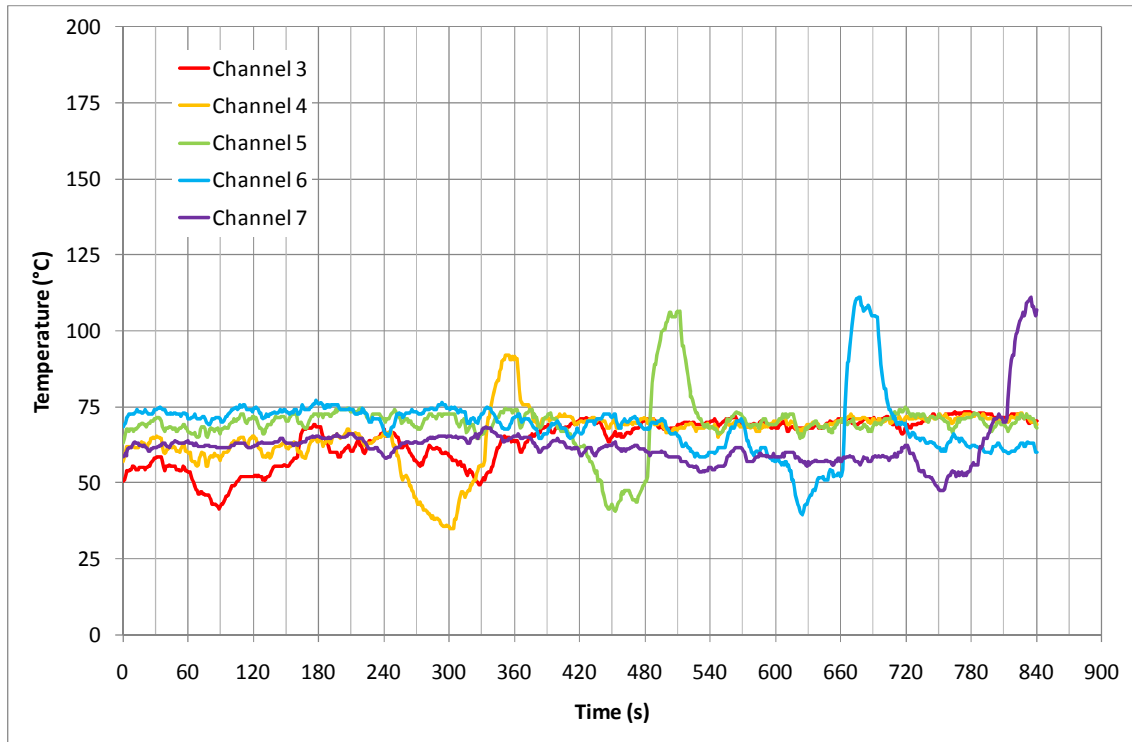
200°C 5 Minutes

Test 1



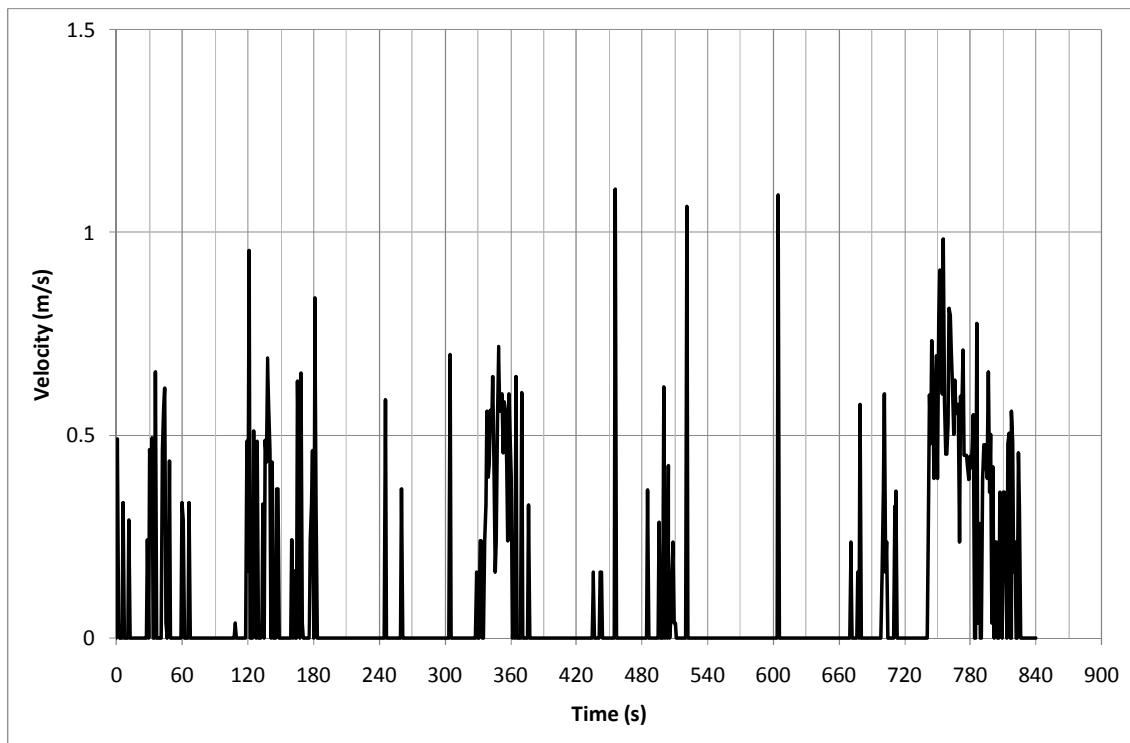
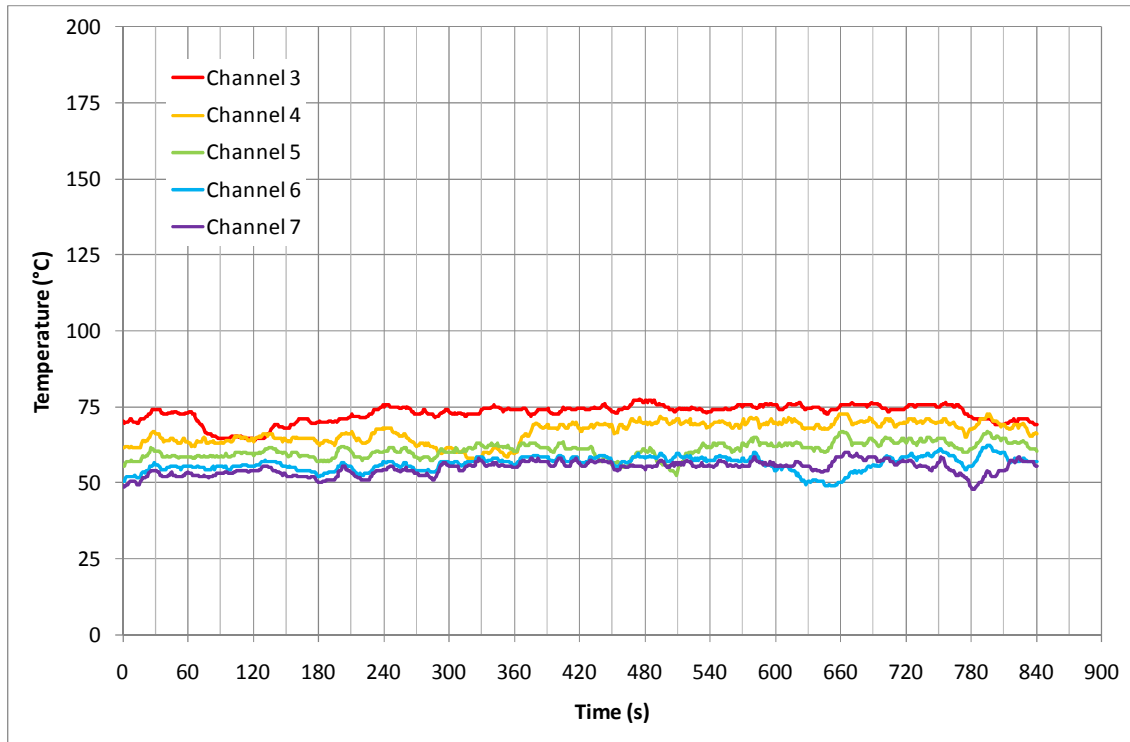
Bar	Point	Time (s)	Temperature (°C)	Velocity (m/s)
1	1	60	74.90	0.00
1	2	90	66.00	0.00
1	3	120	60.55	0.00
1	4	150	64.15	0.00
1	5	180	85.20	0.36
2	1	240	85.00	0.39
2	2	270	80.65	0.39
2	3	300	58.10	0.00
2	4	330	55.95	0.00
2	5	360	76.50	0.00
3	1	390	79.30	0.00
3	2	420	75.05	0.00
3	3	450	68.70	0.00
3	4	480	65.55	0.00
3	5	510	75.85	0.00
4	1	570	85.20	0.00
4	2	600	82.95	0.00
4	3	630	70.60	0.00
4	4	660	69.15	0.00
4	5	690	78.65	0.72
5	1	720	93.85	0.32
5	2	750	84.10	0.00
5	3	780	77.20	0.00
5	4	810	78.05	0.00
5	5	840	80.05	0.43

Test 2



Bar	Point	Time (s)	Temperature (°C)	Velocity (m/s)
1	1	60	54.35	0.00
1	2	90	42.95	0.00
1	3	120	52.00	0.50
1	4	150	55.60	0.00
1	5	180	67.90	0.81
2	1	240	64.75	0.00
2	2	270	49.00	0.00
2	3	300	36.15	0.00
2	4	330	52.50	0.00
2	5	360	91.20	0.26
3	1	390	70.10	0.00
3	2	420	63.95	0.59
3	3	450	44.10	0.00
3	4	480	46.15	0.00
3	5	510	100.90	0.70
4	1	570	69.70	0.00
4	2	600	58.90	0.00
4	3	630	41.85	0.00
4	4	660	53.20	0.00
4	5	690	102.20	0.61
5	1	720	60.45	0.00
5	2	750	50.70	0.00
5	3	780	53.35	0.00
5	4	810	71.20	0.00
5	5	840	108.30	1.89

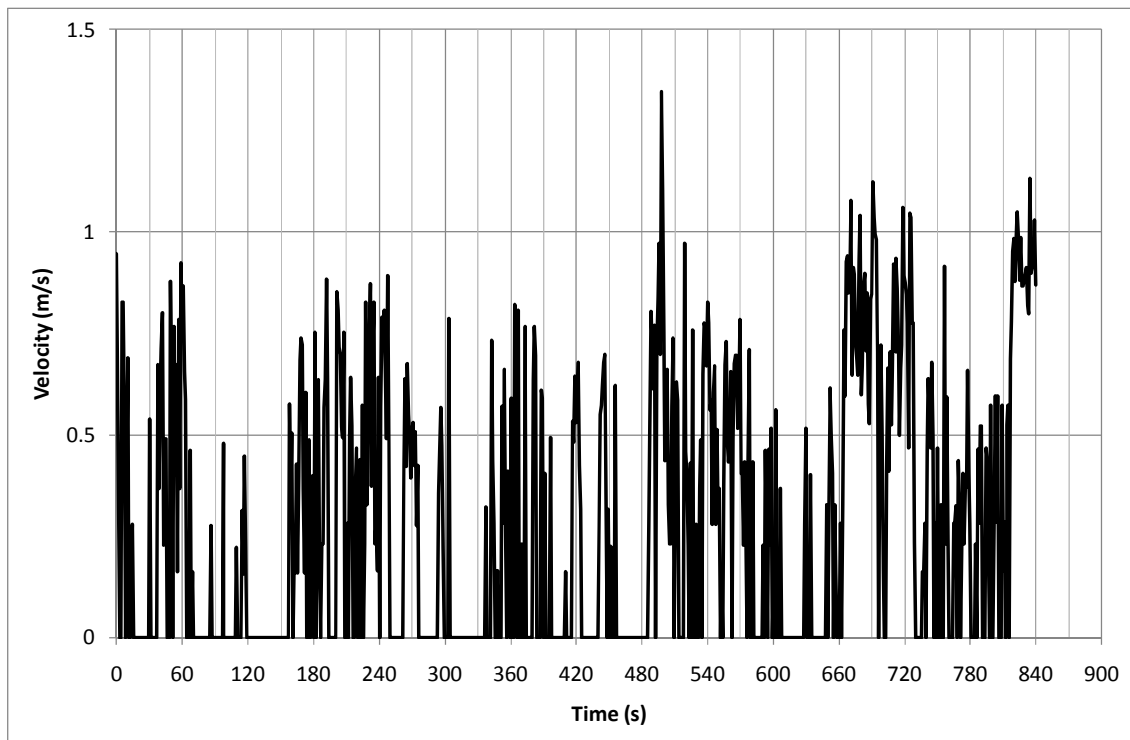
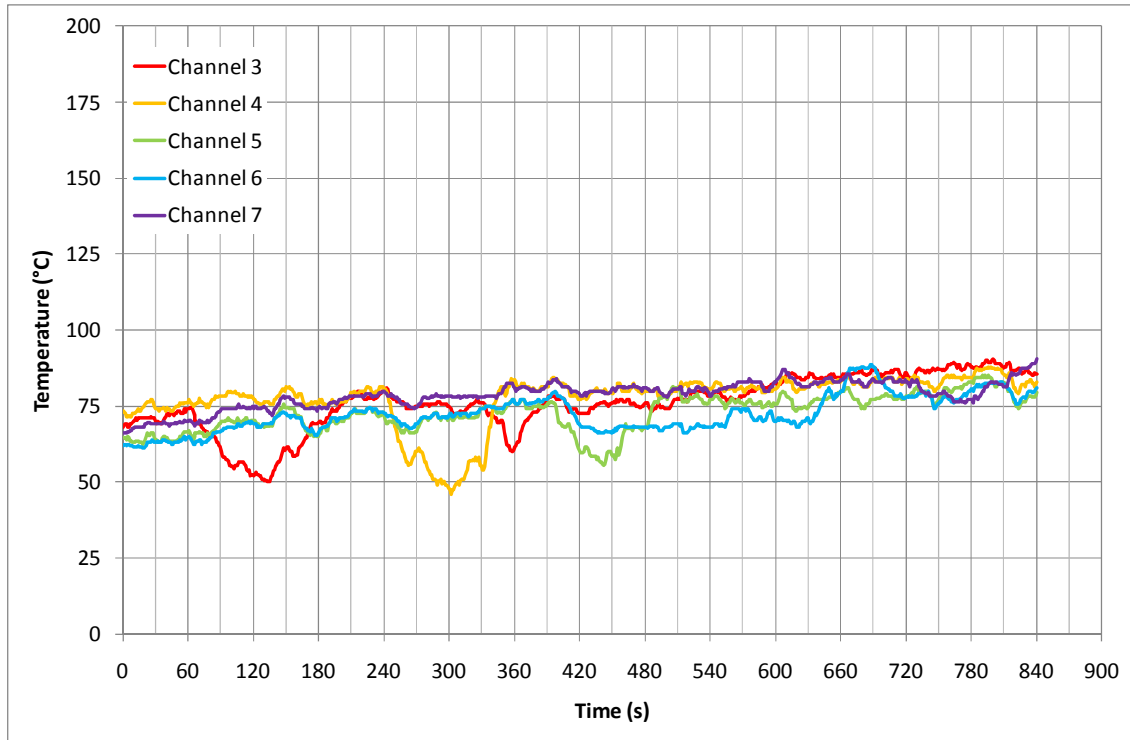
Test 3



Bar	Point	Time (s)	Temperature (°C)	Velocity (m/s)
1	1	60	72.75	0.00
1	2	90	65.25	0.00
1	3	120	64.60	0.00
1	4	150	68.60	0.00
1	5	180	69.20	0.00
2	1	240	67.20	0.00
2	2	270	64.00	0.00
2	3	300	60.50	0.00
2	4	330	57.45	0.00
2	5	360	59.30	0.52
3	1	390	61.75	0.00
3	2	420	61.20	0.00
3	3	450	57.55	0.00
3	4	480	59.90	0.00
3	5	510	54.60	0.05
4	1	570	57.40	0.00
4	2	600	55.60	0.00
4	3	630	51.00	0.00
4	4	660	49.35	0.00
4	5	690	55.15	0.00
5	1	720	56.75	0.00
5	2	750	55.00	0.40
5	3	780	51.25	0.49
5	4	810	50.75	0.50
5	5	840	50.75	0.50

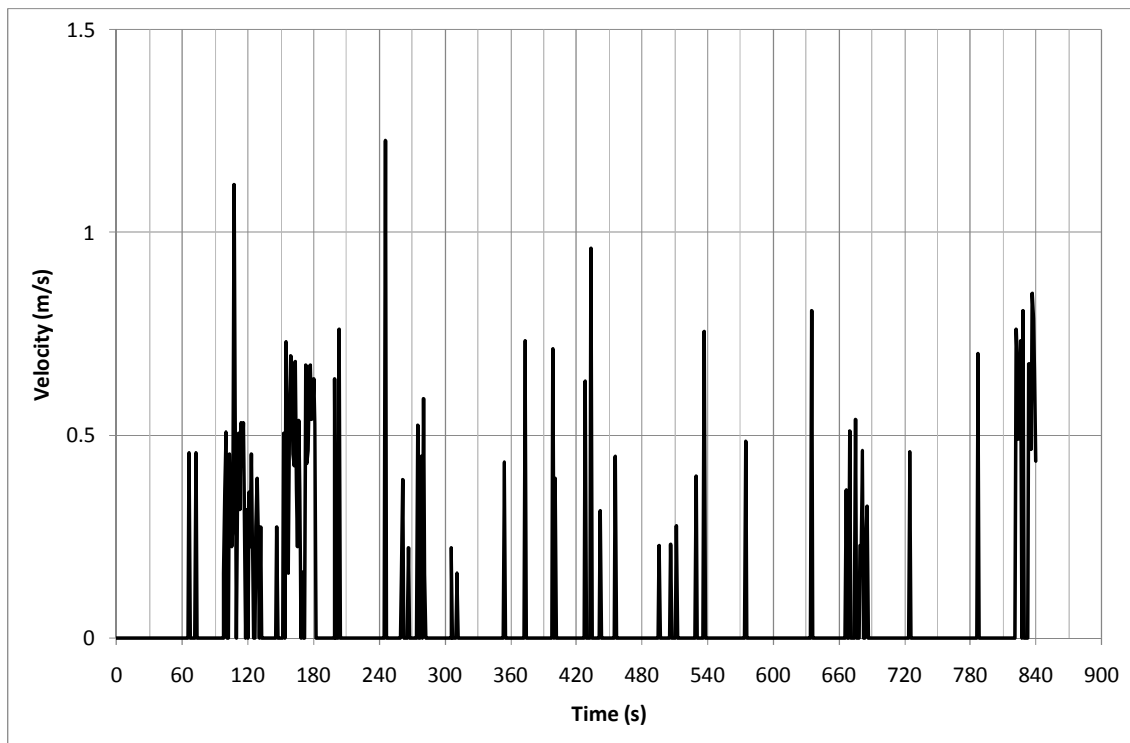
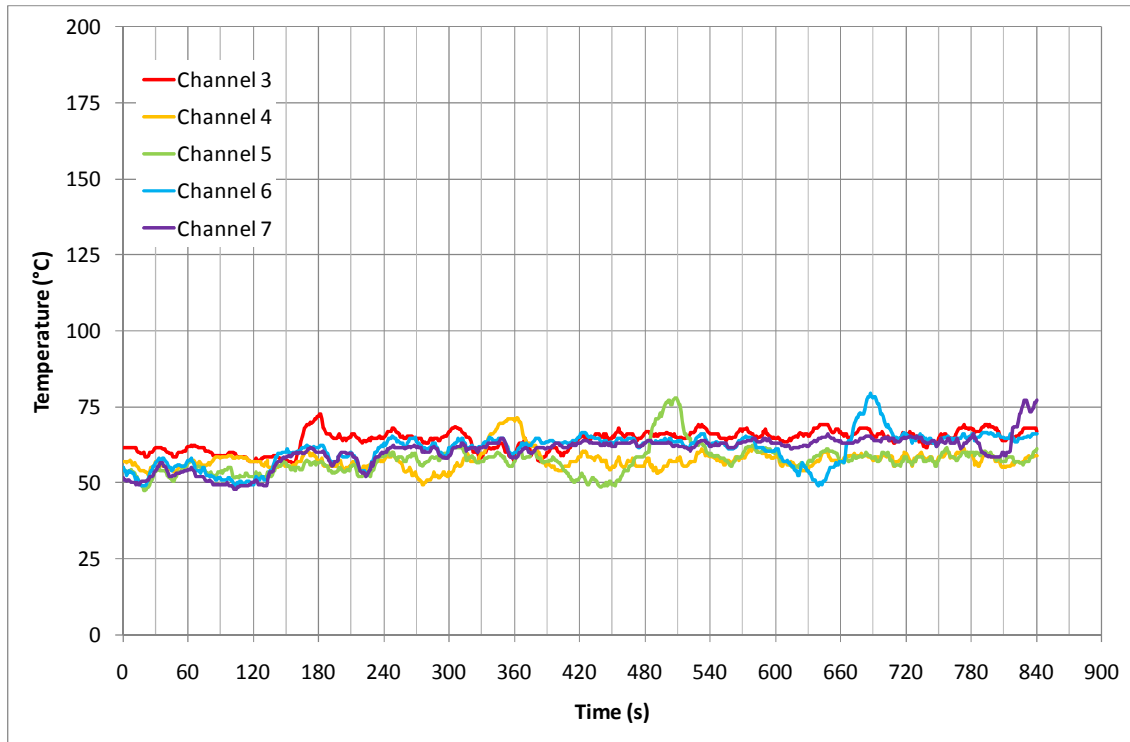
10 Minutes

Test 1



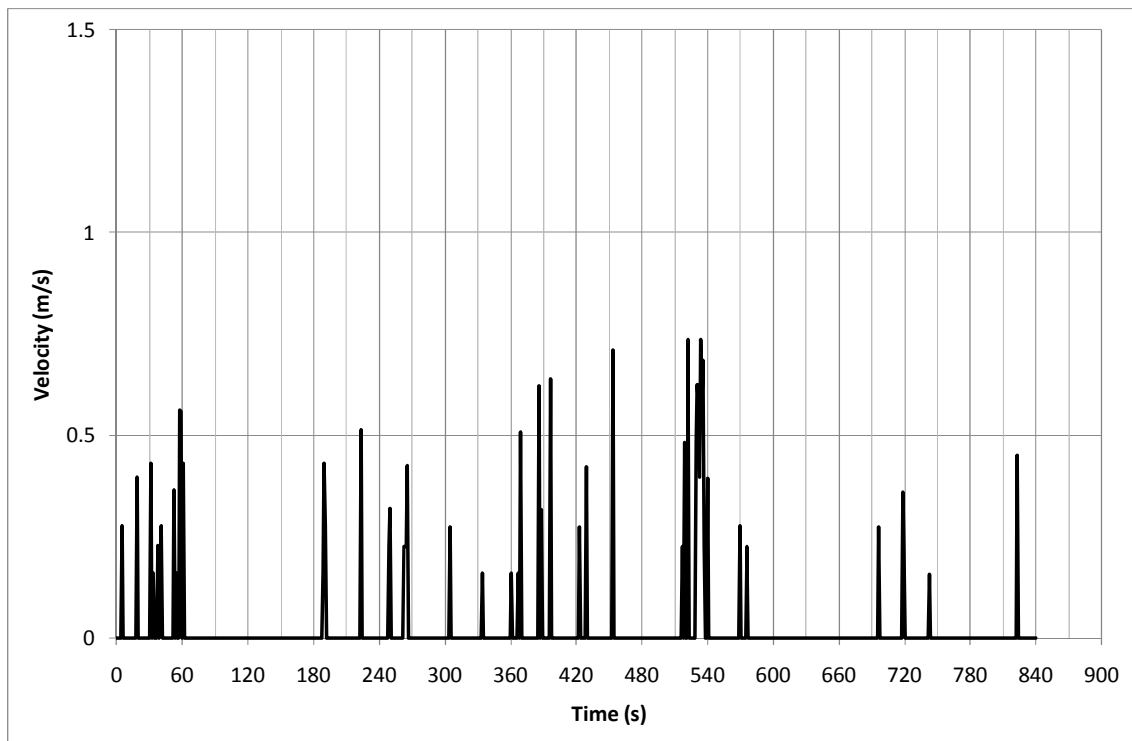
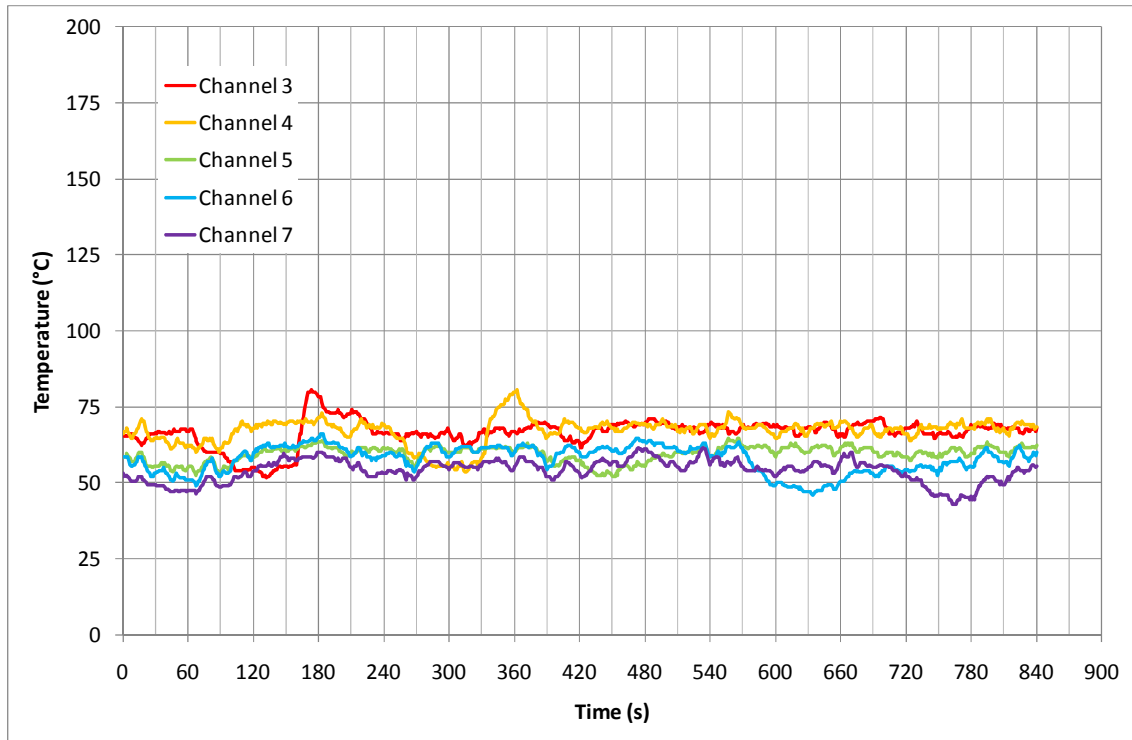
Bar	Point	Time (s)	Temperature (°C)	Velocity (m/s)
1	1	60	73.30	0.60
1	2	90	63.90	0.00
1	3	120	54.30	0.09
1	4	150	57.55	0.00
1	5	180	69.10	0.23
2	1	240	80.40	0.59
2	2	270	57.10	0.45
2	3	300	49.55	0.16
2	4	330	57.20	0.00
2	5	360	81.45	0.17
3	1	390	74.95	0.44
3	2	420	65.75	0.00
3	3	450	58.00	0.47
3	4	480	67.70	0.00
3	5	510	78.90	0.42
4	1	570	73.85	0.60
4	2	600	71.65	0.25
4	3	630	69.65	0.00
4	4	660	78.80	0.26
4	5	690	87.50	0.75
5	1	720	83.15	0.81
5	2	750	78.70	0.43
5	3	780	76.70	0.36
5	4	810	82.35	0.30
5	5	840	88.35	0.93

Test 2



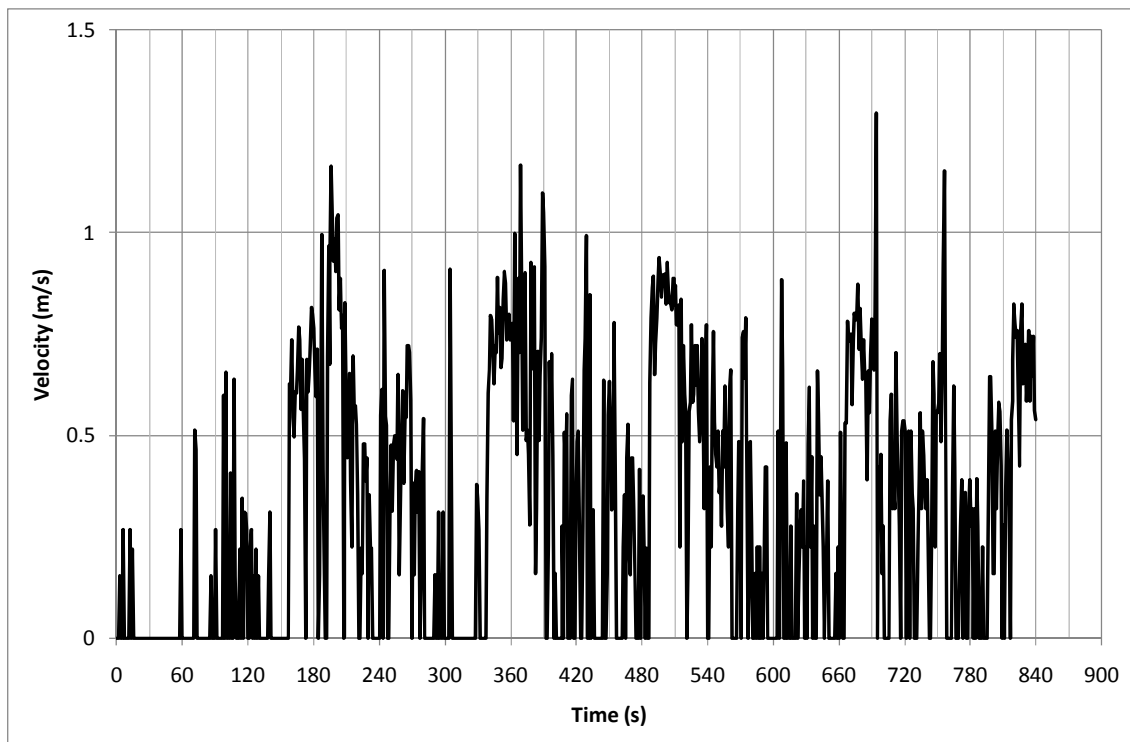
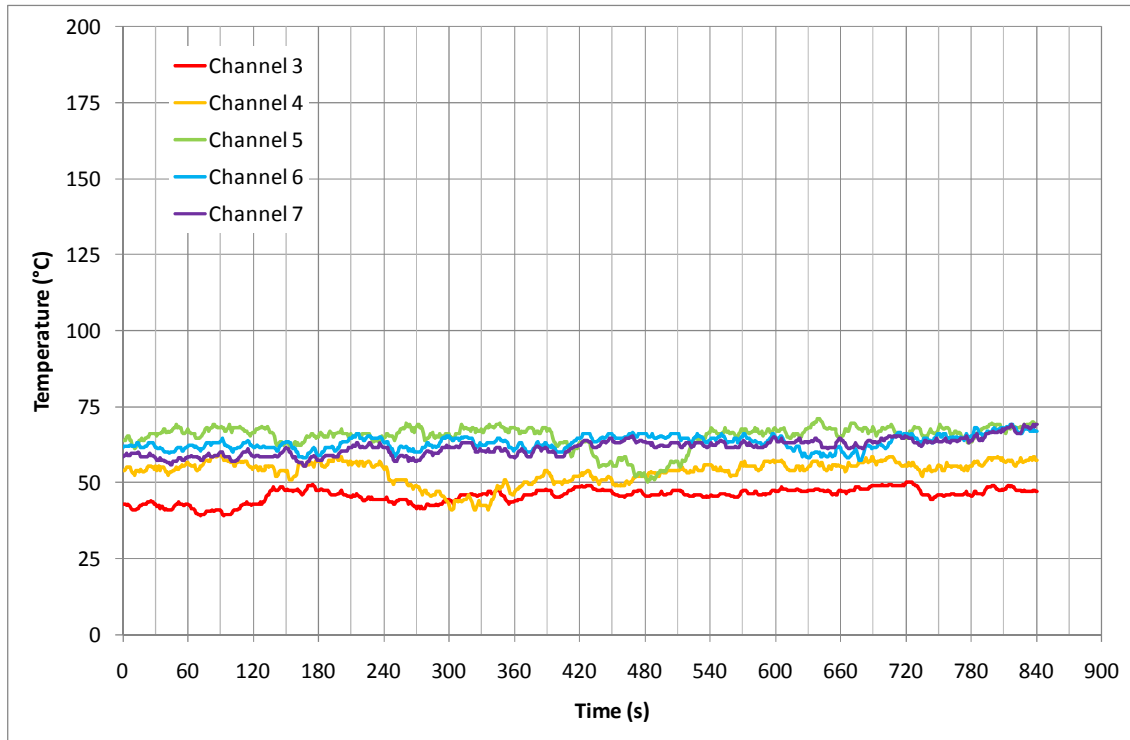
Bar	Point	Time (s)	Temperature (°C)	Velocity (m/s)
1	1	60	60.45	0.00
1	2	90	59.25	0.00
1	3	120	57.80	0.63
1	4	150	58.15	0.34
1	5	180	68.95	0.72
2	1	240	57.00	0.00
2	2	270	53.75	0.45
2	3	300	52.55	0.07
2	4	330	57.40	0.19
2	5	360	70.65	0.34
3	1	390	57.40	0.00
3	2	420	51.20	0.00
3	3	450	49.50	0.36
3	4	480	58.40	0.00
3	5	510	75.60	0.31
4	1	570	62.65	0.00
4	2	600	60.55	0.00
4	3	630	54.50	0.00
4	4	660	55.60	0.00
4	5	690	75.20	0.48
5	1	720	64.15	0.00
5	2	750	63.25	0.25
5	3	780	63.05	0.00
5	4	810	58.85	0.00
5	5	840	75.25	0.69

Test 3



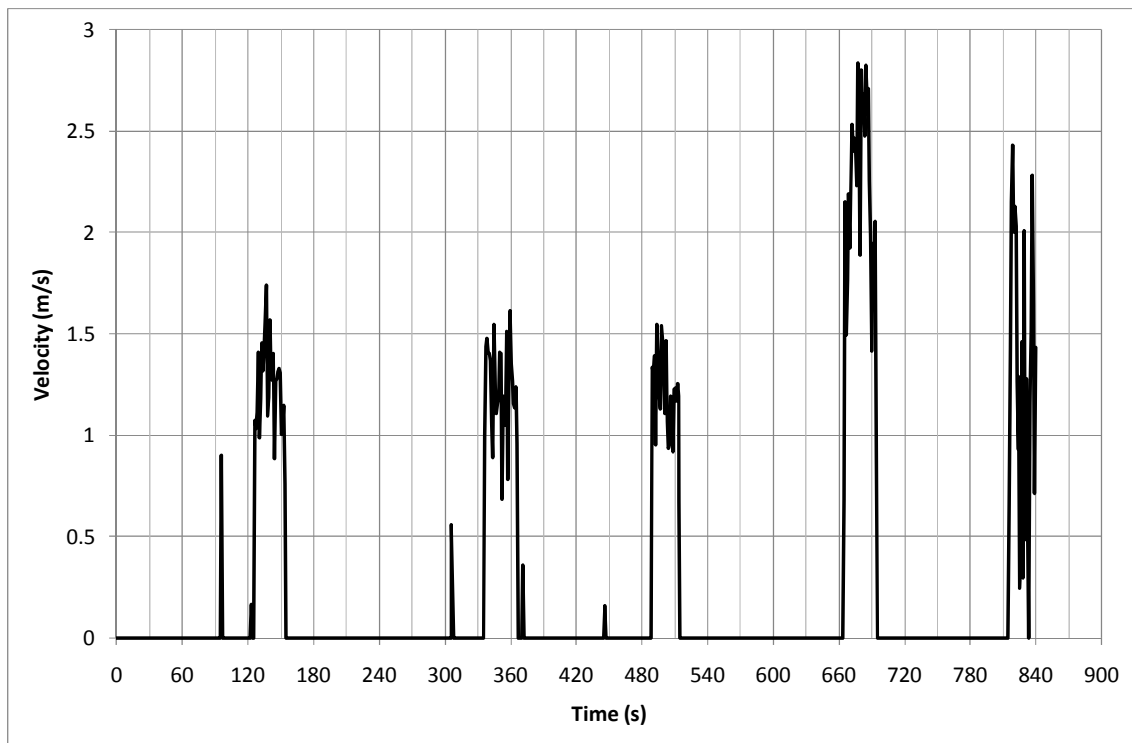
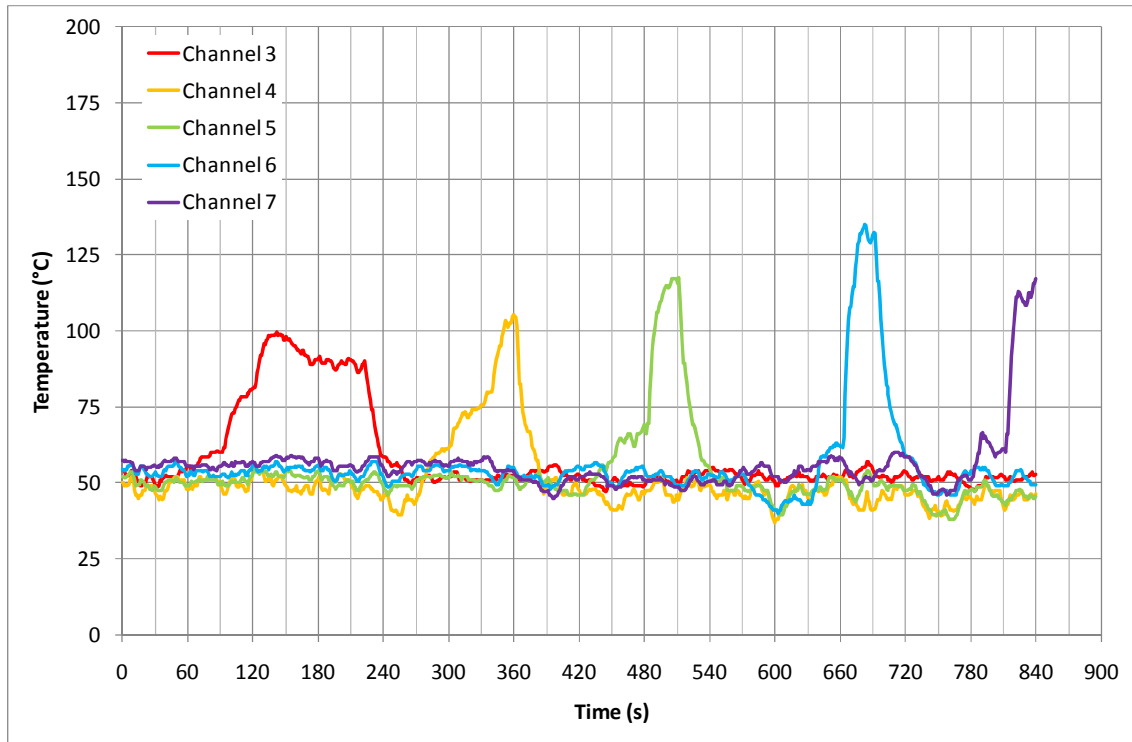
Bar	Point	Time (s)	Temperature (°C)	Velocity (m/s)
1	1	60	67.25	0.00
1	2	90	59.95	0.00
1	3	120	54.50	0.00
1	4	150	55.00	0.00
1	5	180	79.05	0.00
2	1	240	68.45	0.00
2	2	270	59.50	0.00
2	3	300	55.65	0.00
2	4	330	56.60	0.00
2	5	360	77.85	0.00
3	1	390	59.40	0.00
3	2	420	58.10	0.00
3	3	450	52.95	0.00
3	4	480	55.90	0.00
3	5	510	59.25	0.00
4	1	570	62.10	0.00
4	2	600	50.30	0.00
4	3	630	47.70	0.00
4	4	660	48.90	0.00
4	5	690	53.85	0.00
5	1	720	52.80	0.00
5	2	750	46.45	0.00
5	3	780	45.30	0.00
5	4	810	50.50	0.00
5	5	840	54.85	0.00

20 Minutes
Test 1



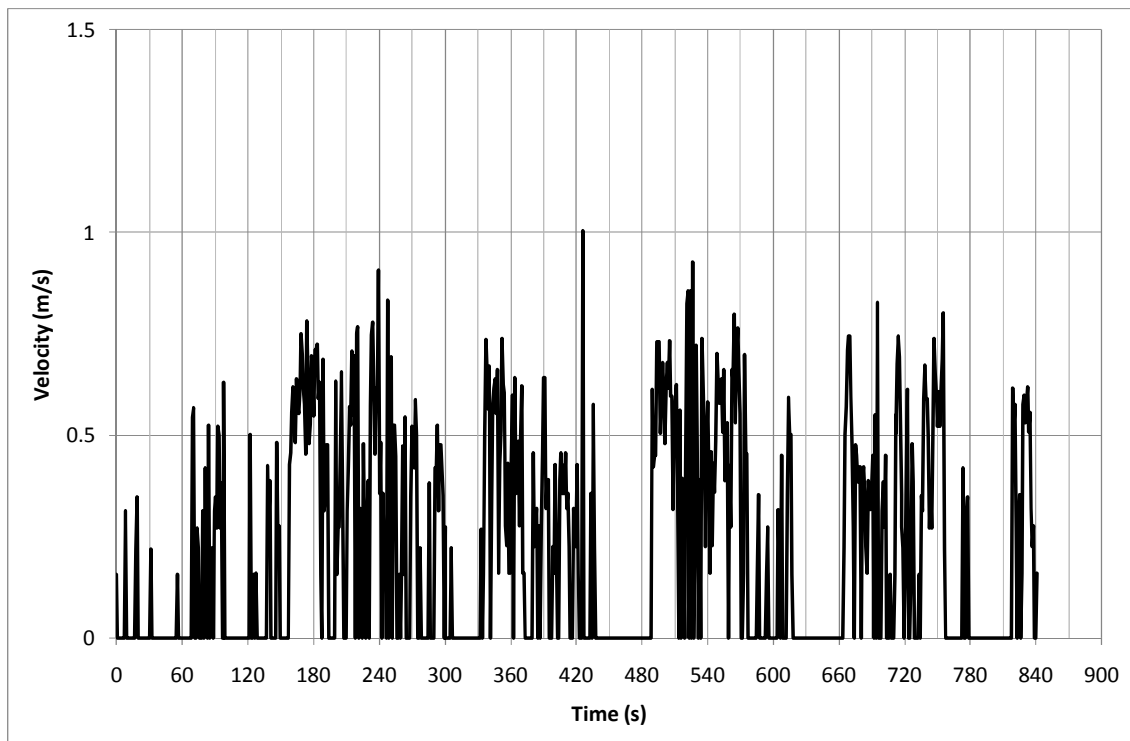
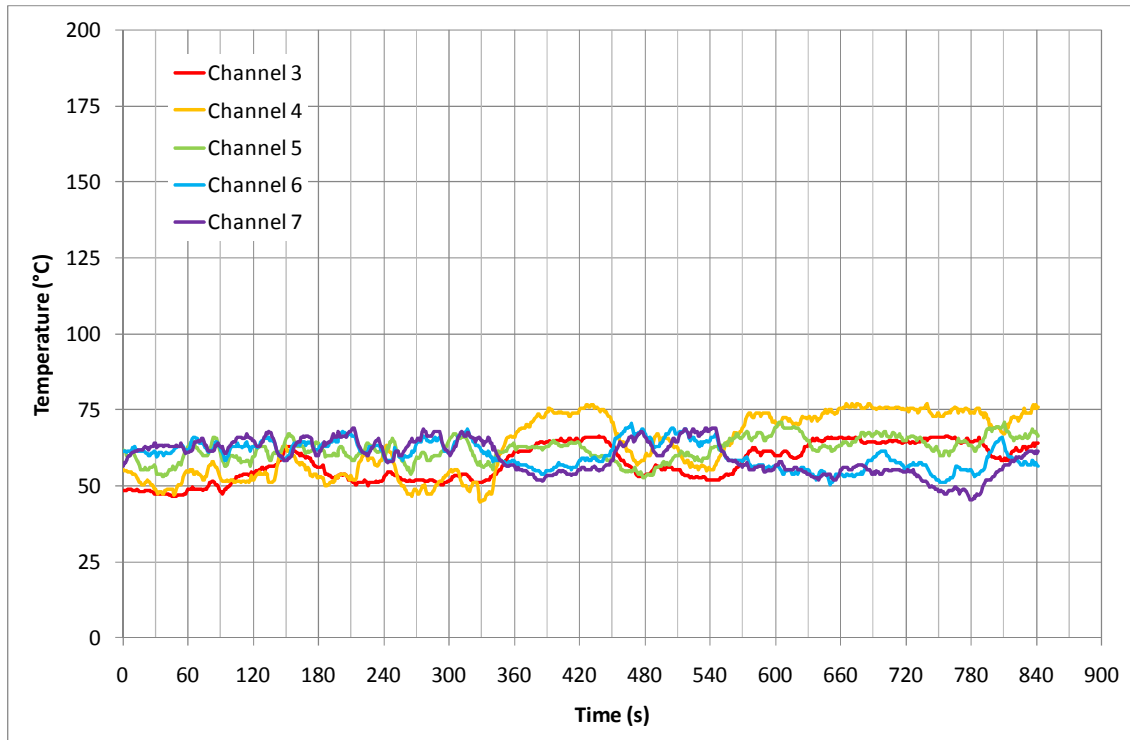
Bar	Point	Time (s)	Temperature (°C)	Velocity (m/s)
1	1	60	42.95	0.00
1	2	90	40.80	0.00
1	3	120	42.95	0.00
1	4	150	47.95	0.00
1	5	180	49.50	0.64
2	1	240	55.75	0.00
2	2	270	49.30	0.55
2	3	300	45.10	0.00
2	4	330	42.45	0.00
2	5	360	48.35	0.79
3	1	390	67.20	0.74
3	2	420	60.60	0.33
3	3	450	56.10	0.11
3	4	480	52.65	0.21
3	5	510	57.30	0.86
4	1	570	64.15	0.32
4	2	600	64.35	0.00
4	3	630	60.05	0.11
4	4	660	60.15	0.00
4	5	690	61.40	0.65
5	1	720	65.10	0.46
5	2	750	63.50	0.36
5	3	780	64.30	0.24
5	4	810	66.80	0.39
5	5	840	68.40	0.67

Test 2



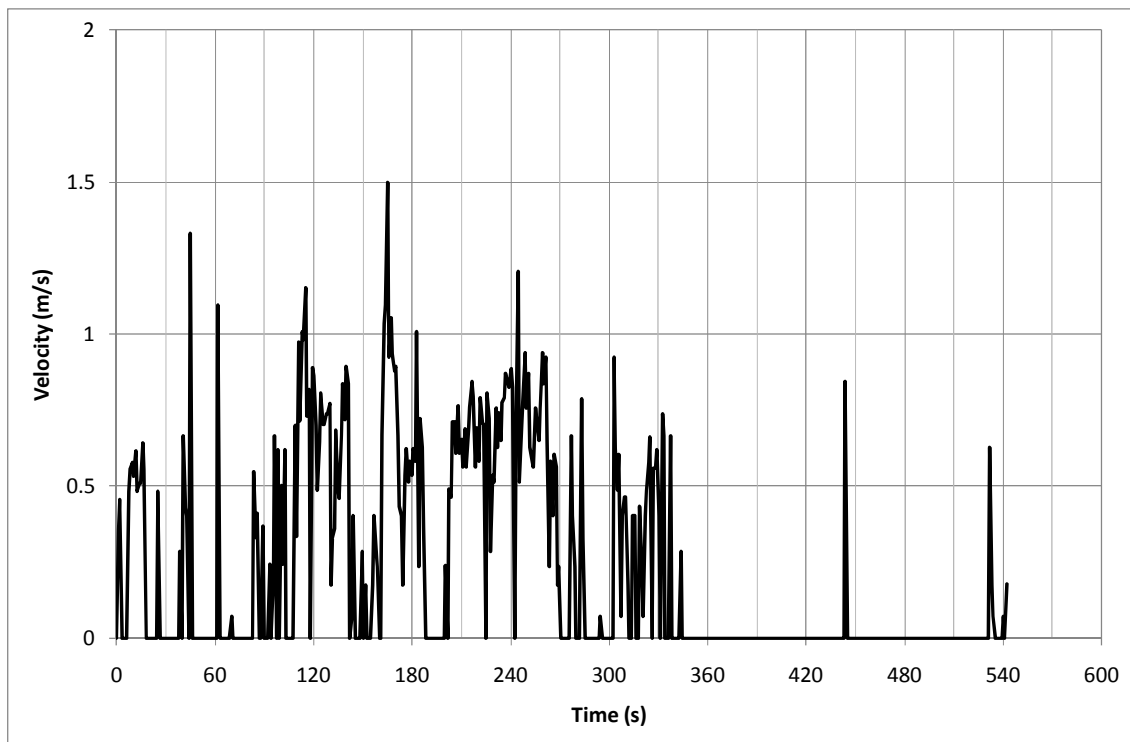
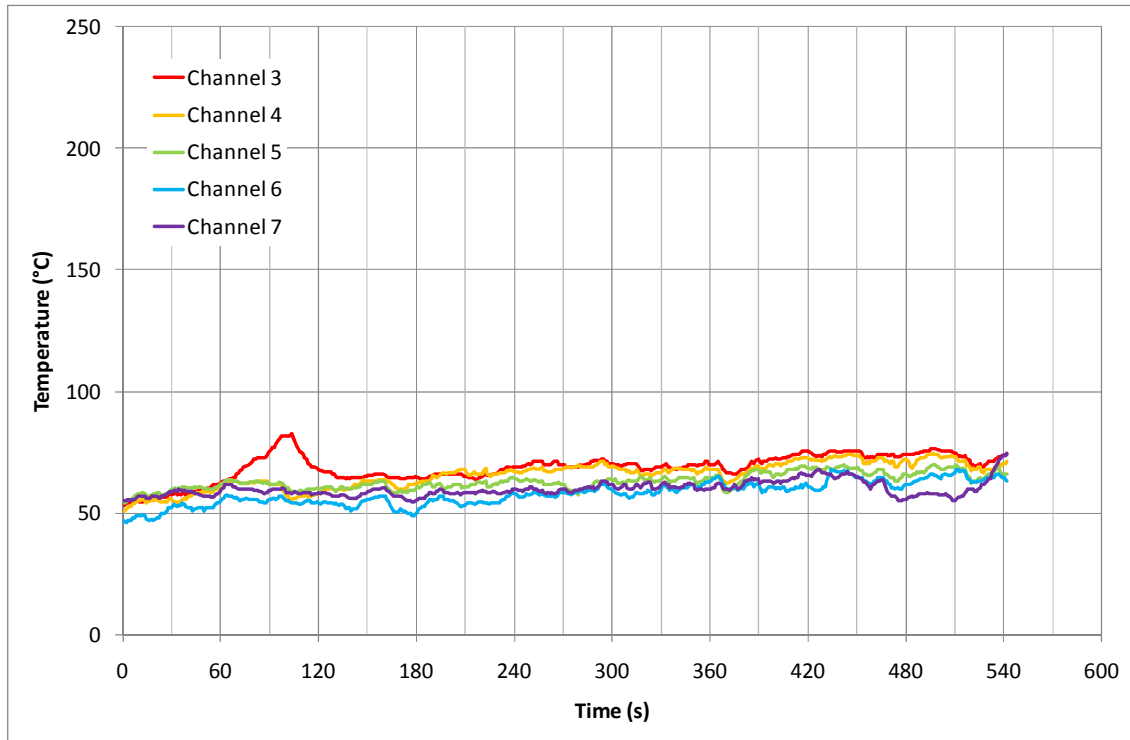
Bar	Point	Time (s)	Temperature (°C)	Velocity (m/s)
1	1	60	53.70	0.00
1	2	90	60.00	0.00
1	3	120	79.20	0.00
1	4	150	98.45	1.30
1	5	180	86.15	0.00
2	1	240	46.20	0.00
2	2	270	44.25	0.00
2	3	300	60.70	0.00
2	4	330	73.90	0.00
2	5	360	97.10	1.26
3	1	390	51.60	0.00
3	2	420	46.20	0.00
3	3	450	55.60	0.00
3	4	480	65.65	0.00
3	5	510	109.35	1.14
4	1	570	52.10	0.00
4	2	600	42.65	0.00
4	3	630	43.70	0.00
4	4	660	62.05	0.00
4	5	690	123.80	2.46
5	1	720	59.45	0.00
5	2	750	47.80	0.00
5	3	780	51.80	0.00
5	4	810	60.00	0.00
5	5	840	111.75	1.34

Test 3



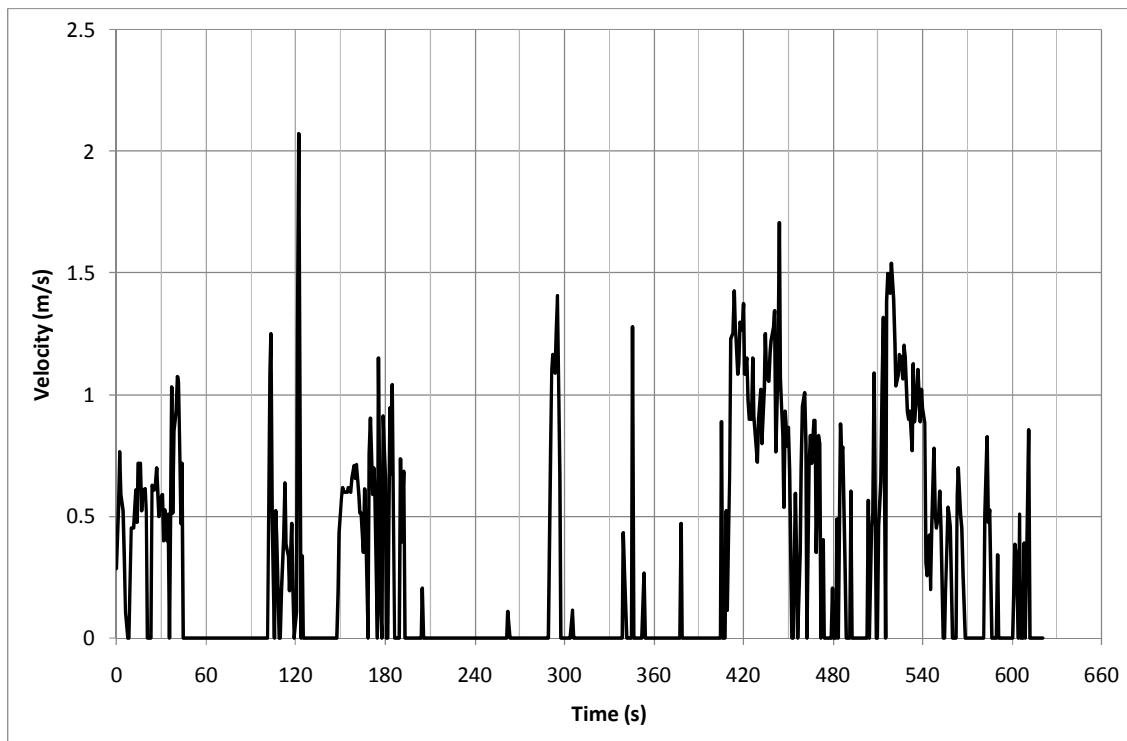
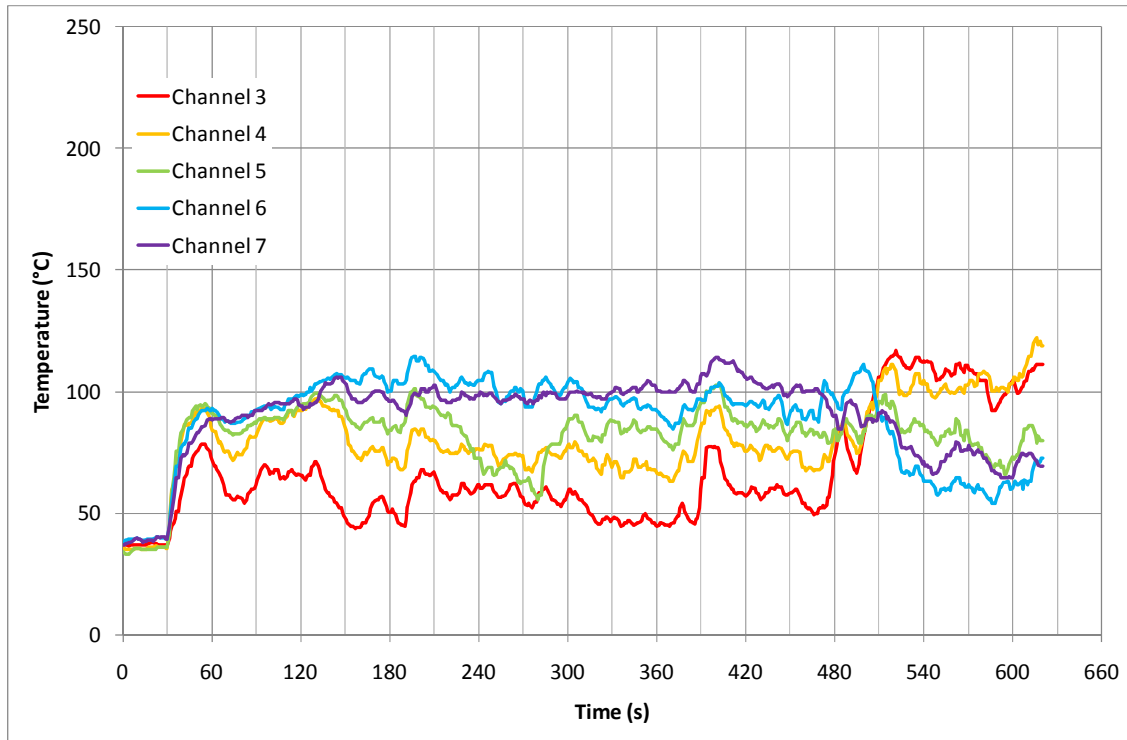
Bar	Point	Time (s)	Temperature (°C)	Velocity (m/s)
1	1	60	47.40	0.00
1	2	90	50.40	0.20
1	3	120	53.95	0.00
1	4	150	58.70	0.04
1	5	180	57.20	0.60
2	1	240	58.05	0.61
2	2	270	47.85	0.21
2	3	300	52.60	0.35
2	4	330	49.10	0.00
2	5	360	65.30	0.46
3	1	360	65.30	0.46
3	2	390	62.60	0.33
3	3	420	64.10	0.00
3	4	450	59.10	0.00
3	5	480	54.25	0.00
4	1	570	58.45	0.62
4	2	600	56.05	0.00
4	3	630	55.35	0.00
4	4	660	52.45	0.00
4	5	690	56.65	0.32
5	1	720	55.00	0.47
5	2	750	49.65	0.53
5	3	780	47.65	0.00
5	4	810	54.70	0.00
5	5	840	61.10	0.45

250°C 5 Minutes
Test 1



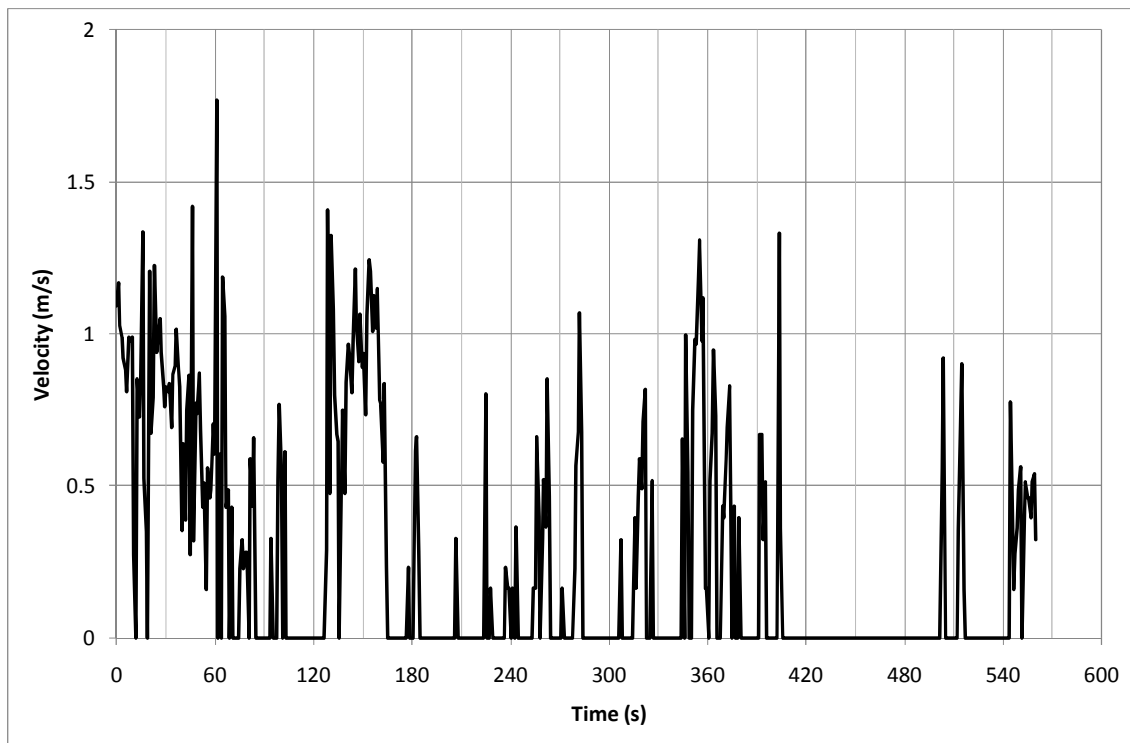
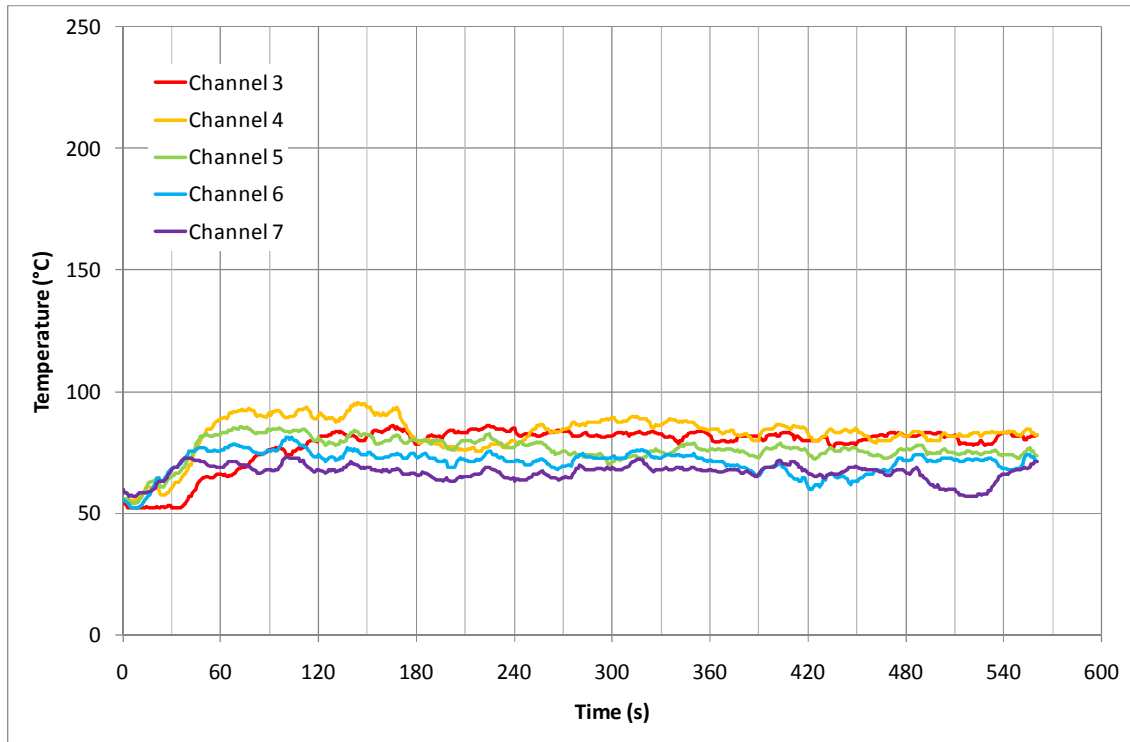
Bar	Point	Time (s)	Temperature (°C)	Velocity (m/s)
1	1	50	59.05	0.00
1	2	80	68.75	0.00
1	3	110	79.10	0.00
1	4	140	59.90	0.60
1	5	170	61.90	0.92
2	1	150	61.95	0.28
2	2	180	60.90	0.56
2	3	210	67.30	0.57
2	4	240	63.15	0.75
2	5	270	61.75	0.57
3	1	250	63.45	0.78
3	2	280	59.55	0.00
3	3	310	62.60	0.43
3	4	340	60.15	0.05
3	5	370	63.25	0.00
4	1	370	63.25	0.00
4	2	400	60.40	0.00
4	3	430	60.15	0.00
4	4	460	62.55	0.00
4	5	490	57.00	0.00
5	1	470	61.85	0.00
5	2	500	58.05	0.00
5	3	530	60.65	0.00
5	4	560	71.30	0.00
5	5	590	71.30	0.00

Test 2



Bar	Point	Time (s)	Temperature (°C)	Velocity (m/s)
1	1	80	56.55	0.00
1	2	100	67.05	0.00
1	3	120	66.20	0.33
1	4	140	63.25	0.00
1	5	160	48.85	0.62
2	1	520	95.90	1.07
2	2	540	86.55	0.96
2	3	560	82.35	0.36
2	4	580	78.15	0.00
2	5	600	69.50	0.00
3	1	180	86.45	0.65
3	2	200	97.00	0.00
3	3	220	91.35	0.00
3	4	240	77.15	0.00
3	5	260	68.20	0.00
4	1	400	109.25	0.00
4	2	420	94.80	1.22
4	3	440	94.70	1.09
4	4	460	91.95	0.53
4	5	480	99.65	0.00
5	1	300	97.85	0.87
5	2	320	98.80	0.00
5	3	340	100.35	0.00
5	4	360	102.80	0.00
5	5	380	101.60	0.00

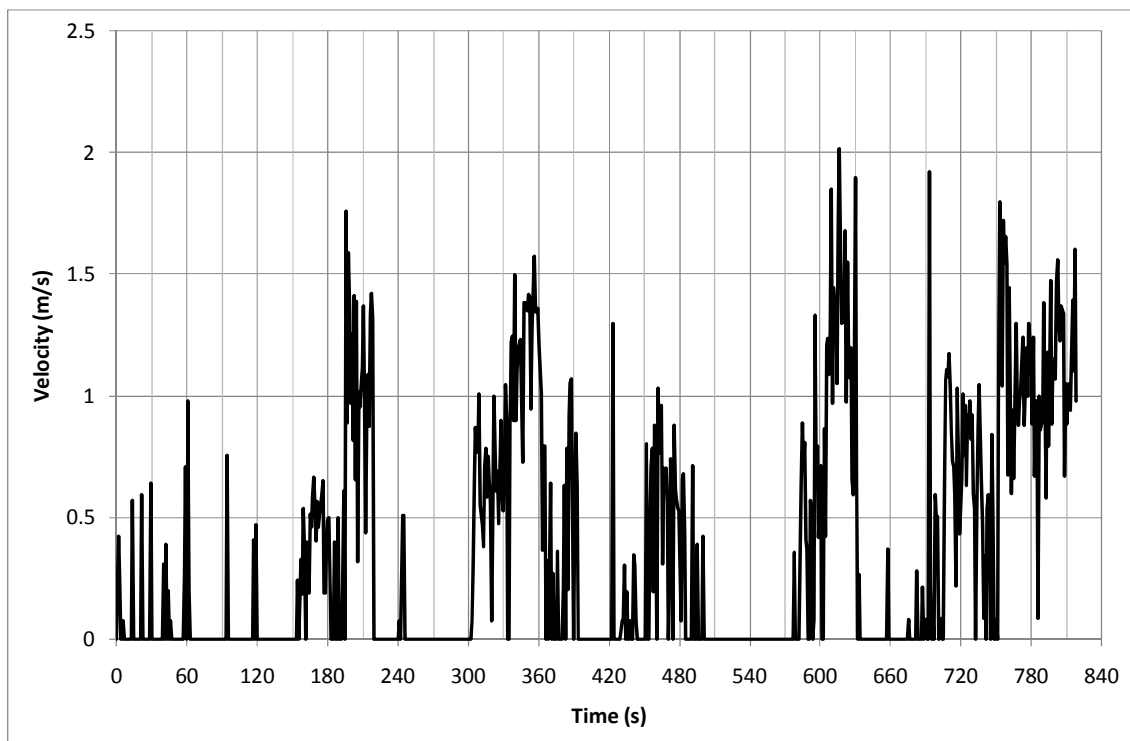
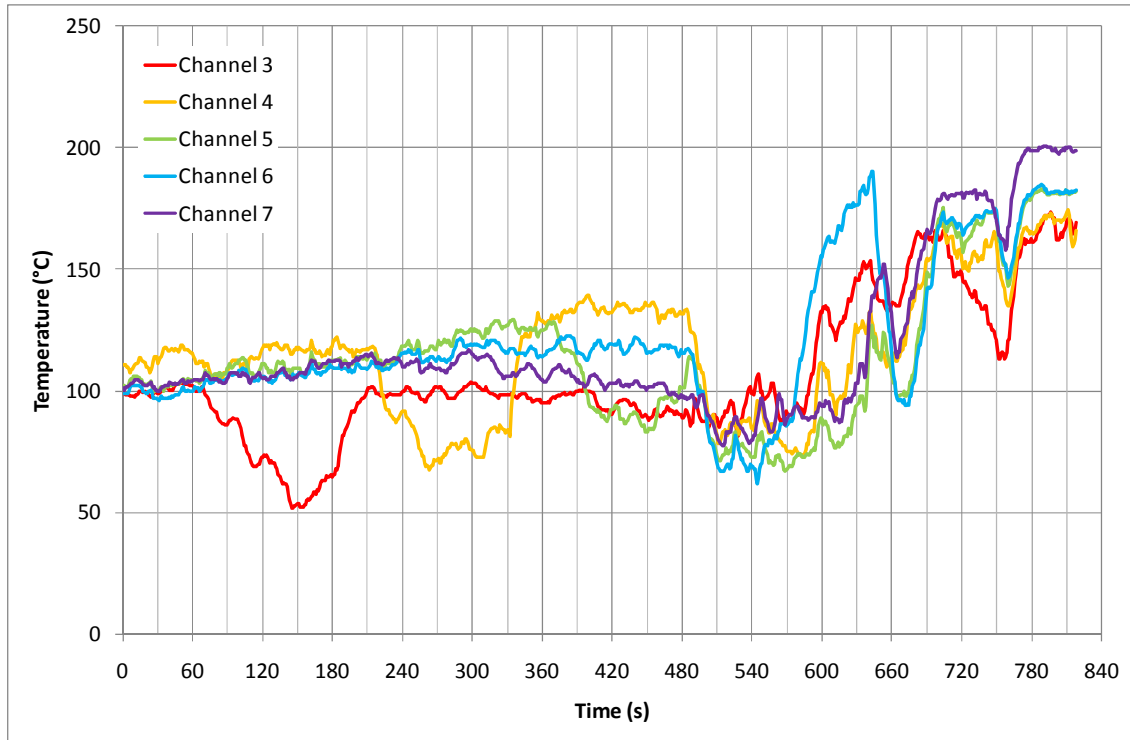
Test 3



Bar	Point	Time (s)	Temperature (°C)	Velocity (m/s)
1	1	50	60.00	0.73
1	2	70	65.85	0.71
1	3	90	74.35	0.00
1	4	110	75.30	0.00
1	5	140	90.10	0.78
2	1	160	91.50	1.04
2	2	180	84.15	0.00
2	3	200	78.00	0.00
2	4	220	76.10	0.00
2	5	240	78.55	0.00
3	1	270	75.40	0.23
3	2	290	73.75	0.27
3	3	310	71.95	0.00
3	4	330	75.00	0.20
3	5	360	72.35	0.85
4	1	390	67.30	0.00
4	2	410	68.45	0.00
4	3	430	61.25	0.00
4	4	450	63.70	0.00
4	5	470	66.95	0.00
5	1	490	67.05	0.00
5	2	510	59.95	0.00
5	3	530	57.55	0.00
5	4	550	67.05	0.00
5	5	570	69.45	0.44

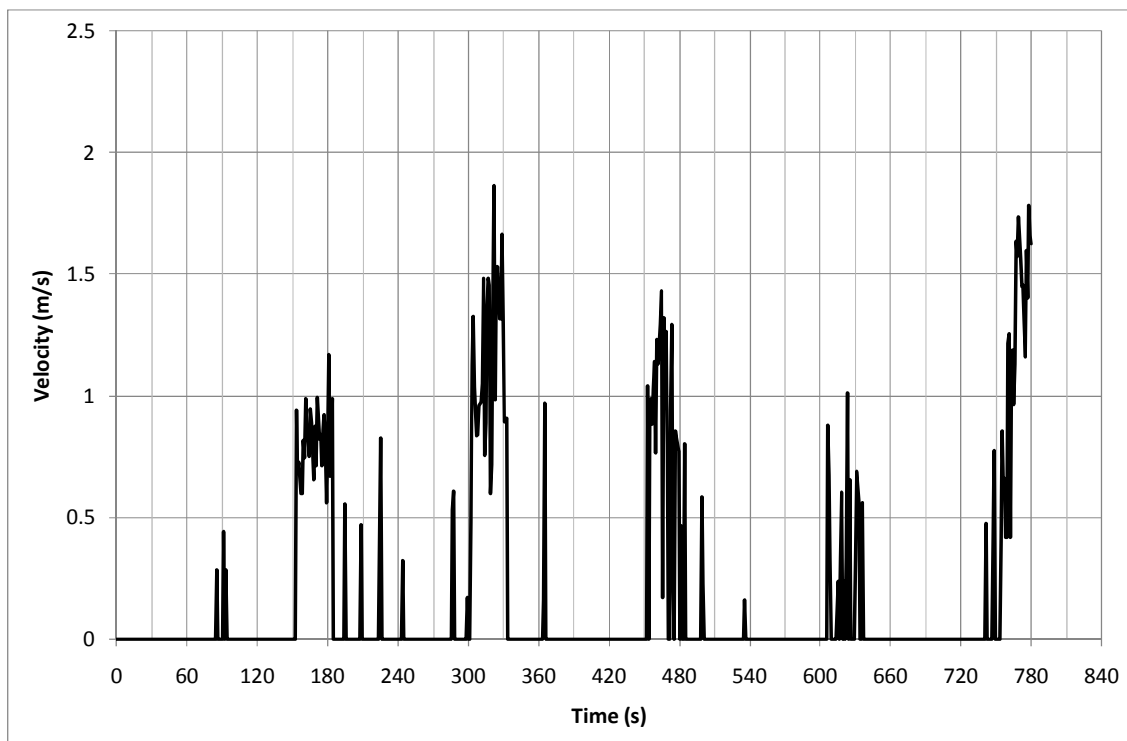
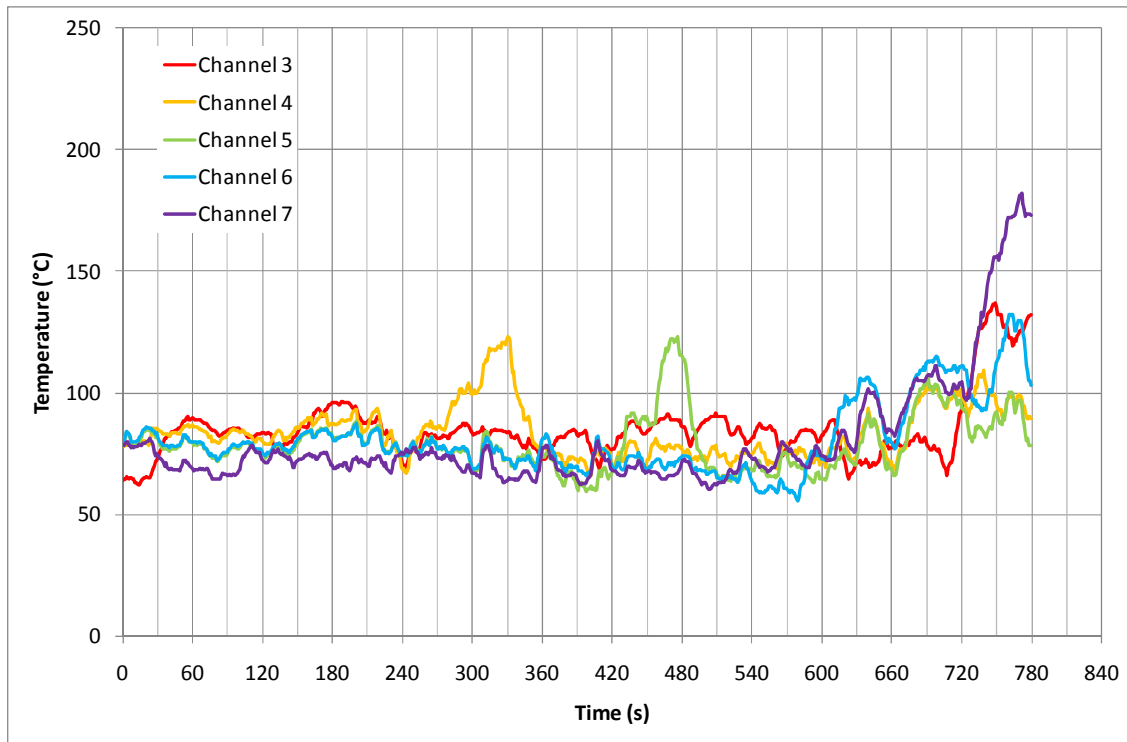
10 Minutes

Test 1



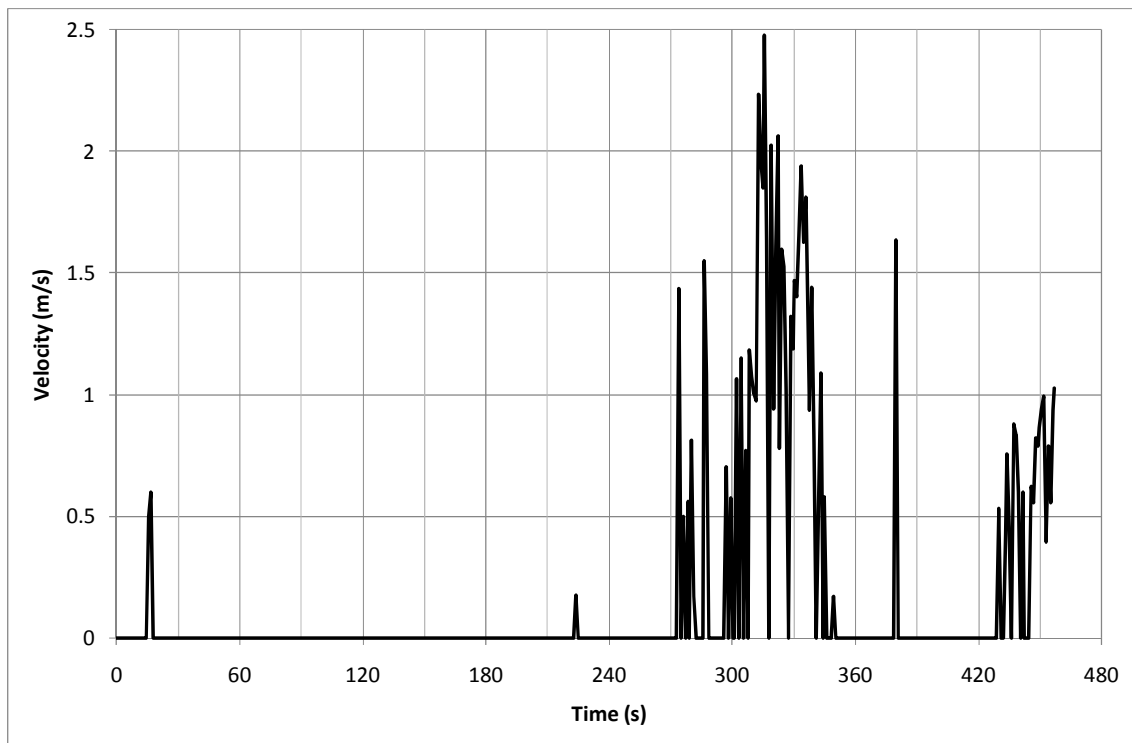
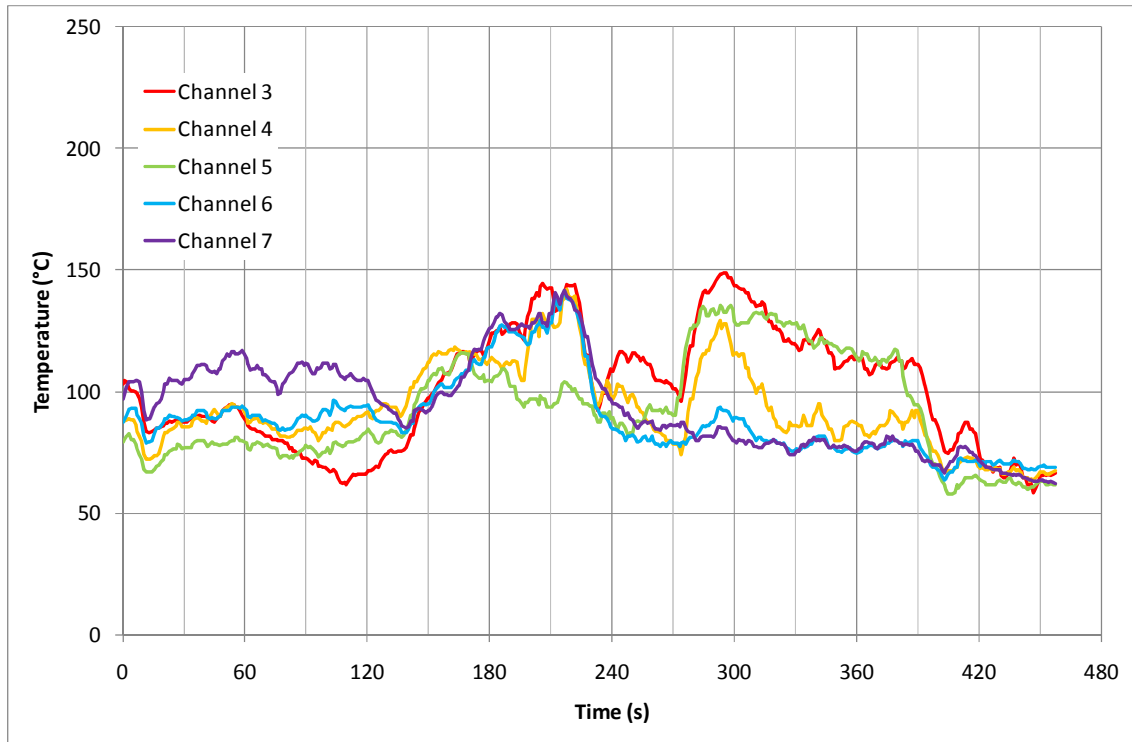
Bar	Point	Time (s)	Temperature (°C)	Velocity (m/s)
1	1	60	102.55	0.00
1	2	90	87.35	0.00
1	3	120	70.25	0.00
1	4	150	54.95	0.00
1	5	180	64.00	0.47
2	1	210	116.80	1.08
2	2	240	89.15	0.00
2	3	270	69.60	0.00
2	4	300	78.25	0.00
2	5	330	83.95	0.66
3	1	360	124.55	1.36
3	2	390	115.15	0.61
3	3	420	89.55	0.00
3	4	450	86.80	0.00
3	5	480	99.30	0.55
4	1	510	80.65	0.00
4	2	540	69.80	0.00
4	3	570	84.50	0.00
4	4	600	145.20	0.50
4	5	630	175.85	1.17
5	1	660	143.80	0.00
5	2	690	155.75	0.00
5	3	720	180.60	0.80
5	4	750	177.00	0.21
5	5	780	198.00	1.11

Test 2



Bar	Point	Time (s)	Temperature (°C)	Velocity (m/s)
1	1	60	88.80	0.00
1	2	90	83.10	0.00
1	3	120	82.35	0.00
1	4	150	80.55	0.00
1	5	180	92.70	0.81
2	1	210	86.90	0.00
2	2	240	77.15	0.00
2	3	270	86.55	0.00
2	4	300	101.00	0.00
2	5	330	119.55	1.37
3	1	360	71.45	0.00
3	2	390	65.10	0.00
3	3	420	67.20	0.00
3	4	450	89.00	0.00
3	5	480	115.40	0.61
4	1	510	67.45	0.00
4	2	540	68.00	0.00
4	3	570	61.50	0.00
4	4	600	75.20	0.00
4	5	630	97.45	0.24
5	1	660	86.35	0.00
5	2	690	105.20	0.00
5	3	720	102.10	0.00
5	4	750	149.05	0.00
5	5	780	175.55	1.51

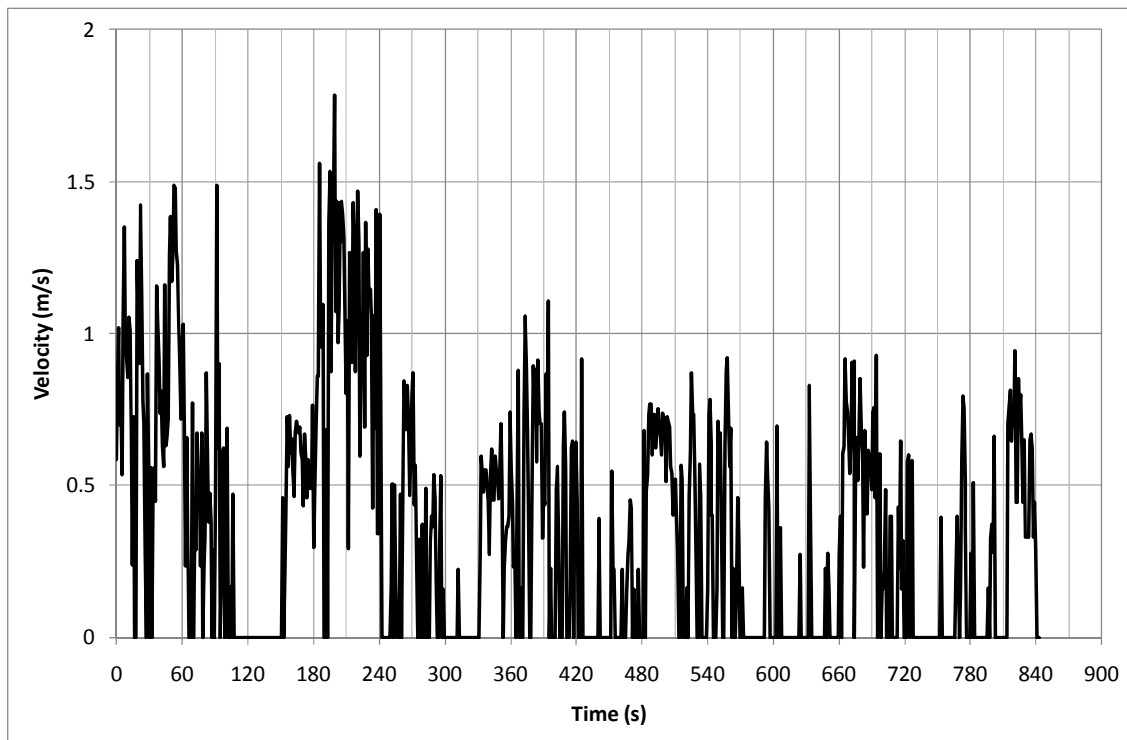
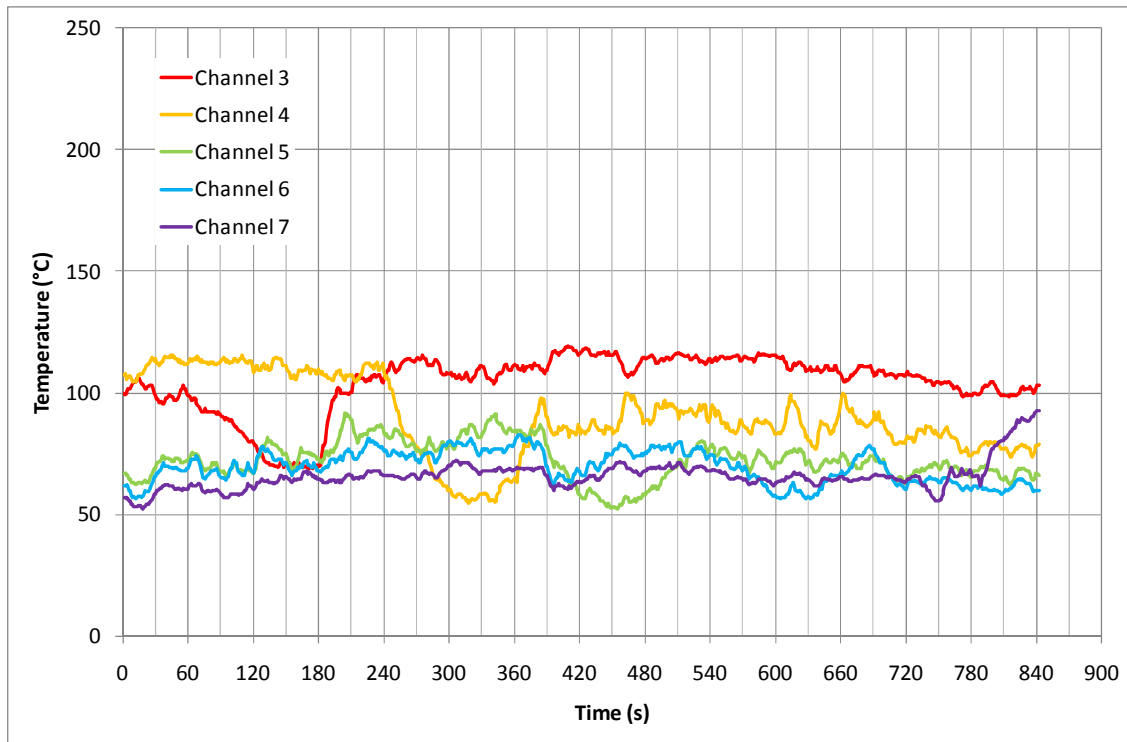
Test3 (Failed not used)



Bar	Point	Time (s)	Temperature (°C)	Velocity (m/s)
1	1	60	92.85	0.00
1	2	90	75.05	0.00
1	3	120	65.05	0.00
1	4	150	88.90	0.00
1	5	180	116.05	0.00
2	1			
2	2			
2	3			
2	4			
2	5			
3	1	250	99.35	0.00
3	2	280	83.15	0.00
3	3	310	111.00	0.48
3	4	340	119.10	1.48
3	5	370	114.05	0.00
4	1			
4	2			
4	3			
4	4			
4	5			
5	1			
5	2			
5	3			
5	4			
5	5			

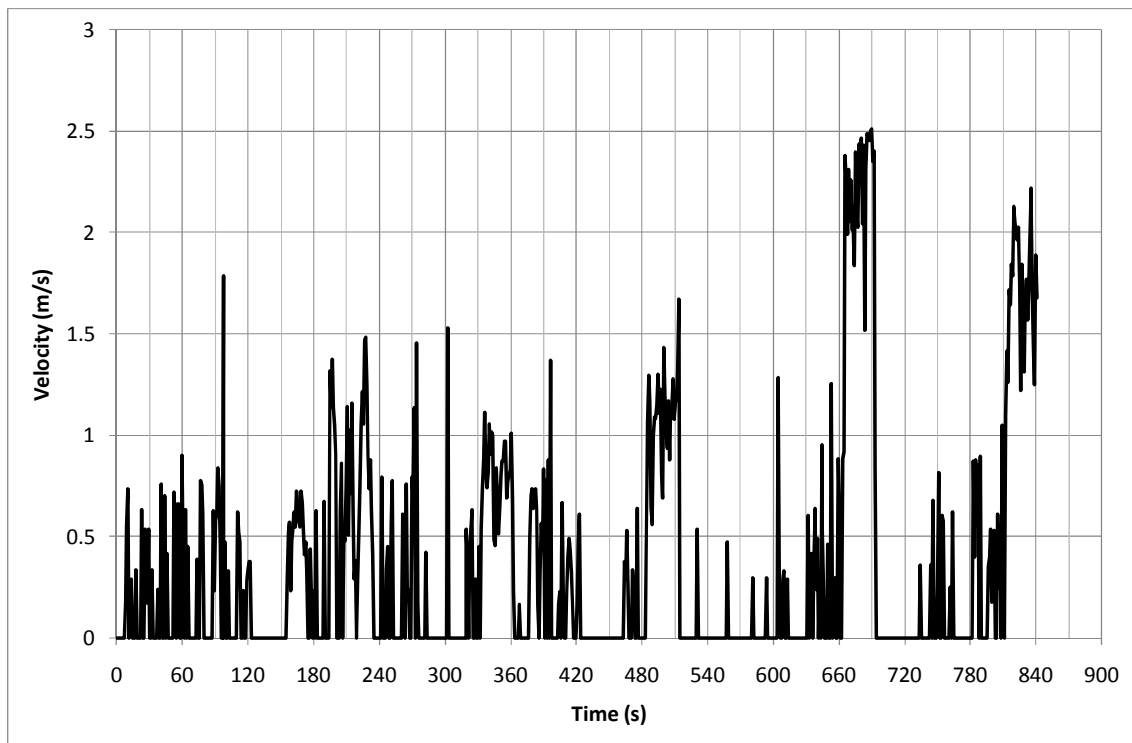
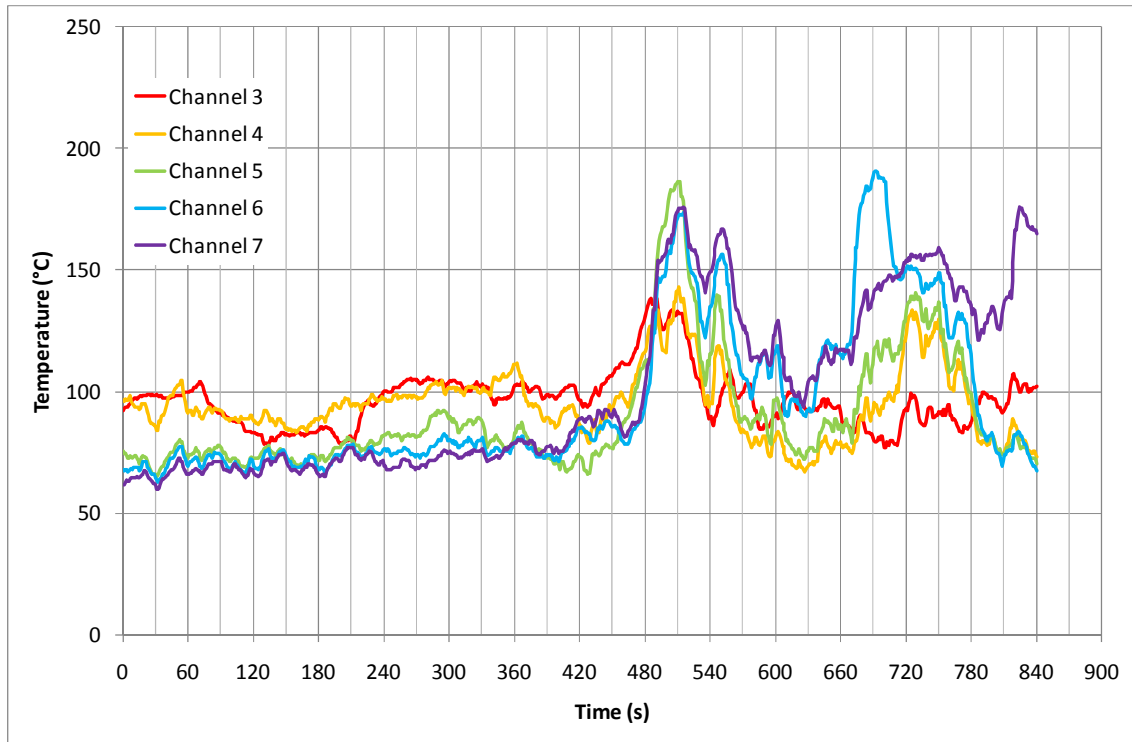
20 Minutes

Test 1



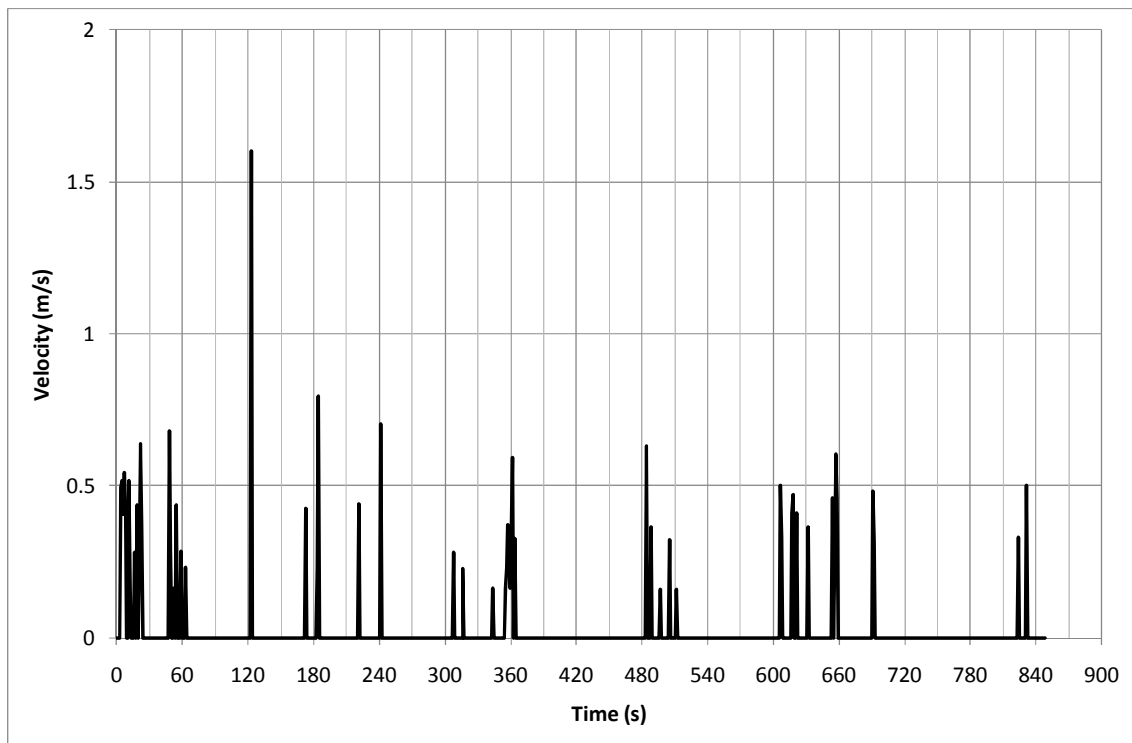
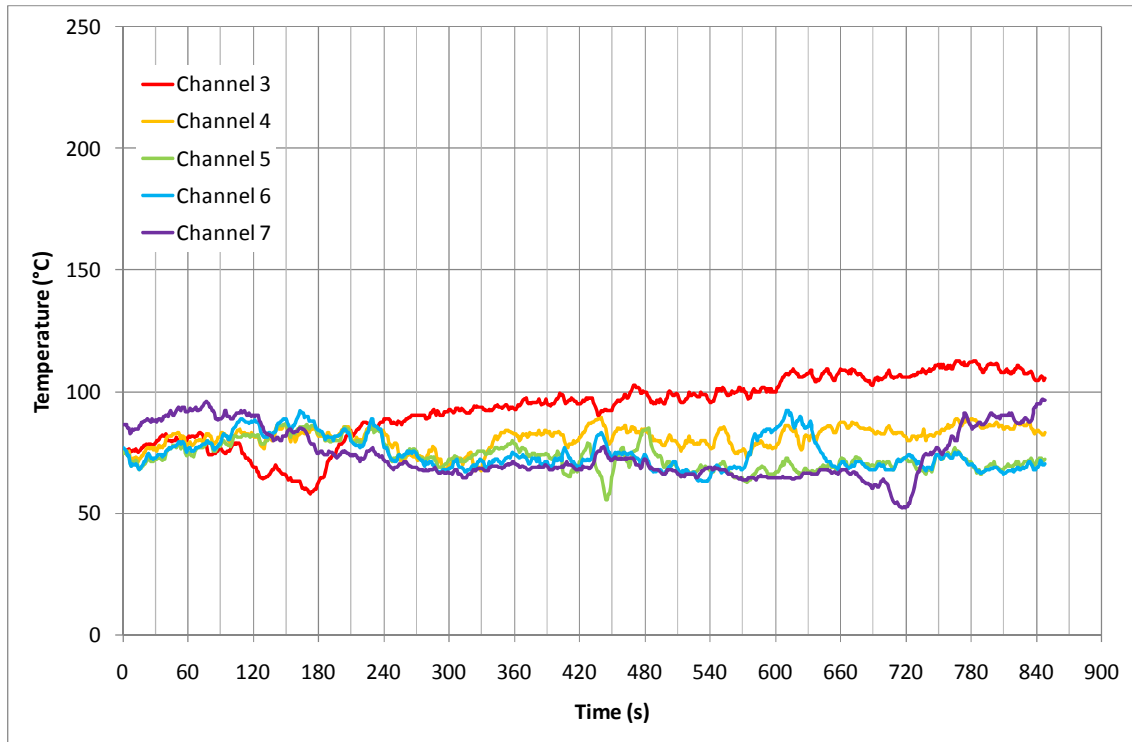
Bar	Point	Time (s)	Temperature (°C)	Velocity (m/s)
1	1	60	100.35	1.17
1	2	90	91.65	0.43
1	3	120	81.25	0.00
1	4	150	70.25	0.00
1	5	180	73.65	0.54
2	1	240	110.85	0.96
2	2	270	80.70	0.66
2	3	300	62.45	0.26
2	4	330	56.90	0.00
2	5	360	65.65	0.46
3	1	390	83.50	0.72
3	2	420	61.95	0.38
3	3	450	54.00	0.00
3	4	480	56.85	0.00
3	5	510	68.45	0.62
4	1	570	69.40	0.26
4	2	600	59.60	0.07
4	3	630	58.45	0.00
4	4	660	66.05	0.00
4	5	690	76.80	0.59
5	1	720	63.80	0.00
5	2	750	57.15	0.00
5	3	780	67.25	0.33
5	4	810	79.25	0.08
5	5	840	89.80	0.46

Test 2



Bar	Point	Time (s)	Temperature (°C)	Velocity (m/s)
1	1	60	99.15	0.34
1	2	90	92.65	0.00
1	3	120	84.05	0.20
1	4	150	81.70	0.00
1	5	180	83.55	0.29
2	1	240	97.20	0.37
2	2	270	98.20	0.33
2	3	300	101.65	0.00
2	4	330	100.85	0.28
2	5	360	104.55	0.83
3	1	390	74.55	0.54
3	2	420	70.40	0.20
3	3	450	77.25	0.00
3	4	480	106.65	0.00
3	5	510	180.60	1.14
4	1	540	128.65	0.00
4	2	570	115.40	0.00
4	3	600	111.65	0.00
4	4	630	92.80	0.00
4	5	660	117.80	0.00
5	1	720	149.20	0.00
5	2	750	156.85	0.00
5	3	780	140.05	0.00
5	4	810	130.15	0.46
5	5	840	168.20	1.74

Test 3

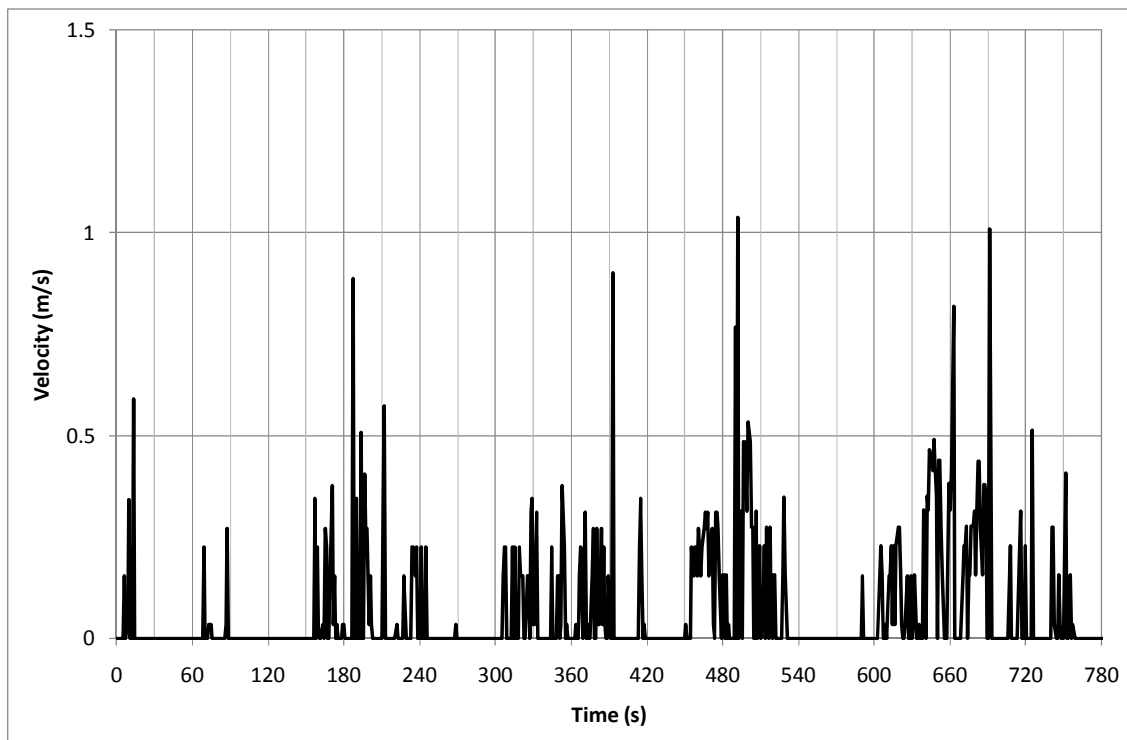
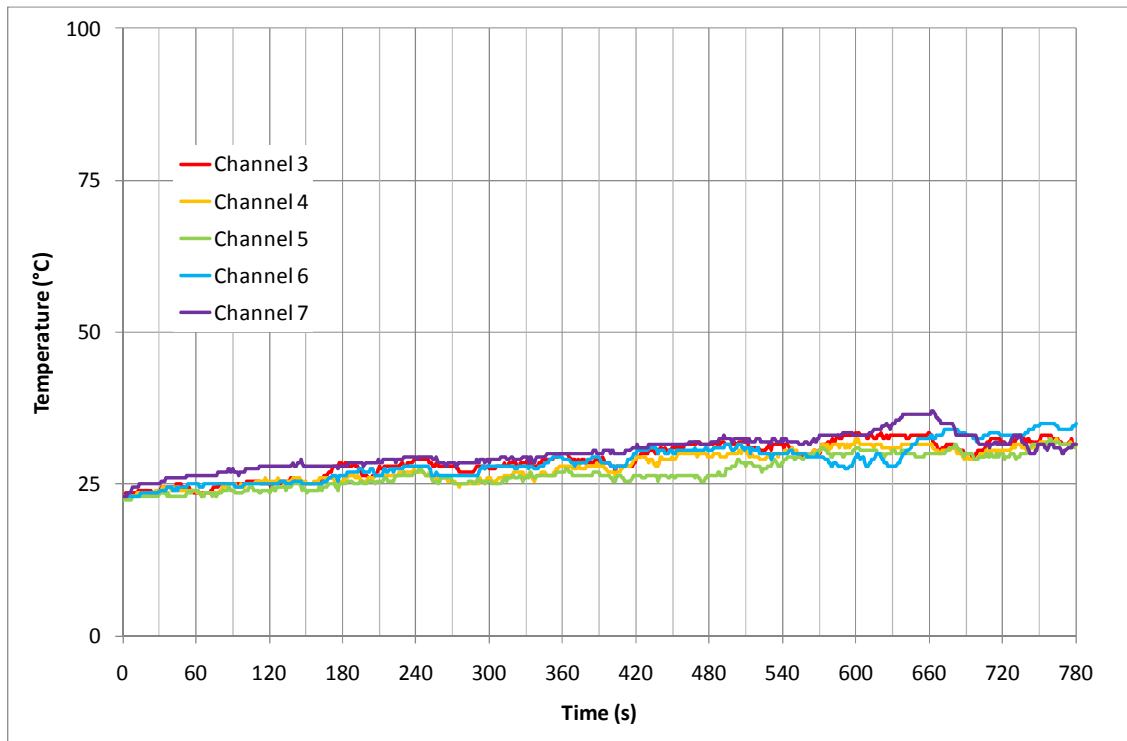


Bar	Point	Time (s)	Temperature (°C)	Velocity (m/s)
1	1	60	80.20	0.00
1	2	90	75.05	0.00
1	3	120	72.35	0.00
1	4	150	67.65	0.00
1	5	180	61.65	0.00
2	1	240	84.60	0.00
2	2	270	73.65	0.00
2	3	300	69.55	0.00
2	4	330	69.65	0.00
2	5	360	78.20	0.00
3	1	390	73.80	0.00
3	2	420	67.00	0.00
3	3	450	59.85	0.00
3	4	480	79.05	0.00
3	5	510	69.65	0.00
4	1	570	68.75	0.00
4	2	600	84.05	0.00
4	3	630	85.15	0.00
4	4	660	66.80	0.00
4	5	690	61.85	0.00
5	1	720	52.95	0.00
5	2	750	75.10	0.00
5	3	780	88.85	0.00
5	4	810	90.05	0.00
5	5	840	90.00	0.00

Appendix C Polyvinyl Chloride Experiment Results

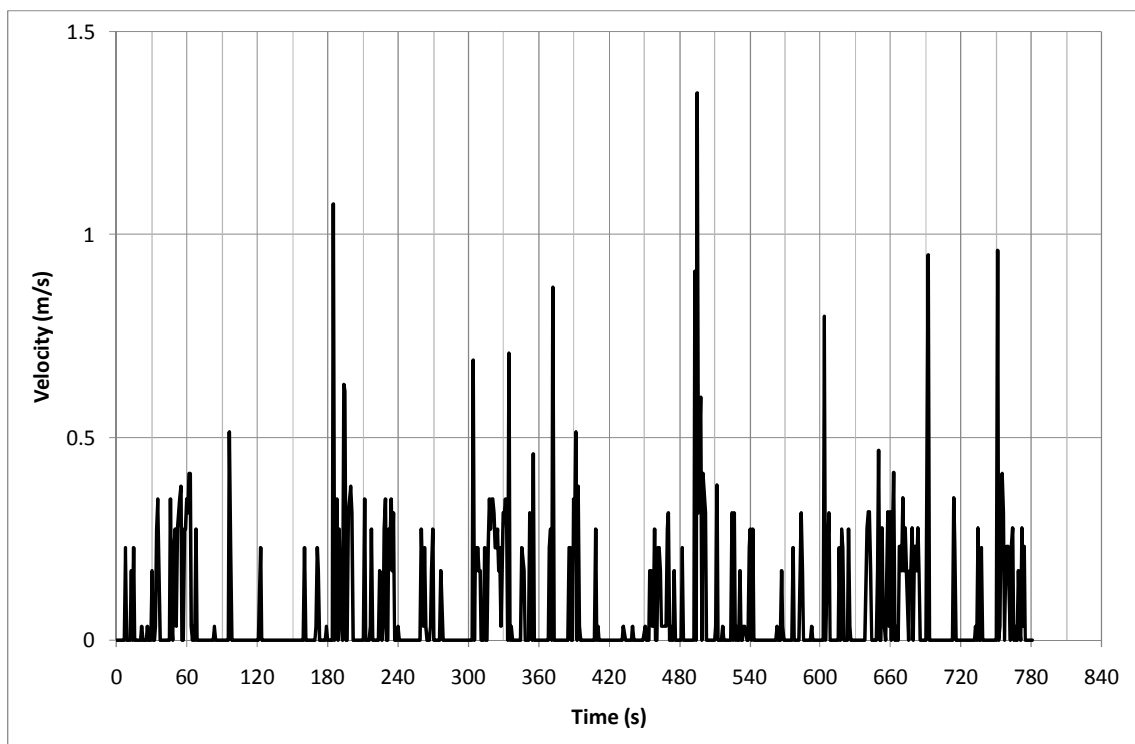
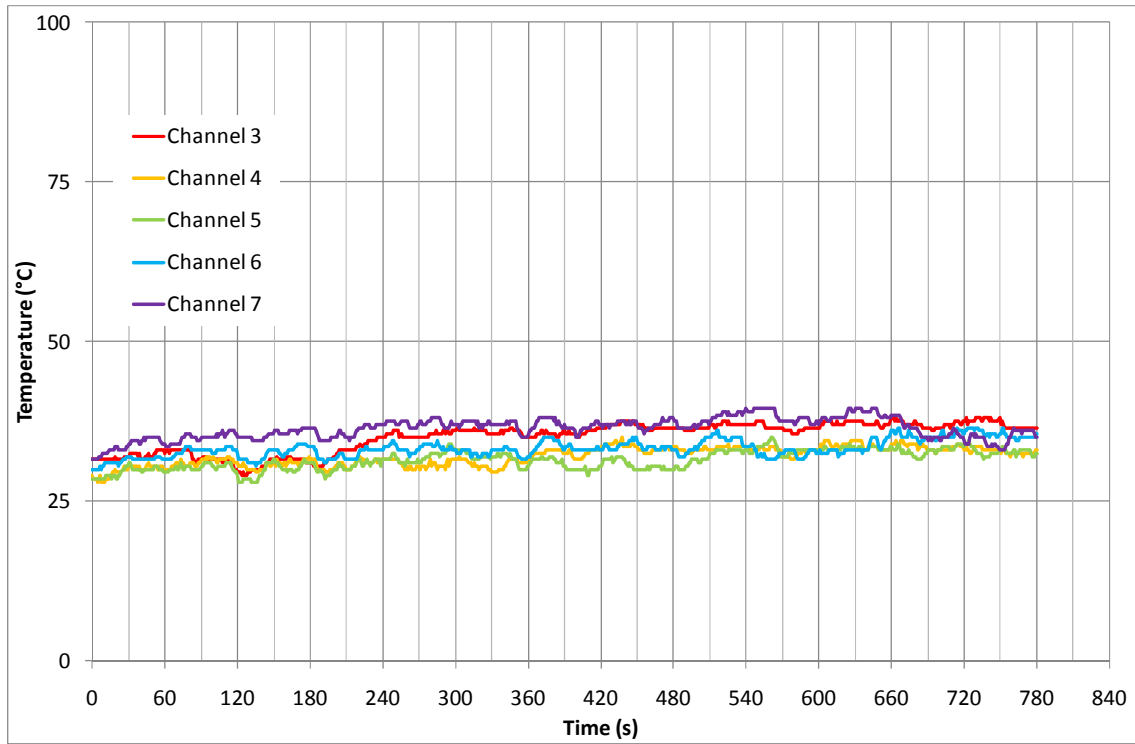
100°C 20 minutes

Test 1



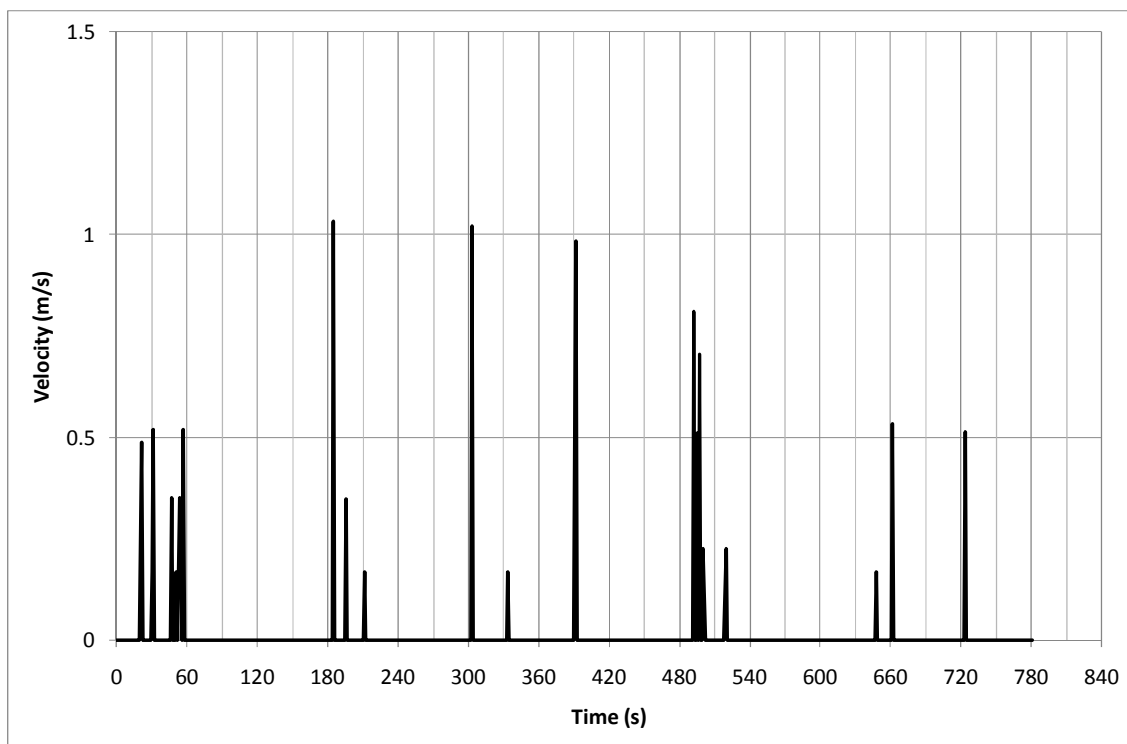
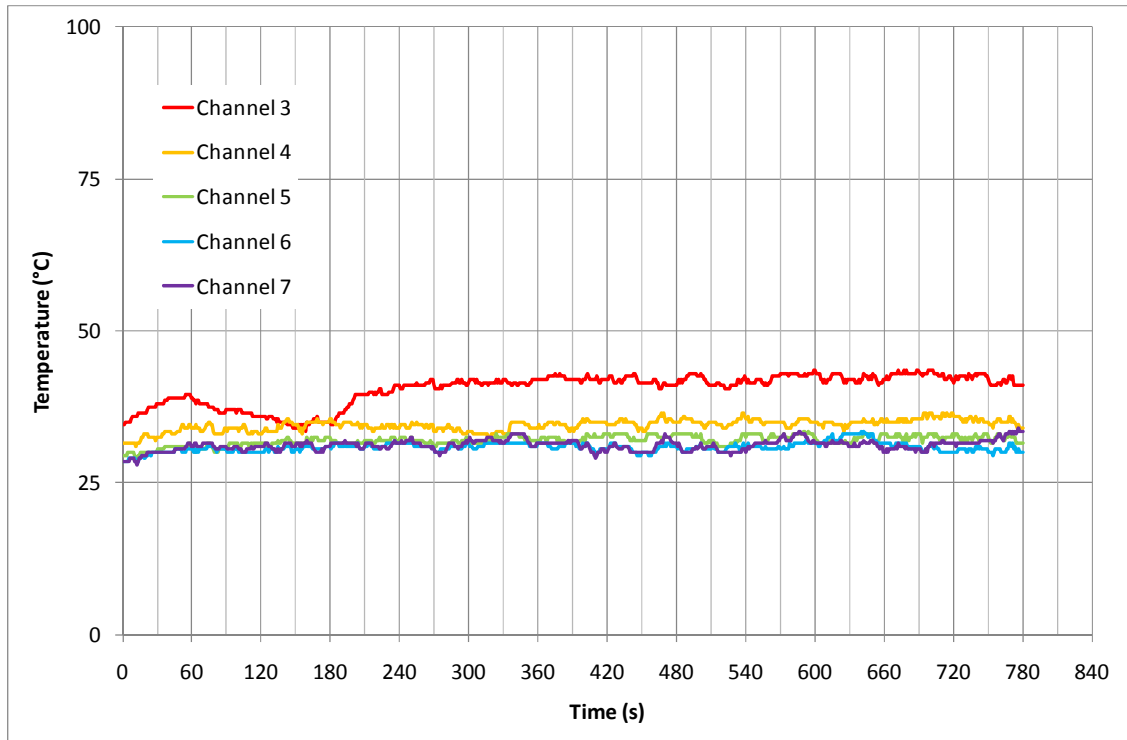
Bar	Point	Time (s)	Temperature (°C)	Velocity (m/s)
1	1	60	24.15	0.00
1	2	90	25.00	0.00
1	3	120	25.15	0.00
1	4	150	25.35	0.00
1	5	180	27.70	0.00
2	1	210	26.20	0.00
2	2	240	27.05	0.00
2	3	270	25.90	0.00
2	4	300	25.55	0.00
2	5	330	26.90	0.16
3	1	360	26.75	0.00
3	2	390	26.75	0.07
3	3	420	25.85	0.00
3	4	450	26.40	0.00
3	5	480	26.40	0.19
4	1	510	31.05	0.25
4	2	540	29.85	0.00
4	3	570	29.55	0.00
4	4	600	28.15	0.00
4	5	630	29.15	0.00
5	1	660	36.50	0.21
5	2	690	33.25	0.30
5	3	720	31.60	0.00
5	4	750	30.55	0.00
5	5	780	30.95	0.00

Test 2



Bar	Point	Time (s)	Temperature (°C)	Velocity (m/s)
1	1	60	32.75	0.24
1	2	90	31.60	0.00
1	3	120	30.75	0.00
1	4	150	31.00	0.00
1	5	180	31.35	0.00
2	1	210	30.70	0.00
2	2	240	31.25	0.09
2	3	270	30.25	0.00
2	4	300	31.05	0.00
2	5	330	30.30	0.26
3	1	360	30.35	0.00
3	2	390	31.15	0.00
3	3	420	29.95	0.00
3	4	450	30.55	0.00
3	5	480	30.35	0.00
4	1	510	34.50	0.00
4	2	540	34.60	0.00
4	3	570	31.90	0.00
4	4	600	32.75	0.00
4	5	630	33.60	0.00
5	1	660	38.15	0.20
5	2	690	35.45	0.00
5	3	720	35.50	0.00
5	4	750	33.60	0.00
5	5	780	35.85	0.00

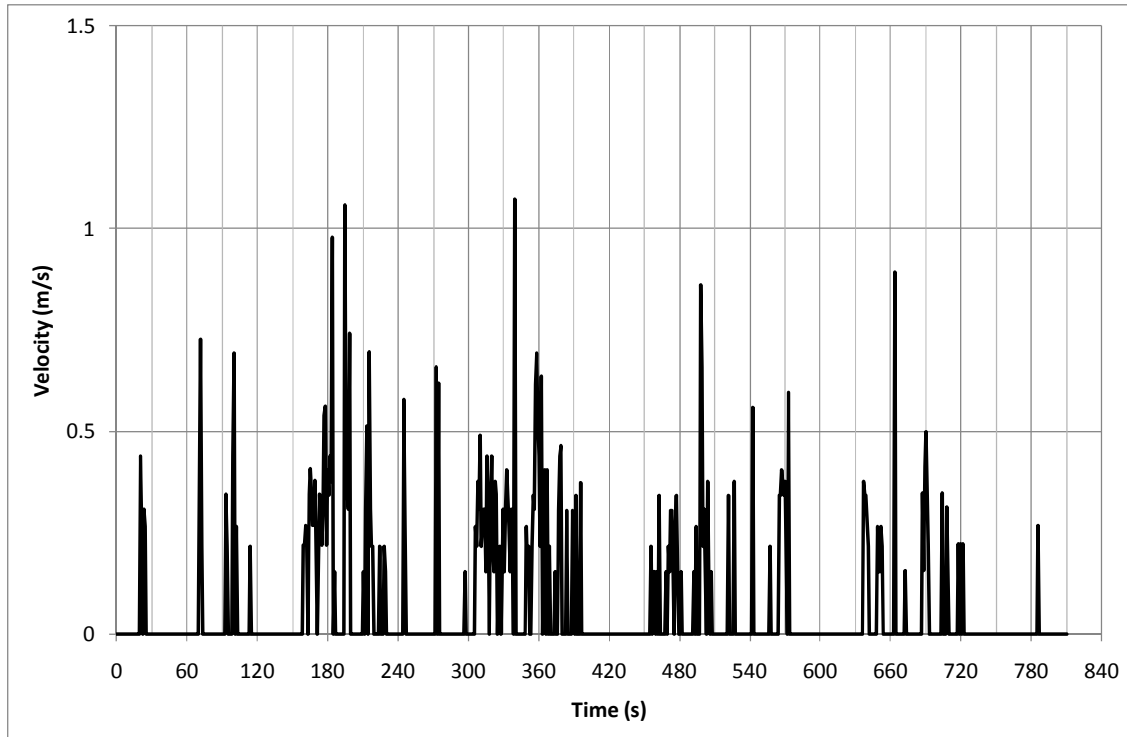
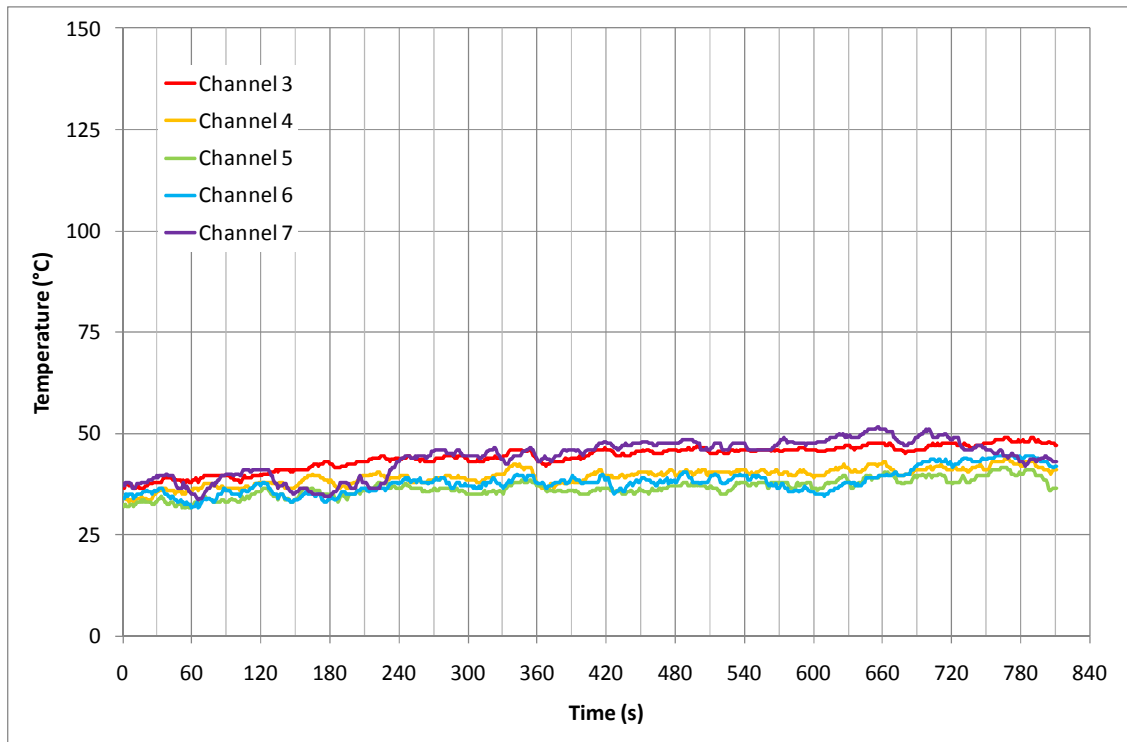
Test 3



Bar	Point	Time (s)	Temperature (°C)	Velocity (m/s)
1	1	60	39.25	0.00
1	2	90	36.70	0.00
1	3	120	36.15	0.00
1	4	150	34.45	0.00
1	5	180	35.05	0.00
2	1	210	34.45	0.00
2	2	240	34.25	0.00
2	3	270	34.25	0.00
2	4	300	33.40	0.00
2	5	330	33.30	0.00
3	1	360	32.15	0.00
3	2	390	31.65	0.00
3	3	420	32.65	0.00
3	4	450	32.05	0.00
3	5	480	32.50	0.00
4	1	510	30.65	0.00
4	2	540	30.95	0.00
4	3	570	30.60	0.00
4	4	600	31.60	0.00
4	5	630	32.70	0.00
5	1	660	31.10	0.00
5	2	690	30.45	0.00
5	3	720	31.60	0.00
5	4	750	31.85	0.00
5	5	780	33.40	0.00

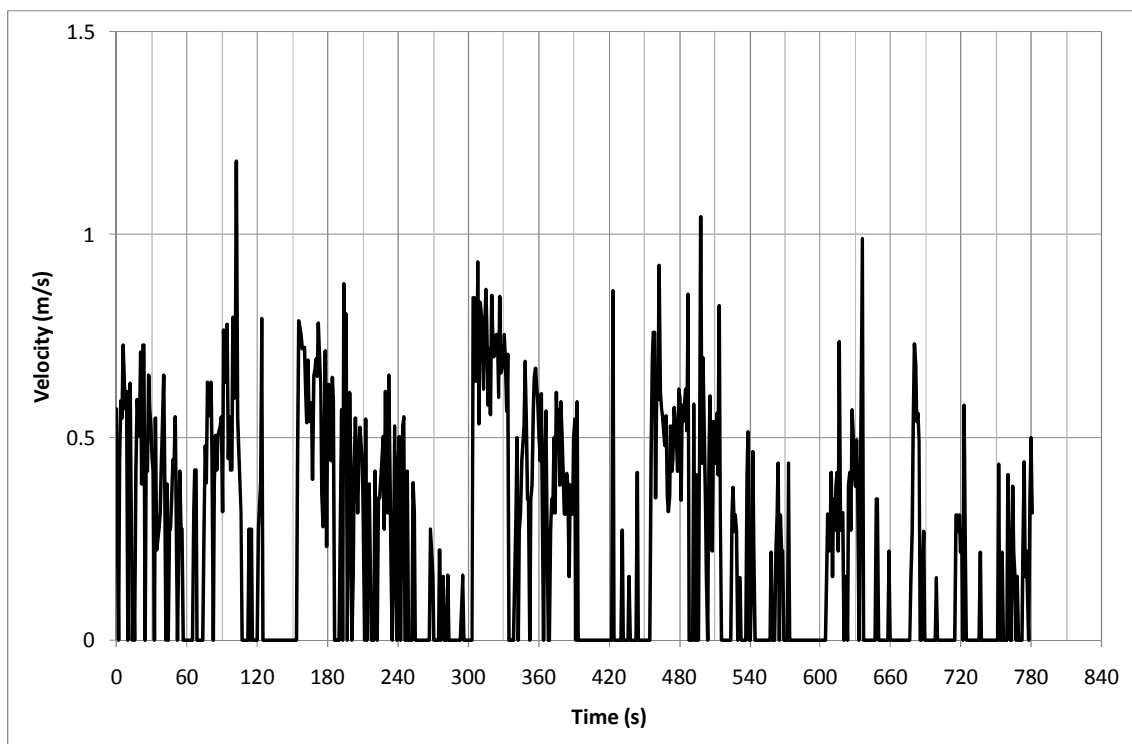
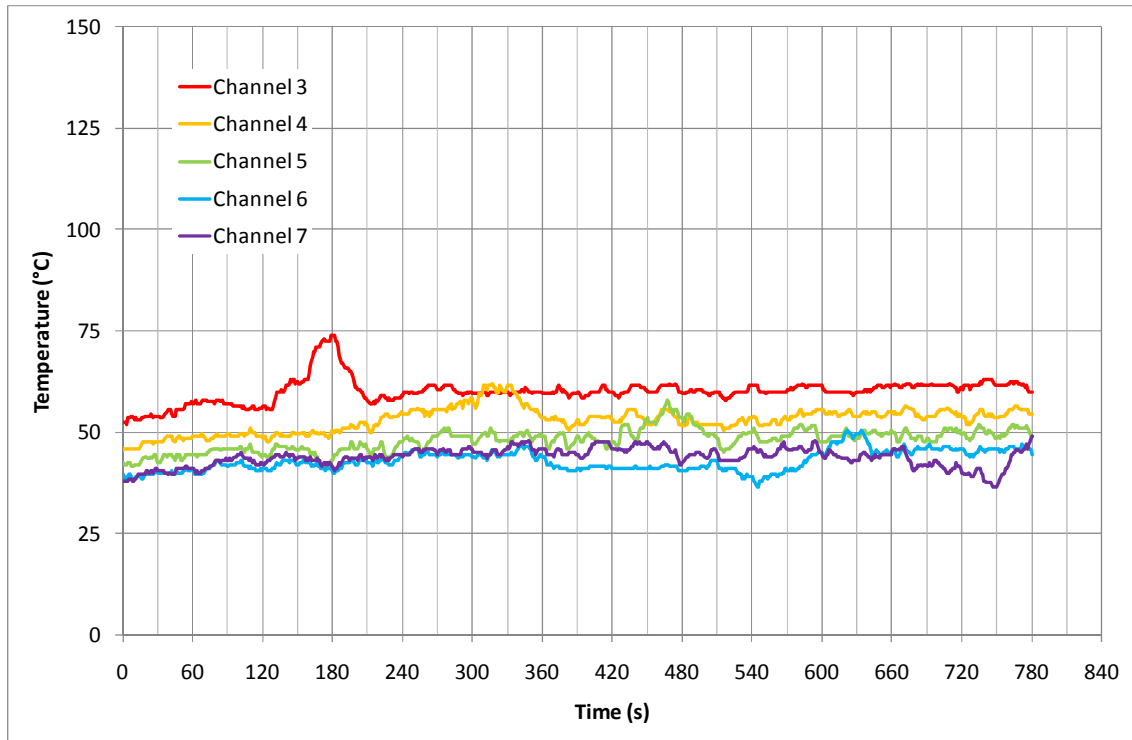
150°C 5 Minutes

Test 1



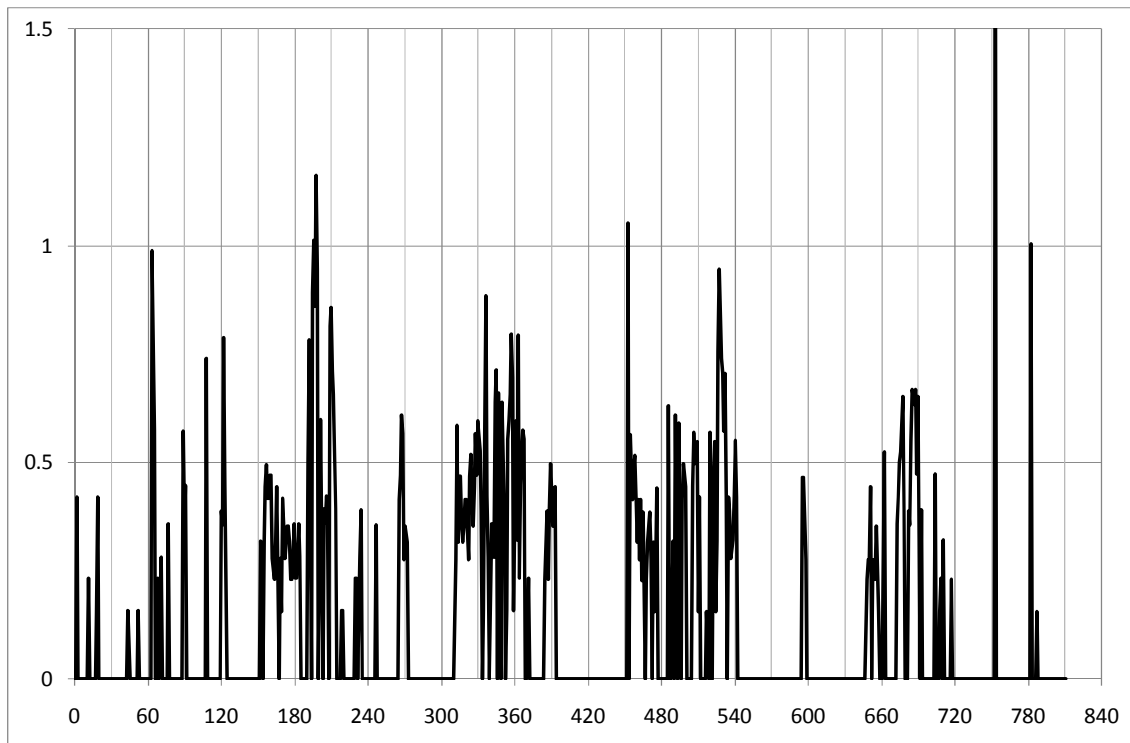
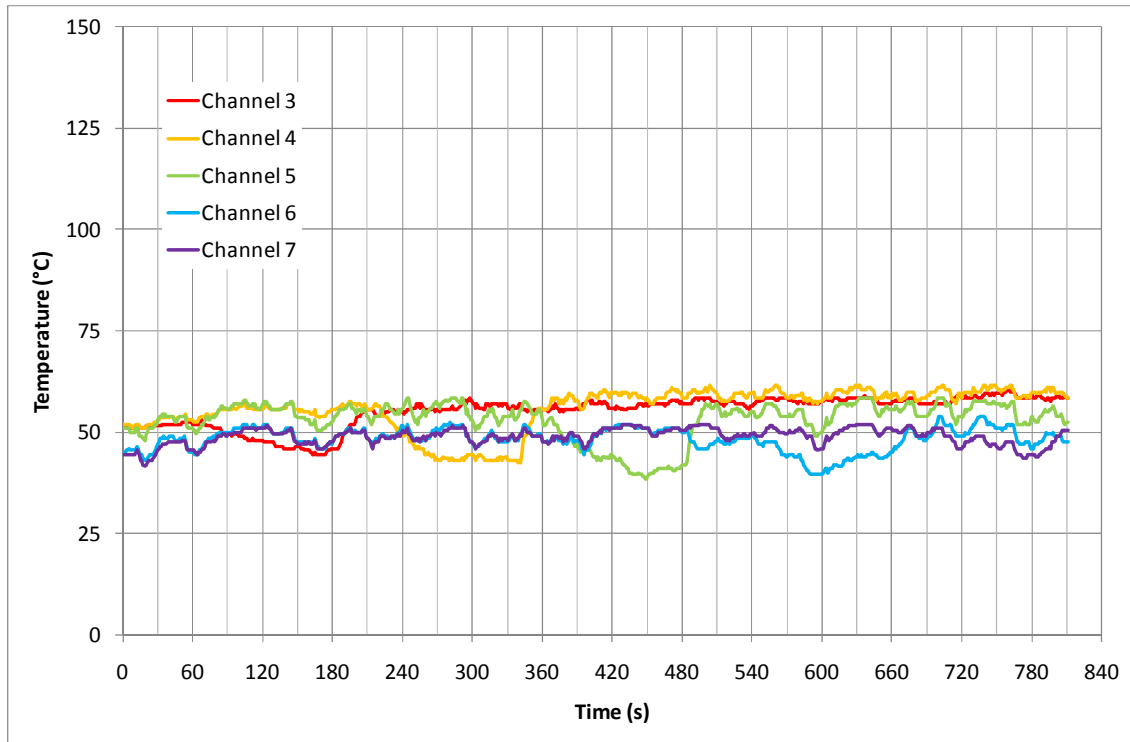
Bar	Point	Time (s)	Temperature (°C)	Velocity (m/s)
1	1	60	38.20	0.00
1	2	90	39.50	0.00
1	3	120	39.35	0.00
1	4	150	40.90	0.00
1	5	180	42.25	0.34
2	1	210	38.75	0.00
2	2	240	38.95	0.00
2	3	270	38.25	0.00
2	4	300	38.95	0.00
2	5	330	39.65	0.25
3	1	360	37.95	0.36
3	2	390	35.75	0.00
3	3	420	36.35	0.00
3	4	450	35.65	0.00
3	5	480	36.90	0.22
4	1	540	39.50	0.00
4	2	570	37.05	0.17
4	3	600	36.10	0.00
4	4	630	37.30	0.00
4	5	660	39.20	0.00
5	1	690	47.85	0.00
5	2	720	49.30	0.00
5	3	750	46.75	0.00
5	4	780	44.35	0.00
5	5	810	43.70	0.00

Test 2



Bar	Point	Time (s)	Temperature (°C)	Velocity (m/s)
1	1	60	56.50	0.00
1	2	90	57.50	0.46
1	3	120	55.95	0.00
1	4	150	62.25	0.00
1	5	180	70.45	0.56
2	1	210	52.05	0.38
2	2	240	54.10	0.35
2	3	270	54.95	0.00
2	4	300	57.65	0.00
2	5	330	60.45	0.73
3	1	360	48.75	0.49
3	2	390	47.10	0.37
3	3	420	47.10	0.00
3	4	450	50.45	0.00
3	5	480	53.50	0.48
4	1	510	42.45	0.42
4	2	540	39.05	0.08
4	3	570	39.80	0.18
4	4	600	44.65	0.00
4	5	630	49.60	0.35
5	1	660	44.40	0.00
5	2	690	41.70	0.43
5	3	720	41.10	0.00
5	4	750	37.20	0.00
5	5	780	46.35	0.17

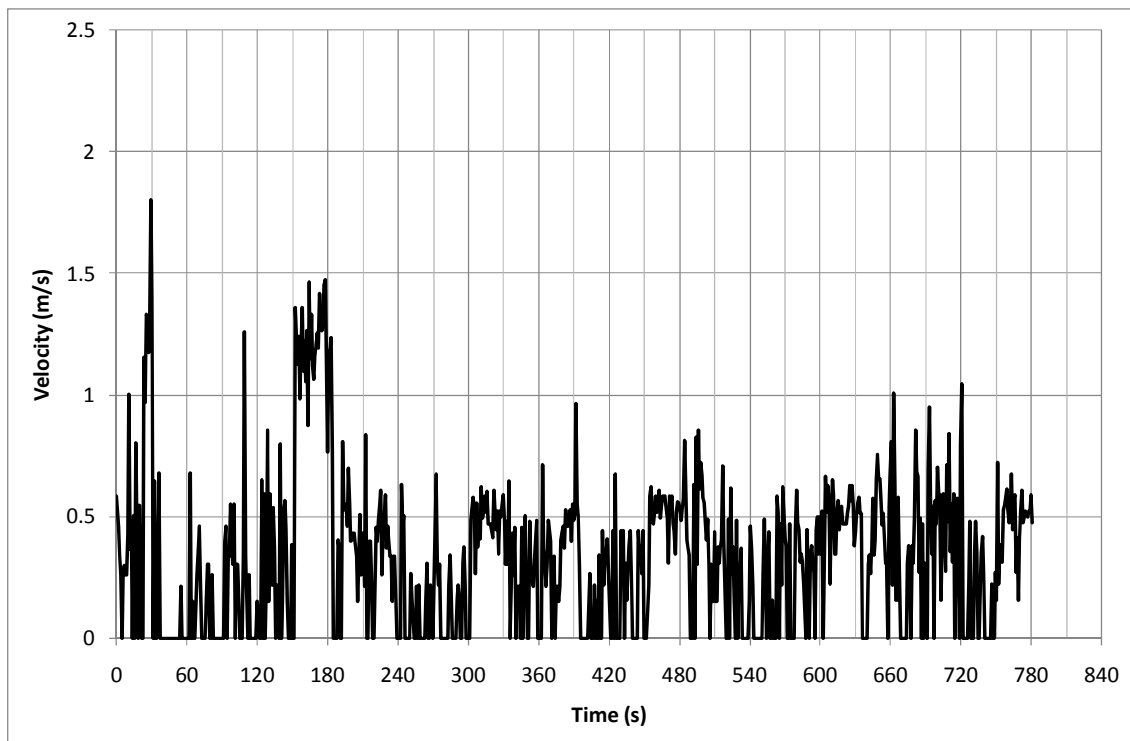
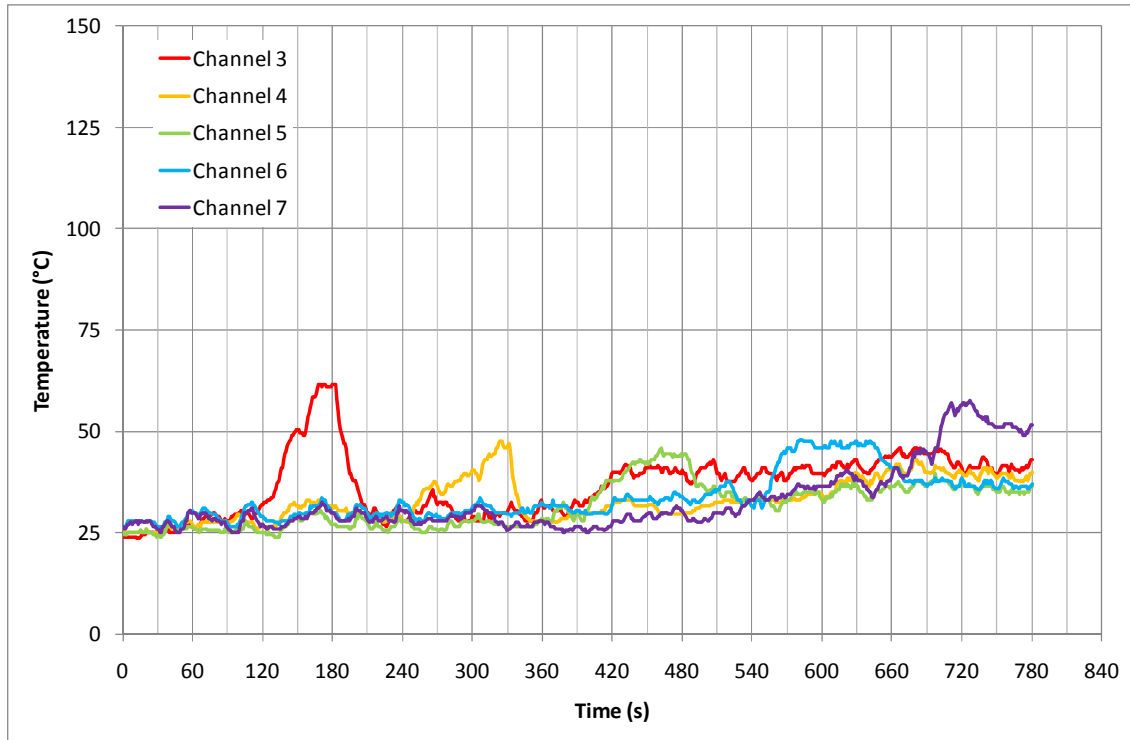
Test 3



Bar	Point	Time (s)	Temperature (°C)	Velocity (m/s)
1	1	60	52.40	0.00
1	2	90	50.25	0.00
1	3	120	48.05	0.00
1	4	150	46.10	0.00
1	5	180	46.10	0.32
2	1	210	56.55	0.47
2	2	240	50.90	0.00
2	3	270	44.25	0.16
2	4	300	44.00	0.00
2	5	330	43.50	0.44
3	1	360	54.85	0.51
3	2	390	47.60	0.24
3	3	420	43.85	0.00
3	4	450	39.25	0.00
3	5	480	41.80	0.21
4	1	540	48.60	0.47
4	2	570	45.40	0.00
4	3	600	39.50	0.00
4	4	630	43.40	0.00
4	5	660	44.10	0.23
5	1	690	49.15	0.49
5	2	720	46.95	0.00
5	3	750	47.05	0.00
5	4	780	44.10	0.00
5	5	810	49.60	0.00

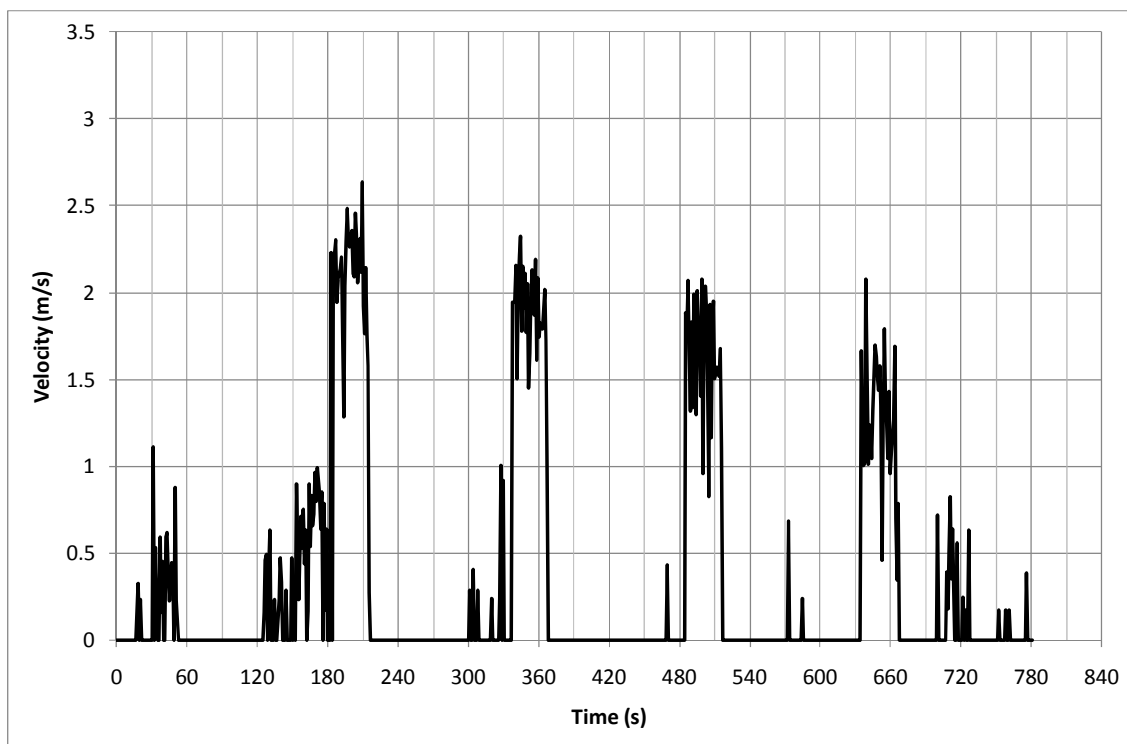
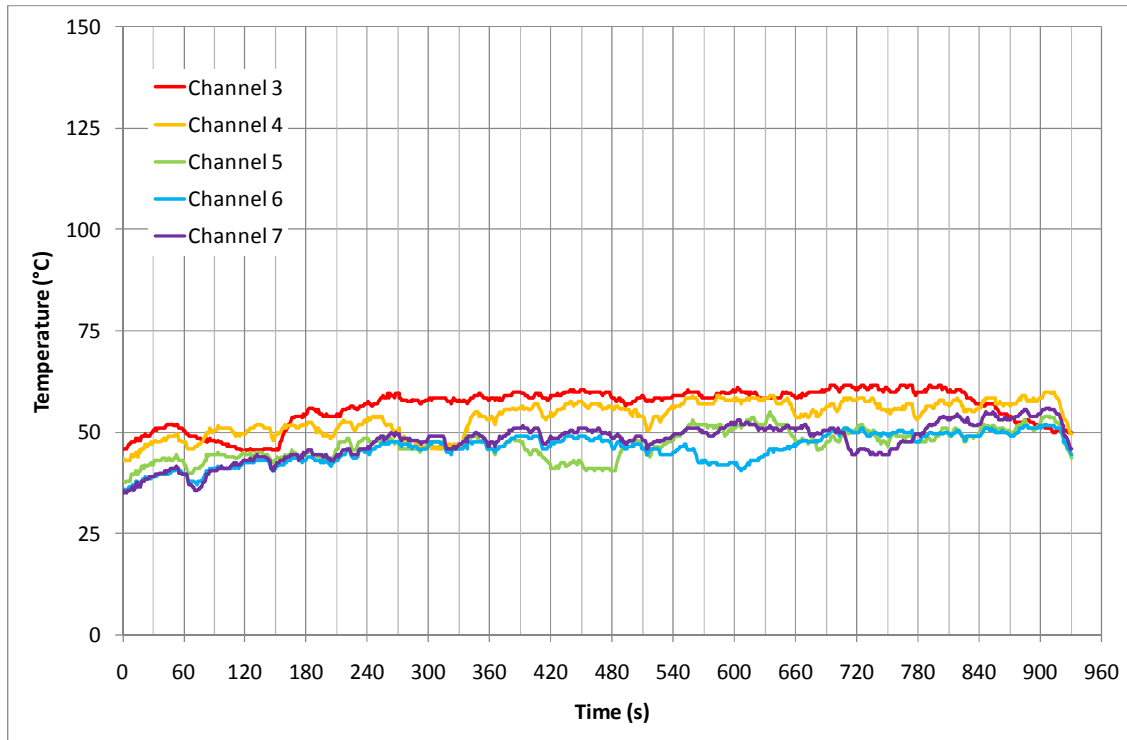
10 Minutes

Test 1



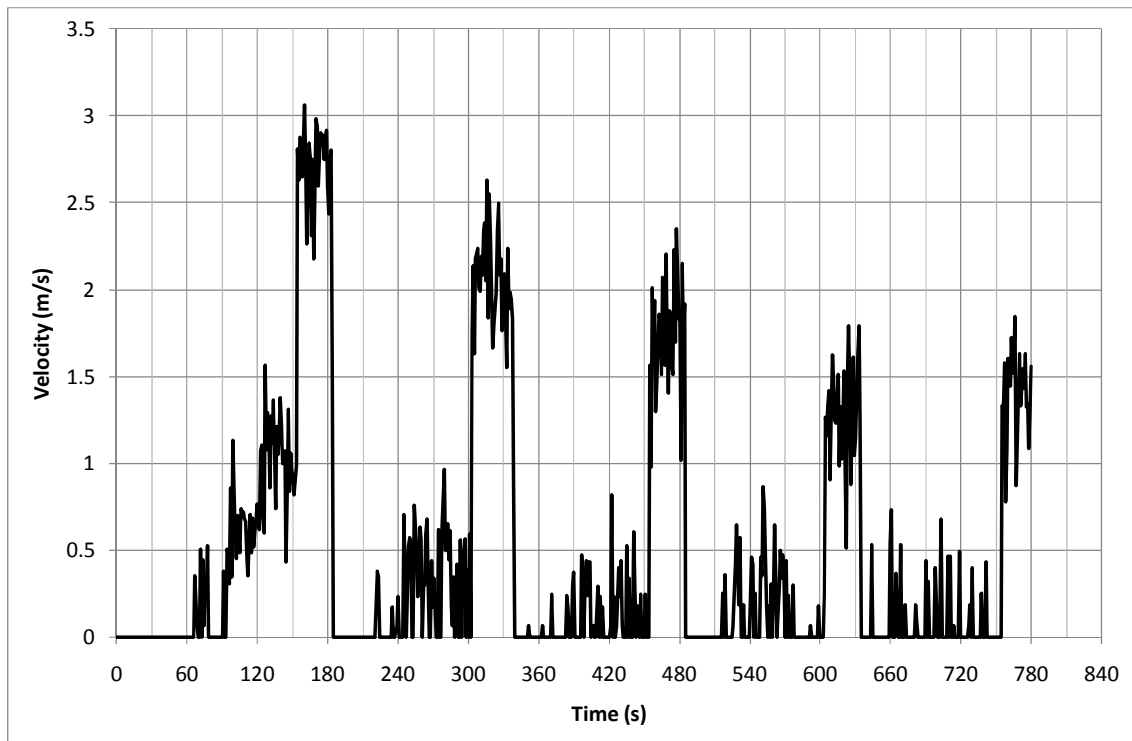
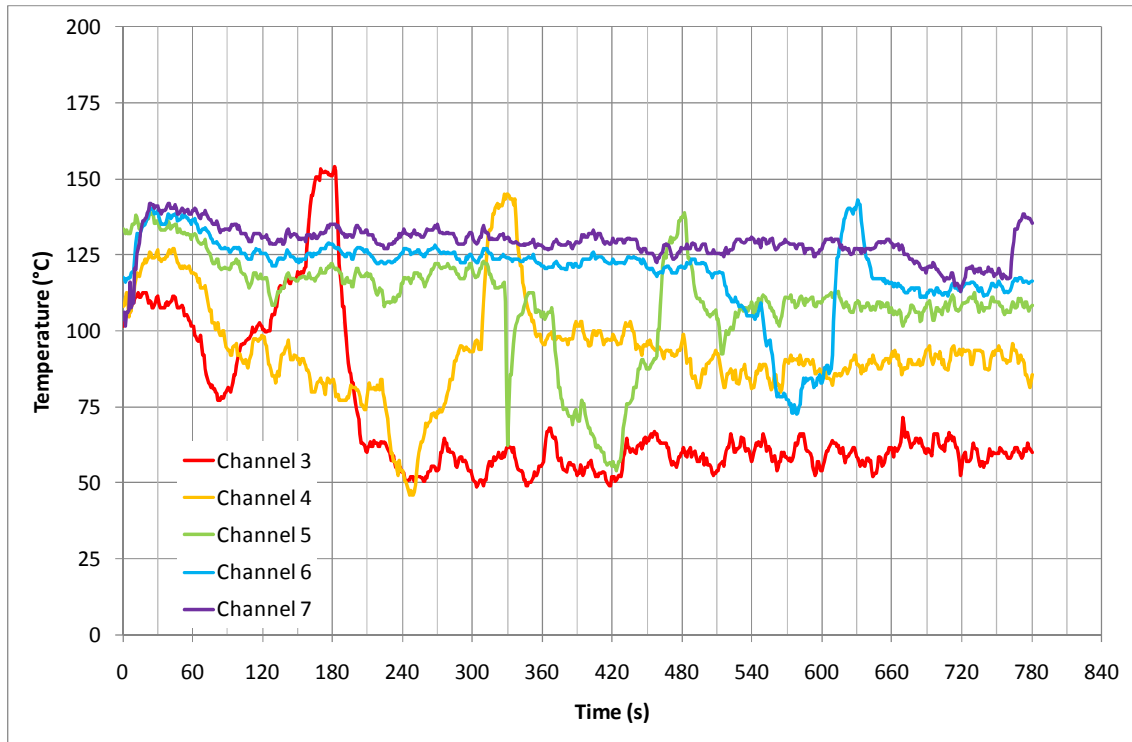
Bar	Point	Time (s)	Temperature (°C)	Velocity (m/s)
1	1	60	26.55	0.00
1	2	90	28.40	0.00
1	3	120	29.95	0.00
1	4	150	48.20	0.27
1	5	180	58.15	1.26
2	1	210	29.95	0.38
2	2	240	28.85	0.28
2	3	270	36.65	0.00
2	4	300	39.25	0.14
2	5	330	44.65	0.50
3	1	360	27.20	0.28
3	2	390	29.60	0.47
3	3	420	37.25	0.27
3	4	450	42.50	0.20
3	5	480	43.05	0.50
4	1	510	34.85	0.38
4	2	540	32.20	0.00
4	3	570	43.45	0.28
4	4	600	46.45	0.35
4	5	630	46.65	0.53
5	1	660	37.45	0.51
5	2	690	45.00	0.49
5	3	720	55.60	0.44
5	4	750	52.10	0.00
5	5	780	50.00	0.52

Test 2



Bar	Point	Time (s)	Temperature (°C)	Velocity (m/s)
1	1	810	61.00	0.00
1	2	840	57.70	0.00
1	3	870	54.35	0.00
1	4	900	52.15	0.00
1	5	930	50.35	0.31
2	1	210	49.15	0.00
2	2	240	52.10	0.00
2	3	270	50.90	0.00
2	4	300	46.60	0.00
2	5	330	46.80	0.24
3	1	360	47.15	0.14
3	2	390	48.05	0.00
3	3	420	43.35	0.00
3	4	450	42.65	0.00
3	5	480	41.45	0.27
4	1	510	46.75	0.00
4	2	540	44.55	0.00
4	3	570	43.40	0.00
4	4	600	42.30	0.00
4	5	630	43.55	0.00
5	1	660	51.15	0.00
5	2	690	49.90	0.00
5	3	720	45.50	0.00
5	4	750	44.65	0.00
5	5	780	49.45	0.00

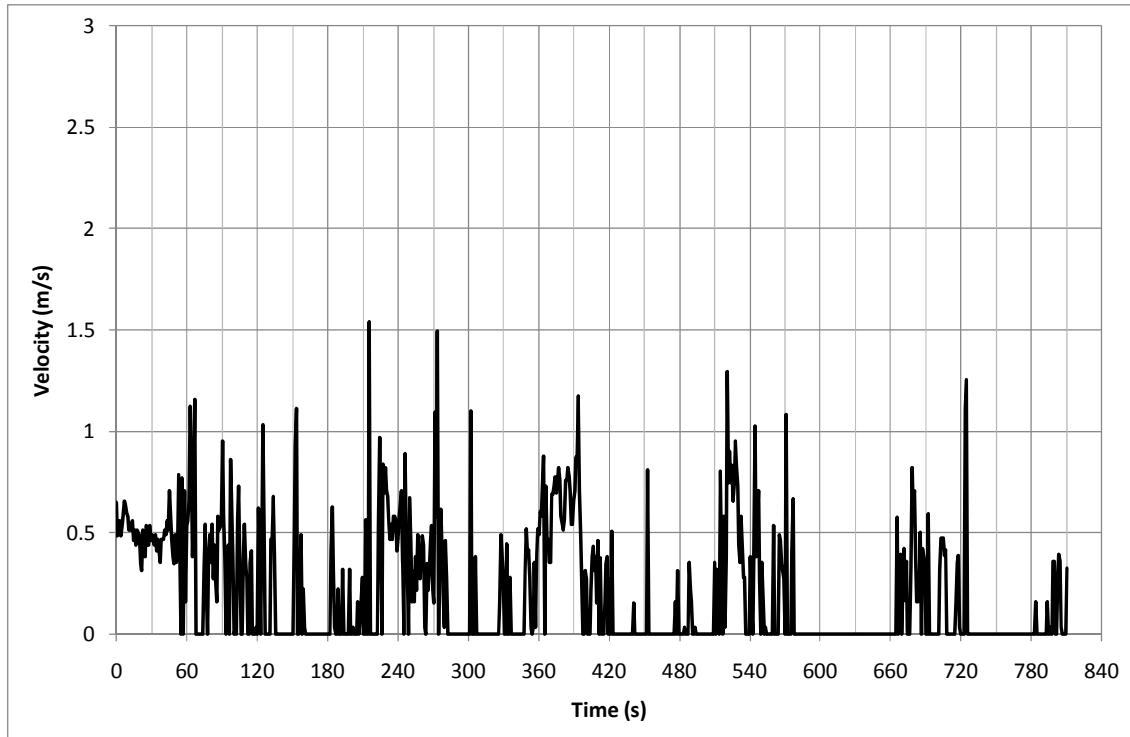
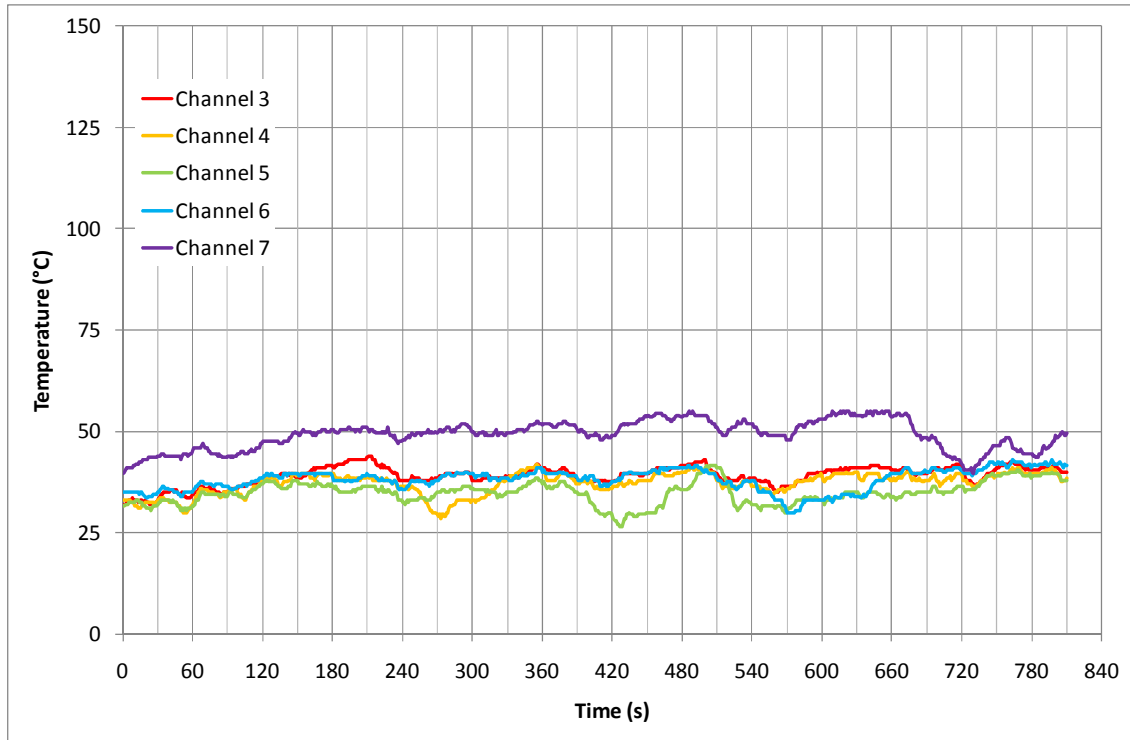
Test 3



Bar	Point	Time (s)	Temperature (°C)	Velocity (m/s)
1	1	30	109.60	0.00
1	2	60	114.95	0.00
1	3	90	118.85	0.00
1	4	120	117.50	0.00
1	5	150	123.50	0.67
2	1	180	126.30	0.00
2	2	210	126.30	0.00
2	3	240	120.25	0.00
2	4	270	119.00	0.00
2	5	300	126.00	0.43
3	1	330	127.10	0.00
3	2	360	119.70	0.00
3	3	390	115.70	0.00
3	4	420	113.45	0.00
3	5	450	127.45	0.00
4	1	510	126.85	0.00
4	2	540	123.85	0.00
4	3	570	114.80	0.00
4	4	600	95.95	0.00
4	5	630	126.40	1.20
5	1	660	114.35	0.00
5	2	690	115.85	0.00
5	3	720	103.60	0.00
5	4	750	112.40	0.00
5	5	780	121.35	1.97

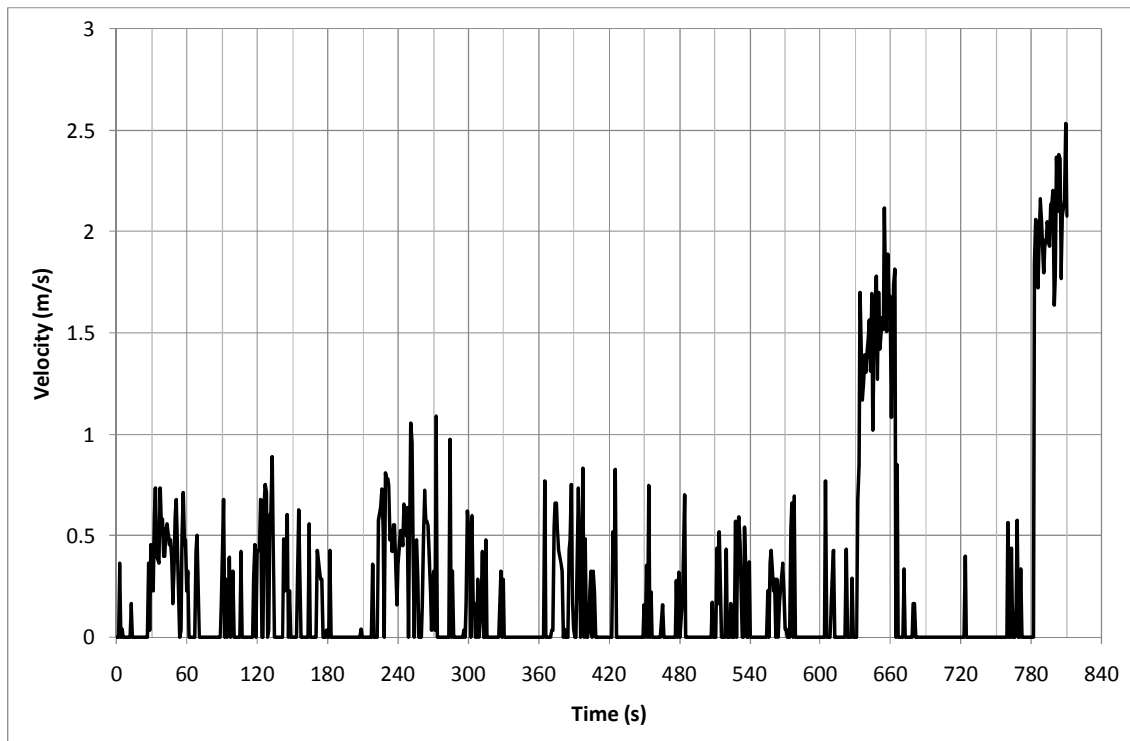
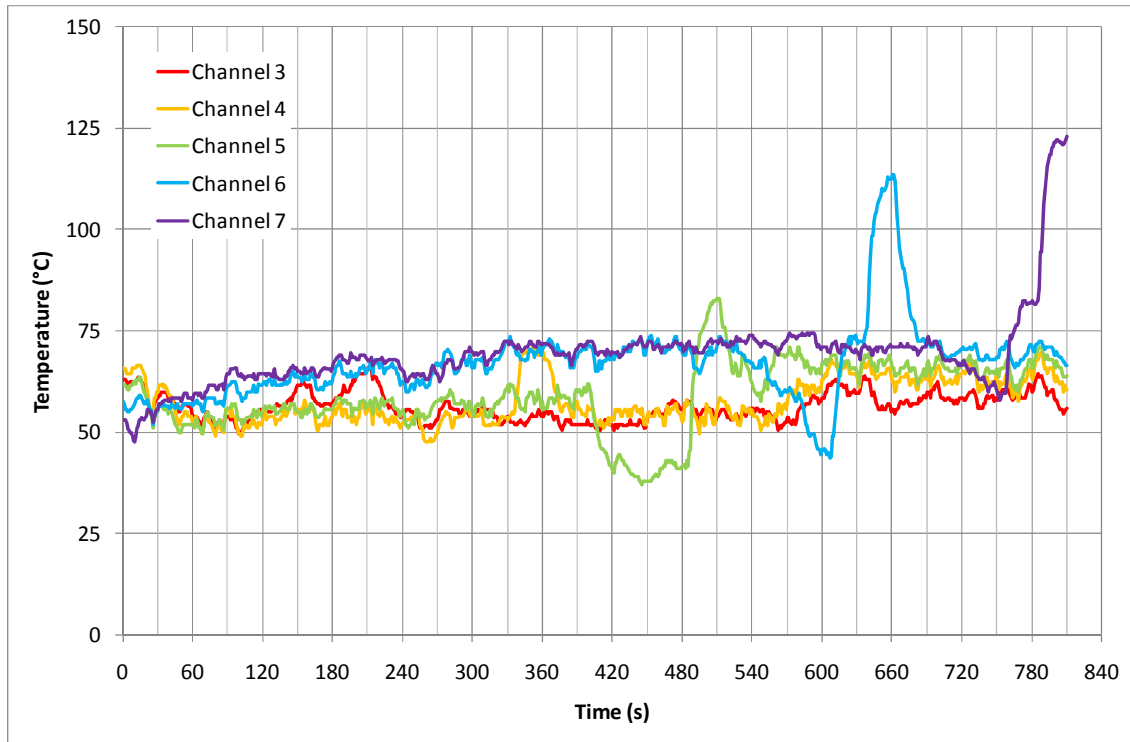
20 Minutes

Test 1



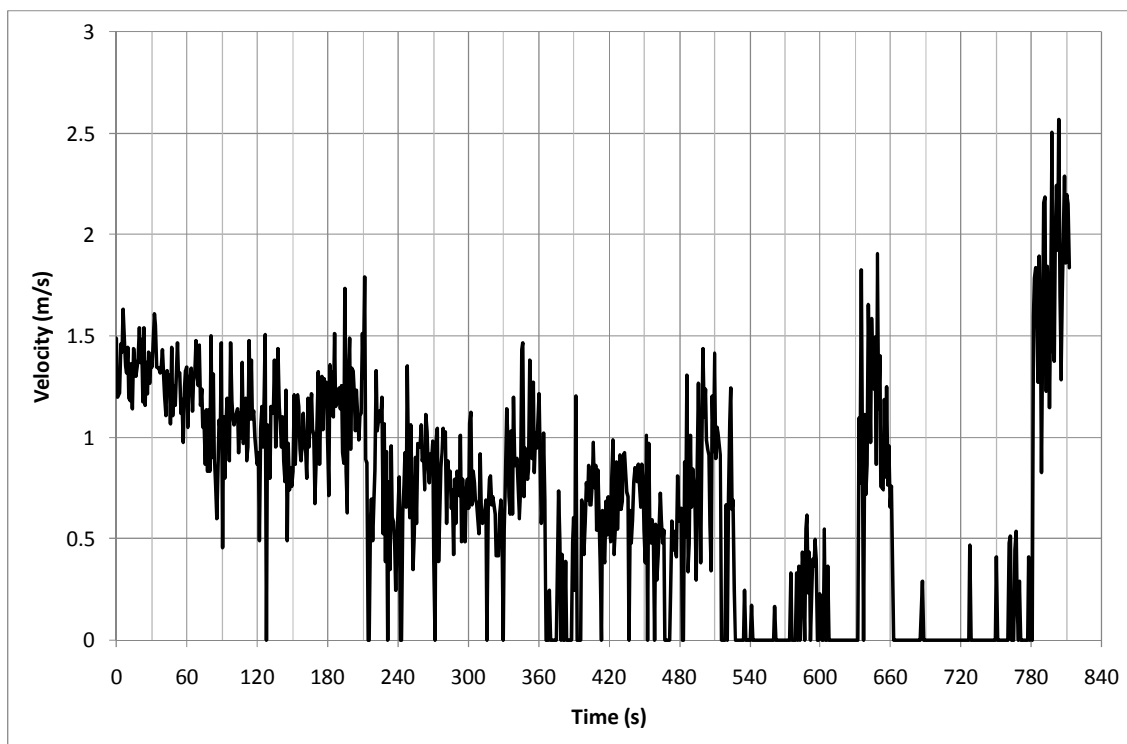
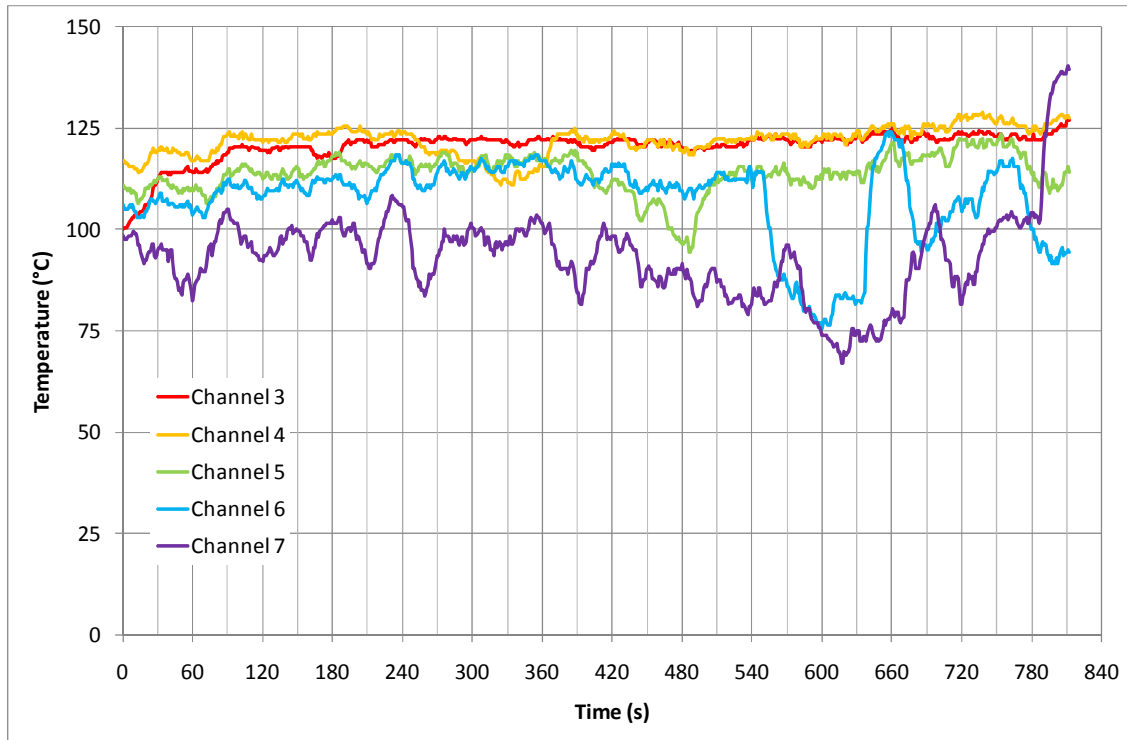
Bar	Point	Time (s)	Temperature (°C)	Velocity (m/s)
1	1	90	34.85	0.51
1	2	120	37.15	0.00
1	3	150	39.15	0.00
1	4	180	41.30	0.00
1	5	210	43.00	0.00
2	1	240	36.95	0.56
2	2	270	30.80	0.35
2	3	300	32.95	0.00
2	4	330	37.30	0.00
2	5	360	41.20	0.30
3	1	390	35.90	0.67
3	2	420	29.60	0.20
3	3	450	29.45	0.00
3	4	480	35.85	0.00
3	5	510	41.10	0.00
4	1	540	37.40	0.28
4	2	570	32.35	0.07
4	3	600	33.00	0.00
4	4	630	34.35	0.00
4	5	660	40.10	0.00
5	1	690	48.75	0.33
5	2	720	43.15	0.00
5	3	750	45.40	0.00
5	4	780	44.65	0.00
5	5	810	48.95	0.00

Test 2



Bar	Point	Time (s)	Temperature (°C)	Velocity (m/s)
1	1	90	52.60	0.00
1	2	120	54.80	0.00
1	3	150	58.65	0.12
1	4	180	56.85	0.00
1	5	210	64.35	0.00
2	1	240	52.65	0.57
2	2	270	48.15	0.45
2	3	300	54.75	0.00
2	4	330	52.90	0.00
2	5	360	68.65	0.00
3	1	390	58.10	0.23
3	2	420	44.50	0.00
3	3	450	38.15	0.00
3	4	480	41.80	0.00
3	5	510	80.60	0.00
4	1	540	68.20	0.30
4	2	570	60.25	0.20
4	3	600	47.10	0.00
4	4	630	72.45	0.00
4	5	660	106.75	1.69
5	1	690	70.65	0.00
5	2	720	67.40	0.00
5	3	750	61.40	0.00
5	4	780	81.85	0.00
5	5	810	121.55	2.14

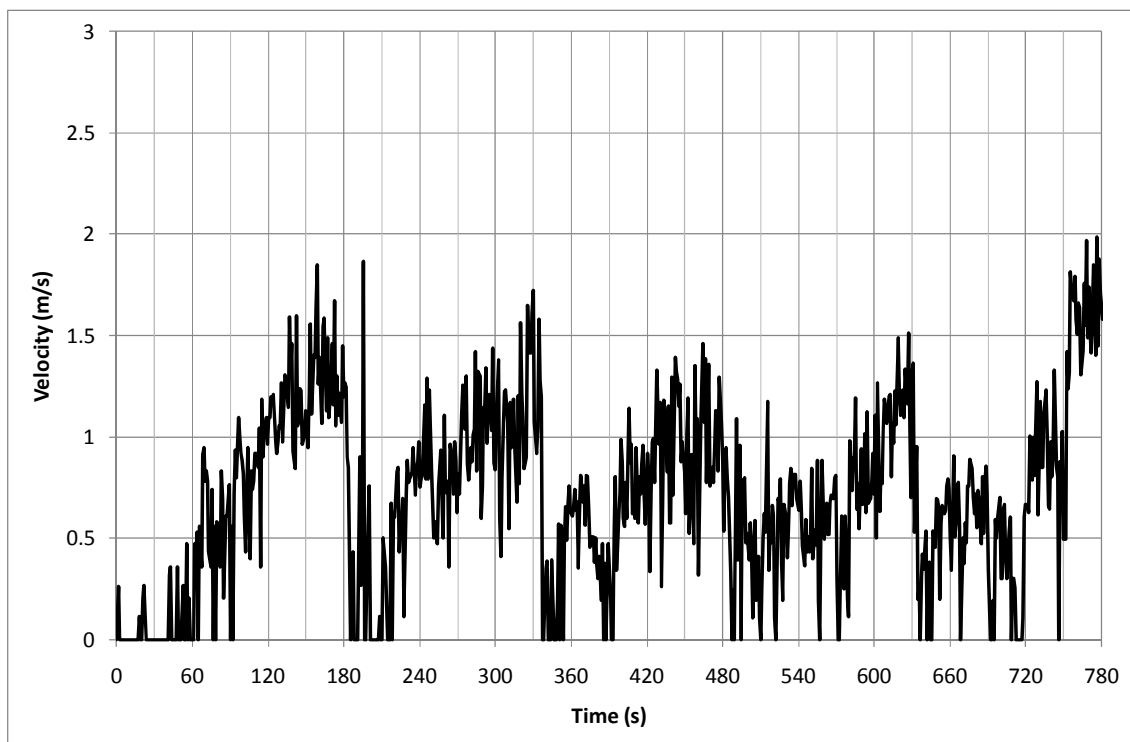
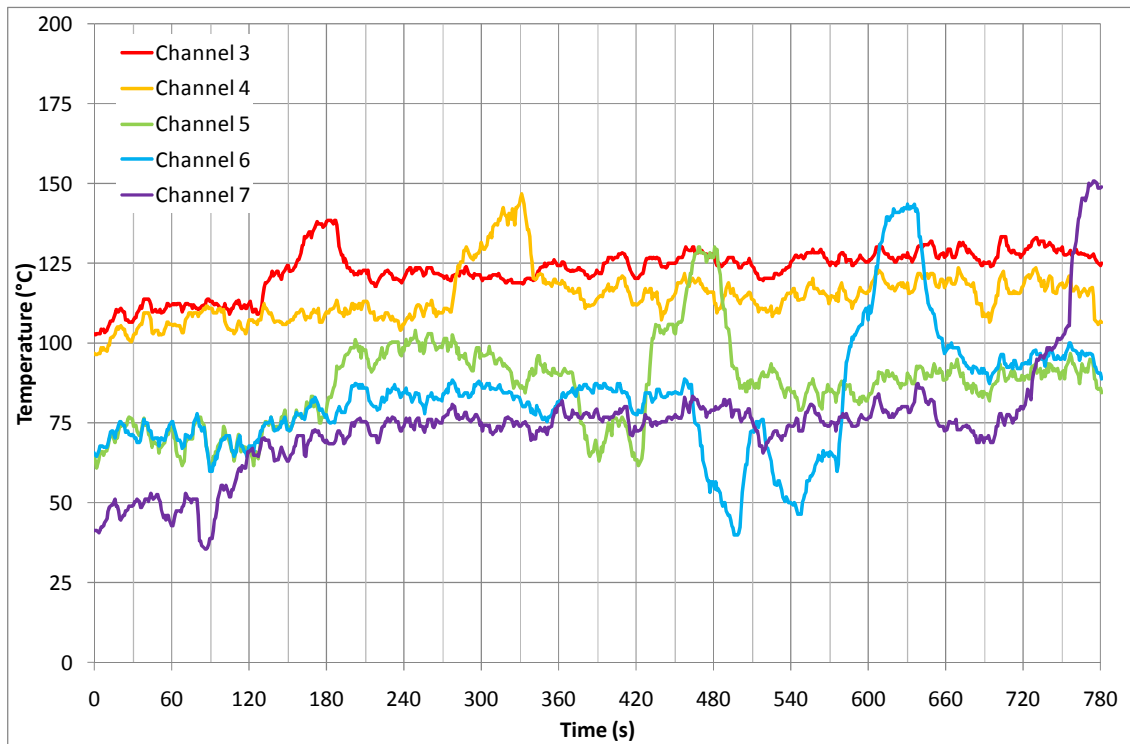
Test 3



Bar	Point	Time (s)	Temperature (°C)	Velocity (m/s)
1	1	90	117.70	0.85
1	2	120	119.95	0.93
1	3	150	120.45	0.64
1	4	180	118.10	0.94
1	5	210	121.90	1.02
2	1	240	123.75	0.00
2	2	270	118.90	0.67
2	3	300	116.90	0.35
2	4	330	112.10	0.00
2	5	360	114.95	0.85
3	1	390	118.70	0.00
3	2	420	110.10	0.00
3	3	450	103.50	0.45
3	4	480	98.25	0.00
3	5	510	110.40	0.80
4	1	540	113.30	0.00
4	2	570	88.35	0.00
4	3	600	78.25	0.00
4	4	630	83.10	0.00
4	5	660	118.00	0.77
5	1	690	93.95	0.00
5	2	720	87.05	0.00
5	3	750	99.45	0.00
5	4	780	102.10	0.00
5	5	810	137.95	1.82

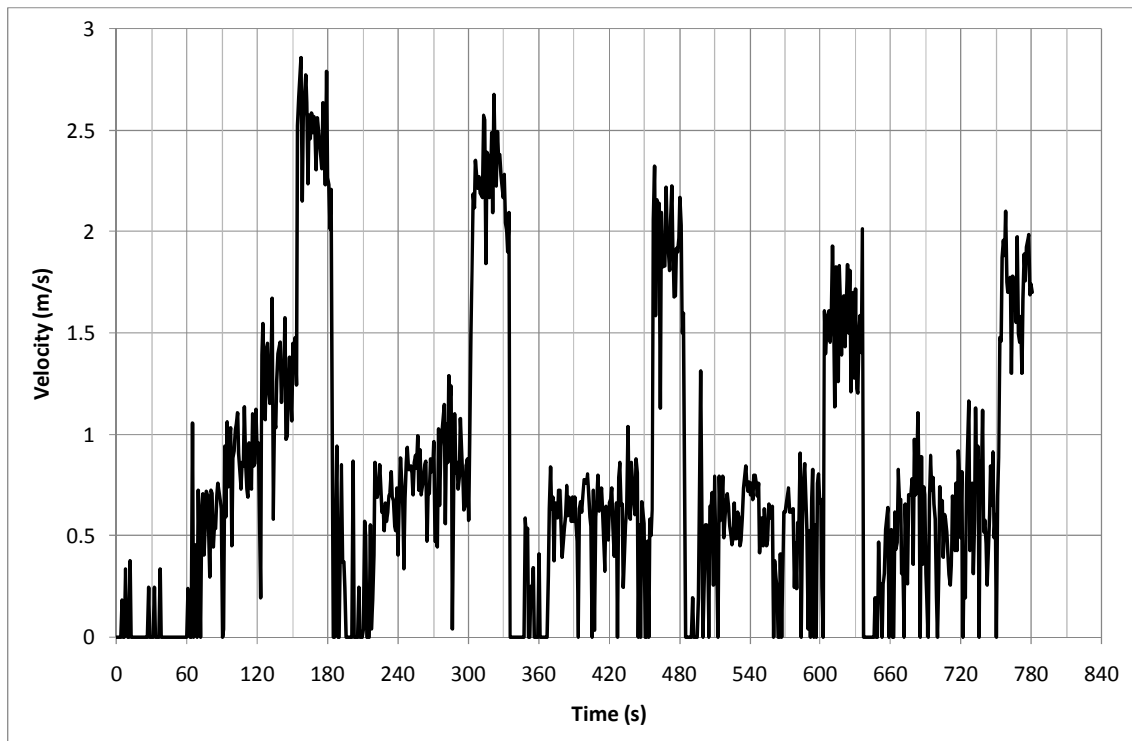
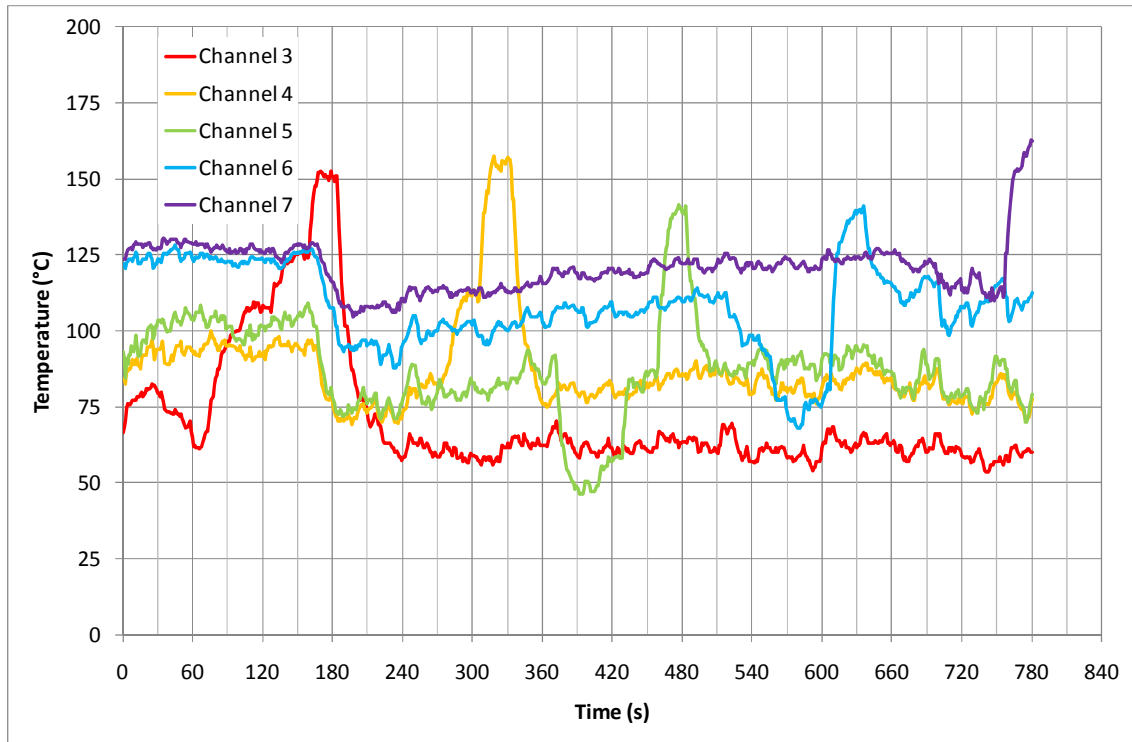
200°C 5 Minutes

Test 1



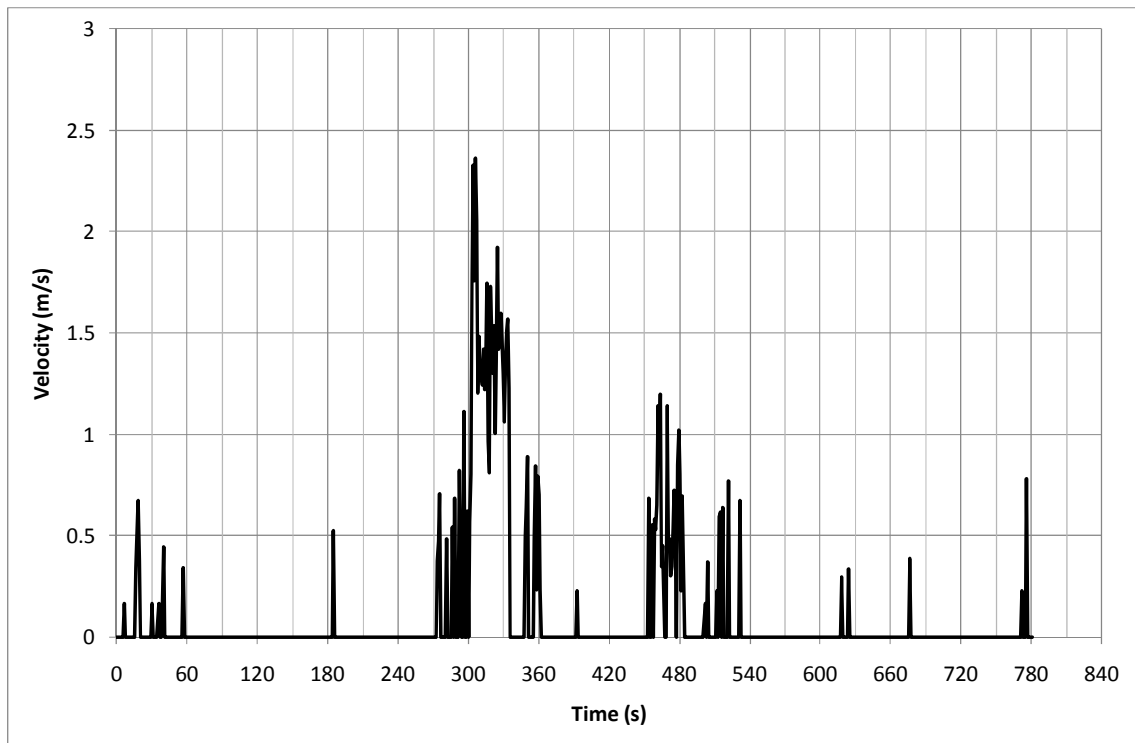
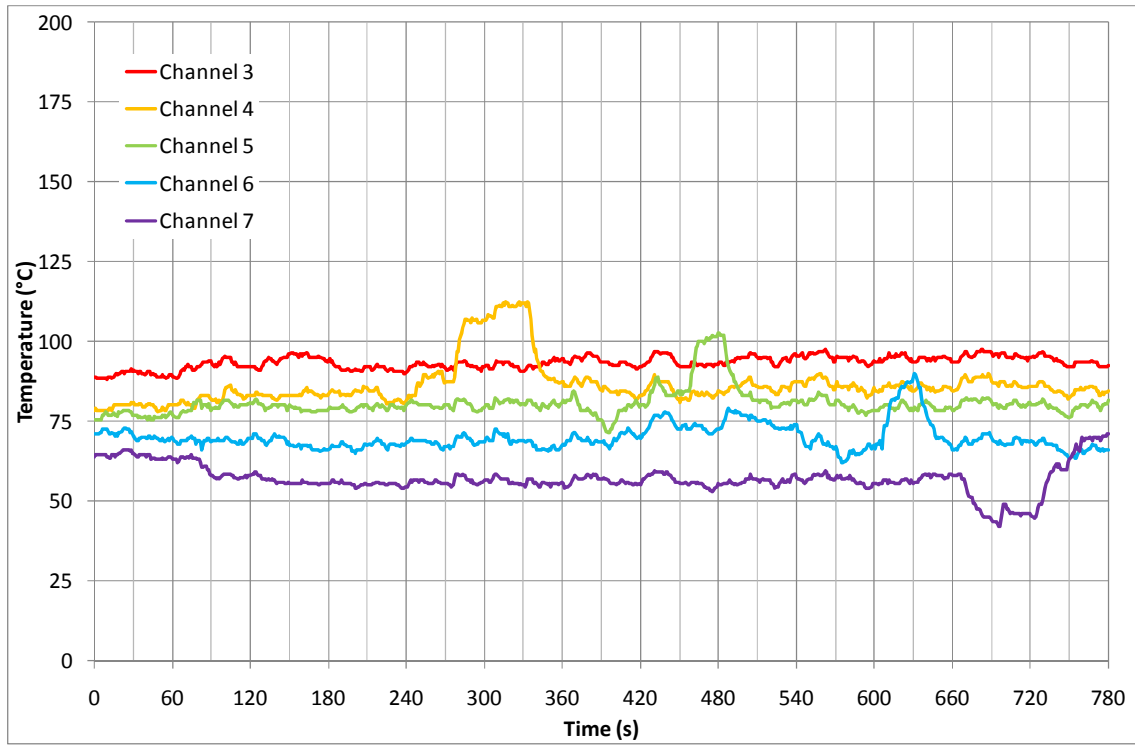
Bar	Point	Time (s)	Temperature (°C)	Velocity (m/s)
1	1	60	111.00	0.00
1	2	90	112.20	0.55
1	3	120	111.90	0.95
1	4	150	122.15	1.13
1	5	180	134.35	1.28
2	1	210	111.85	0.00
2	2	240	106.45	0.85
2	3	270	110.45	0.79
2	4	300	128.00	1.13
2	5	330	140.40	1.35
3	1	360	90.95	0.51
3	2	390	67.65	0.29
3	3	420	70.50	0.75
3	4	450	104.75	1.13
3	5	480	120.55	0.98
4	1	510	60.75	0.38
4	2	540	52.90	0.69
4	3	570	64.55	0.66
4	4	600	106.85	0.81
4	5	630	141.55	1.17
5	1	660	76.05	0.65
5	2	690	70.55	0.69
5	3	720	77.80	0.15
5	4	750	99.50	0.89
5	5	780	149.65	1.67

Test 2



Bar	Point	Time (s)	Temperature (°C)	Velocity (m/s)
1	1	60	69.05	0.00
1	2	90	91.30	0.61
1	3	120	107.70	0.88
1	4	150	123.40	1.23
1	5	180	143.70	2.46
2	1	210	74.10	0.00
2	2	240	71.20	0.66
2	3	270	83.50	0.77
2	4	300	111.20	0.80
2	5	330	154.70	2.36
3	1	360	87.50	0.00
3	2	390	51.55	0.61
3	3	420	55.80	0.62
3	4	450	82.75	0.60
3	5	480	136.15	1.91
4	1	510	110.45	0.52
4	2	540	97.10	0.67
4	3	570	77.20	0.23
4	4	600	76.40	0.57
4	5	630	136.55	1.58
5	1	660	125.65	0.35
5	2	690	120.85	0.74
5	3	720	114.95	0.60
5	4	750	111.60	0.62
5	5	780	158.15	1.71

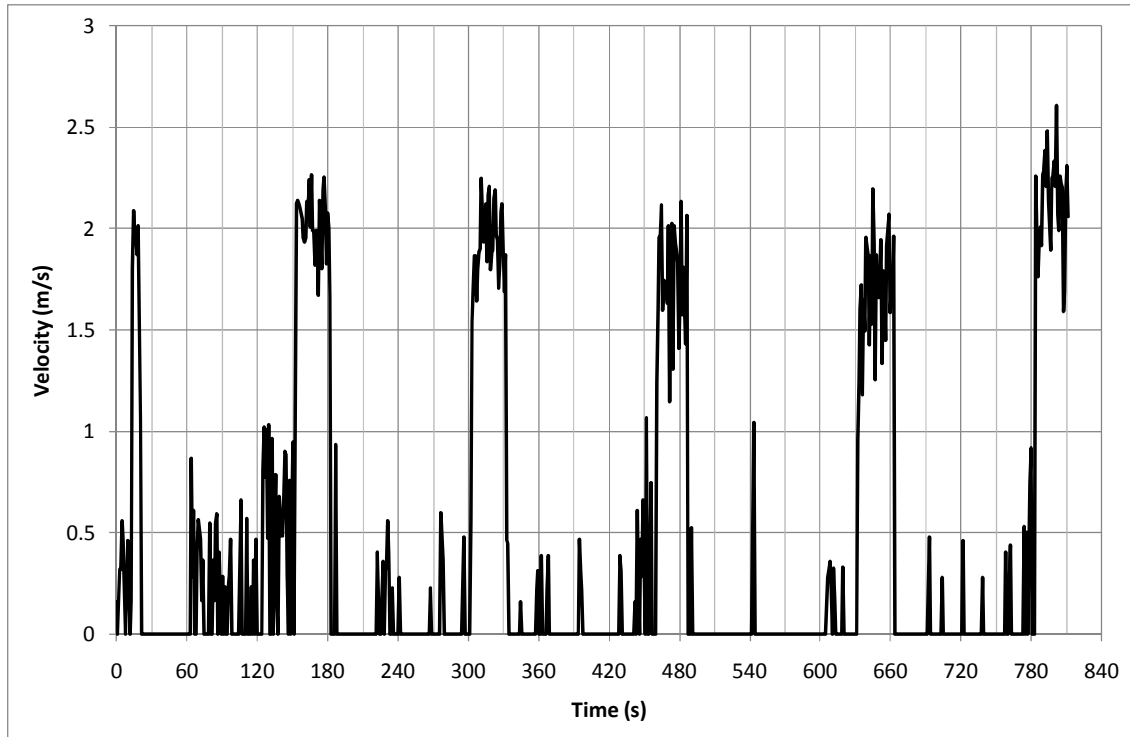
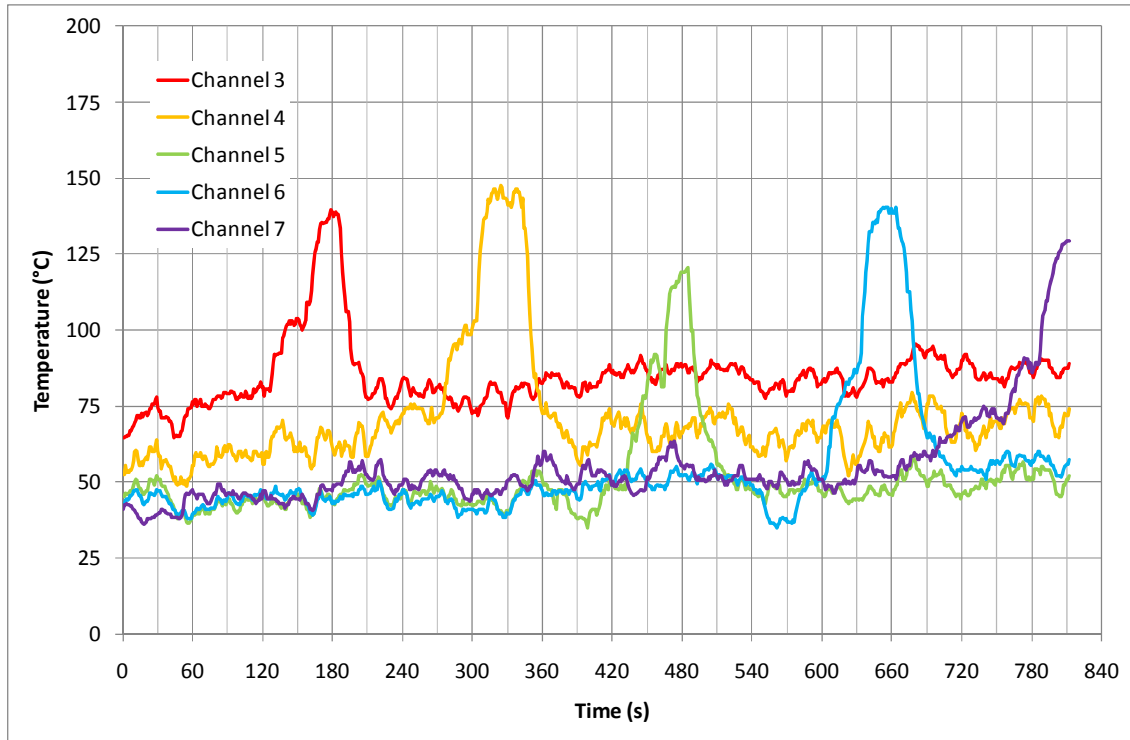
Test 3



Bar	Point	Time (s)	Temperature (°C)	Velocity (m/s)
1	1	60	89.15	0.00
1	2	90	93.35	0.00
1	3	120	92.00	0.00
1	4	150	94.55	0.00
1	5	180	93.55	0.00
2	1	210	84.85	0.00
2	2	240	81.25	0.00
2	3	270	89.55	0.00
2	4	300	106.45	0.00
2	5	330	111.50	1.46
3	1	360	80.35	0.43
3	2	390	76.95	0.00
3	3	420	80.20	0.00
3	4	450	83.35	0.00
3	5	480	98.25	0.58
4	1	510	76.25	0.00
4	2	540	73.10	0.00
4	3	570	67.60	0.00
4	4	600	66.75	0.00
4	5	630	86.45	0.00
5	1	660	57.90	0.00
5	2	690	45.55	0.00
5	3	720	45.95	0.00
5	4	750	60.60	0.00
5	5	780	70.15	0.00

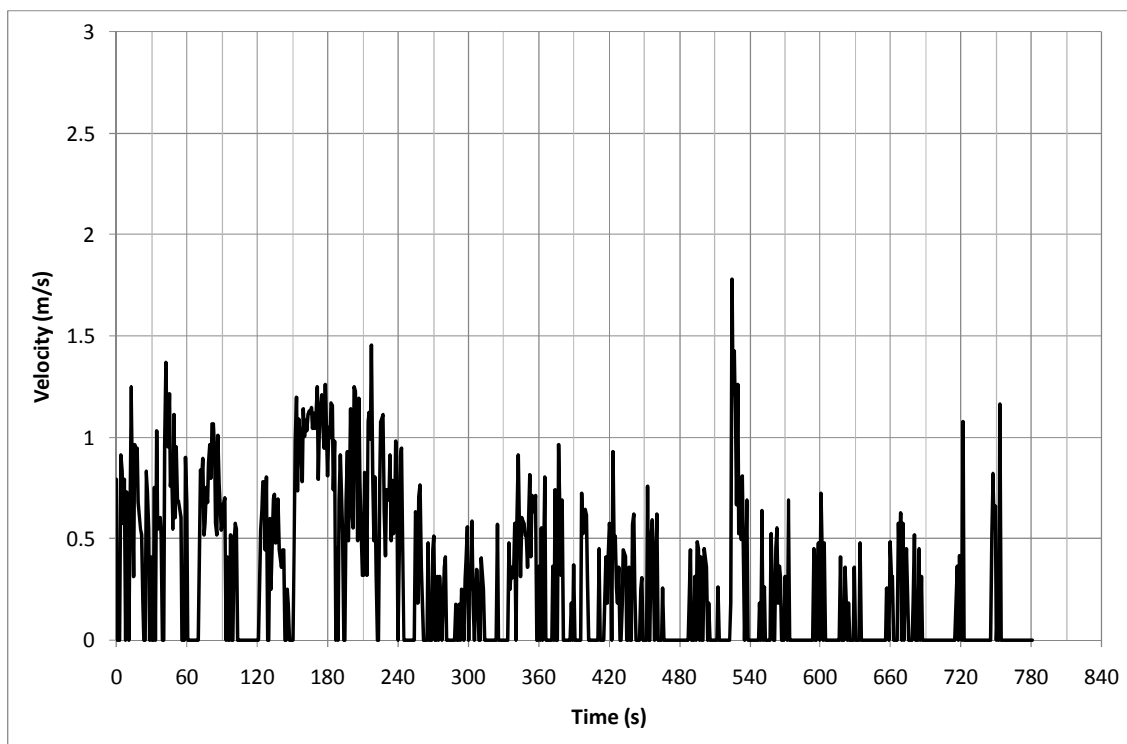
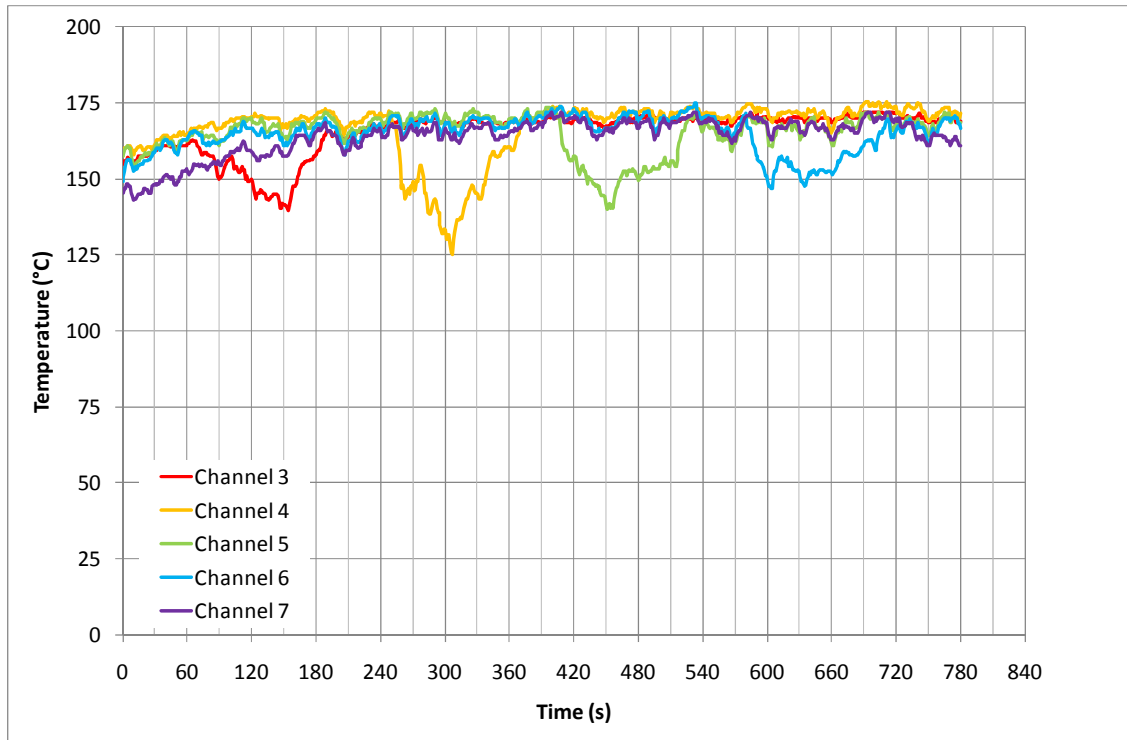
10 Minutes

Test 1



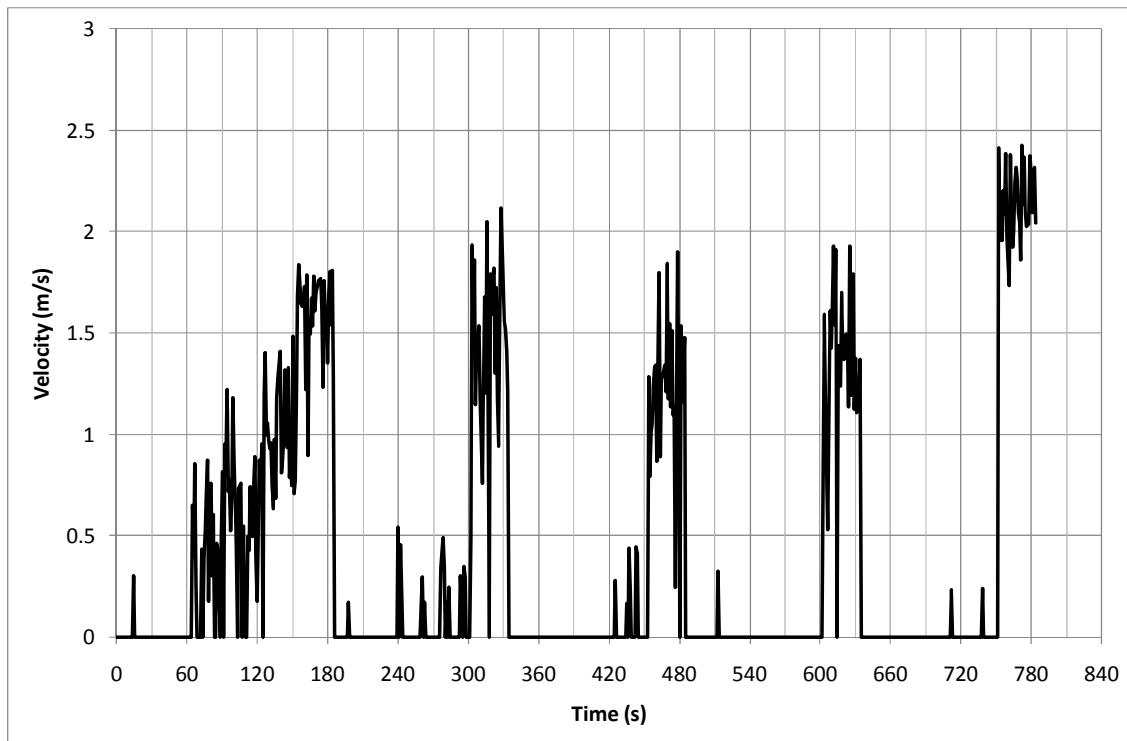
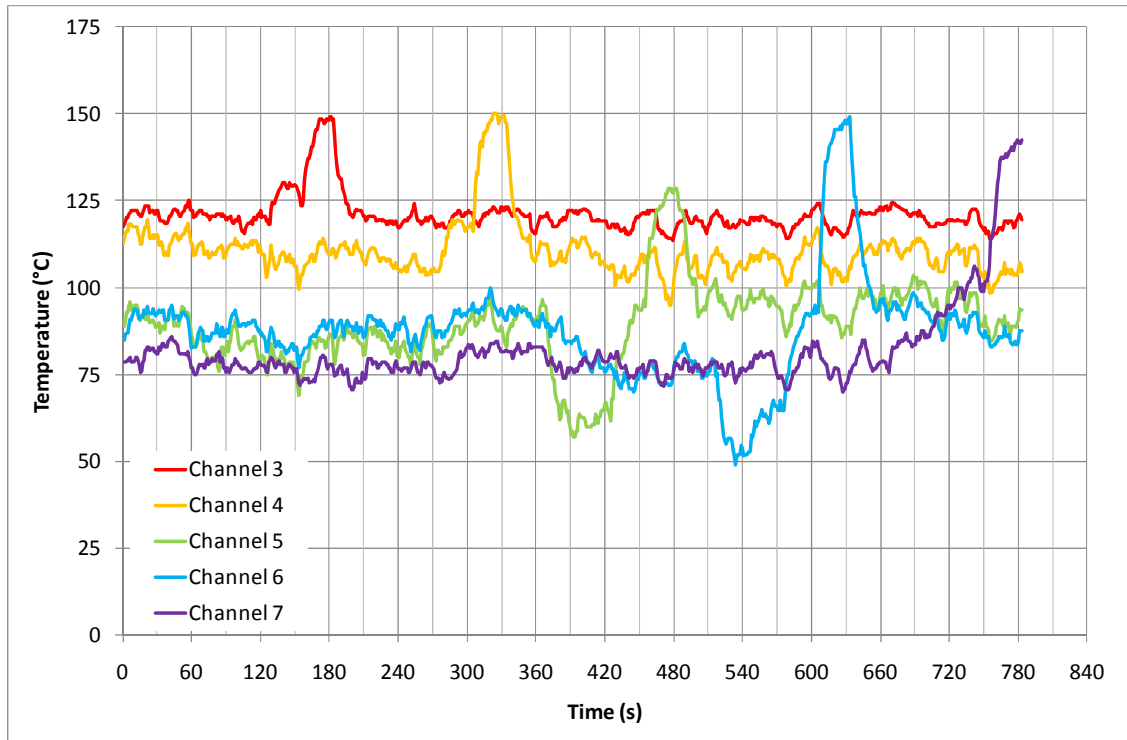
Bar	Point	Time (s)	Temperature (°C)	Velocity (m/s)
1	1	60	71.65	0.00
1	2	90	78.65	0.24
1	3	120	80.20	0.00
1	4	150	102.30	0.58
1	5	180	128.90	2.01
2	1	210	65.25	0.00
2	2	240	69.25	0.09
2	3	270	70.70	0.00
2	4	300	99.15	0.00
2	5	330	144.95	1.98
3	1	360	52.85	0.00
3	2	390	41.30	0.00
3	3	420	47.85	0.00
3	4	450	72.40	0.00
3	5	480	108.80	1.76
4	1	540	50.35	0.00
4	2	570	37.10	0.00
4	3	600	51.15	0.00
4	4	630	83.95	0.00
4	5	660	139.70	1.74
5	1	690	58.80	0.00
5	2	720	67.15	0.00
5	3	750	73.00	0.00
5	4	780	89.25	0.00
5	5	810	126.15	2.12

Test 2



Bar	Point	Time (s)	Temperature (°C)	Velocity (m/s)
1	1	60	160.90	0.53
1	2	90	155.25	0.82
1	3	120	151.45	0.00
1	4	150	143.25	0.00
1	5	180	157.85	1.06
2	1	210	167.05	0.85
2	2	240	171.45	0.73
2	3	270	146.30	0.00
2	4	300	136.95	0.00
2	5	330	145.70	0.00
3	1	360	159.45	0.54
3	2	390	170.80	0.00
3	3	420	157.95	0.24
3	4	450	146.00	0.00
3	5	480	152.05	0.00
4	1	510	156.50	0.00
4	2	540	172.50	0.59
4	3	570	165.10	0.20
4	4	600	154.50	0.00
4	5	630	153.30	0.00
5	1	660	152.50	0.00
5	2	690	159.65	0.00
5	3	720	170.50	0.00
5	4	750	163.15	0.00
5	5	780	162.50	0.00

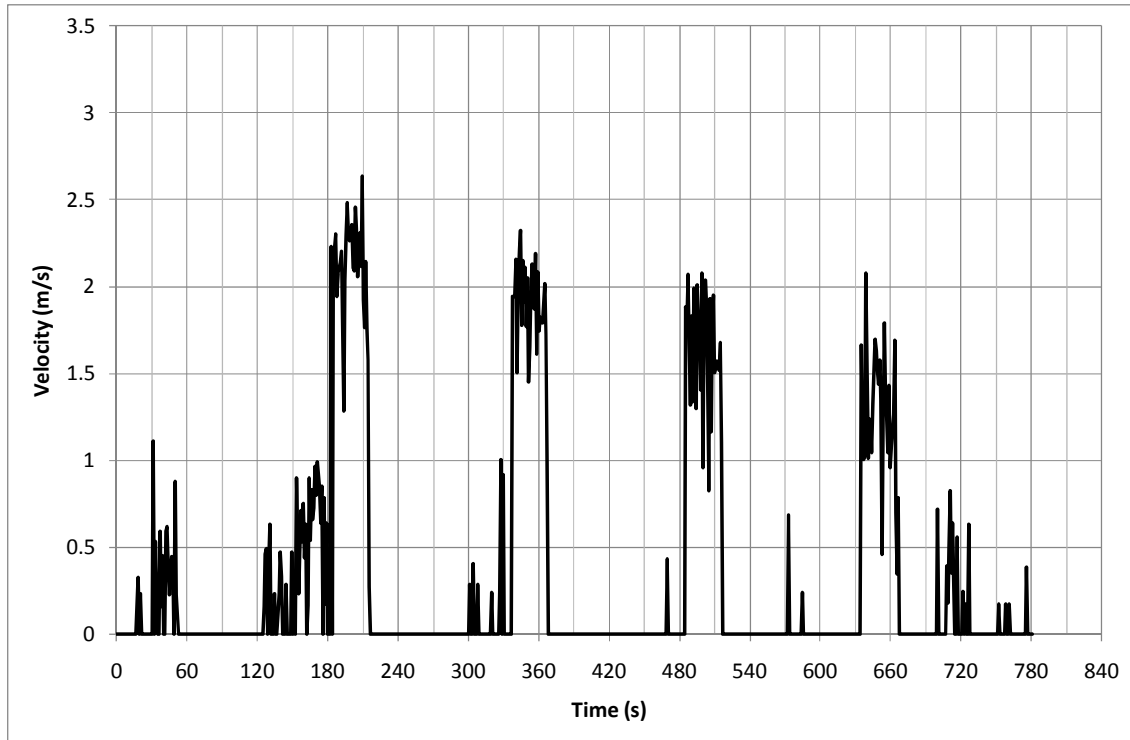
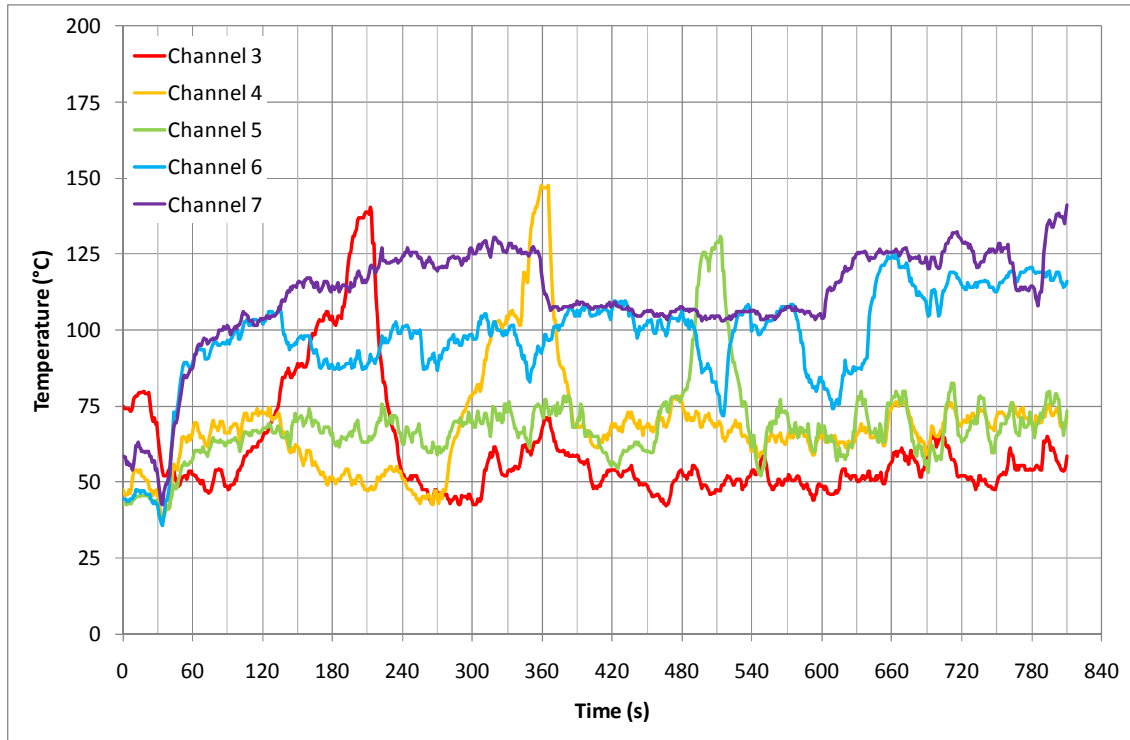
Test 3



Bar	Point	Time (s)	Temperature (°C)	Velocity (m/s)
1	1	60	122.50	0.00
1	2	90	120.65	0.86
1	3	120	119.55	0.91
1	4	150	129.30	1.26
1	5	180	144.15	1.79
2	1	210	110.65	0.00
2	2	240	106.80	0.33
2	3	270	104.45	0.62
2	4	300	118.20	0.56
2	5	330	148.60	1.78
3	1	360	91.50	0.00
3	2	390	64.10	0.16
3	3	420	62.70	0.38
3	4	450	91.55	0.43
3	5	480	126.75	1.46
4	1	510	75.30	0.00
4	2	540	52.80	0.00
4	3	570	64.25	0.18
4	4	600	90.85	0.00
4	5	630	145.95	1.66
5	1	660	77.50	0.00
5	2	690	84.60	0.00
5	3	720	92.95	0.30
5	4	750	103.00	0.29
5	5	780	139.90	2.30

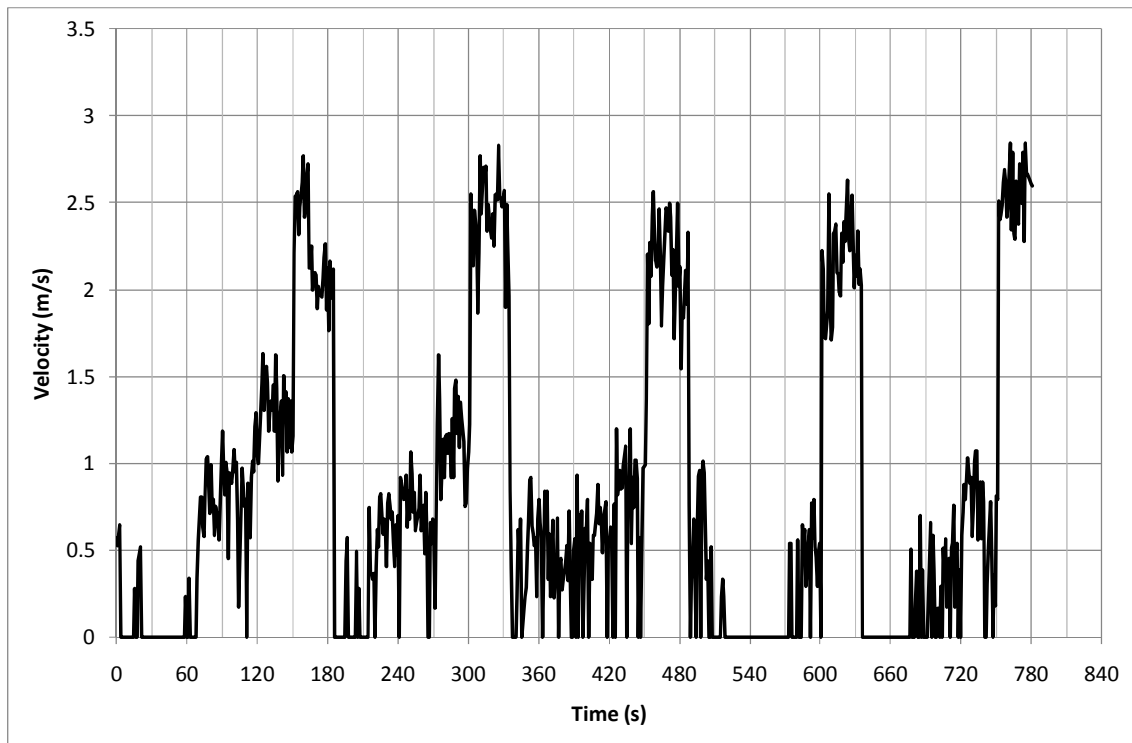
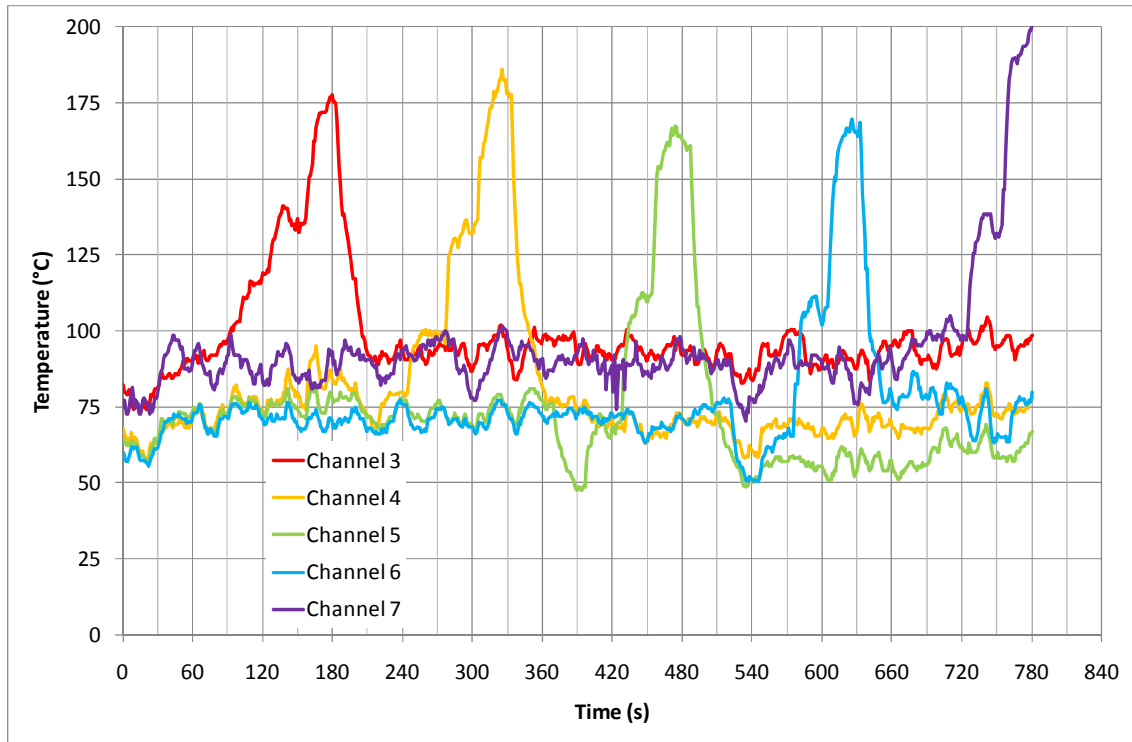
20 Minutes

Test 1



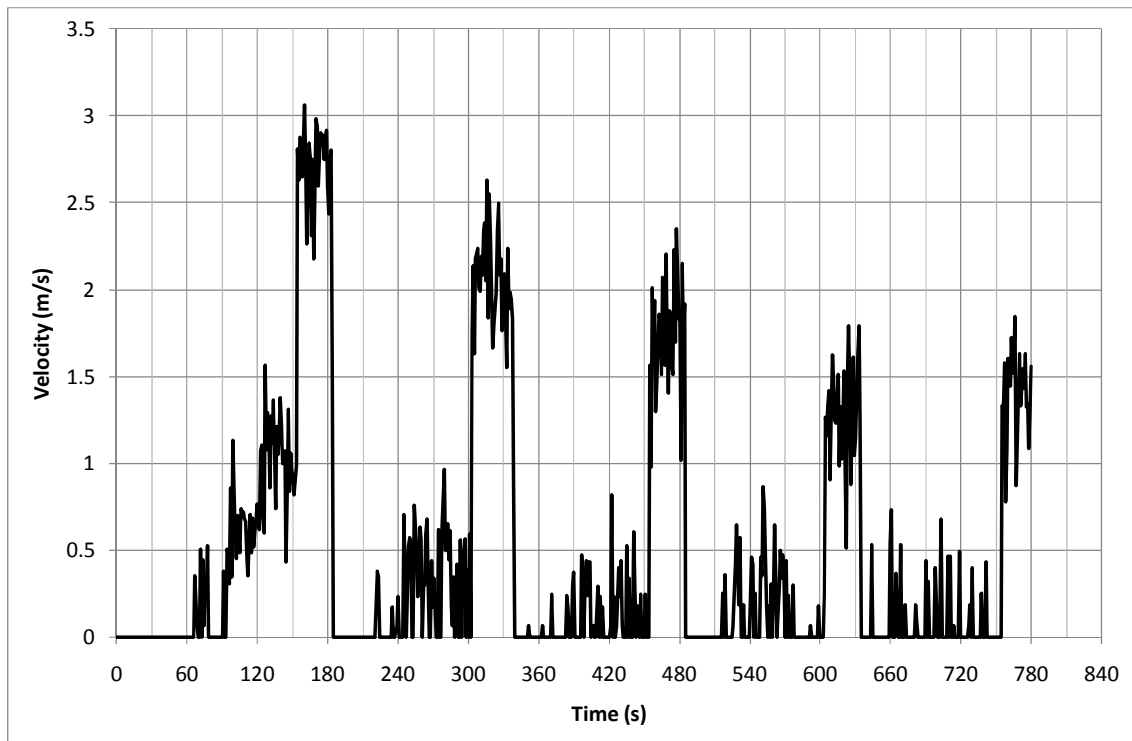
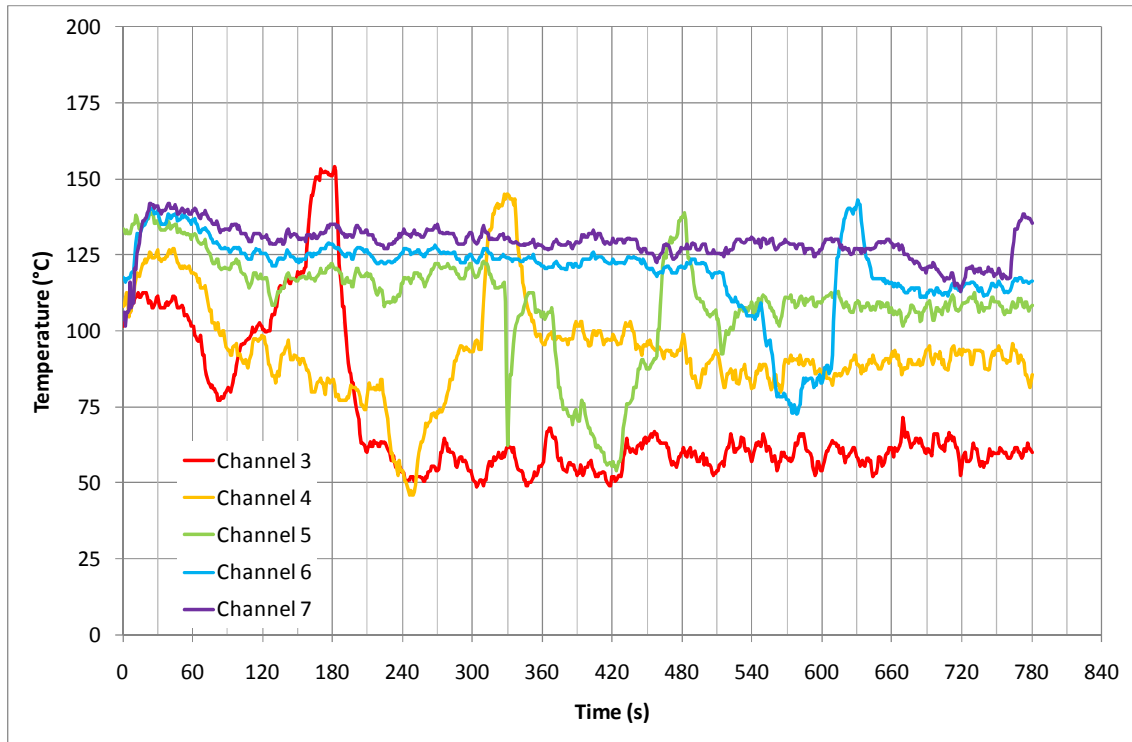
Bar	Point	Time (s)	Temperature (°C)	Velocity (m/s)
1	1	90	51.90	0.00
1	2	120	62.05	0.00
1	3	150	85.95	0.00
1	4	180	104.40	0.64
1	5	210	136.35	2.29
2	1	240	53.75	0.00
2	2	270	45.10	0.00
2	3	300	74.25	0.00
2	4	330	102.35	0.16
2	5	360	133.40	1.89
3	1	390	73.15	0.00
3	2	420	58.55	0.00
3	3	450	61.55	0.00
3	4	480	77.30	0.00
3	5	510	124.95	1.65
4	1	540	106.00	0.00
4	2	570	106.55	0.00
4	3	600	82.25	0.00
4	4	630	87.10	0.00
4	5	660	122.20	1.33
5	1	690	123.05	0.00
5	2	720	131.20	0.25
5	3	750	125.90	0.00
5	4	780	113.75	0.00
5	5	810	137.35	1.57

Test 2



Bar	Point	Time (s)	Temperature (°C)	Velocity (m/s)
1	1	60	89.85	0.00
1	2	90	95.20	0.82
1	3	120	115.95	0.91
1	4	150	136.50	1.26
1	5	180	174.15	2.05
2	1	210	75.70	0.00
2	2	240	79.40	0.64
2	3	270	99.15	0.56
2	4	300	133.55	1.11
2	5	330	181.10	2.50
3	1	360	79.65	0.65
3	2	390	51.85	0.40
3	3	420	67.90	0.63
3	4	450	109.95	0.73
3	5	480	165.15	2.21
4	1	510	74.70	0.41
4	2	540	52.85	0.00
4	3	570	65.05	0.00
4	4	600	108.40	0.55
4	5	630	166.55	2.33
5	1	660	90.45	0.00
5	2	690	95.95	0.00
5	3	720	100.15	0.41
5	4	750	136.05	0.37
5	5	780	194.65	2.63

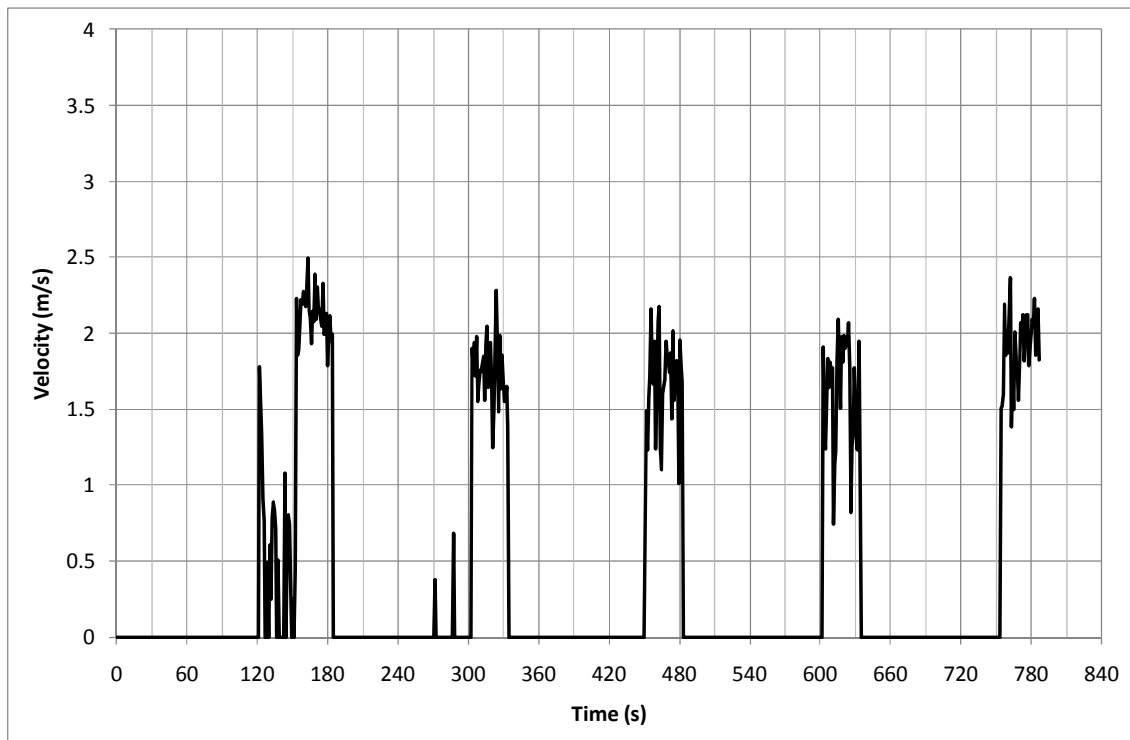
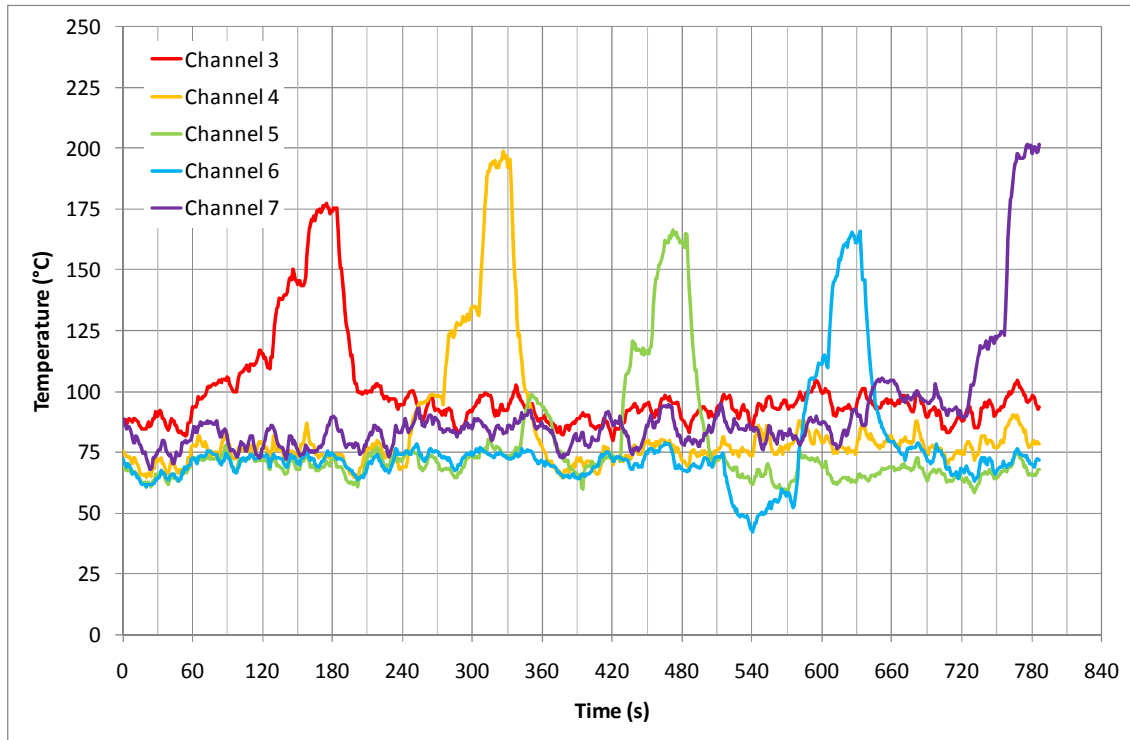
Test 3



Bar	Point	Time (s)	Temperature (°C)	Velocity (m/s)
1	1	60	104.85	0.00
1	2	90	78.45	0.00
1	3	120	100.90	0.60
1	4	150	116.90	1.00
1	5	180	145.00	2.81
2	1	210	77.80	0.00
2	2	240	56.25	0.00
2	3	270	71.30	0.33
2	4	300	94.05	0.12
2	5	330	142.25	2.05
3	1	360	108.40	0.00
3	2	390	72.55	0.00
3	3	420	58.00	0.00
3	4	450	87.70	0.00
3	5	480	131.40	1.83
4	1	510	119.35	0.00
4	2	540	106.25	0.00
4	3	570	78.90	0.34
4	4	600	83.55	0.00
4	5	630	138.35	1.31
5	1	660	129.50	0.00
5	2	690	121.10	0.00
5	3	720	116.05	0.00
5	4	750	119.35	0.00
5	5	780	137.20	1.41

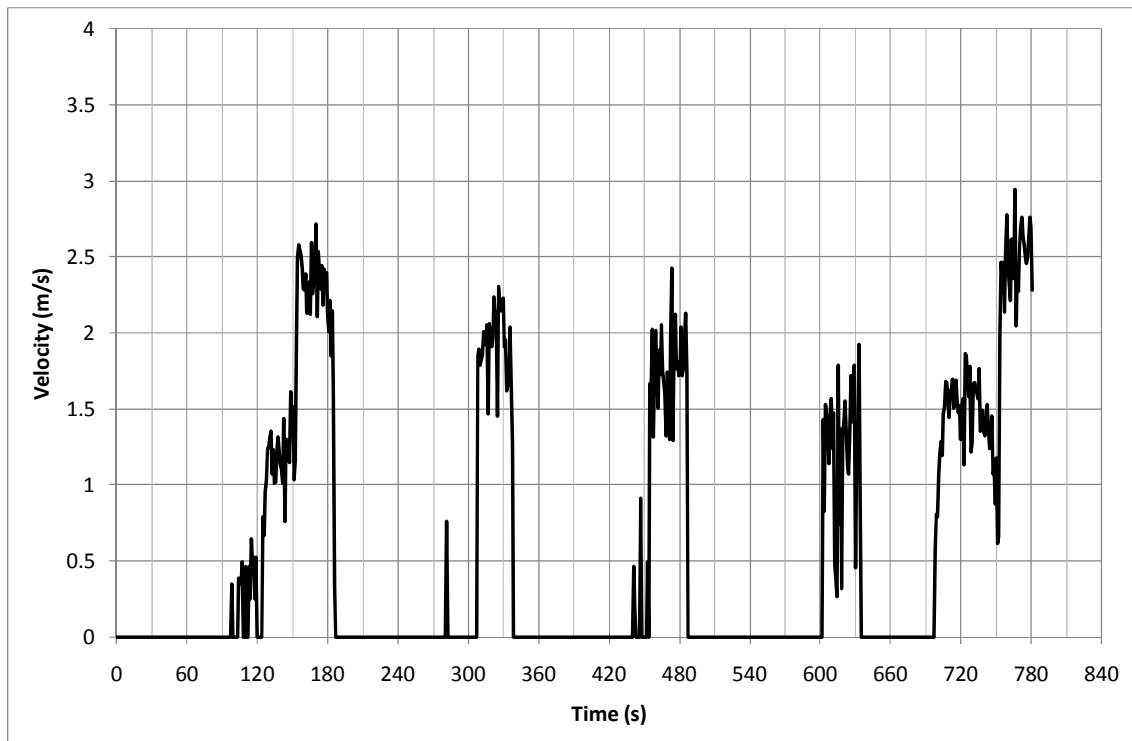
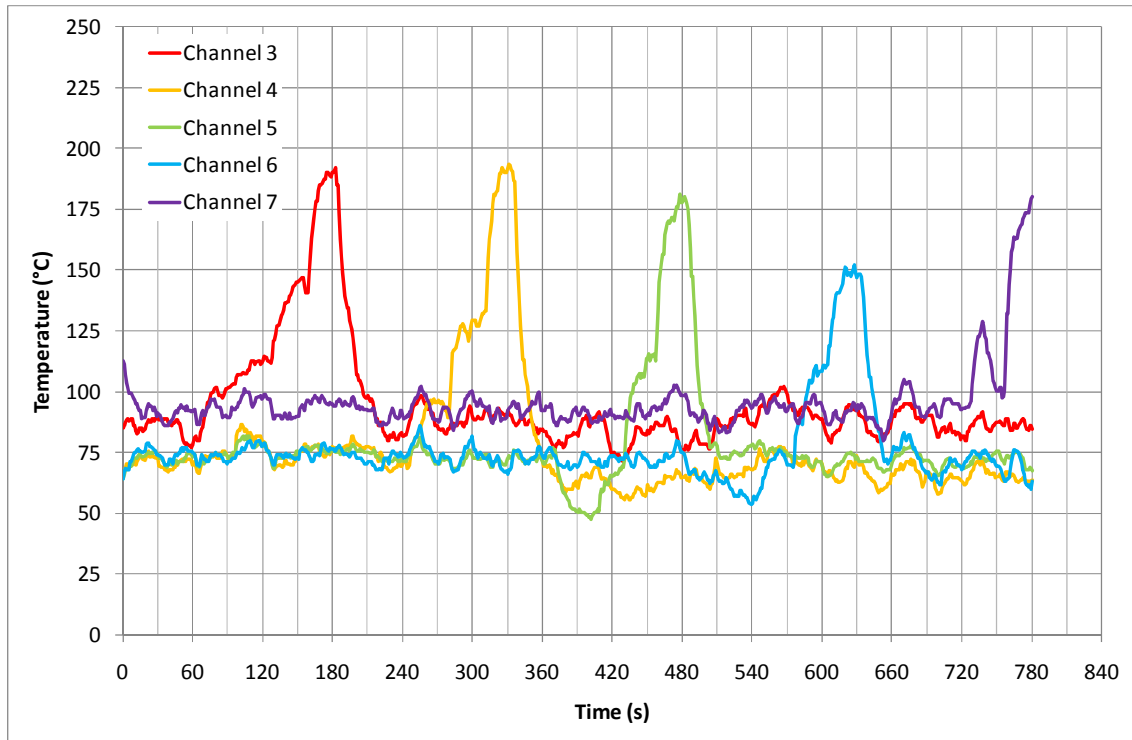
250°C 5 Minutes

Test 1



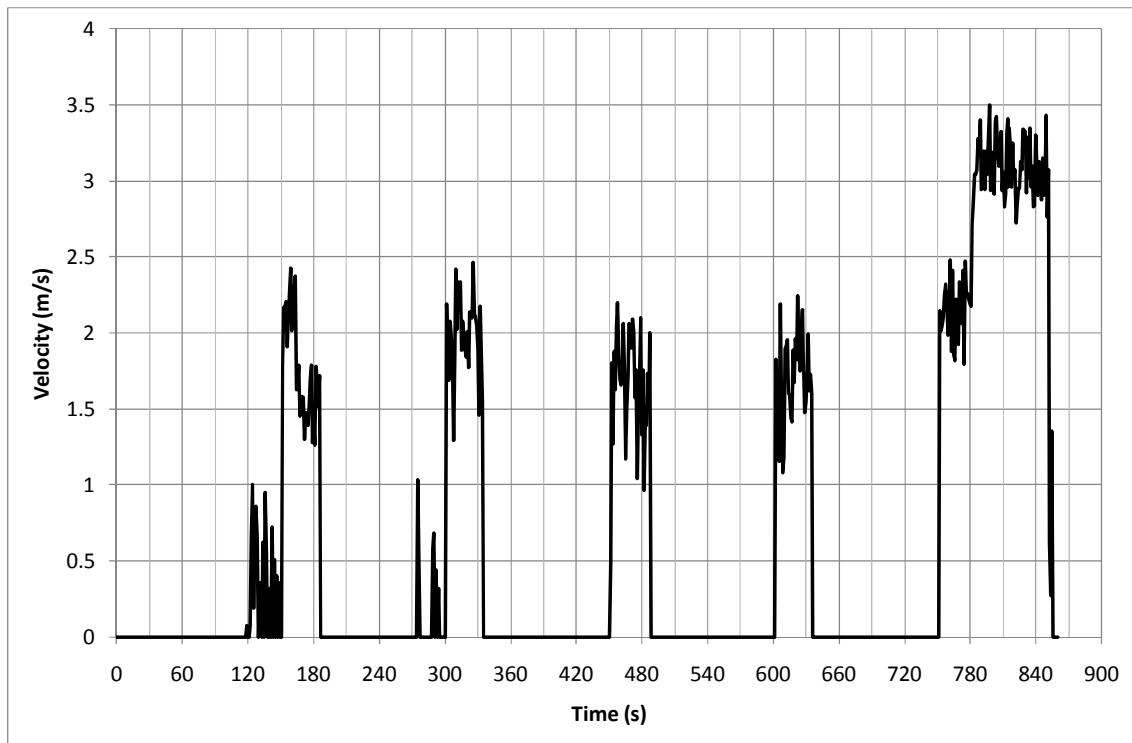
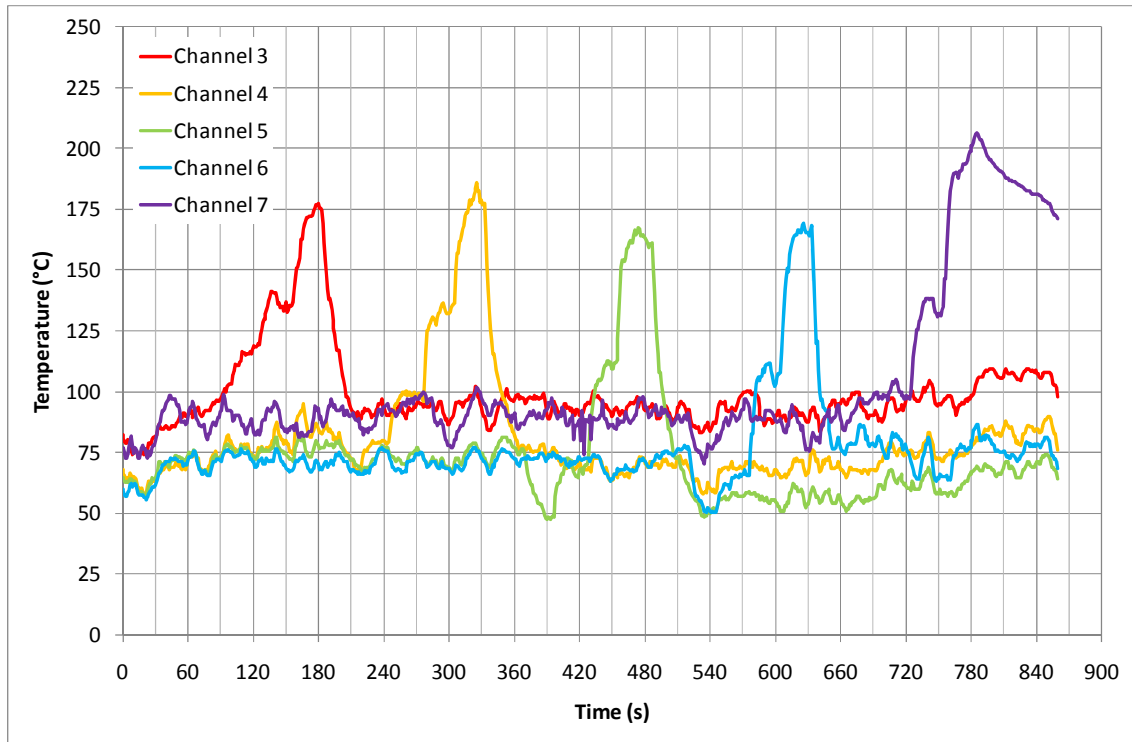
Bar	Point	Time (s)	Temperature (°C)	Velocity (m/s)
1	1	60	85.20	0.00
1	2	90	104.45	0.00
1	3	120	113.00	0.00
1	4	150	145.45	0.41
1	5	180	165.00	2.11
2	1	210	69.75	0.00
2	2	240	71.85	0.00
2	3	270	97.80	0.00
2	4	300	130.70	0.00
2	5	330	194.80	1.77
3	1	360	96.65	0.00
3	2	390	68.65	0.00
3	3	420	72.50	0.00
3	4	450	117.00	0.00
3	5	480	154.45	1.69
4	1	510	71.30	0.00
4	2	540	47.85	0.00
4	3	570	57.00	0.00
4	4	600	107.60	0.00
4	5	630	155.60	1.68
5	1	660	104.40	0.00
5	2	690	97.75	0.00
5	3	720	91.85	0.00
5	4	750	120.20	0.00
5	5	780	198.80	1.98

Test 2



Bar	Point	Time (s)	Temperature (°C)	Velocity (m/s)
1	1	60	79.35	0.00
1	2	90	99.50	0.00
1	3	120	111.90	0.36
1	4	150	140.65	1.24
1	5	180	177.00	2.36
2	1	210	77.45	0.00
2	2	240	69.05	0.00
2	3	270	95.35	0.00
2	4	300	125.50	0.00
2	5	330	187.25	2.08
3	1	360	72.40	0.00
3	2	390	53.35	0.00
3	3	420	61.40	0.00
3	4	450	106.80	0.00
3	5	480	164.20	1.82
4	1	510	64.50	0.00
4	2	540	56.75	0.00
4	3	570	74.10	0.00
4	4	600	107.40	0.00
4	5	630	149.50	1.46
5	1	660	84.55	0.00
5	2	690	91.45	0.00
5	3	720	94.70	1.56
5	4	750	112.15	1.27
5	5	780	173.10	2.62

Test 3

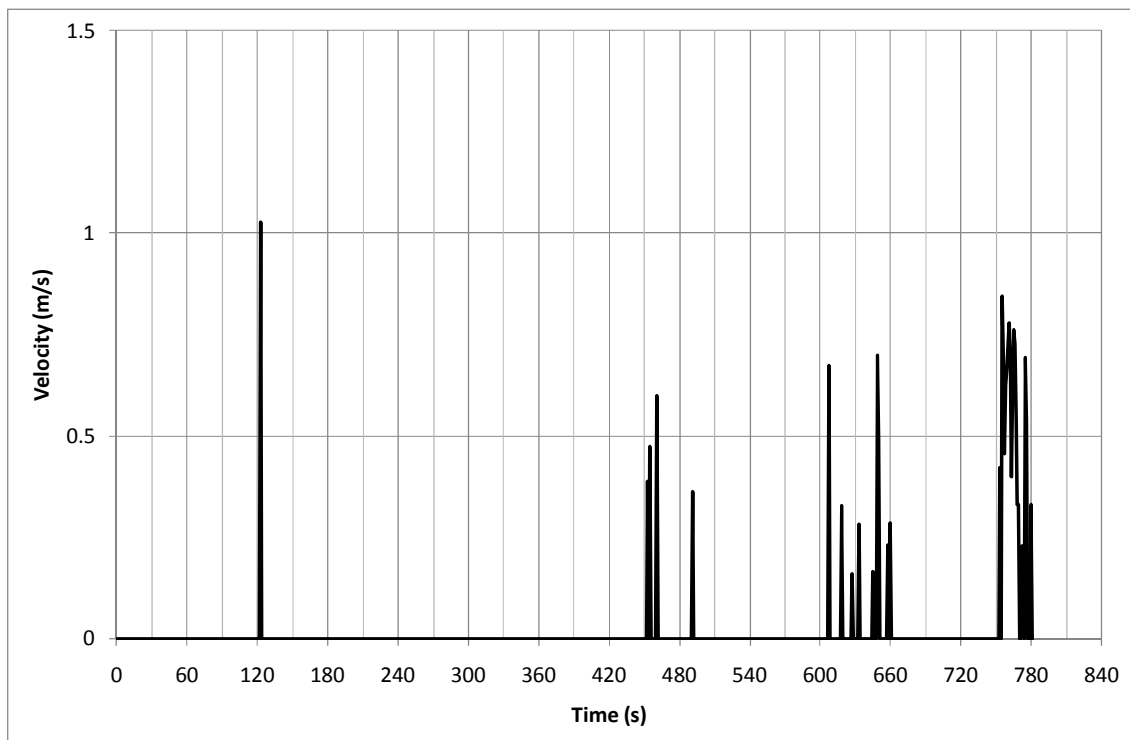
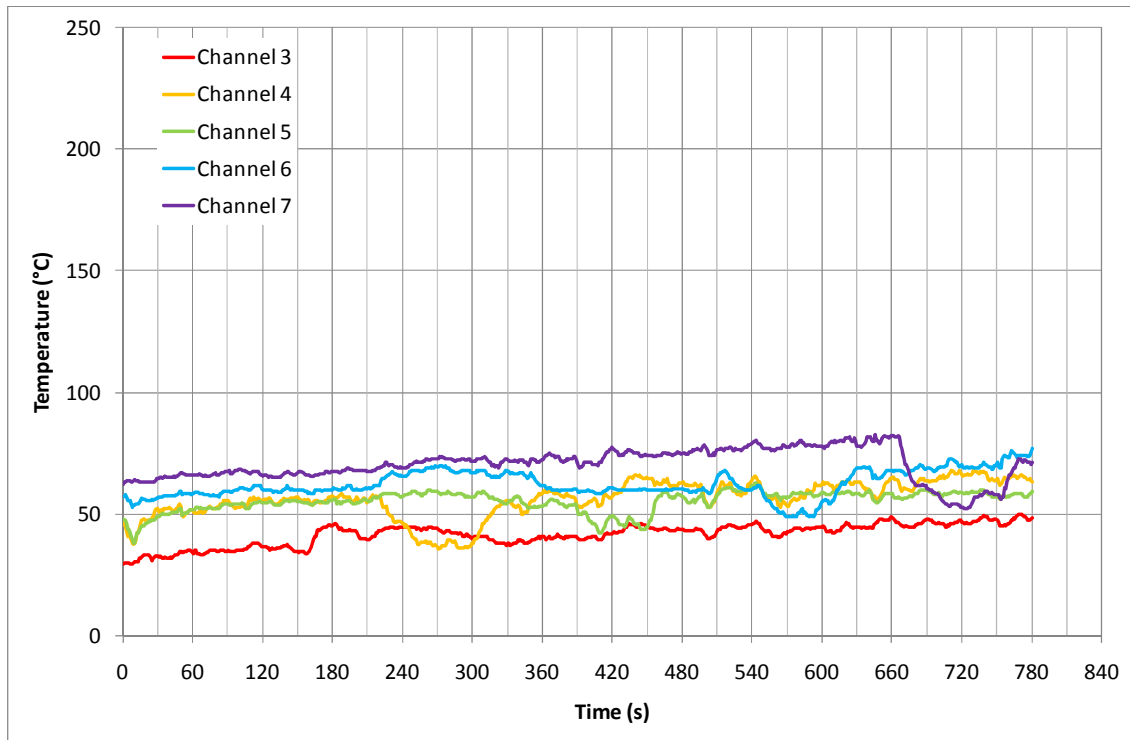


Bar	Point	Time (s)	Temperature (°C)	Velocity (m/s)
1	1	60	89.85	0.00
1	2	90	95.20	0.00
1	3	120	115.95	0.00
1	4	150	136.50	0.00
1	5	180	164.85	1.50
2	1	210	75.70	0.00
2	2	240	79.40	0.00
2	3	270	99.15	0.00
2	4	300	133.55	0.00
2	5	330	181.10	2.08
3	1	360	79.65	0.00
3	2	390	51.85	0.00
3	3	420	67.90	0.00
3	4	450	109.95	0.00
3	5	480	155.95	1.72
4	1	510	74.70	0.00
4	2	540	52.85	0.00
4	3	570	65.05	0.00
4	4	600	108.40	0.00
4	5	630	157.65	1.87
5	1	660	90.45	0.00
5	2	690	95.95	0.00
5	3	720	100.15	0.00
5	4	750	136.05	0.00
5	5	780	194.65	2.23

Appendix D Acrylic Experiment Results

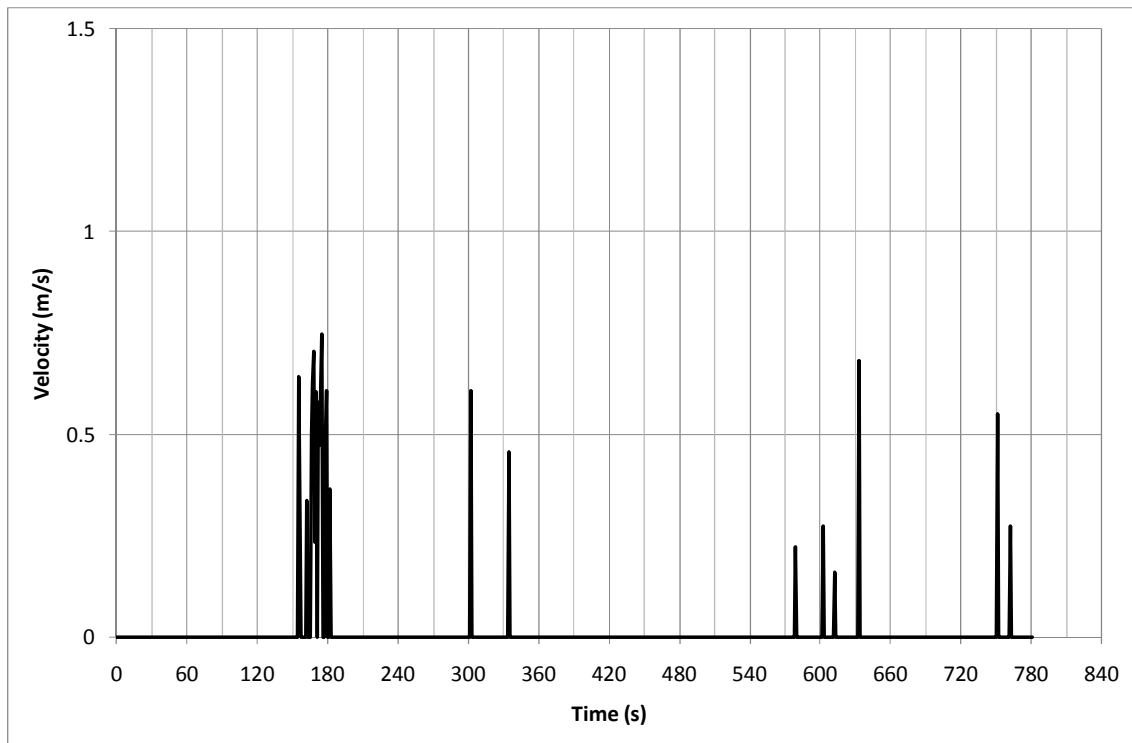
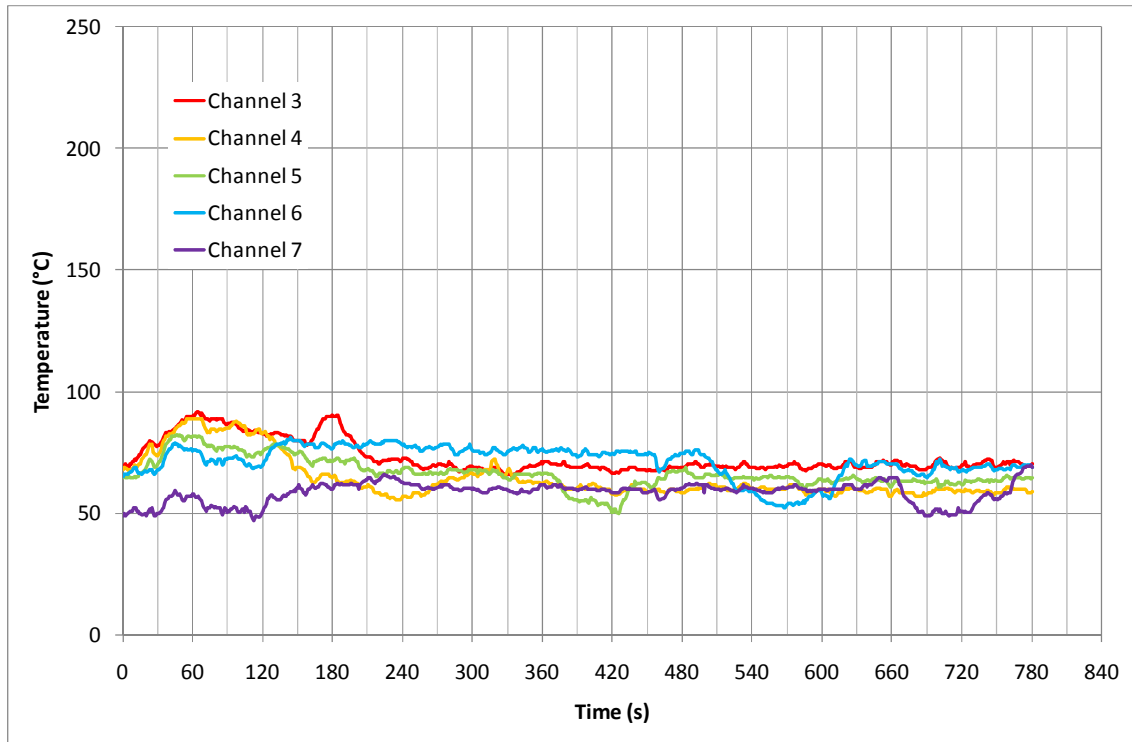
250°C 10 Minutes

Test 1



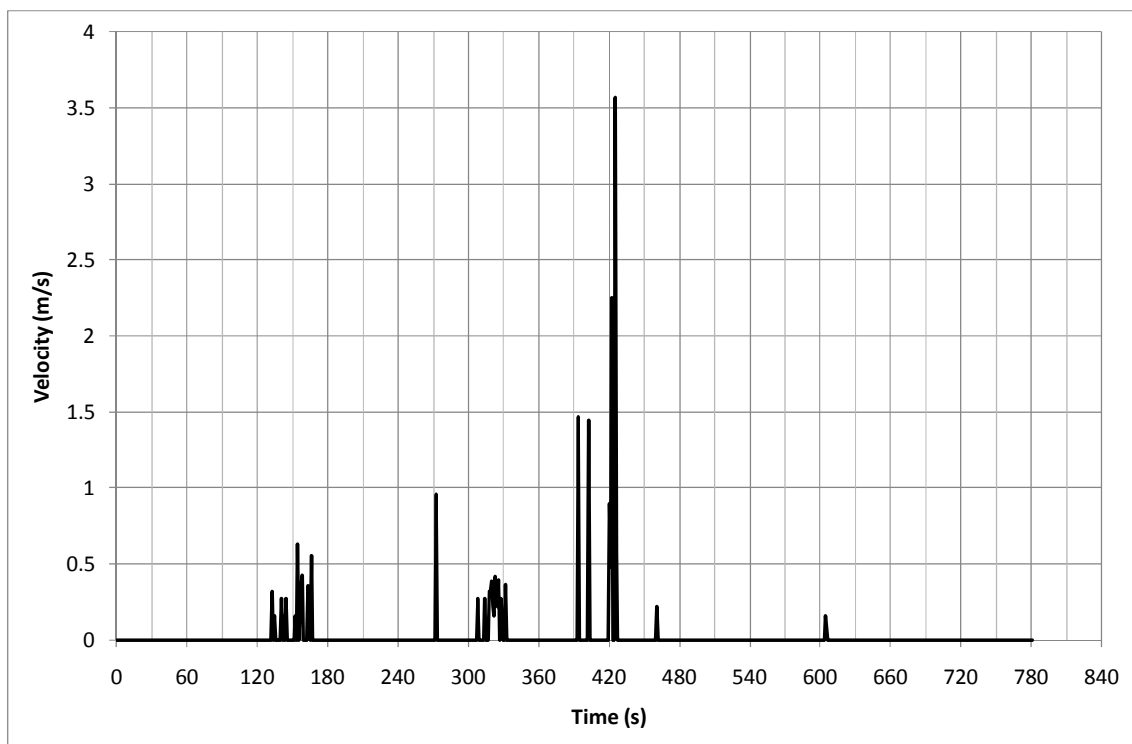
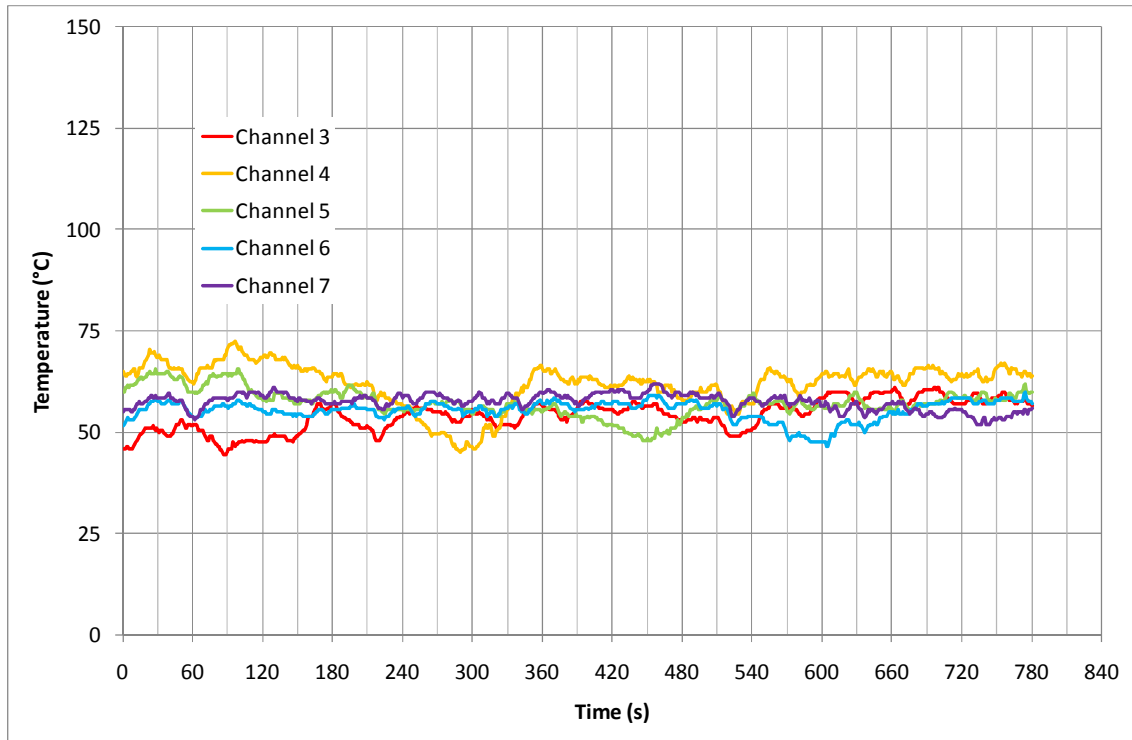
Bar	Point	Time (s)	Temperature (°C)	Velocity (m/s)
1	1	60	34.45	0.00
1	2	90	34.70	0.00
1	3	120	37.55	0.00
1	4	150	35.75	0.00
1	5	180	45.95	0.00
2	1	210	55.85	0.00
2	2	240	47.30	0.00
2	3	270	37.75	0.00
2	4	300	36.50	0.00
2	5	330	53.70	0.00
3	1	360	52.70	0.00
3	2	390	53.25	0.00
3	3	420	45.55	0.00
3	4	450	44.40	0.00
3	5	480	57.70	0.00
4	1	510	60.60	0.00
4	2	540	60.30	0.00
4	3	570	50.70	0.00
4	4	600	51.15	0.00
4	5	630	65.20	0.00
5	1	660	81.10	0.00
5	2	690	61.55	0.00
5	3	720	53.50	0.00
5	4	750	58.80	0.00
5	5	780	71.40	0.13

Test 2



Bar	Point	Time (s)	Temperature (°C)	Velocity (m/s)
1	1	60	89.10	0.00
1	2	90	88.10	0.00
1	3	120	83.25	0.00
1	4	150	80.95	0.00
1	5	180	86.75	0.40
2	1	210	61.05	0.00
2	2	240	55.85	0.00
2	3	270	60.20	0.00
2	4	300	65.60	0.00
2	5	330	67.50	0.00
3	1	360	65.95	0.00
3	2	390	56.20	0.00
3	3	420	53.10	0.00
3	4	450	62.25	0.00
3	5	480	68.00	0.00
4	1	510	70.60	0.00
4	2	540	59.55	0.00
4	3	570	52.80	0.00
4	4	600	58.40	0.00
4	5	630	69.80	0.00
5	1	660	64.05	0.00
5	2	690	50.60	0.00
5	3	720	50.30	0.00
5	4	750	57.25	0.00
5	5	780	68.80	0.00

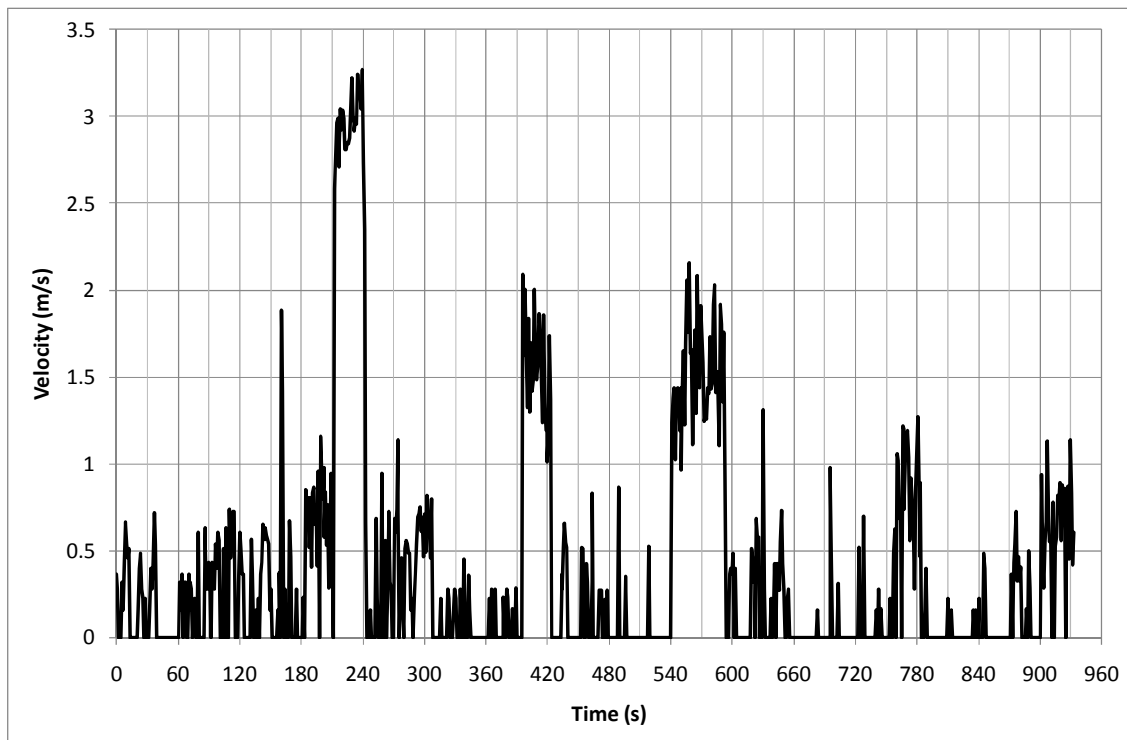
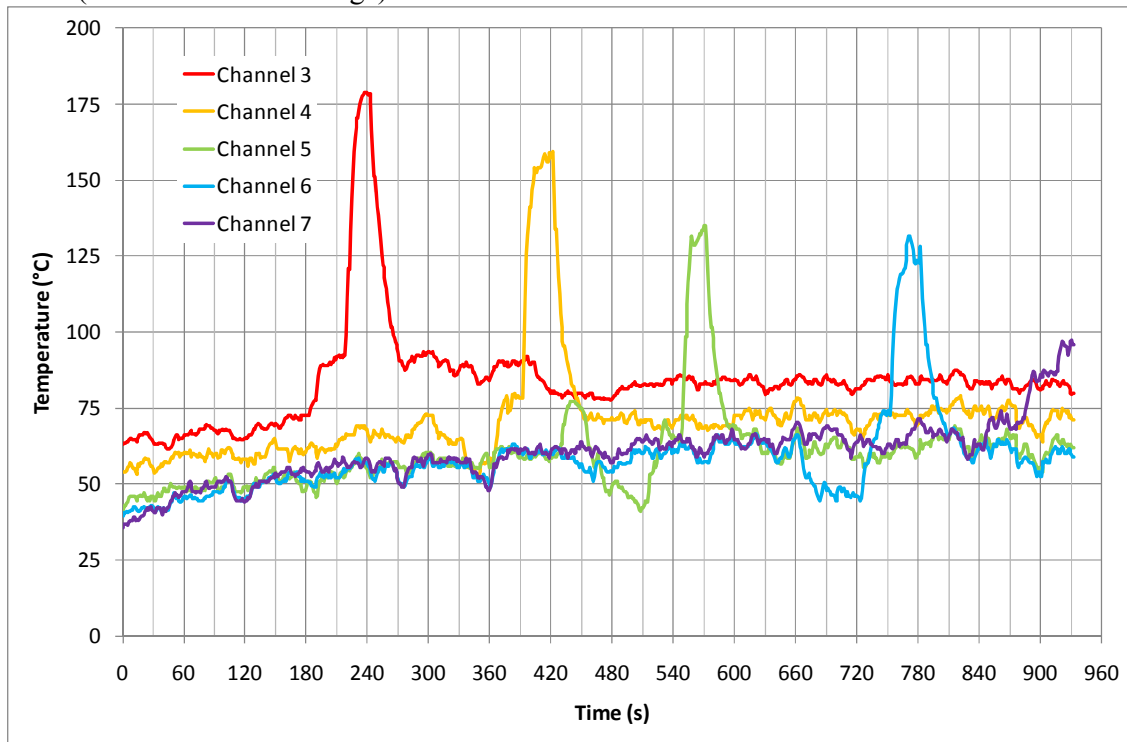
Test 3



Bar	Point	Time (s)	Temperature (°C)	Velocity (m/s)
1	1	60	51.95	0.00
1	2	90	45.45	0.00
1	3	120	47.70	0.00
1	4	150	48.20	0.00
1	5	180	56.80	0.00
2	1	210	61.70	0.00
2	2	240	57.35	0.00
2	3	270	50.05	0.00
2	4	300	46.45	0.00
2	5	330	52.15	0.27
3	1	360	55.25	0.00
3	2	390	54.25	0.00
3	3	420	52.20	0.00
3	4	450	48.60	0.00
3	5	480	52.05	0.00
4	1	510	56.50	0.00
4	2	540	53.60	0.00
4	3	570	51.90	0.00
4	4	600	47.50	0.00
4	5	630	52.40	0.00
5	1	660	56.40	0.00
5	2	690	54.80	0.00
5	3	720	55.55	0.00
5	4	750	52.65	0.00
5	5	780	55.15	0.00

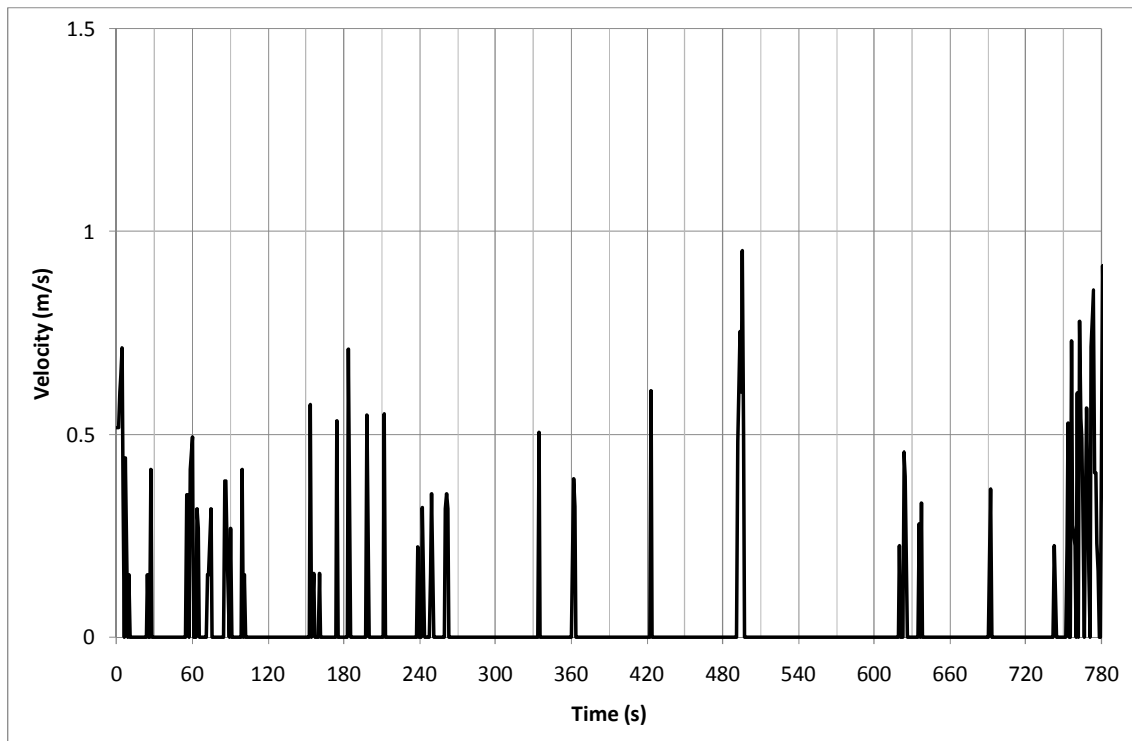
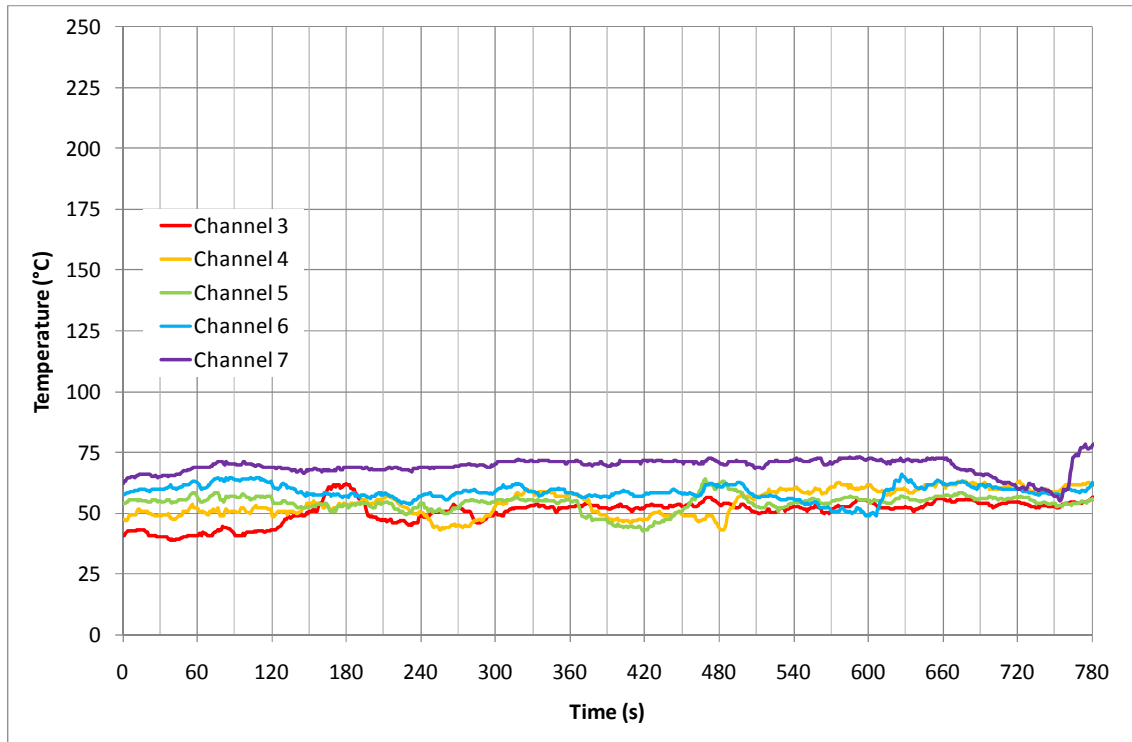
10 Minutes

Test 1(Not used due to damage)



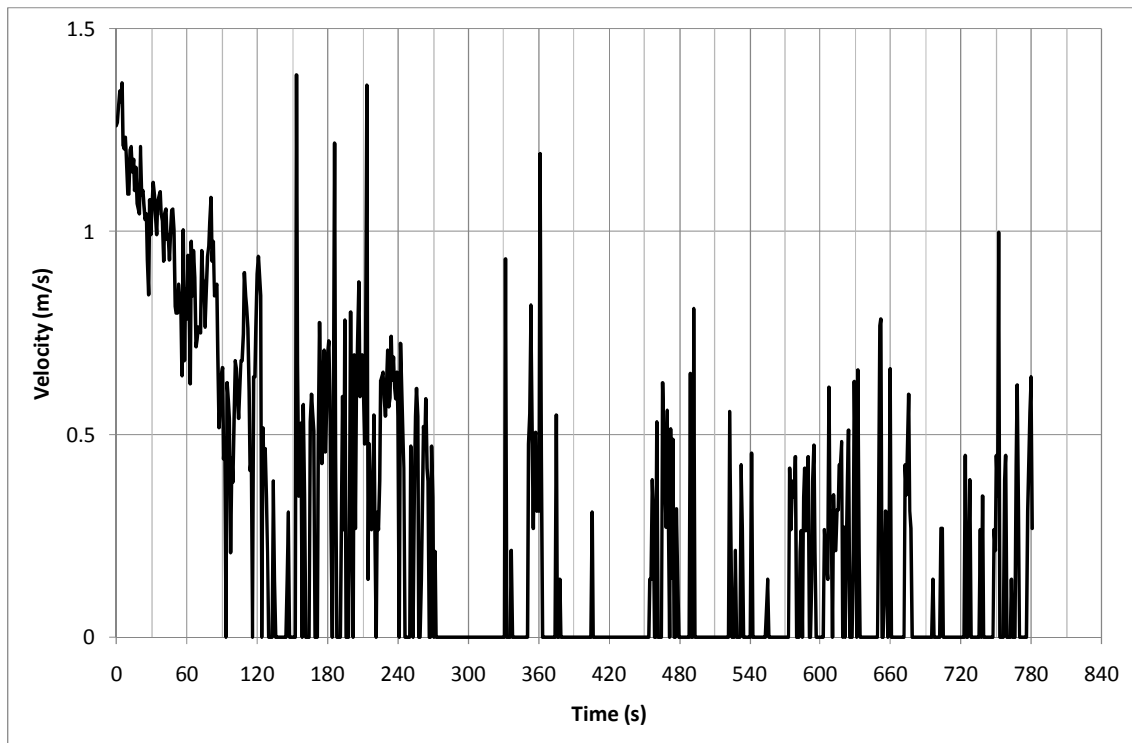
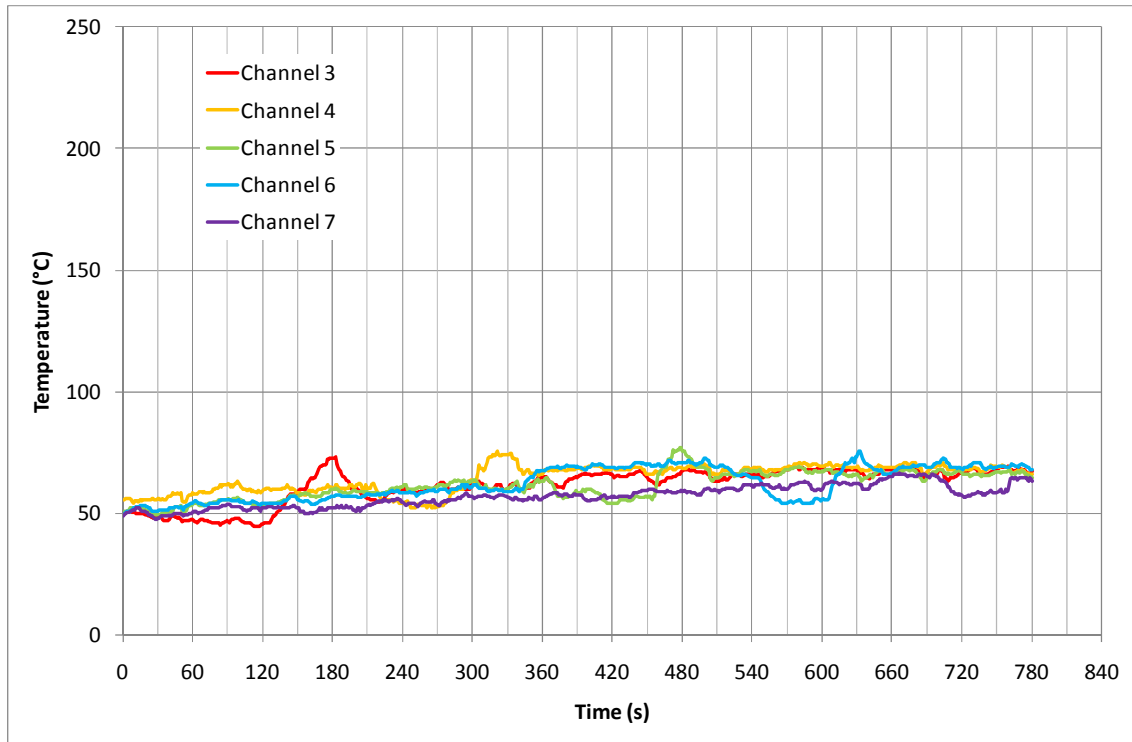
Bar	Point	Time (s)	Temperature (°C)	Velocity (m/s)
1	1	120	64.70	0.42
1	2	150	69.10	0.52
1	3	180	71.95	0.00
1	4	210	90.20	0.71
1	5	240	175.80	3.07
2	1	300	71.75	0.60
2	2	330	63.60	0.00
2	3	360	56.75	0.00
2	4	390	78.20	0.00
2	5	420	156.65	1.52
3	1	450	76.35	0.00
3	2	480	49.00	0.00
3	3	510	43.15	0.00
3	4	540	67.70	0.00
3	5	570	131.10	1.61
4	1	660	61.85	0.00
4	2	690	47.65	0.00
4	3	720	46.30	0.00
4	4	750	71.50	0.00
4	5	780	68.00	0.90
5	1	810	65.85	0.00
5	2	840	61.60	0.00
5	3	870	71.40	0.00
5	4	900	84.60	0.00
5	5	930	95.45	0.71

Test 2



Bar	Point	Time (s)	Temperature (°C)	Velocity (m/s)
1	1	60	40.90	0.18
1	2	90	43.25	0.00
1	3	120	42.45	0.00
1	4	150	49.40	0.00
1	5	180	60.45	0.00
2	1	210	55.00	0.00
2	2	240	50.45	0.00
2	3	270	44.65	0.00
2	4	300	49.85	0.00
2	5	330	58.95	0.00
3	1	360	55.00	0.00
3	2	390	47.45	0.00
3	3	420	43.95	0.00
3	4	450	49.50	0.00
3	5	480	61.20	0.00
4	1	510	58.55	0.00
4	2	540	55.75	0.00
4	3	570	52.10	0.00
4	4	600	50.60	0.00
4	5	630	63.35	0.00
5	1	660	72.35	0.00
5	2	690	66.90	0.00
5	3	720	61.75	0.00
5	4	750	59.20	0.00
5	5	780	76.90	0.36

Test 3

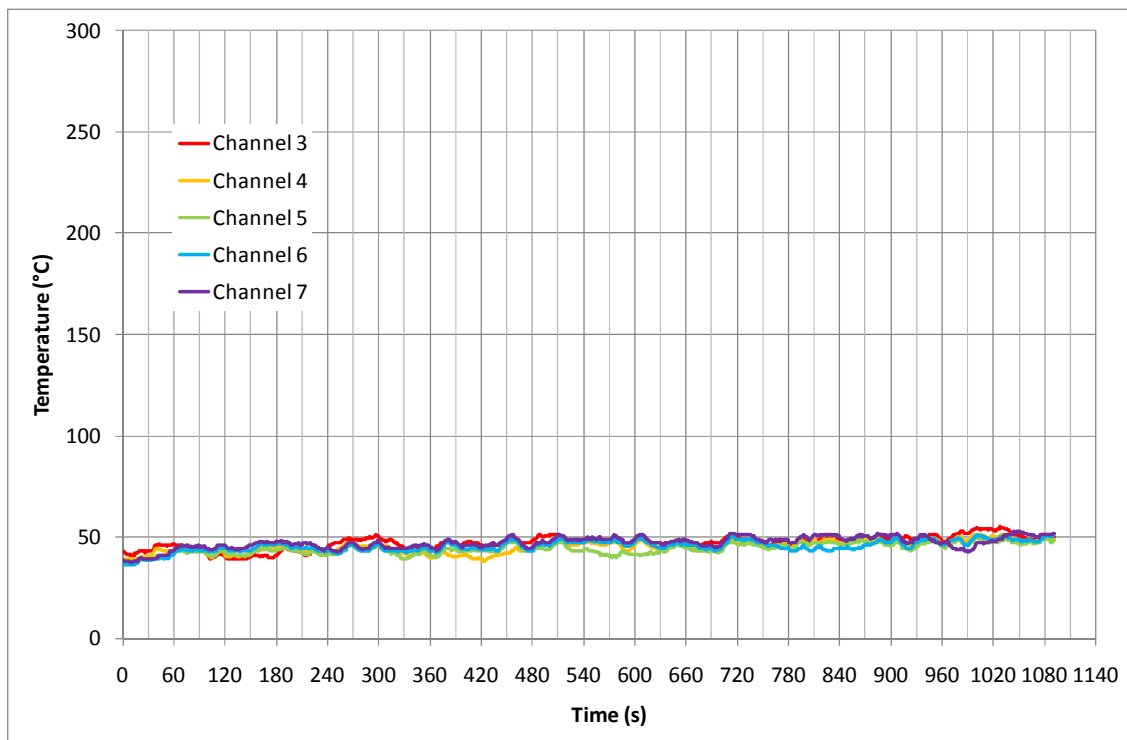
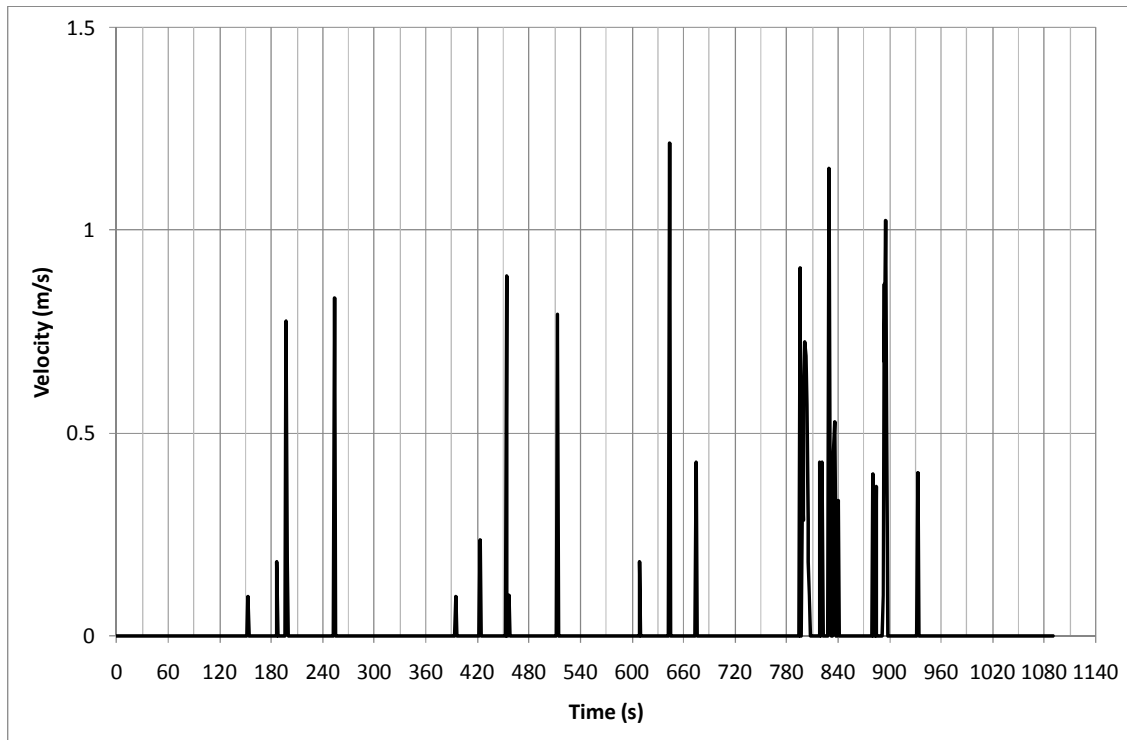


Bar	Point	Time (s)	Temperature (°C)	Velocity (m/s)
1	1	60	47.10	0.42
1	2	90	46.05	0.44
1	3	120	44.95	0.00
1	4	150	57.40	0.00
1	5	180	69.90	0.00
2	1	210	61.10	0.00
2	2	240	54.80	0.00
2	3	270	52.60	0.00
2	4	300	61.75	0.00
2	5	330	74.05	0.00
3	1	360	62.45	0.00
3	2	390	57.60	0.00
3	3	420	54.75	0.00
3	4	450	56.75	0.00
3	5	480	74.70	0.00
4	1	510	70.15	0.00
4	2	540	65.55	0.00
4	3	570	54.65	0.00
4	4	600	55.20	0.00
4	5	630	71.35	0.00
5	1	660	64.30	0.00
5	2	690	65.65	0.00
5	3	720	58.25	0.00
5	4	750	58.55	0.00
5	5	780	64.20	0.00

Appendix E Glass-Fibre Reinforced Polyester Results

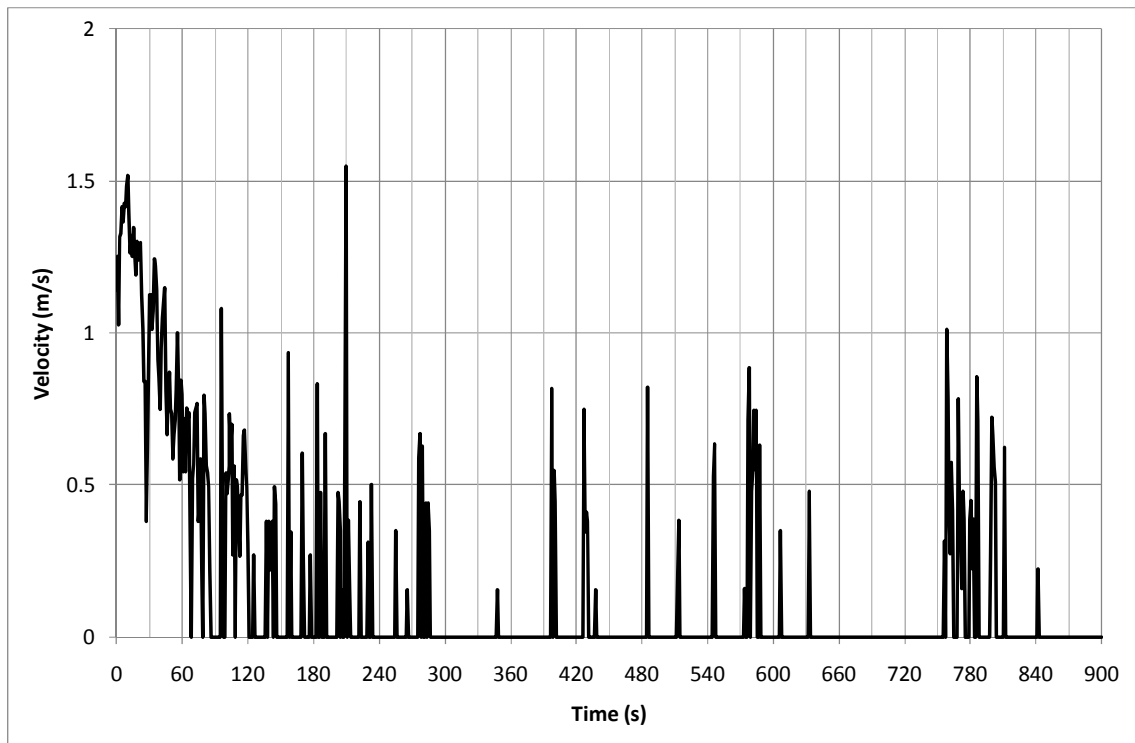
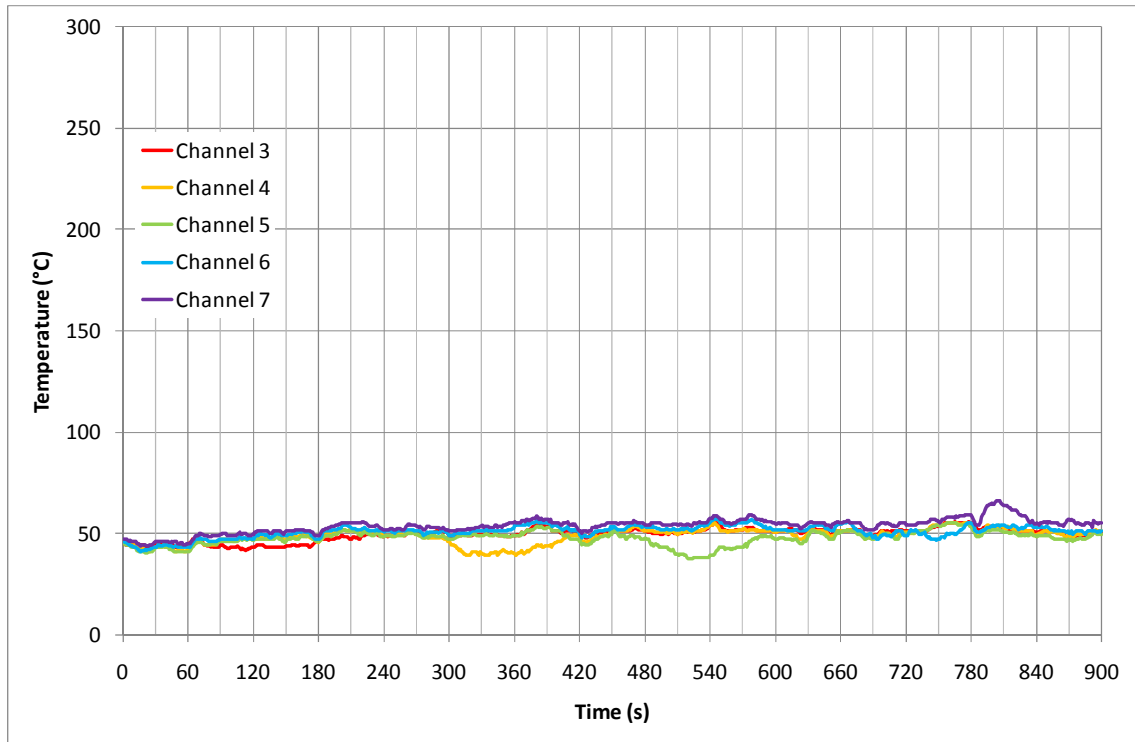
300°C 120 minutes

Test 1



Bar	Point	Time (s)	Temperature (°C)	Velocity (m/s)
1	1	90	44.50	0.00
1	2	120	41.40	0.00
1	3	150	39.75	0.00
1	4	180	40.30	0.00
1	5	210	42.95	0.00
2	1	330	42.75	0.00
2	2	360	41.40	0.00
2	3	390	40.85	0.00
2	4	420	39.55	0.00
2	5	450	41.60	0.00
3	1	510	45.90	0.00
3	2	540	43.20	0.00
3	3	570	41.20	0.00
3	4	600	41.65	0.00
3	5	630	42.20	0.00
4	1	750	47.65	0.00
4	2	780	44.60	0.00
4	3	810	43.65	0.40
4	4	840	44.20	0.39
4	5	870	44.35	0.00
5	1	930	44.35	0.00
5	2	960	44.35	0.00
5	3	990	44.35	0.00
5	4	1020	44.35	0.00
5	5	1050	44.35	0.00

Test 2



Bar	Point	Time (s)	Temperature (°C)	Velocity (m/s)
1	1	60	44.15	0.00
1	2	90	43.50	0.00
1	3	120	42.30	0.00
1	4	150	43.15	0.00
1	5	180	44.85	0.00
2	1	270	50.25	0.00
2	2	300	47.40	0.00
2	3	330	40.55	0.00
2	4	360	48.75	0.00
2	5	390	53.00	0.00
3	1	450	49.05	0.00
3	2	480	48.10	0.00
3	3	510	52.15	0.00
3	4	540	53.95	0.00
3	5	570	54.85	0.00
4	1	630	51.60	0.00
4	2	660	54.95	0.00
4	3	690	52.30	0.00
4	4	720	54.80	0.00
4	5	750	56.55	0.00
5	1	780	59.00	0.15
5	2	810	65.20	0.00
5	3	840	56.15	0.00
5	4	870	54.80	0.00
5	5	900	55.10	0.00

Appendix F Calculation of Biot number

The Biot number is calculated as if the condition of $Bi < 0.1$ is met the lumped capacitance method can be used.

The dimensions for the polycarbonate and PVC sheets are:

$$length = 0.328 \text{ m}$$

$$width = 0.300 \text{ m}$$

$$depth = 0.001 \text{ m}$$

Note that the width is longer than the width of the frame due to the corrugations.

Biot Number

$$Bi = \frac{hL_c}{k}$$

Where

$h = \text{convective heat transfer coefficient}$

$k = \text{thermal conductivity}$

$L_c = \text{the characteristic length}$

$$L_c = \frac{V}{A_s}$$

Where

$V = \text{volume}$

$A_s = \text{Surface Area}$

For polycarbonate and PVC

Surface Area

$$A_s = 2 \times length \times width$$

$$A_s = 2 \times .328 \times .300$$

$$A_s = 0.1968 \text{ m}^2$$

Volume

$$V = \text{length} \times \text{width} \times \text{depth}$$

$$V = 0.328 \times 0.300 \times 0.001$$

$$V = 9.84 \times 10^{-5} \text{m}^3$$

Characteristic Length

$$L_c = \frac{V}{A_s}$$

$$L_c = \frac{9.84 \times 10^{-5}}{0.1968}$$

$$L_c = 5 \times 10^{-4} \text{ m}$$

For the acrylic sheet the dimensions are

$$\text{length} = 0.328 \text{ m}$$

$$\text{width} = 0.275 \text{ m}$$

$$\text{depth} = 0.004 \text{ m}$$

Surface Area

$$A_s = 2 \times \text{length} \times \text{width}$$

$$A_s = 2 \times .328 \times .275$$

$$A_s = 0.1804 \text{ m}^2$$

Volume

$$V = \text{length} \times \text{width} \times \text{depth}$$

$$V = 0.328 \times 0.275 \times 0.004$$

$$V = 3.30 \times 10^{-4} \text{m}^3$$

Characteristic Length

$$L_c = \frac{V}{A_s}$$

$$L_c = \frac{3.30 \times 10^{-4}}{0.1804}$$

$$L_c = 1.8 \times 10^{-3} \text{ m}$$

The value of h has been estimated from (Incropera et al. 2007) as free convection of gases. This gives a range from 2 to 25 W/m²K

$$h = 25 \frac{W}{m^2K}$$

$$h = 2 \frac{W}{m^2K}$$

The value for the thermal conductivity is from Table 16 in section 4.8

$$k_{PVC} = 0.16 \frac{W}{mK}$$

$$K_{PC} = 0.23 \frac{W}{mK}$$

$$K_A = 0.20 \frac{W}{mK}$$

The Biot number for PVC

$$Bi = \frac{25 \times 5 \times 10^{-4}}{0.16}$$

$$Bi = 0.078$$

$$Bi = \frac{2 \times 5 \times 10^{-4}}{0.16}$$

$$Bi = 0.006$$

The Biot number for polycarbonate

$$Bi = \frac{25 \times 5 \times 10^{-4}}{0.23}$$

$$Bi = 0.054$$

$$Bi = \frac{25 \times 5 \times 10^{-4}}{0.23}$$

$$Bi = 0.004$$

The Biot number for acrylic

$$Bi = \frac{25 \times 1.8 \times 10^{-3}}{0.20}$$

$$Bi = 0.225$$

$$Bi = \frac{2 \times 1.8 \times 10^{-3}}{0.20}$$

$$Bi = 0.018$$

The condition for which the Lumped capacitance method can be used if

$$Bi < 0.1$$

For PVC and Polycarbonate the highest Biot numbers are less than 0.1

$$0.078 < 0.1$$

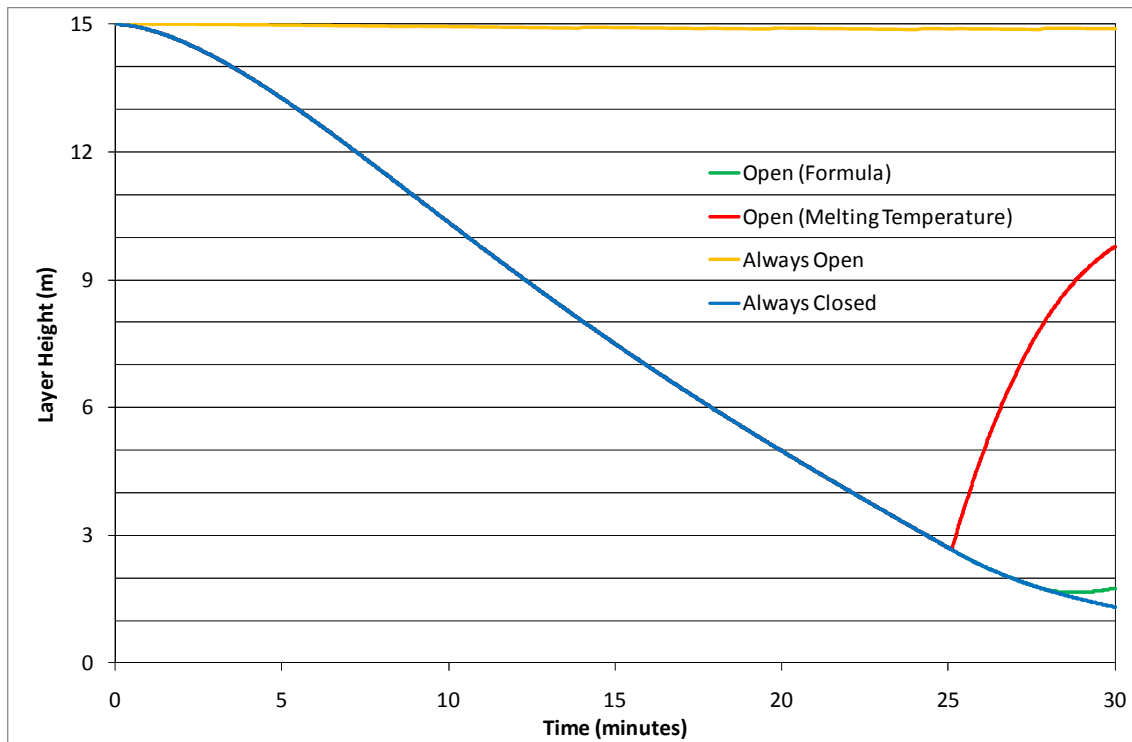
$$0.054 < 0.1$$

However for acrylic the range of the Biot number encompasses the criteria value of 0.1. The lumped heat capacitance method may not be applicable.

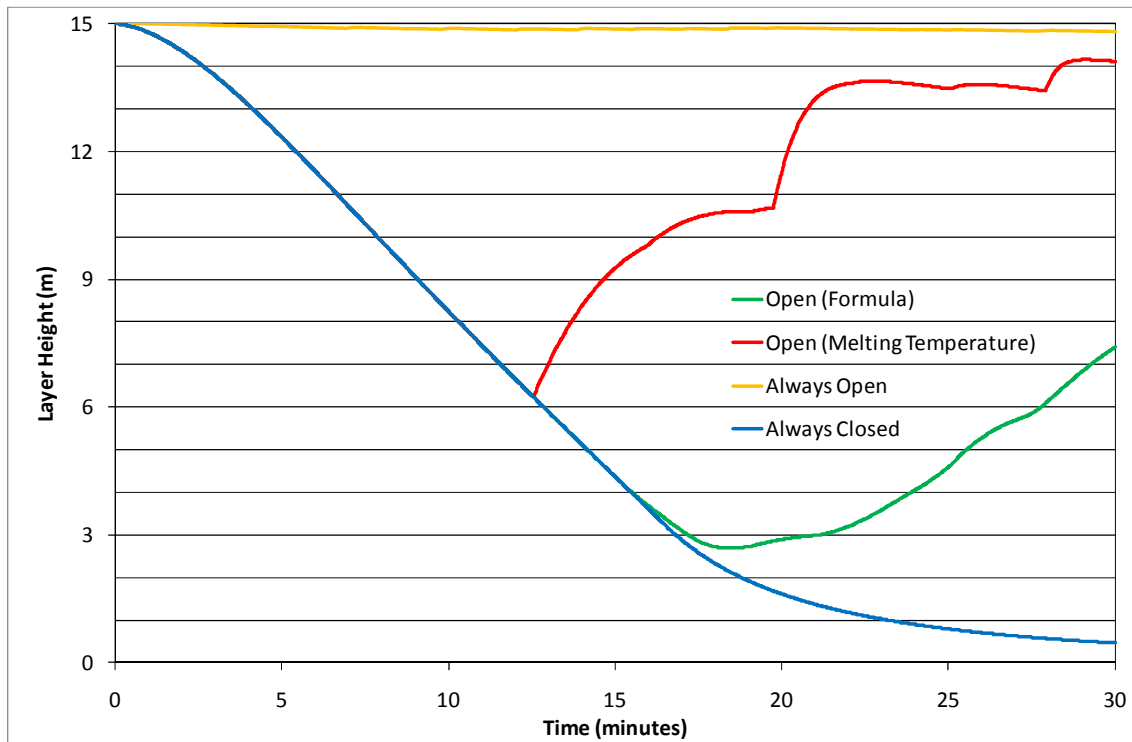
The condition is met and therefore the lumped capacitance method can be used.

Appendix G Model Results

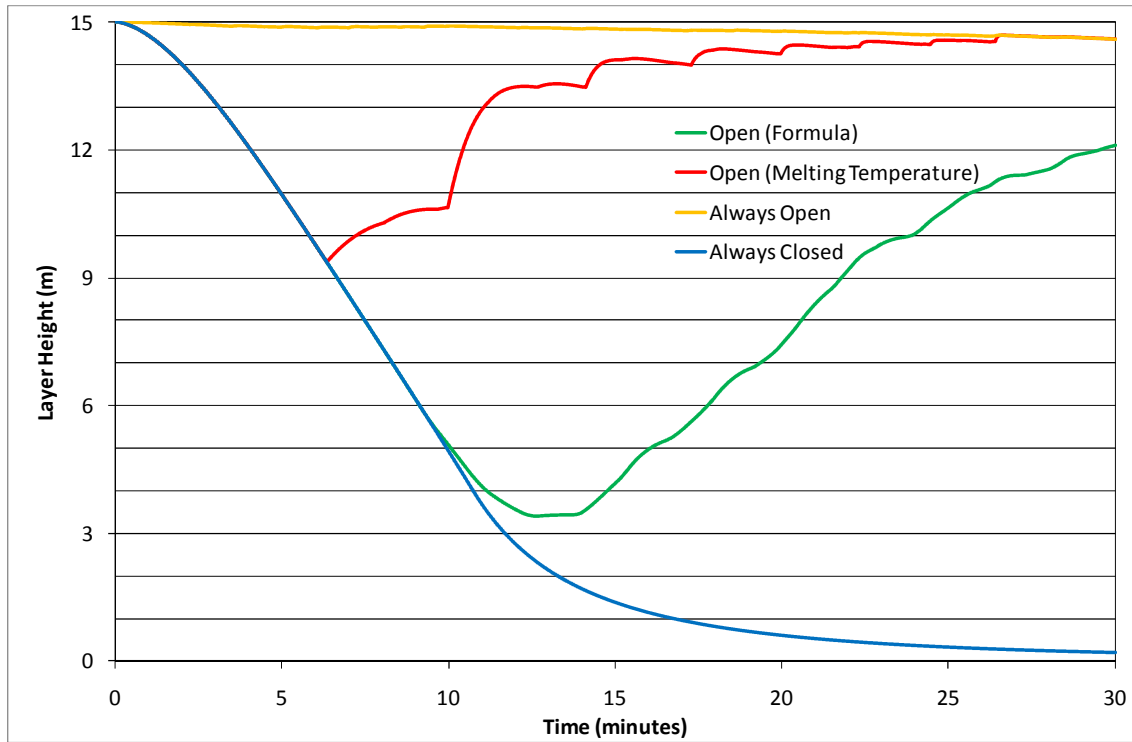
Acrylic
Slow



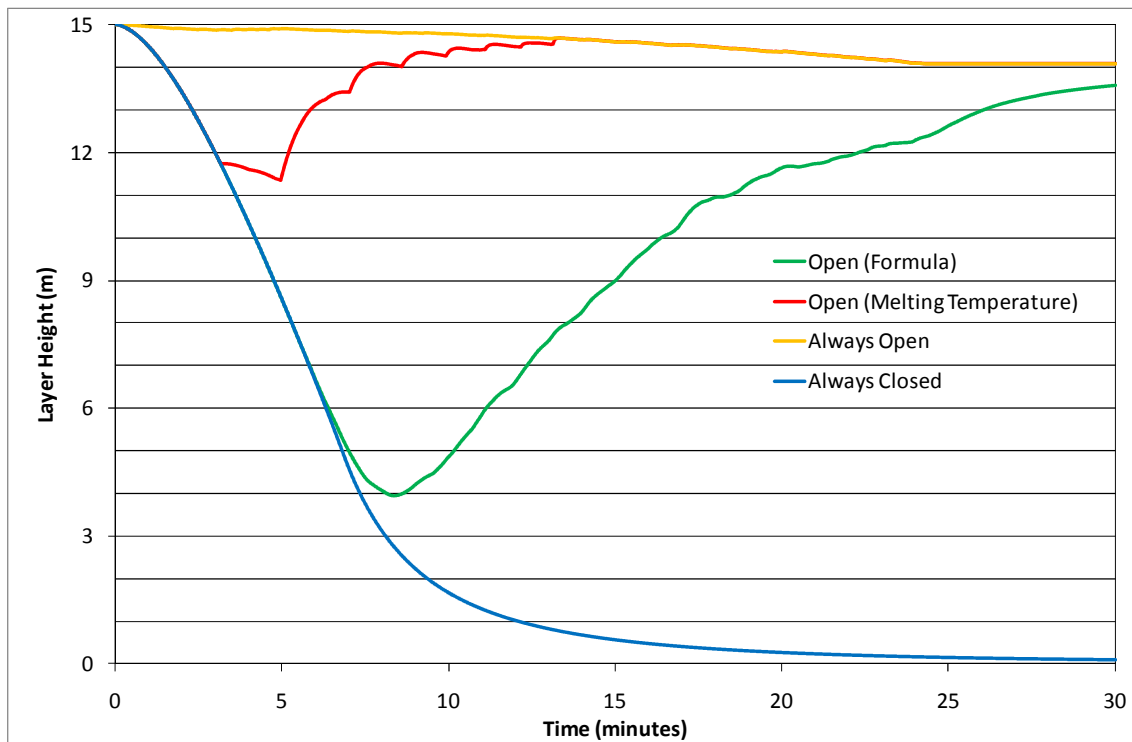
Medium



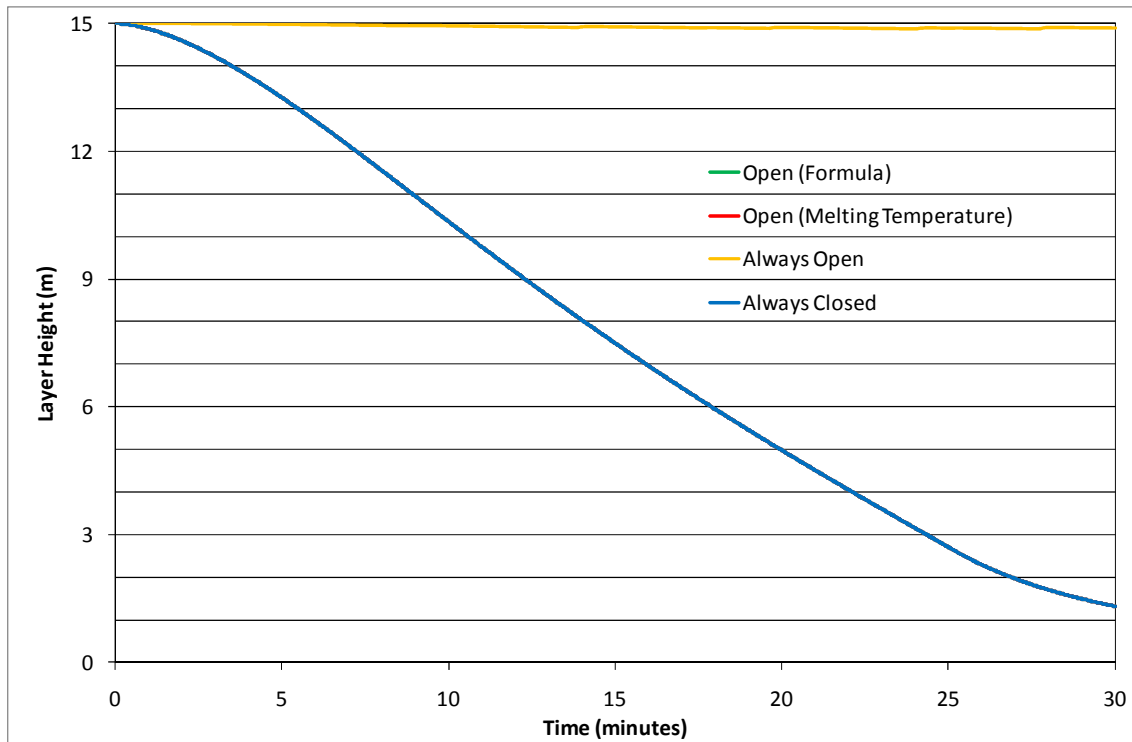
Fast



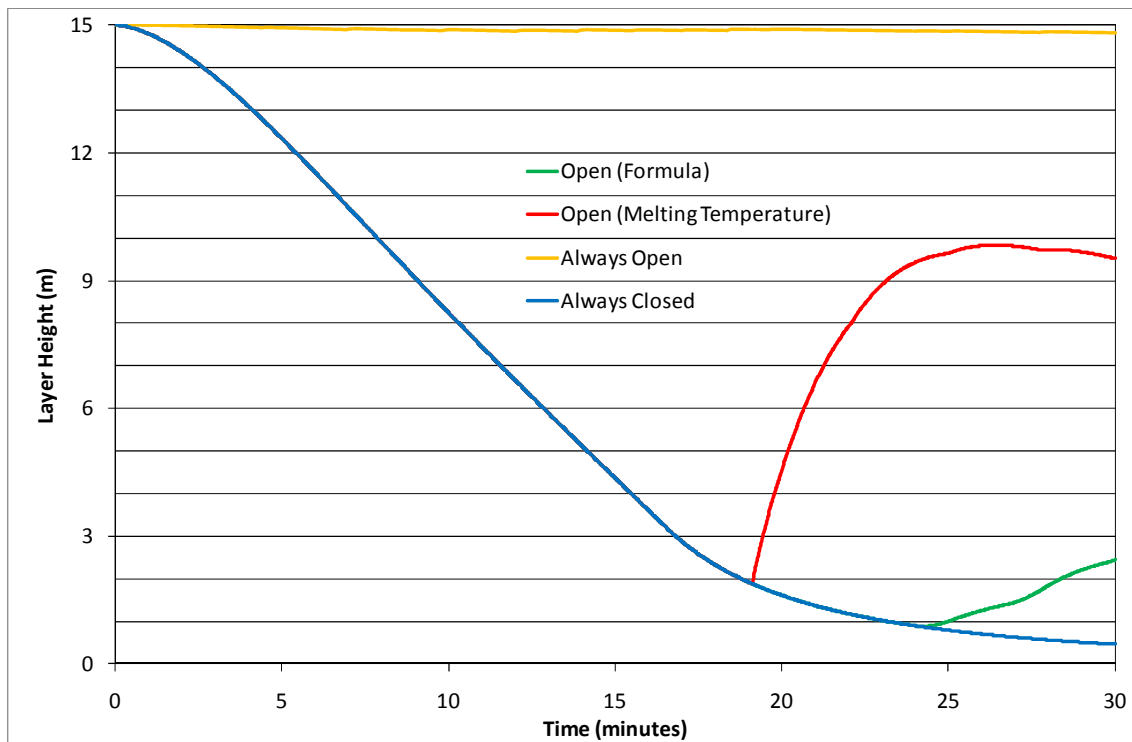
Ultra Fast



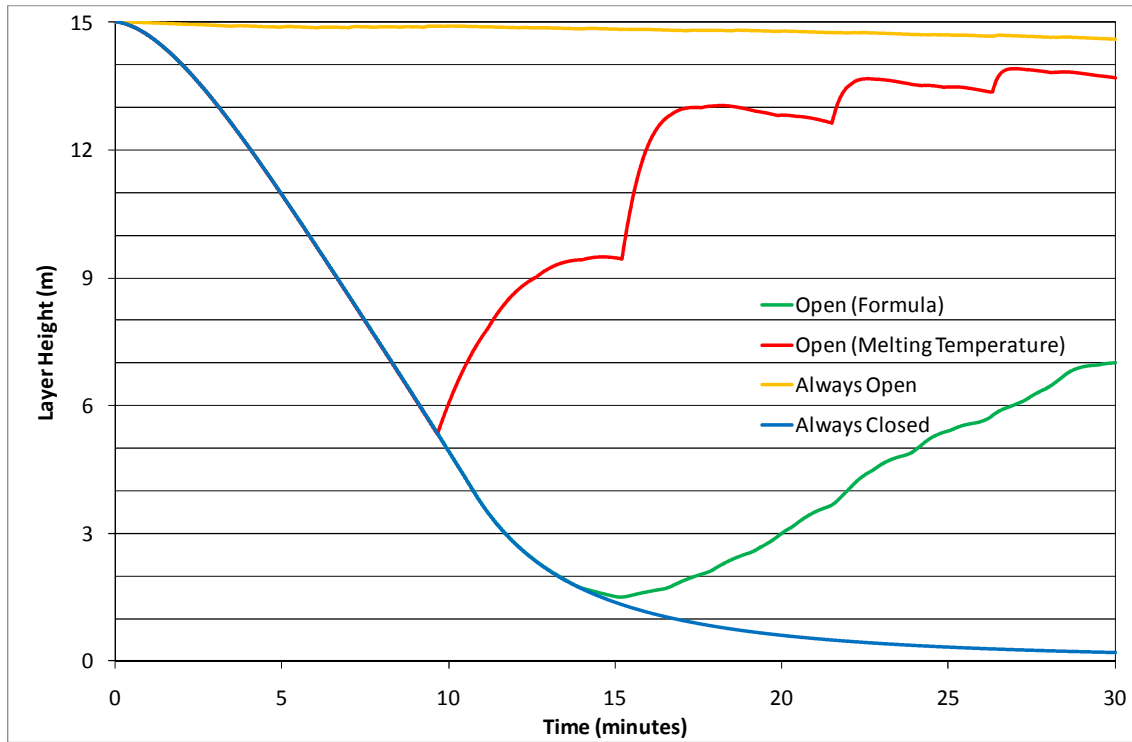
Polycarbonate
Slow



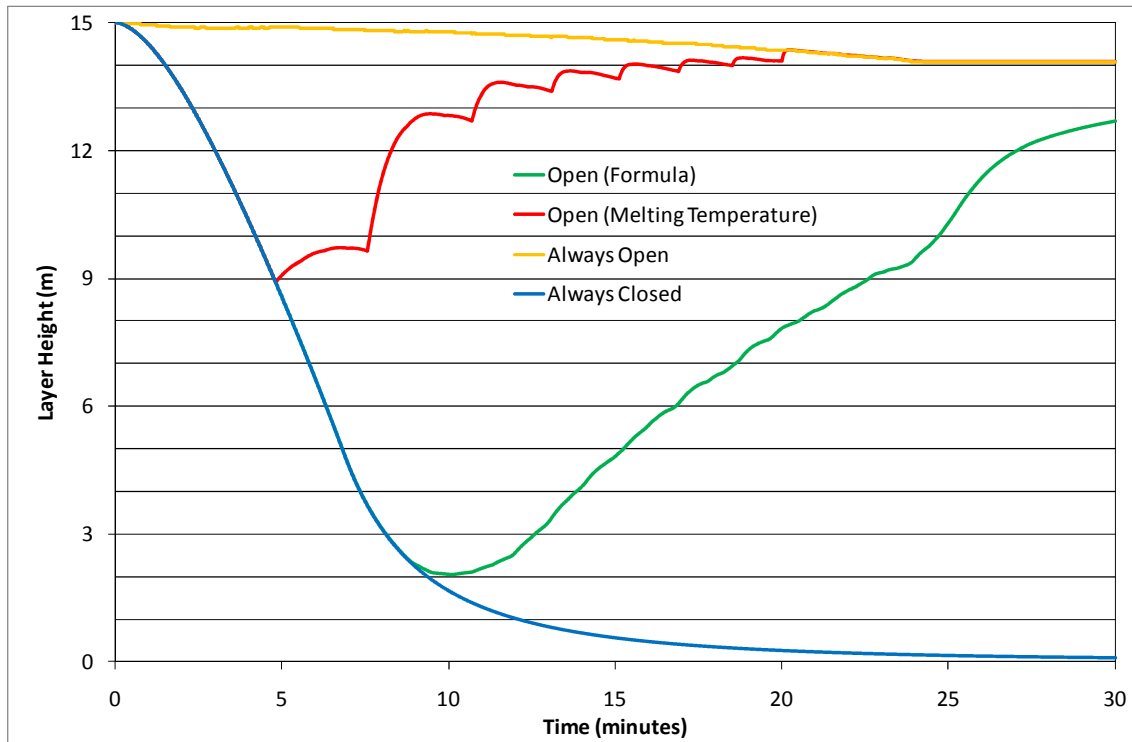
Medium



Fast

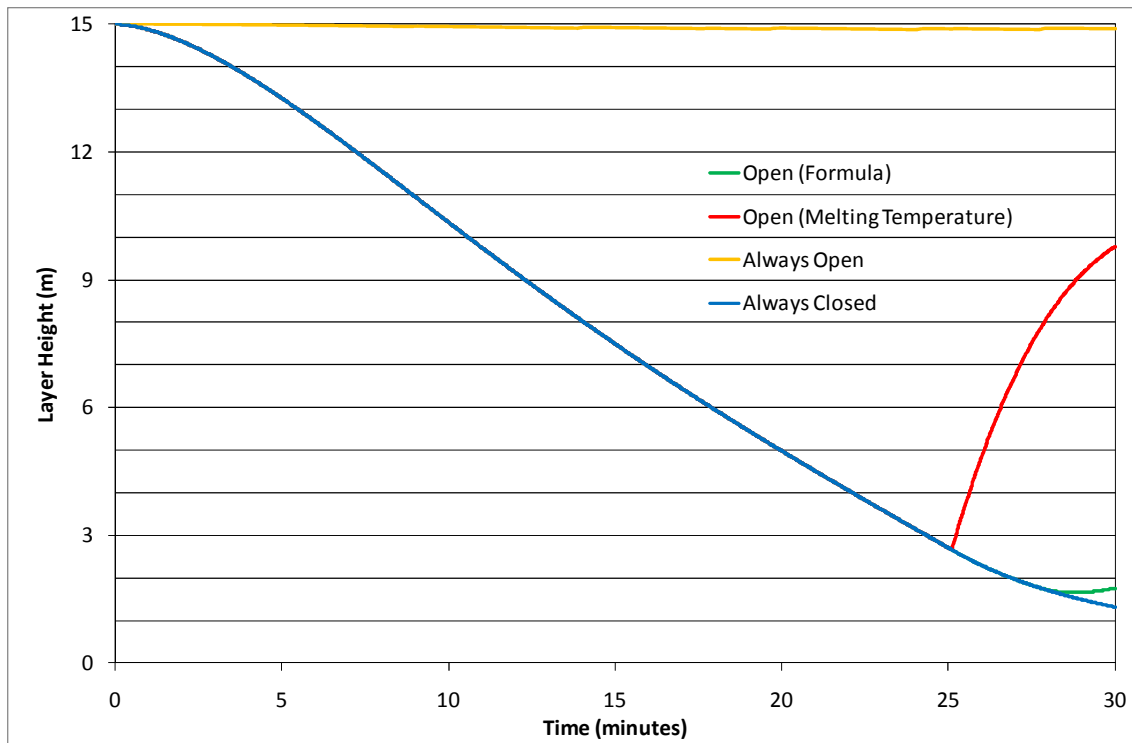


Ultra Fast

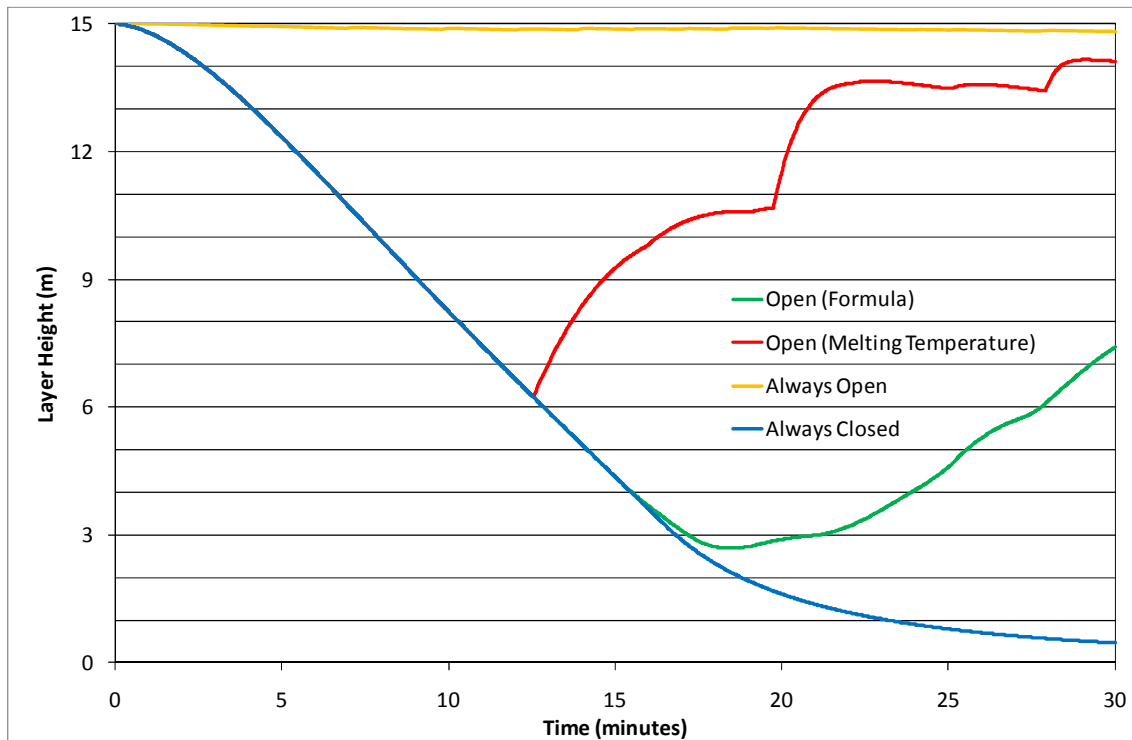


Polyvinyl Chloride

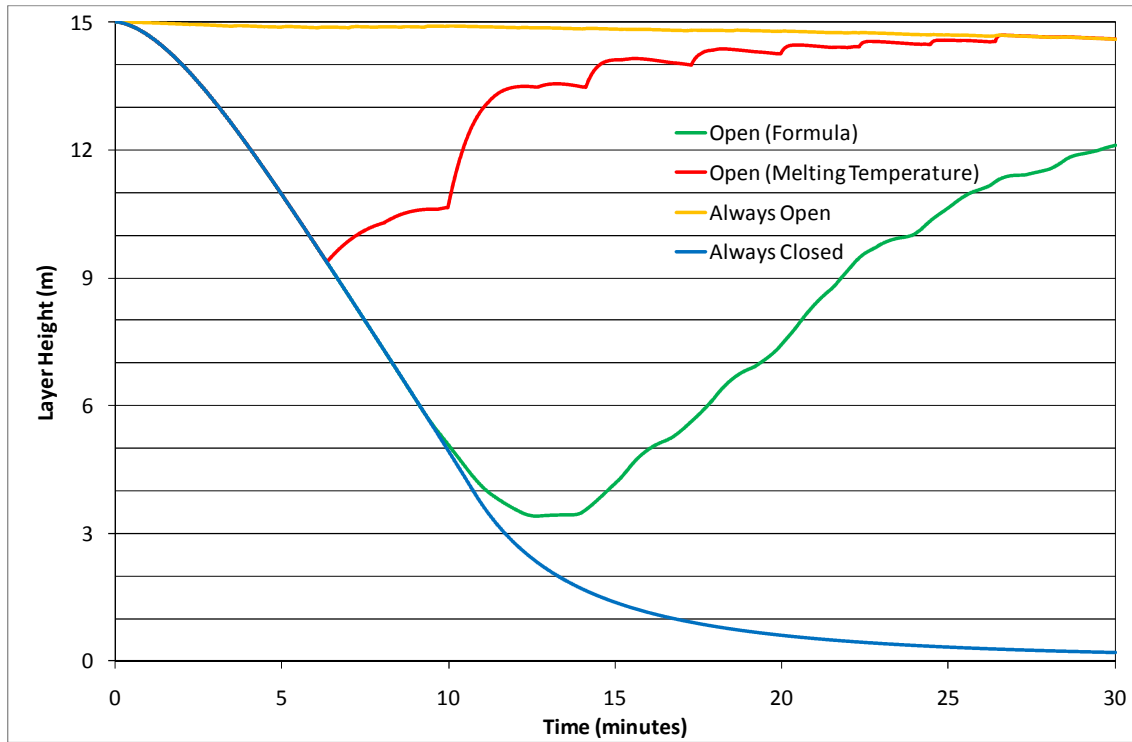
Slow



Medium



Fast



Ultra Fast

